



**Departamento de Ingeniería Química. Universidad de Sevilla**

**VALORIZACIÓN DE SUBPRODUCTOS Y RESIDUOS DE LA INDUSTRIA  
DEL CANGREJO ROJO EN BASE A SU CONTENIDO PROTEICO**

*“Valorisation of wastes and by-products from Red-Crayfish Industry  
based on their protein content”*

**MANUEL FÉLIX ÁNGEL**

Sevilla, 30 de noviembre de 2015





Departamento de Ingeniería Química. Universidad de Sevilla

## TESIS DOCTORAL

**VALORIZACIÓN DE SUBPRODUCTOS Y RESIDUOS DE LA INDUSTRIA  
DEL CANGREJO ROJO EN BASE A SU CONTENIDO PROTEICO**

*“Valorisation of wastes and by-products from Red-Crayfish Industry  
based on their protein content”*

**Tesis Doctoral presentada por D. Manuel Félix Ángel.**

**Dirigida por los Doctores:**

**D. Antonio Francisco Guerrero Conejo y D. Alberto Romero García**

**Los Directores**

**El Doctorando**

Fdo. D. Antonio Guerrero Conejo Fdo. D. Alberto Romero García Fdo. D. Manuel Félix Ángel

**Sevilla, 30 de noviembre de 2015**





---

D. ANTONIO FRANCISCO GUERRERO CONEJO Y D. ALBERTO ROMERO  
GARCÍA, PROFESORES DE LA UNIVERSIDAD DE SEVILLA

INFORMAN:

Que la presente Memoria titulada “VALORIZACIÓN DE SUBPRODUCTOS Y RESIDUOS DE LA INDUSTRIA DEL CANGREJO ROJO EN BASE A SU CONTENIDO PROTEICO” presentado por D. MANUEL FÉLIX ÁNGEL para optar al grado de Doctor con Mención Internacional, ha sido realizada en su mayoría en el Departamento de Ingeniería Química de esta Universidad bajo nuestra dirección, por lo que autorizamos su presentación.

Y para que conste y en cumplimiento de la legislación vigente, firmamos el presente en Sevilla, a 30 de noviembre de 2015.



**D. Antonio Guerrero Conejo**



**D. Alberto Romero García**

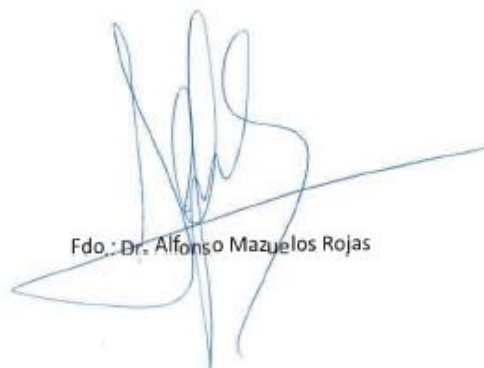


---

Dr. D. Alfonso Mazuelos Rojas, Director del Departamento de Ingeniería  
Química de la Universidad de Sevilla:

CERTIFICA:

Que la Tesis Doctoral que presenta D. Manuel Félix Ángel ha sido  
realizada dentro de la línea "Reología aplicada y tecnología de fluidos  
complejos".



Fdo.: Dr. Alfonso Mazuelos Rojas



## INDEX

1. ACKNOWLEDGEMENTS.	15
2. SYNOPSIS	21
3. BACKGROUND	31
<b>3.1. Proteins</b>	<b>33</b>
3.1.1. Amino acids	33
3.1.2. Peptides and proteins	35
3.1.3. Protein structure	35
3.1.3.1. Primary structure	36
3.1.3.2. Secondary structure	36
3.1.3.3. Tertiary structure	36
3.1.3.4. Quaternary structure	37
3.1.4. Protein separation and characterisation	38
3.1.4.1. Dialysis	38
3.1.4.2. Column chromatography	39
3.1.4.2.1. Ion-exchange chromatography	39
3.1.4.2.2. Size-exclusion chromatography	39
3.1.4.2.3. Affinity chromatography	40
3.1.4.2.4. High-performance liquid chromatography (HPLC)	40
3.1.4.3. Electrophoresis	40
3.1.5. Protein denaturation	42
3.1.5.1. Non-covalent forces in a protein	43
3.1.5.2. Mechanism of denaturation	46
3.1.5.2.1. Temperature-induced denaturation	46
3.1.5.2.2. Pressure-induced denaturation	48
3.1.5.2.3. Denaturation by small-molecular weight additives	49
3.1.5.2.4. Denaturation induced by pH	50
3.1.6. Techno-functional properties of food proteins	51
3.1.6.1. Protein solubility	52
3.1.6.1.1. Effect of pH	52
3.1.6.1.2. Salt concentration's	52
3.1.6.1.3. Denaturation of protein	53
3.1.6.2. Gelation	53
3.1.6.2.1. Thermally irreversible (thermoset) gels	53
3.1.6.2.2. High Pressure Processing (HHP) in food processing	54
3.1.6.3. Water binding	55
3.1.6.4. Emulsification	57
3.1.6.5. Foaming	58

3.1.6.6.	Enzymatic modification of protein to improve techno-functional properties	59
3.1.7.	Crayfish proteins	60
3.1.7.1.	Crustacean shell fish	60
3.1.7.2.	Muscle proteins	60
3.1.7.2.1.	Sarcoplasmic Proteins	61
3.1.7.2.2.	Myofibrillar Proteins	62
3.1.7.2.3.	Stromal Proteins	63
3.1.7.3.	Techno-functional properties of muscle proteins	63
3.1.7.3.1.	Water Retention	64
3.1.7.3.2.	Solubility	64
3.1.7.3.3.	Viscosity of protein solutions	64
3.1.7.3.4.	Gelation	65
3.1.7.3.5.	Emulsification	65
3.1.7.3.6.	Foaming	66
<b>3.2.</b>	<b>Rheology</b>	<b>67</b>
3.2.1.	Definition	67
3.2.2.	Flow laws	67
3.2.3.	Shear stress	68
3.2.4.	Shear rate	68
3.2.5.	Dynamic viscosity	69
3.2.6.	Non-Newtonian liquids. Non-ideal liquids	69
3.2.6.1.	Pseudoplastic fluids	70
3.2.6.2.	Dilatant fluids	71
3.2.6.3.	Yield point	71
3.2.6.4.	Thixotropic fluids	72
3.2.7.	Elastic Behaviour	73
3.2.7.1.	Shear modulus	73
3.2.8.	Viscoelastic fluids	74
3.2.8.1.	The Maxwell model	74
3.2.8.2.	The Kelvin-Voigt model	77
3.2.9.	Viscoelastic tests	79
3.2.9.1.	Creep tests	79
3.2.9.1.1.	Models for creep test	80
3.2.9.1.2.	Models for relaxation tests	81
3.2.9.2.	Oscillatory tests	82
3.2.9.2.1.	Theoretical aspects of dynamic testing	83
3.2.10.	The oscillatory response of real systems	88
<b>3.3.</b>	<b>Interfacial Assessment</b>	<b>91</b>
3.3.1.	Interfacial tension and adsorption	91
3.3.2.	Surfactants	93
3.3.2.1.	Amphiphiles	93

3.3.2.2.	Polymers	94
3.3.3.	Proteins adsorption	94
3.3.3.1.	Adsorbed layers at solid surfaces	95
3.3.3.2.	Adsorbed layers at fluid interfaces	96
3.3.3.3.	Simulation model of a globular protein adsorbed layer	98
3.3.3.4.	Competitive adsorption	99
3.3.4.	Interfacial Measurements	100
3.3.4.1.	Surface pressure-area	100
3.3.4.2.	Dilatational Droplet Tension	102
3.3.4.3.	Interfacial Shear Rheology	103
<b>3.4.</b>	<b>Products from protein</b>	<b>105</b>
3.4.1.	Emulsions	105
3.4.1.1.	Methods of Emulsification	105
3.4.1.1.1.	Role of Surfactants in Emulsion Formation	106
3.4.1.2.	Emulsion breakdown	107
3.4.1.2.1.	Creaming and Sedimentation	108
3.4.1.2.2.	Flocculation	108
3.4.1.2.3.	Ostwald Ripening	109
3.4.1.2.4.	Coalescence	109
3.4.1.2.5.	Phase Inversion	109
3.4.1.3.	Stabilization of systems	110
3.4.1.3.1.	Prevention of Creaming or Sedimentation	110
3.4.1.3.2.	Prevention of flocculation	111
3.4.1.3.3.	Prevention of coalescence	111
3.4.1.4.	Food emulsions	112
3.4.1.5.	Emulsion characterisation	113
3.4.1.5.1.	Rheology of emulsions	113
3.4.1.5.2.	Interfacial Rheology	114
3.4.1.5.3.	Bulk rheology	115
3.4.1.5.4.	Microscopy	117
3.4.2.	Food Gels	119
3.4.2.1.	Definition	119
3.4.2.2.	Protein gelation	120
3.4.2.2.1.	Heat-induced gelation	120
3.4.2.2.2.	High-pressure gelation	122
3.4.2.2.3.	pH-induced gelation	122
3.4.2.3.	Physicochemical properties of protein gels	122
3.4.2.3.1.	Protein interactions	123
3.4.2.3.2.	Denaturation and Formation of Extended Protein Chains	124
3.4.2.3.3.	Opacity/transparency	125
3.4.2.3.4.	Thermal reversibility	125
3.4.2.3.5.	Rheological properties	126
3.4.2.3.6.	Gel Strength	130

3.4.2.3.7.	Water holding capacity (WHC)	130
3.4.2.3.8.	Microscopy	130
3.4.2.4.	Nutritional properties	131
3.4.2.4.1.	Antioxidant properties of food gels	131
3.4.3.	Bioplastics	133
3.4.3.1.	Materials used in the bioplastic manufacturing	133
3.4.3.1.1.	Natural raw-materials	134
3.4.3.1.2.	Plasticisers	134
3.4.3.2.	Methods for protein-based bioplastics manufacturing	135
3.4.3.2.1.	General approach	135
3.4.3.2.2.	Solvent casting	136
3.4.3.2.3.	Thermo-mechanical processing	137
3.4.3.3.	Properties of the protein bioplastics	139
3.4.3.3.1.	Barrier properties	139
3.4.3.3.2.	Thermal properties	140
3.4.3.3.3.	Microstructural properties	141
3.4.3.3.4.	Viscoelastic behaviour.	141
3.4.3.3.5.	Differential Scanning Calorimetry	142
3.4.3.3.6.	Tensile measurements	142
3.4.3.4.	Applications of protein bioplastics	144
3.4.3.5.	Composite materials	145
<b>4.</b>	<b>MATERIALS AND METHODS</b>	<b>149</b>
<b>4.1.</b>	<b>Materials</b>	<b>151</b>
4.1.1.	Crayfish powder	151
4.1.2.	Materials for Emulsions	153
4.1.3.	Materials for gels	154
4.1.4.	Materials for Bioplastics	155
<b>4.2.</b>	<b>Methods</b>	<b>157</b>
4.2.1.	pH-adjustment of proteins dispersions	157
4.2.2.	Protein characterisation	157
4.2.2.1.	pH- Value	157
4.2.2.2.	Protein content	157
4.2.2.3.	Lipid content	158
4.2.2.4.	Moisture content	159
4.2.2.5.	Ash content	159
4.2.2.6.	Protein solubility	160
4.2.2.7.	Surface hydrophobicity	160
4.2.2.8.	Free and total sulfhydryl	161
4.2.2.9.	Differential scanning calorimetry	161
4.2.2.10.	High performance liquid chromatography (HPLC)	162
4.2.2.11.	Water imbibing capacity (WIC)	163



4.2.3.	Specific methods	163
4.2.3.1.	Emulsions performing	163
4.2.3.2.	Emulsion characterisation	167
4.2.3.2.1.	Droplet size distribution measurements	167
4.2.3.2.2.	Rheological characterization	168
4.2.3.2.3.	Physical stability	169
4.2.3.2.4.	Confocal laser scanning microscopy (CLSM)	170
4.2.3.3.	Gel performing	170
4.2.3.4.1.	Temperature ramp test	170
4.2.3.4.2.	Frequency sweep tests	171
4.2.3.4.3.	Protein interactions	171
4.2.3.4.4.	Water holding capacity (WHC)	172
4.2.3.4.5.	Bio-active properties	172
4.2.3.5.	Bioplastic manufacturing	175
4.2.3.5.1.	Mixing stage	175
4.2.3.5.2.	Injection stage	175
4.2.3.6.	Bioplastic characterisation	176
4.2.3.6.1.	Dynamic Mechanical Temperature Analysis	176
4.2.3.6.2.	Tensile strength measurements	177
4.2.3.6.3.	Water uptake capacity	178
4.2.3.6.4.	X-Ray diffraction (XRD)	179
5.	<b>RESULTS</b>	<b>183</b>
5.1.	<b>Protein Characterisation</b>	<b>185</b>
5.1.1.1.	Amino acid characterisation	185
5.1.1.2.	Protein solubility	186
5.2.	<b>Crayfish-based high oleic/water emulsions</b>	<b>193</b>
5.2.1.	Selection of emulsification conditions	193
5.2.2.1.	Adsorption kinetics	195
5.2.3.	Emulsion characterisation	202
5.2.3.1.	Droplet size distribution (DSD)	202
5.2.3.2.1.	Rheological properties of the continuous phase	212
5.2.3.2.2.	Linear viscoelastic properties of emulsions	213
5.2.3.2.3.	Flow properties of emulsions	218
5.2.3.3.	Light scattering measurements	222
5.2.3.4.	Optical measurements	225
5.3.	<b>Antioxidant Crayfish Gels</b>	<b>229</b>
5.3.1.	CF2L-based protein gels	229
5.3.1.1.	Viscoelastic characterisation	229
5.3.1.1.1.	Gel formation	229
5.3.1.1.2.	Gel characterisation	231

5.3.2.	CF2L-Protein hydrolysate gels	240
5.3.2.1.	Gel Characterisation	240
5.3.2.1.1.	Viscoelastic characterisation	240
5.3.2.1.2.	Protein interactions	247
5.3.2.1.3.	Water holding capacity	250
5.3.2.1.4.	Bio-Active Characterisation	252
<b>5.4.</b>	<b>Crayfish-based bioplastics</b>	<b>259</b>
5.4.1.	Crayfish-bioplastic with chemical modifiers	262
5.4.1.1.	Blends characterisation	262
5.4.1.1.1.	Preparation of blends by thermoplastic mixing	262
5.4.1.1.2.	Rheological characterisation of blends	265
5.4.1.2.	Injection moulding process	268
5.4.1.3.	Characterization of bioplastic probes	269
5.4.1.3.1.	Dynamic Mechanical Temperature Analysis	269
5.4.1.3.2.	Uniaxial tensile strength measurements	272
5.4.2.	Crayfish-bioplastic with a synthetic polymer. Composite materials	275
5.4.2.1.	Blends characterisation	275
5.4.2.1.1.	Preparation of blends by thermoplastic mixing	275
5.4.2.1.2.	Thermal characterization of blends	277
5.4.2.2.	Injection moulding process	280
5.4.3.	Biocomposite characterisation	280
5.4.3.1.1.	Dynamic Mechanical Temperature Analysis	280
5.4.3.1.2.	Uniaxial tensile strength measurements	285
5.4.3.2.	X-Ray Diffraction (XRD)	289
5.4.4.	CF and CF2L protein-based bioplastic comparison	292
5.4.4.1.	Dynamic Mechanical analysis	292
5.4.4.2.	Uniaxial tensile strength	293
<b>6.</b>	<b>CONCLUSIONS</b>	<b>297</b>
6.1.	Conclusions from protein characterisation	299
6.2.	Conclusions from Crayfish-based Emulsions	301
6.3.	Conclusions from Antioxidant Crayfish Gels	303
6.4.	Conclusions from Crayfish bioplastic	305
<b>7.</b>	<b>REFERENCES</b>	<b>307</b>
<b>8.</b>	<b>APPENDIX</b>	<b>329</b>



## 1. Acknowledgements.

---



Como ya se dijo hace muchos años, *no sólo de pan vive el hombre*. Así, durante estos años en los que he realizado el trabajo de tesis doctoral en el Departamento de Ingeniería Química, no sólo he crecido profesionalmente, sino que además he estado rodeado de una familia que me ha acompañado en muchos momentos de mi vida, es por ello que ha llegado la hora de rendir tributo a todos ellos y agradecerles cada vez que han estado ahí para lo que les he necesitado.

Por ello, quiero recrear el recorrido que podría haber hecho un día cualquiera a la entrada en el departamento.

Tras abrir la puerta de entrada del departamento, y enfilarme en ese pasillo, que bien podría ser el de uno de esos hospitales que antaño llamaban de beneficencia, cabe recordar aquellas veces en las que tras entrar Pepe me ofrecía té verde o bien si estaba, como él dice, “condimentado”, un té moruno. Tras esta pequeña pausa en la que no sólo había degustado una bebida con fantásticas propiedades antioxidantes, sino que también discutimos sobre la burocracia de la Universidad, me adentro en el departamento donde paso por Secretaría donde se encuentra Montse y sus ayudas con todo los trámites administrativos (que no fueron pocos y van en aumento) que tenemos que realizar o a Manolo y todos sus paseos al Pabellón de Brasil, entregando todos los documentos para que estuvieran a tiempo. Finalmente, como no, ese rincón a la izquierda del departamento me recuerda a Felipe y sus mil quehaceres con las tareas de director de departamento y Antonio y su doble pantalla, que tanta utilidad tiene para trabajar juntos y evitar la tan conocida tortícolis y sus consiguientes masajes terapéuticos.

Tras salir de ese rincón del Departamento con un caramelo que Montse me ha ofrecido, paso por la puerta del laboratorio 3 y no puedo dejar de recordar la salud de la maceta de Mari Carmen, que con sus mimos la hace estar resplandeciente, o la sonrisa de Jenny que se encuentra hablando con Luisma. Bueno como todo cambia, con Luis, que aunque parezca mentira, Luisma hace ya unos cuantos meses que se fue y con él el “Re-lio” del departamento.

Como no recordar aquellas idas y venidas a ese laboratorio, donde tantas dudas se solucionaban, y donde otras tantas surgían como agua en proceso de licuefacción tras el terremoto de lo que somos, *química*. La misma que da forma a las endorfinas y oxitocinas, la misma que nos permite alcanzar la plenitud como ser humano, la misma que nos permite alcanzar aquello conocido como felicidad, la misma que ha permitido que ésta última madure en una gran amistad. Sin saberlo, comenzamos con 18 años una andadura juntos, el destino hizo que compartiéramos una parte de nuestras vidas, y será el tiempo el encargado de labrar cada uno de nuestros caminos.

Entrando ya en el laboratorio 4 para imprimir unos artículos, saludo a Pablo, que me cuenta las nuevas travesuras de su peque, y a Carlos, sorprendiéndome al entrar en su despacho con una señal que indica, ¡Peligro Canguros! ¿Por qué si aquí no hay de esos? ¡Ahh!, es un recuerdo de cuando estuviste en Australia, me quedo mucho más tranquilo. Tras salir, Lucía me comenta una de esas aventuras deportivas que ha vivido el fin de semana, siempre me ha gustado el deporte, ciertamente éste no es más que un reflejo de esa vida que cuando somos pequeños nos espera fuera de las instalaciones deportivas, y como no, nos ayuda a madurar, a crecer. No puedo olvidarme que después de hacer deporte, hay que recuperar fuerzas y nada mejor que uno de esas cuñas, frescas por supuesto, que Aurora nos trae de Los Palacios.

Antes de llegar al Laboratorio 6, me cruzo con Ana Martín que viene llegando escuchando música, y en la “L” me topo con Juan Carlos, con él comento la ruina hacia la que se dirige el Betis, recuerdo aquellos maratones de prácticas, dónde teníamos nuestro descanso para comernos nuestro abanico, ibérico por supuesto, y comentar el trascurso de esos pequeños momentos que construyen la vida. Pregunto por Paco, pero está en la Escuela, allí donde se pasa tantas y tantas horas, y donde también hemos compartido algunas horas en ese laboratorio de la edad moderna. Finalmente, Nieves me da con la mejor de las sonrisas el matraz de fondo redondo que le pedí el día anterior, pero mirando bien, hay alguien más, Nati, que además de adecentar todo aquello por donde pasa, tantas risas gasta en este lugar llamado “L”.

Tras salir, me encuentro con José Antonio, que viene de su laboratorio 5 y me comenta sus últimos logros en el Battlefield, su inestabilidad en el pH del agua de la pecera o los últimos arañazos que le ha propiciado su gata. Nos dirigimos a visitar a Paco, a hacerle una de esas preguntas que no pueden ser otra cosa más que ocurrencia de José Antonio. Paco intenta comprenderla sin poner cara de “yo no entiendo nada”, tras lo que no puede hacer más que reír. Nuria nos escucha, y me comenta que este fin de semana va a pasarse por La Palma, MI PUEBLO!! ¡Cuidado! por allí hay gente peligrosa, le advierto. De camino al laboratorio 6, saludo a Mc. Alfaro y paso por el despacho de Cecilio, bueno despacho o confesionario, porque creo que lo que ese despacho no haya oído..., porque CEcilio siempre tiene 5 minutos para escuchar a cualquiera, para solucionar cualquier duda, para hacer aquello con lo que si todos hiciéramos el Mundo iría mejor: escuchar y ser amable, olvidando todos aquellos prejuicios, orgullos y celos que nos prohíben ser felices.

Tras todas las paradas en todos esos rincones que forma el departamento, se va haciendo tarde, así que ya tengo que entrar en el laboratorio 6, donde están Alberto y Víctor. Víctor está terminando uno de esos trabajos del Máster que tanta “emoción” genera, y Alberto preparándose una de esas clases que luego tanto éxito tiene entre sus alumnos, una de esas clases en las que alumnos suyos, que a la vez son conocidos míos, me paran y me comentan su magnífica escenificación. Ha llegado la hora de trabajar, con la ilusión de hacer las cosas bien, sin tener miedo al futuro, a sabiendas que tras la defensa del trabajo de tantos años se cerrará una etapa, pero con la ilusión que tras el cierre de una puerta se abre un ventanal.

Durante estos años de tesis, también han formado parte de mí mis amigos y aquellas personas con las que he vivido, Dani, Mary, Javi, Moi, Juanjo, Jorge e Inma, así como con todos aquellos con los que he tomado una cerveza y he amenizado los fines de semana en la Palma, Ismael, Juandi, Juan, Jaime, fran, así como de otros tanto que han estado conmigo en las duras y en las maduras. Aquellas personas que por suerte o azar del destino he conocido en los otros lugares donde he llevado a cabo mi labor investigadora, a Heline y Raf en Bélgica, a Turid,

## *Acknowledgements*

Trude, Siri, Giancarlos en Noruega o a Adri, Espe, Isa, Ortega, Rocío o Inma en Huelva.

Por último, no puedo olvidarme de mi familia, aquellos que han formado parte de mi vida desde que nací (puesto que soy el hermano pequeño), aquellos que me han visto alegre y enfadado, aquellos que me han guiado a lo largo de tantos años, aquellos que sé que nunca me abandonarán y siempre me querrán, aquellos a los que dedicaré unas líneas más adelante. No puedo olvidarme de aquellas personas que ya no forman parte de aquello que conocemos como familia, bien porque ya no están entre nosotros, como mis abuelos, bien porque actualmente no lo sean, pero lo serán. Aquellos en los que tendrá influencia este presente, que para entonces será pasado, aquellos en los que influiré e influirán en un futuro. A todos ustedes os tengo en mente en este preciso momento.





## 2. Synopsis





Every year food and agricultural industry produce a big amount of surpluses and wastes which are discarded or used as a low added value by-product. A particularly relevant example of this fact is located in Andalusia (southern Spain) and it is associated to the red-swamp crayfish. This crustacean was introduced in the middle of the twentieth century and due to favourable weather conditions, abundant food and the lack of predators, it has undergone a fast widespread growth (Kirjavainen and Westman 1999). This rapid growth has contributed to the development of a strong local crayfish industry at the marshes of the Guadalquivir River (Geiger, Alcorlo et al. 2005). A currently attractive way to valorise these products is taking benefits from its relatively high protein content.

Crustaceans constitute an excellent source of high-quality protein, rich not only in essential amino acids and lipids, including long-chain polyunsaturated fatty acids from  $\omega$ -3, but also containing other components of functional value such as astaxanthin that possess a high antioxidant capacity, even higher than others important antioxidants such as  $\beta$ -carotene or vitamin E (Miki 1991). The quality of this protein concentrate will contribute to increase the functional properties in their products and derivatives.

To obtain a useful crayfish protein concentrate for these three applications, a previous stage of characterization and optimization of different flours from crayfish pulp has been carried out. This stage was developed by PEVESA, who selected the temperature, pH, extraction procedure and protein-dispersion fraction in order to obtain the phase with the highest content of soluble protein.

This study is focused on different applications of crayfish protein systems derived from their functional properties, aiming at the achievement of high value-added crayfish-based products. The applications considered in this

study will be: emulsification ability, gel formation and bioplastics processing, and.

First of all, one application come from food industry, which is really interested in produce stable oil-in-water (o/w) emulsions containing a protein different to egg-yolk protein as the only emulsifier in order to produce food products such as mayonnaise and salad dressings. These alternative proteins would avoid the presence of cholesterol from yolk, the development of salmonella in yolk-containing food products or allergic reactions, which nowadays are more and more frequent. Other authors have used previously myofibrillar proteins such as actomyosin to produce emulsions and have demonstrated that actomyosin from hake had higher emulsifying activity and stability than the actomyosin from chicken and pork (Cofrades, Carballo et al. 1996). Protein from crayfish may constitute an excellent source of protein which may contribute to stabilize o/w emulsions.

In addition, other functional property is the ability of proteins to denature form aggregates and adopt gel-structure after a controlled heating. This application contributes to design a wide variety of food systems with the desire rheological consistency, microstructure and texture. Crustacean meat contents mainly sarcoplasmatic and myofibrillar proteins. Sarcoplasmic fraction with a globular and relatively simple structure, show a weak gelation capacity and, therefore, a little contribution to the texture of processed foods. On the other hand, myofibrillar proteins, specially myosin and actomyosin, constitute multiples dominions that tend to form viscoelastic networks and gels with high consistency (Damodaran 1997). Finally, an interesting area of research is the antioxidant characterisation of these gels. Due to the presence of the above mentioned functional ingredients, these gels may constitute an excellent source of protein for the human nutrition.

Finally, a currently attractive way to valorise these by-products is through the use of this protein concentrate as renewable resources in the manufacture of “green materials”, replacing hardly degradable plastic materials from oil-based synthetic polymers. Recently, some important applications for bioplastics are beginning to emerge in the areas of food-packaging, pharmaceuticals, electronics, automotive industry and biomedicine. Thus, among other applications, bioplastics from proteins can be used in food packaging, fruit coating, encapsulation, textiles, absorbent materials or tissue engineering (Sharma and Luzinov 2012, Soroudi and Jakubowicz 2013). This wide variety of potential applications allows us to envisage an increasingly use of biobased-plastic materials in a near future.

Thus, one of the main objectives of this study has been to evaluate the potentials of crayfish concentrate as emulsifier to obtain highly concentrated oil/water emulsions such as mayonnaise-like. First of all, it was necessary to optimize the processing and composition parameters that would lead to long-term stable emulsions. In this context, interfacial measurements were performed in order to facilitate prediction of emulsion stability. Relevant ultimate information on emulsion stability was obtained by characterizing the rheological properties and microstructure of crayfish-based emulsions. The rheological characterization has been focused on the linear viscoelastic properties of the emulsions, determined by means of small-amplitude oscillatory shear (SAOS). Microstructural parameters have been evaluated through droplet size distributions analysis. Microstructure has also been characterised by Confocal Laser Scanning Microscopy (CLSM).

Another additional objective has been to evaluate the gel ability and the bioactive potential of gels made from non-denatured crayfish protein concentrate at different pH values. To explore improvements in both, the gelation and bioactive ability, different hydrolysates were obtained

with different degree of hydrolysis. Pancreatic trypsin was the protease-enzyme chosen to hydrolyse the crayfish concentrate protein. On the other hand, transglutaminase was eventually added to a selected system (based on his bioactive properties) in order to improve the mechanical properties of its gels. To characterise mechanical properties, rheological measurements of aqueous CF protein dispersions were performed in order to follow the gelation process by means of temperature ramps, as well as frequency sweep tests to obtain the mechanical spectra of CF-based gels. Finally, bioactive ability of the different gels was evaluated behind three different reference compounds.

Finally, the last objective of this study has been to evaluate the potentials of crayfish concentrate protein to produce plasticized crayfish bio-based plastic materials by means of a conventional, highly versatile and widely used polymer processing technique such as injection moulding, as an alternative to plastic materials based on polymers derived from fossil fuel. Glycerol (GL) has to be used in this process as a plasticiser. Results from crayfish protein concentrate were compared with those obtained using a low valued crayfish protein flour in order to reduce bioplastics costs, since, as is widely known, these kind of products are involved in a well-developed industry and very competitive market. Furthermore, the effect of using different chemical additives on the properties of CF-based products was also evaluated. The additives assessed in this study were sodium sulphite (SS) or bisulphite (BS) as reducing agents, urea (U) as a denaturing agent and L-cysteine (LC) as a crosslinking agent. An interesting alternative to achieve this objective involves using CF protein in combination with a synthetic polymer, preferably one showing some biodegradable properties such as polycaprolactone (PCL). This polymer is classified as a biodegradable polyester from fossil source and it has been widely used as the polymer matrix in the development of a variety of new materials. As for bioplastic processing, regardless of its formulation, injection moulding has been selected since it is one of the most versatile and

extended polymer processing technique, being particularly useful for polymeric materials (e.g. protein) that deviate from a typical thermoplastic behaviour. This process requires a previous mixing stage of polymeric materials and plasticiser (and additives, if any) to obtain homogenised blends with suitable properties for their subsequent injection. This stage was carried out by means of a mixing-rheometer that allows an exhaustive control of the blend by recording torque and temperature over mixing. Rheological and Differential Scanning Calorimetry measurements of the blends obtained were carried out in order to obtain information that may be useful in the selection of suitable processing parameters for injection moulding operations (temperature and residence time in the pre-injection cylinder as well as moulding temperature). Eventually, all the probes were characterised by means of dynamic mechanical analysis (DMA) and tensile strength measurements in order to obtain the mechanical characterisation.







*A mi familia*

*Por hacerme persona,  
Por inculcarme todos aquellos valores que hacen al hombre ser humano,  
Por quererme siempre incondicionalmente,  
A mis padres y hermana, por ser quienes son y hacerme ser quien soy.*





### 3. Background

---



## 3.1. Proteins

Proteins are the intermediate in every process that takes place in a living being. Proteins also are the most abundant biological macromolecules, being considered even as biopolymers.

All proteins are built from the same set of 20 amino acids which are covalently linked in a characteristic linear sequence. Each type of protein has a unique sequence of amino acids which provides each of them with distinctive chemical properties. This group of 20 precursor molecules may be considered as the alphabet used to write the protein structure and functionality. Proteins are found in a wide range of sizes, from relatively small peptides to huge biopolymer with molecular weight over the millions (Lehninger, Nelson et al. 2005).

### 3.1.1. Amino acids

All of the 20 amino acid are  $\alpha$ -amino acids. Each of them have a carboxyl group and an amino group bonded to the same carbon atom (the  $\alpha$ -carbon), and an "R" group. They differ from each other in their "R" groups, which vary in structure, size, and electric charge. For all the amino acids except for the glycine, the  $\alpha$ -carbon is bonded to four different groups: a carboxyl group, an amino group, the "R" group, and a hydrogen atom. According to this structure, the  $\alpha$ -carbon atom is a chiral centre. Thus, the four different groups can occupy two unique spatial arrangements due to the tetrahedral arrangement of the bonding orbitals around the  $\alpha$ -carbon atom, such that each amino acid have two possible stereoisomer L and D. However, all the amino acids synthesized by living being are L-amino acid (Aluru 2005). Figure 3.1-1 shows the 20 amino acids classified by "R" group nature (non-polar, polar-uncharged, polar-positively charged, polar-negatively charged and aromatic).

## Background. Proteins

Amino acids in aqueous solution also can act as acids and bases. The amino and carboxyl groups of amino acids, along with the ionisable R groups of some amino acids, can work as weak acids and bases. When an amino acid loses an ionisable R group and is dissolved in water at neutral pH, it exists in solution as the dipolar ion, or zwitterion which can act as either an acid or a base. These kind of substances which have an amphoteric behaviour are named ampholytes (Lehninger, Nelson et al. 2005). The twenty amino acids are: Glycine, (Gly); Histidine, (His); Isoleucine, (Ile); Leucine, (Leu); Lysine, (Lys); Methionine, (Met); Phenylalanine, (Phe); Proline, (Pro); Serine, (Ser); Threonine, (Thr); Tryptophan, (Trp); Tyrosine, (Tyr); Valine, (Val).

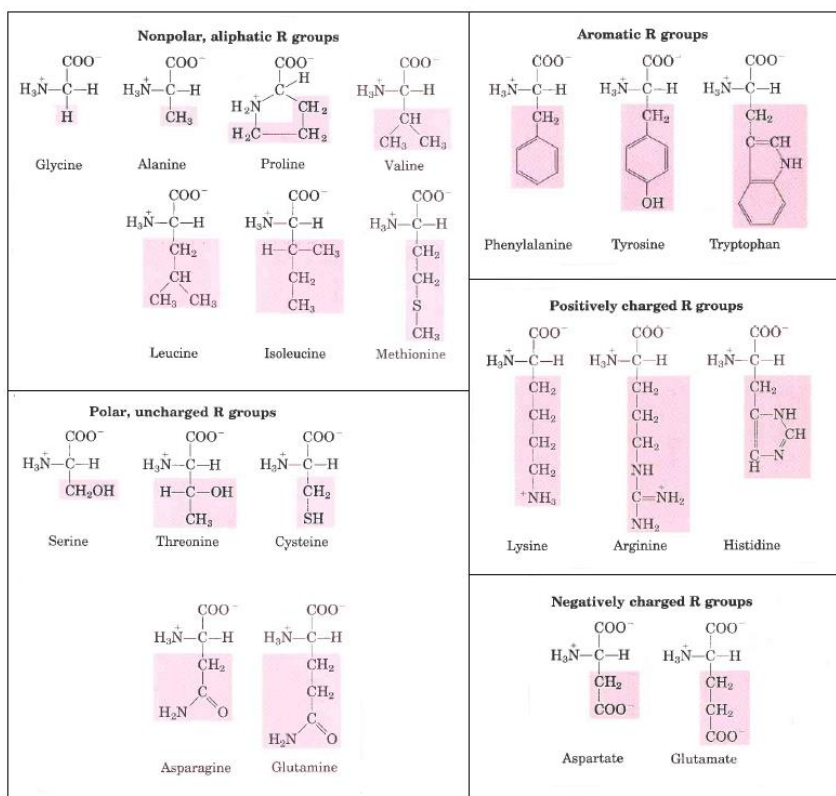


Figure 3.1-1: Chemical composition and structure of the twenty amino acids, classified by "R" group nature

### 3.1.2. Peptides and proteins

Peptides and proteins are the polymers of amino acids. Two amino acid molecules can be covalently bounded through an amide linkage, leading a dipeptide. Such a linkage is formed by removal of one hydroxyl-group from the carboxyl group of the starting amino acid and one hydrogen from the amino group of the followed amino acid. As a consequence, formation of a peptide bond is a condensation reaction where each peptide joining release a molecule of water. Figure 3.1-2 schematises this chemical reaction.

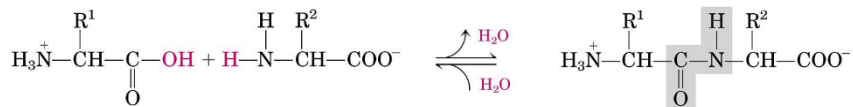


Figure 3.1-2: Formation of peptide bond from two amino acids

Three amino acids can be joined by two peptide bonds to form a tripeptide. In the same way, amino acids can be joined to form tetrapeptides, pentapeptides, etc. When a few amino acids are linked in this way, the structure is called an oligopeptide (from 6 to c.a. 20 amino acids). When many amino acids are joined, the product is called a polypeptide. Proteins have thousands of amino acid. In fact, polypeptides whose molecular weight is higher than 10.000 Da, are generally called proteins (Lehninger, Nelson et al. 2005).

### 3.1.3. Protein structure

For large macromolecules such as proteins, the task of describing and understanding structure is approached at several levels of complexity, arranged in a kind of conceptual hierarchy. For proteins, four levels of protein structure are commonly define (Aluru 2005).

### 3.1.3.1. Primary structure

The most important element of the primary structure is the sequence of amino acid residues. The differences in primary structure can be especially informative. Each protein has a distinctive number and sequence of amino acid residue. The function of a protein depends on its amino acid sequence.

### 3.1.3.2. Secondary structure

Secondary structure is referred to particularly stable arrangements of amino acid residues giving rise to recurring structural patterns. Thus, the term secondary structure refers to any chosen segment of a polypeptide chain, describing the local spatial arrangement of its main-chain atoms, without regard to its relationship to other segments.

A regular secondary structure occurs when each dihedral angle ( $\phi$  and  $\psi$ ) remains the same. The most commonly structure are  $\alpha$ -helix and  $\beta$ -conformations. Where a regular pattern is not found, the secondary structure is sometimes referred to a random coil. However, this conformation does not describe properly a structure.

### 3.1.3.3. Tertiary structure

Tertiary structure describes all aspects of the three-dimensional folding of a polypeptide. Thus, the overall three-dimensional arrangement of all atoms in a protein is referred to as the protein's tertiary structure. Amino acids that are far apart in the polypeptide sequence and are in different types of secondary structure may interact within the completely folded structure of a protein. The location of bends in the polypeptide chain and the direction and angle of these bends are determined by the number and the location of specific bend-producing conformation. Different interacting segments of polypeptide chains are held in their characteristic tertiary location, such as



several kinds of weak interactions or even by covalent bonds (e.g. disulphide bonds) between different protein segments.

### 3.1.3.4. Quaternary structure

When a protein has two or more polypeptide subunits, their arrangement in space is referred to as quaternary structure. Thus, the arrangement of proteins which contain two or more separate polypeptide chains, or subunits, in three-dimensional complexes constitutes the quaternary structure. Considering these higher levels of structure, it is very useful to classify proteins into two main groups: fibrous proteins (whose polypeptide chains are arranged in long strands or sheets) and globular proteins (whose polypeptide chains are folded into a spherical or globular shape) (Lehninger, Nelson et al. 2005).

Figure 3.1-3 illustrate the four different conformations which are adopted by a protein:

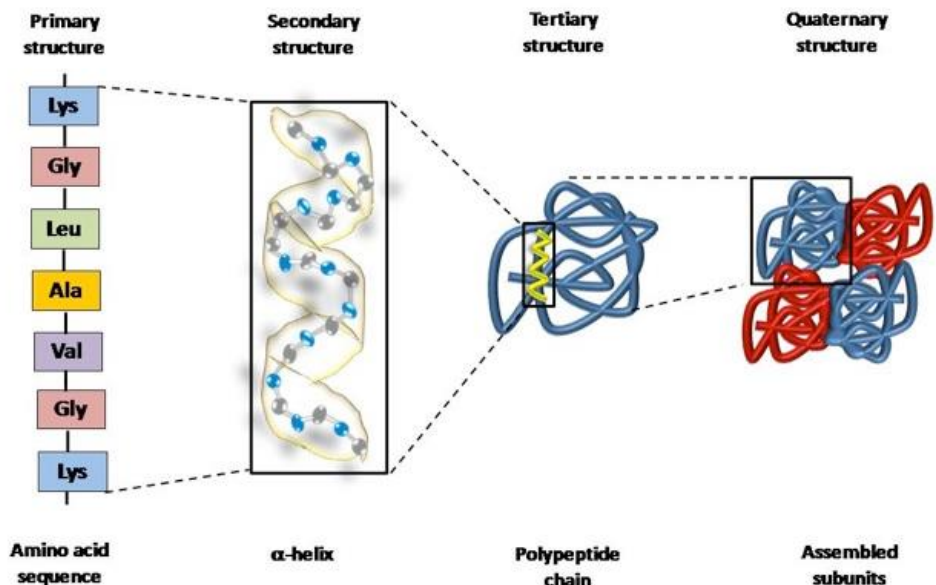


Figure 3.1-3: Conformations adopted by a protein.

### **3.1.4. Protein separation and characterisation**

To study a protein in detail, the researcher must be able to separate it from other proteins in pure form and must have the techniques to determine its properties which allow to understand its behaviour and its relationship with other macro and micro molecular systems.

Thus, in any protein purification, the first step is the proteins solubilisation into a solution, which is called a crude extract, is the separation. Several methods are available for separating one or more of the proteins from the crude extract. Usually, the extract is subjected to treatments that separate the proteins into different fractions based on a physical property such as size or charge. A separation based on protein solubility (which depends on pH, temperature and salt concentration, among other factors) is commonly used in an early fractionation step. For instance, the solubility of proteins is generally lowered at high salt concentrations. Thus, the addition of certain salts in the right amount can selectively precipitate some proteins, while others will remain in solution (Lehninger, Nelson et al. 2005).

#### **3.1.4.1. Dialysis**

A solution containing the protein of interest must usually be modified before the subsequent purification step. Dialysis is a procedure that separates proteins from small solutes because of the larger size of proteins. The partially purified extract is placed in a bag or tube made of a semipermeable membrane. When this is suspended in a much larger volume of buffered solution of appropriate ionic strength, the membrane allows the exchange of salt and buffer but not of proteins. Thus, dialysis retains large proteins within the membranes, allowing the concentration of other solutes in the protein preparation to change until they come into equilibrium with the solution outside the membrane.

### 3.1.4.2. Column chromatography

The most powerful methods for fractionating proteins make use of column chromatography technique, where a buffered solution (the mobile phase) percolates through it. The protein-containing solution, layered on the top of the column, percolates through the solid matrix. Individual proteins migrate faster or more slowly through the column depending on their physical properties.

#### 3.1.4.2.1. Ion-exchange chromatography

This technique makes use of differences in the sign and magnitude of the net electric charge of proteins at a selected pH. The column matrix is a synthetic polymer containing bound charged groups. If those groups are bound with anionic groups from protein are, the column will be called cation exchangers column, and those with bound cationic groups are called anion exchangers. The affinity of each protein for the charged groups on the column is influenced by the pH (which determines the ionization state of the molecule) and the concentration of free salt ions in the surrounding solution.

Separation can be optimized by gradually changing the pH and/or salt concentration of the mobile phase so as to create a pH or salt gradient.

#### 3.1.4.2.2. Size-exclusion chromatography

This technique is also called gel filtration because it separate proteins according to size. In this method, large proteins emerge from the column sooner than small ones. The solid phase consists of cross-linked-polymer beads with engineered pores or cavities of a particular size. Large proteins cannot enter the cavities and take a short (and rapid) path through the column, around the beads. By the contrary, small proteins enter the cavities and are slowed by the longer path through the column.

### 3.1.4.2.3. *Affinity chromatography*

This technique is based on binding affinity. The beads in the column have a covalently attached chemical group called ligand (a group or molecule that binds to a macromolecule such as a protein). When a protein mixture is added to the column, any protein with affinity for this ligand binds to the beads, and its migration through the matrix is retarded.

### 3.1.4.2.4. *High-performance liquid chromatography (HPLC)*

HPLC makes use of high-pressure pumps that speed the movement of the protein molecules down the column, as well as higher-quality chromatographic materials that can withstand the crushing force of the pressurized flow. By reducing the transit time on the column, HPLC can limit diffusional spreading of protein bands and thus greatly improve resolution (Lehninger, Nelson et al. 2005).

### 3.1.4.3. **Electrophoresis**

Electrophoresis is one of the most commonly technique for the separation of proteins based on the migration of charged proteins in an electric field.

This procedure is not generally used to purify proteins in large amounts, because usually are available simpler alternatives than electrophoretic methods, which often affect the structure and, as a consequence the function of proteins. Electrophoresis is however especially useful as an analytical method. Its advantage is that proteins can be visualized as well as separated, permitting a researcher to estimate quickly the number of different proteins in a mixture or the degree of purity of a particular protein preparation. Also, electrophoresis allows determination of crucial properties of a protein such as its isoelectric point and approximate molecular weight.

Electrophoresis of proteins is generally carried out in gels made up of the cross-linked polymer polyacrylamide (PAGE). The polyacrylamide gel acts as a molecular sieve, slowing the migration of proteins approximately in proportion to their charge-to-mass ratio. Migration may also be affected by protein shape. In electrophoresis, the force moving the macromolecule is the electrical potential,  $E$ . The electrophoretic mobility,  $\mu$ , of a molecule is the ratio of its velocity,  $V$ , to the electrical potential. Electrophoretic mobility is also equal to the net charge,  $Z$ , of the molecule divided by the frictional coefficient,  $f$ , which reflects in part the protein's shape. Thus:

$$\mu = \frac{V}{E} = \frac{Z}{f} \quad (3.1-1)$$

Thus, as can be deduced from Equation 3.1-1 (3.1-1) the migration of a protein in a gel during electrophoresis may be regarded as a function of its size and shape.

An electrophoretic method commonly employed for estimation of purity and molecular weight makes use of the surfactant sodium dodecyl sulphate (SDS), then the electrophoresis is called SDS-PAGE. SDS binds to most proteins in amounts roughly proportional to the molecular weight of the protein, about one molecule of SDS for every two amino acid residues. The bounded SDS contributes a large net negative charge, rendering the intrinsic charge of the protein insignificant and conferring on each protein a similar charge-to-mass ratio. In addition, SDS binding partially unfolds proteins, such that most SDS-bounded proteins assume a similar shape. Therefore, electrophoresis in the presence of SDS separates proteins almost exclusively on the basis of mass (molecular weight), with smaller polypeptides migrating faster. After electrophoresis, the proteins are visualized by adding a dye, such as Coomassie blue, which binds to proteins but not to the gel itself. The molecular weight of each protein fractions is obtained by comparison with standard proteins whose molecular weight is known. If the protein has two or

more different subunits, the subunits are generally separated by the SDS treatment, and a separate band appears for each one. Figure 3.1-4 illustrates the method followed to perform this technique and the gel obtained after application of the electric field (Lehninger, Nelson et al. 2005).

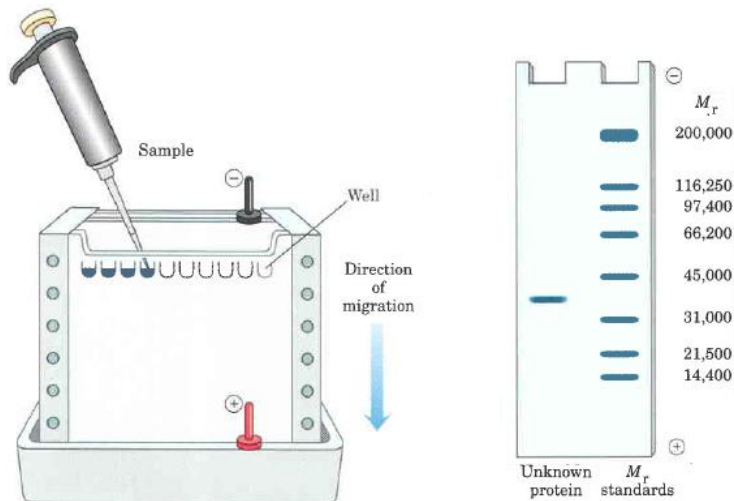


Figure 3.1-4: Sample preparation and gel obtained after performing electrophoresis method.

### 3.1.5. Protein denaturation

Techno-functional properties of proteins, which have also been termed techno-functional, emanate mainly from two molecular attributes such as hydrodynamic properties and physicochemical attributes of the protein's surface. This is particularly important in food proteins in view of the relevance of techno-functional properties in food products. While the hydrodynamic properties are related to the size and shape of the molecule, the properties of a protein's surface are linked to its topology and to the pattern of distribution of polar and non-polar patches. Both type of properties can be precisely determined from their crystallographic structure, using different techniques, provided that proteins remain in their native state. However, protein denaturation, which inevitably occurs in food processing, would alter

hydrodynamic and surface attributes making difficult to predict their functionality in a complex food milieu. The extent of denaturation of proteins in a food product depends on the susceptibility of intra-molecular interactions that hold the compact native protein structure to temperature, pressure, pH, ionic strength, types of ions, as well as specific and non-specific interactions with other food components such as sugars, polysaccharides, lipids, and other additives.

Thus, denaturation is a phenomenon where a protein change from a well-defined initial state of a protein formed under physiological conditions to an ill-defined final state by the application of a denaturing agent. However, it is worth mentioning that denaturation does not involve any chemical change in the protein (Damodaran 1997).

### **3.1.5.1. Non-covalent forces in a protein**

Folding of a protein from an elementary unfolded state to a folded native conformation is driven by several non-covalent interactions between different surrounding molecules. These interactions are mainly: van der Waals forces, steric strains, hydrogen bonding, electrostatic, and hydrophobic interactions.

The Van der Waals interactions are short range in nature and, as a consequence, involve interactions between neighbouring atoms. Steric strains indirectly limit the number of configurations accessible to various segments of polypeptides. As regards hydrogen bonds, the greatest number of hydrogen bonds in proteins occurs between the amine and carboxyl groups, although other groups may also be involved. The majority of hydrogen bonds in proteins take place in  $\alpha$ -helix and  $\beta$ -sheet structures. In fact, the stability of these secondary structures is partly attributable to these hydrogen bonds. However, because water itself can hydrogen bond with amide groups in proteins, formation of hydrogen bonds between amide groups in proteins is not thermodynamically stable in an aqueous environment. As a consequence,

they cannot act as the driving force for protein folding. Thus, their existence in  $\alpha$ -helix and  $\beta$ -sheet structures might be the result of other interactions that create a non-polar environment where the hydrogen bonding and other macro dipole-dipole interactions become stable. Based on these considerations, it is fair to say that hydrogen bonds in proteins are only pseudostable and their stability depends on maintenance of the non-polar environment (Damodaran 1997).

Electrostatic interactions in proteins at neutral pH appear mainly between the positively charged  $\epsilon$ -amino groups of lysine, arginine, and histidine residues and the side-chain carboxyl groups of glutamate and aspartate residues. The stability of electrostatic interactions is dependent on the dielectric constant of the local environment. They are stronger in a non-polar environment than in a polar environment. In aqueous solutions, because of the high dielectric effect of water on charged groups, attractive and repulsive electrostatic interactions between charged groups in proteins are very insignificant. Thus, charged groups located on the surface of the protein do not greatly influence the stability of protein structure.

Hydrophobic interactions between non-polar sidechain groups are considered to be the major driving force for protein folding in aqueous solutions. These interactions appear as a result of thermodynamically unfavourable interaction between solvent water and non-polar groups in proteins. The origin of hydrophobic interactions is due to the much greater affinity between water molecules than between water and hydrocarbon. Because of this preferential affinity water tends to minimize the surface area of direct contact with hydrocarbon chains and maximize its interaction with other water molecules, forcing the hydrocarbon chains to aggregate. As a consequence, as the non-polar residues are removed from the aqueous environment, the non-polar regions created within the molecule allow



formation of hydrogen bonds in such water-deficient regions as the interior of  $\alpha$ -helix and  $\beta$ -sheet structures.

From the above discussions, it can be summarized that the folding of a protein from a nascent unfolded state to a folded native state is driven by a thermodynamic requirement that a majority of non-polar groups has to be buried in the interior of the protein while the majority of hydrophilic and charged groups has to be located in contact with the surrounding aqueous phase. The structural stability of the folded state under a given set of solution conditions depends on two opposing forces: the sum of the energetics of hydrophobic interactions and other non-covalent interactions, attractive and repulsive electrostatic interaction, and van der Waals interactions, which favour folding of the polypeptide chain, and the conformational entropy of the polypeptide chain which opposes folding of the chain.

Thus, the net stability of a folded protein molecule can be calculated using EQ. (3.1-2):

$$\Delta G_{U \leftrightarrow N} = (\Delta G_{H-bond} + \Delta G_{elec} + \Delta G_{H\phi} + \Delta G_{vdW}) - T\Delta S \quad (3.1-2)$$

where  $\Delta G_{U \leftrightarrow N}$  represents the net stability of the protein from the unfolding to nature state,  $\Delta G_{H-bond}$ ,  $\Delta G_{elec}$ ,  $\Delta G_{H\phi}$ , and  $\Delta G_{vdW}$  are the free energy changes for hydrogen bonding and electrostatic, hydrophobic and van der Waals interactions, respectively. Finally,  $T\Delta S$  is the free energy change obtained from the decrease in configurationally entropy of the polypeptide chain as a result of folding at temperature (T). For most proteins the transformation from an unfolded state (U) to the folded state (N) is spontaneous, thus  $\Delta G_{U \leftrightarrow N}$  is negative although moderate (ranging from -20 to -80 kJ/mol)(Damodaran, Parkin et al. 2007).

### 3.1.5.2. Mechanism of denaturation

The low values typically found for  $\Delta G_{U \leftrightarrow N}$  indicate that the tertiary structure of proteins is only marginally stable. Any change in the thermodynamic environment of the protein, such as pH, ionic strength, temperature, pressure, or presence of other solutes, can readily cause a shift in the equilibrium in favour of the denatured state. Two type of alterations in protein structure are often identified. Slight changes in the tertiary structure, which do not greatly alter the topographical features of the protein, are usually denoted as conformational adaptation. This kind of change in structure usually takes place when a substrate, inhibitor, or a low-molecular weight ligand binds to a protein. More remarkable changes leading to breakdown of tertiary structure along with unfolding of secondary structures is often termed denaturation. As previously mentioned, an ill-defined final state is typically achieved after denaturation in contrast with the fairly well-defined protein structure of the native state (Damodaran 1997).

#### 3.1.5.2.1. Temperature-induced denaturation

Many unit operations in food processing and preservation involve heating and cooling. These processes invariably cause protein denaturation. Proteins may exhibit huge differences in their thermal stability, however non-enzyme proteins, especially food proteins such as whey proteins and legume proteins, are usually stable up to 70-80°C.

The mechanism of temperature-induced denaturation of proteins primarily involves the effect of temperature on the stability of non-covalent interactions. In this respect, the hydrogen bonding and electrostatic interactions, which are exothermic in nature, are destabilized, and hydrophobic interactions, which are endothermic, are stabilized as the temperature is increased. In addition to non-covalent interactions, temperature dependence of conformational entropy,  $T\Delta S_{conf}$ , also plays an

important role in the stability of proteins. The net stability of a protein at a given temperature is then the result of a balance of these interactions.

In globular proteins, the majority of charged groups are located on the surface of the protein molecule, fully exposed to the high dielectric aqueous medium. Because of the dielectric screening effect of water, attractive and repulsive electrostatic interactions between charged residues are greatly reduced. Thus, the influence of temperature on electrostatic interactions in proteins would be very low. Similarly, hydrogen bonds are unstable in an aqueous environment and therefore their stability in proteins is strongly dependent on hydrophobic interactions. This implies that so long as a non-polar environment is maintained, the hydrogen bonds in proteins would remain intact when the temperature is increased. These facts suggest that although polar interactions are affected by temperature, they generally do not play a significant role in heat-induced denaturation of proteins. Based on these considerations, the stability of the native state of a protein can be simply regarded as the net free energy difference emanating from hydrophobic interactions that tend to minimize the nonpolar surface area of the protein molecule and the positive free energy change rising from the loss of conformational entropy of the chain ( $T\Delta S$ ).

In dilute solutions under certain heating conditions, thermal denaturation of globular proteins is completely reversible. At high concentration, e.g., > 1 wt. %, protein-protein interactions between unfolded protein molecules interfere with protein refolding. Prolonged heating of protein solutions at high temperatures, e.g. 90°C, can cause irreversible denaturation of proteins regardless of the protein concentration. This is mainly due to chemical changes in proteins, such as destruction of cysteine and cysteine residues and de-amidation of asparagine and glutamine.

In addition, several proteins have been shown to undergo denaturation at cold temperatures. The cold temperature-induced denaturation of proteins is mainly due to a decrease in the stability of hydrophobic interactions at low temperatures. The fact that the hydrophobic and the conformational entropy are the two relevant forces, controlling thermodynamic stability of proteins tentatively suggests that the stability of proteins might be in some way dependent on the amino acid composition.

Finally, factors such as water content of dry protein powders or the presence of small-molecular-weight substances affect thermal protein denaturation. Thus, as the water content is increased, the denaturation temperature of proteins decreases asymptotically towards a value that is similar to the denaturation temperature of the protein in a dilute solution. This is due to the plasticizing effect of water, which promotes segmental mobility in proteins. On the other hand, small-molecular-weight solutes, such as salts and sugars, generally leads to an increase in the denaturation temperature of proteins.

### 3.1.5.2.2. *Pressure-induced denaturation*

Proteins are inherently highly flexible. This high flexibility is the underlying reason for their marginal stability under physiological conditions. The flexibility of proteins arises because of unfilled spaces or cavities in the interior of the protein. These cavities are created by imperfect packing of the residues as the protein chain collapses on itself during folding, the partial specific volume ( $\bar{v}^0$ ), of a protein consists of EQ. (3.1-3):

$$\bar{v}^0 = v_c + v_{cav} + \Delta v_{sol} \quad (3.1-3)$$

where  $v_c$  is the sum of constitutive specific volumes of atoms in the protein,  $\Delta v_{sol}$  is the specific volume of cavities in the protein, and  $\Delta v_{sol}$  is the specific volume change because of the hydration process. The first term is

constant for a given protein, while the last two terms are the main parameters affecting the specific volume of proteins.

Under very high hydrostatic pressure, the collapse of the cavities formed as a result of imperfect packing of amino acid residues causes unfolding of the protein. In the unfolded state, elimination of the cavities decreases the volume, and hydration of the exposed hydrophobic residues also leads to a reduction in the volume of the solvent. Despite, pressure-induced gels are softer in texture than heat-induced gels, and feature the capability of retaining colour, flavour, vitamins and other nutrients that are destroyed to some extent in thermally processed foods and in heat-induced gels (Damodaran 1997).

### 3.1.5.2.3. *Denaturation by small-molecular weight additives*

Several small-molecular-weight solutes, such as urea, guanidine hydrochloride, surfactants, sugars, and neutral salts, affect protein stability in aqueous solutions. While urea, guanidine hydrochloride, and small-molecular-weight surfactants destabilize the native conformation of proteins, sugars tend to stabilize the native structure. As for neutral salts, while certain salts termed as kosmotropes tend to stabilize protein structure (e.g. sulphate and fluoride salts of sodium), other salts, such as bromide, iodide, perchlorate, and thiocyanate, termed as kosmotropes, destabilize protein structure.

The stabilizing or destabilizing effects of small molecular-weight additives on proteins is believed to follow a general mechanism. This is related to their preferential interaction with the aqueous phase and the protein surface.

Additives that stabilize protein structure bind very weakly to the protein surface but enhance preferential hydration of the protein surface. Such additives are generally excluded from the region surrounding the protein and,

as a result, their concentration near the protein is lower than in the bulk solution. This concentration gradient presumably creates an osmotic pressure gradient surrounding the protein molecule, sufficient enough to elevate the thermal denaturation temperature.

In the case of additives that destabilize protein structure, the opposite seems to be true. That is, those additives that decrease the stability of proteins preferentially bind to the protein surface and cause dehydration of the protein. In such cases, water molecules are excluded from the region surrounding the protein and the concentration of the additive in this water-excluded region is higher than in the bulk solvent. Favourable interactions of such additives with protein surfaces, particularly the non-polar surfaces, promote unfolding of the protein such that the buried nonpolar surfaces are further exposed for favourable interactions with chaotrope additives.

Anionic surfactants such as sodium dodecyl sulphate (SDS), are potent denaturing agents with the skill of developing strong binding to hydrophobic groups in the crevices of protein molecules, which leads to destabilization and solubilisation of buried hydrophobic regions. Because of this high binding capacity, proteins in SDS solution become highly negatively charged. The resultant electrostatic repulsions between segments also play a role in protein unfolding as well as in preventing protein aggregation.

#### 3.1.5.2.4. *Denaturation induced by pH*

With regards to pH-induced denaturation, proteins are either negatively or positively charged at neutral pH. Native proteins, at this physiological pH, present an equilibrium structure with a global minimum free energy that has already taken into account the pre-existing repulsive and attractive electrostatic interactions. However, at pH values far away from the neutral pH, changes in the state of ionization of various charged residues in proteins alter the electrostatic free energy, resulting in conformational changes. Most

proteins are very stable at their isoelectric point (IEP), pH at which the net charge of the protein is zero and electrostatic repulsive interactions are at a minimum. However, proteins typically unfold at pH values far from the IEP, that is, below 4 and above 10.

This unfolding is not simply because of changes in the ionization state of the charged residues on the surface of the protein, but is related to ionization of residues that are partially or fully buried in the protein (Hui 2006).

### **3.1.6. Techno-functional properties of food proteins**

Functionality has been described as the set of non-nutritive roles that food constituents play in a food system. More formally, techno-functional properties are the physical and chemical properties that affect the behaviour of molecular constituents in food systems.

Proteins in foods are multifunctional and may be the principal structural component in many food systems, including products from meat and poultry, eggs, dairy, cereals, and legumes. In fact, proteins contribute significantly to the sensory attributes and overall quality of food products. In this sense, protein functionality is considered critical for the improvement or existing food products or the development of new ones. An example is the use of less expensive protein sources as replacements in traditional food products. Use of less expensive proteins not only allows for cost reduction, but also can increase the utilization of food materials that previously might have been considered waste products.

Techno-functional properties commonly associated with proteins include solubility, gelation, emulsification, foaming, and water-holding capacity (Damodaran 1997, Aluru 2005).

### 3.1.6.1. Protein solubility

The solubility of a protein, which is determined by its primary structure, is very often the key factor in delimiting its use in foods. If a protein has a polar surface due to the presence of polar amino acids, it will have good solubility in a polar solvent such as water. On the other hand, proteins with higher contents of hydrophobic amino acids, fewer charges on their surface, or those which contain many subunits tend to have limited water solubility (Damodaran, Parkin et al. 2007).

#### 3.1.6.1.1. Effect of pH

Surfaces of proteins have net charges due to their amino acid content depending on the pH of their environment. A protein shows minimal solubility when it has a net charge of zero, that is, equal numbers of positive and negative charges on its surface. This is called the isoelectric point of the protein (IEP). There is minimal solubility because intermolecular repulsion is at a minimum and proteins will tend to aggregate. At pH values above the isoelectric point of a protein, it has a net negative charge. At pH values below the isoelectric point, it will have a net positive charge. In both cases the presence of pronounced surface charges will result in intermolecular repulsion and enhanced solubility.

#### 3.1.6.1.2. Salt concentration's

Solubility is also affected by the type and concentration of salts in a food system. As salts content increases proteins become more soluble, which is the so-called "salting-in" effect, attributed to the ability of salt ions to enhance the surface charges on proteins. In foods, sodium chloride is commonly used for this purpose. At high salt concentrations, usually above 1M, which is much higher than the concentration used in foodstuffs molar, protein solubility decreases. This effect is called "salting-out" and is thought to be due to salt competing with the proteins for available water for solvation.



### 3.1.6.1.3. *Denaturation of protein*

As described in section 3.1.5, when denaturation proceeds, protein molecules change in regard to surface charges, shape, size, and hydrophobicity. Most thoroughly denatured proteins are insoluble. In any case, denaturation always results in loss of solubility, and then it is undesirable in many food systems where solubility is important. However, denaturation may cause some desirable changes in some food systems. Therefore, the degree of protein denaturation required depends on the food application, but ensuring its exhaustive control over food processing is essential.

### 3.1.6.2. **Gelation**

A protein gel is a three-dimensional cross-linked network of protein molecules imbedded in an aqueous solvent. Most gels are very high in water content (up to 95-98%), and still have characteristics of solid or rigid food materials (Damodaran, Parkin et al. 2007).

Gelation is based on the denaturation of proteins, followed by their intermolecular association to form matrices which trap water, fat, and other food ingredients. The formation of gels is influenced by heat, pH, pressure or shearing, and solvent conditions. Food gels are divided into two categories: thermally reversible and thermally irreversible gels (Damodaran 1997).

#### 3.1.6.2.1. *Thermally irreversible (thermoset) gels*

Thermally irreversible or thermoset gels form chemical bonds that will not break during reheating of the gel and thus remain rigid if it is reheated. Most thermoset gels are the result of protein unfolding, followed by aggregation of the molecules into a cross-linked network. During this process, heated proteins partially unfold and form aggregates. As the “gel-point” temperature is reached, these aggregates unfold further and rapidly cross-link to form a gel. This network is generally formed via non-covalent bonds such

as hydrophobic interactions and hydrogen bonds. Occasionally, disulphide bonds may be involved.

### 3.1.6.2.2. *High Pressure Processing (HHP) in food processing*

The effect of the high pressure on food preservation was study initially by Hopkins, Hite and Watson (1899). In 1899 some experiments were carried out in West University (Virginia), using high hydrostatic pressure to conserve juice, meat and fruit. These studies demonstrated that some microorganisms could be destroyed after 10 min at 658 MPa. At early 20<sup>th</sup> century, other research proved that egg white could be modified by high pressure. However, the research in this field did not undergo any substantial progress until significant improvements were achieved in the technology of hydraulic presses. This fact encouraged the renewed interest of researchers on HHP applications in the eighties.

When a high pressure is apply to a food dipped in a liquid, the pressure placed on the sample is the same in all points. This is one of the advantages of this procedure, avoiding the differences found in the thermal treatment. In addition, compared to the thermal treatments, pressurisation and depressurisation cycles are faster, reducing processing time.

As above mentioned, HHP can leads to the destruction of microorganisms without markedly altering the taste and flavour or the nutrient content of foods. In general, bacteria, which are in the logarithmic growth phase, are the most sensitive. Moderate pressures (300-600 MPa) involve the death of the vegetative cell. Usually a pressure of 400 MPa is apply for 5 min to reduce the population ten times (Hoover, Metrick et al. 1989). To destroy bacteria spores, a higher pressure is needed, however if the pressure is combined to a soft heating (60°C), spores are destroyed at about 400 MPa. Thus, a combination of high pressure and soft heating can suppose a synergic effect (Galazka and Ledward 1995).

The enzyme activity strongly depends on pH, composition, temperature and pressure. Some enzymes can be disabled at 100 MPa, however other needs higher pressures (even 1,000 MPa) (Cano, Hernandez et al. 1997)

In addition of microorganisms inactivation. HHP can also unfold proteins, solidify lipids, showing advantages in the preservation of sensory (colour, taste, flavour, texture, etc.) and nutritional properties (Tewari, Jayas et al. 1999). In addition, high pressure can induce conformational changes in proteins, which can involve important modifications of their techno-functional properties. As a consequence, proteins can undergo aggregation and gelation, depending on the pressure applied, as well as protein nature, composition, and environmental factors such as pH or ionic force.

Because the aggregation and gelation are directly related to protein-protein interactions, HHP processing will have a high influence on protein structure, since application of HHP may exerts a marked effect on non-covalent interactions (electrostatic, hydrophobic and hydrogen bonds). Thus, HHP treatment may lead to a breakdown of the tertiary and quaternary protein structure of globular proteins, but it has a very limited influence on secondary structure.

In general, low pressures induce reversible changes such as protein-complex dissociation, ligands, and conformational changes, whereas high pressures (> 500 MPa) generally involve irreversible protein modifications (Hereman, Van Camp et al. 1997).

### **3.1.6.3. Water binding**

Water-binding capacity is the amount of water that is bound or retained by a protein under well-defined conditions. Thus, water binding is an important techno-functional property for several reasons:

- Most foods contain high amounts of water and it is necessary to avoid chemical changes that might cause the formation of free water or drip loss.
- Increasing the amount of water a product can hold effectively can increase the profitability of a given product
- Both product yield and sensory quality are highly dependent on the proper moisture content of a finished food.

Water is usually bounded to the surface of a protein by hydrogen bonding, which is sometimes called dipole bonding. Hydrogen bonding results from water's interaction with the R group of amino acids which are dipoles. Water bound to the surface of proteins in this manner is called "monolayer" water and is very tightly associated with the protein. Other water associated with the protein or protein matrices can be trapped in capillary structures and pores. If water is not associated with the monolayer on the protein surface is called free water and moves unhindered throughout the food system.

With regards to factors which influence water binding, the most important are small polar molecules (e.g. sugars), temperature, salt content and pH. Small polar molecules and temperature will generally enhance water binding by proteins. In some cases temperature may induce formation of protein gels, which will enhance the binding of water by the system. Sodium chloride binds to charged groups on protein surfaces and weakens intermolecular bonds. This is a positive effect in systems which utilize muscle fibres as part of the structural elements of the food. Salt allows the muscle proteins to distance themselves from others within the muscle fibre and thus increase the number of sites for water to bind. The pH of a system markedly influences its ability to bind water. This is due to changes in the surface

charges on a protein as the pH is altered. Water binding is the lowest at the isoelectric point (IEP) of a protein (Damodaran 1997).

### **3.1.6.4. Emulsification**

An emulsion is a mixture of two immiscible liquids in which one is dispersed in the other in the form of droplets. The liquid in the droplets the dispersed is called internal, or discontinuous phase. In the same way, the surrounding phase is called the external or continuous phase. Emulsions in which the dispersed phase is a lipid are called “oil in water” emulsions (O/W). By the contrary, water in oil emulsions contain droplets of water dispersed in a lipid as continuous phase (W/O) (McClements 2004).

When a liquid is exposed to other phase (e.g. air), the surface between them is in a state of tension. This state of tension is called interfacial tension (or surface tension, in the case of air) and it is a consequence of the attractive forces between molecules in the liquid that are enhanced by exposure to the other phase. The molecules “bunch” together to decrease their exposition to the air surface. The region of contact between two immiscible liquids is called the interface. The interfacial area plays an important role in emulsion formation. Thus, a considerable amount of mechanical energy is required in order to reduce droplet size and to increase interfacial area (Walstra 1993). However, as the interfacial area increases, the stability of the mixture decreases. Unfortunately, most emulsions are thermodynamically unstable and droplets tend to aggregate spontaneously in order to reduce the interfacial area. Therefore, emulsion stability, which is considered to be the primary requirement for the commercial application of emulsions, is in fact a kinetic concept such that an emulsion is considered stable when the number, size distribution, and arrangement of droplets do not undergo any discernible change over the storage time scale.

In order to stabilize emulsions it is necessary to add molecules which decrease the interfacial tension between mixtures of lipids and water. Surfactants are molecules that contain both hydrophobic (non-polar) and hydrophilic (polar) regions in their structure. When added to a system that contains both lipids and water, surfactants rapidly migrate to the interfaces between the two phases. At the interface, the surfactants orient their polar region towards the aqueous phase and their non-polar region towards the lipid phase. Since proteins contain amino acid residues that can be polar and non-polar they can be excellent surfactants in food systems.

Figure 3.1-5 illustrates the coating of oil droplets with proteins. Once the droplet or air bubble is coated, the interfacial tension between the two phases is markedly lowered and the tendency to coalesce is greatly reduced. If a sufficient reduction in interfacial tension is achieved, the emulsion may be stable for long periods of time.

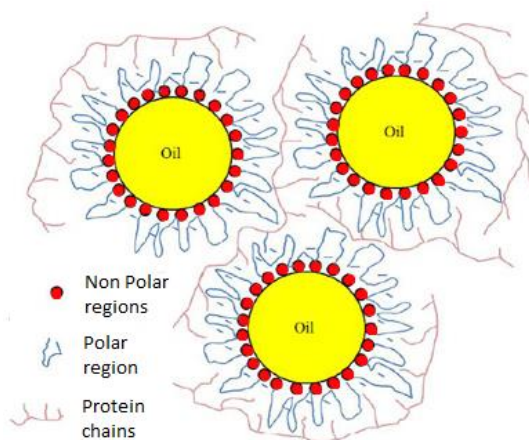


Figure 3.1-5: Coating of oil droplets with proteins.

### 3.1.6.5. Foaming

Foams are dispersed systems, containing two distinct phases, where the continuous phase (liquid or solid) surrounds a dispersed gas. Many times a protein which emulsifies well will also foam well. The first step in the

formation of foams is the migration of proteins to the interface between air bubbles and the aqueous phase. At the interface the protein will unfold and orient their nonpolar regions toward the air phase. As proteins adsorb on the bubble surface, they begin to form layers of partially denatured proteins which encapsulate the air bubble and prevent the foam from collapsing (Damodaran, Parkin et al. 2007).

### **3.1.6.6. Enzymatic modification of protein to improve techno-functional properties**

Enzymatic modification of proteins includes partial hydrolysis, covalent attachment of functional groups, and the incorporation of cross-links between protein molecules.

Protein hydrolysis is the most widely used of these techniques. Proteolysis is easy to control, very rapid, and takes place under ambient conditions. There is very low risk for the formation of toxic residues. Thus, proteolysis is considered by many to be the most cost-effective way to enhance protein functionality. Proteolysis produces peptides that are smaller in size and which contain less secondary structure than the original proteins, their solubility is increased. Enhanced solubility is directly related to the degree of hydrolysis and related to increases in functional properties such as foaming and emulsification.

Depending on the source of protein, optimal peptide size for one functionality, such as foaming, does not always equate to optimal functionality for another, such as emulsification. Proteolysis is quite interesting in that it is possible to fine tune the process to obtain protein ingredients that are optimized for a given functionality.

Finally, enhanced functionality due to cross-linking or covalent attachment of a hydrophilic or hydrophobic residue is also a field arising considerable interest where intense research is required (Hui 2006).

### **3.1.7. Crayfish proteins**

#### **3.1.7.1. Crustacean shell fish**

Crustacean shell fish are characterised by a heavily segmented body and a chitin exoskeleton which provides an outer protective shell that is articulated like body armour. All edible crustaceans are aquatic, with most occupying marine and estuarine habitats, but some crayfish s are found in freshwater.

The general body plan is similar among the decapod crustaceans with two sections making up the body: the fused head and thorax (cephalothorax) and the tail (abdomen). Each section is made up of a series of segments, but the number of segments and specialisation of segments varies among species. Lobsters and crabs have a dorso-ventrally flattened body, with a heavier and stronger exoskeleton, and the strong claws, which is a commercially valuable part of the animal, have a lot of musculature. The abdomen in crabs is reduced and folded under the cephalothorax, provided with large and strong legs that are used as the primary mode of locomotion (Hui 2006). In contrast, crayfish or craw-fish are similar to small lobsters, having a well-developed tail (abdomen). It is the meat in the tail which is prized in crayfish.

#### **3.1.7.2. Muscle proteins**

Proteins are the most important functional components in muscle, conferring many of the desirable physicochemical and sensory attributes of muscle foods.

Muscle proteins are the responsible of 15-22 wt. % of the total muscle weight (about 60-88 wt. % of total mass) and can be divided into three major



groups on the basis of solubility characteristics: sarcoplasmic proteins (water-soluble), myofibrillar proteins (salt-soluble), and stromal proteins (insoluble).

Techno-functional properties of muscle proteins do not carry a simple relationship to their native structures. This is because in meat processing, muscle proteins will undergo a series of structural changes, producing many intermediates when protein denaturation occurs. Structures of partially denatured protein molecules in the transitional stage are subject to specific meat-processing conditions, can vary to a large extent, and are difficult to characterize (Hui 2006).

### 3.1.7.2.1. *Sarcoplasmic Proteins*

This group is composed by proteins which are located inside the sarcolemma and are soluble in low salt concentrations (<0.1 M KCl). Sarcoplasmic proteins comprise about 30-35% of the total muscle proteins or about 5% of the weight of muscle in mature animals. The amount of sarcoplasmic proteins in early embryonic stages may be as high as 70%, but it gradually declines in proportion to the increase in the content of myofibrillar proteins as the animal matures.

Sarcoplasmic proteins may be separated by centrifugation into four different structural components based on their sedimentation velocity: nuclear, mitochondrial, microsomal, and cytoplasmic fractions. Despite their diversity, sarcoplasmic proteins share many common physicochemical properties. For instance, most are of relatively low molecular weight, high isoelectric pH, and have globular or rod-shaped structures. These structural characteristics may be partially responsible for the high solubility of these proteins in water or dilute salt solutions.

Myoglobin is perhaps the single most important sarcoplasmic protein in meat because it is primarily responsible for meat colour and, meat quality. The

distribution of myoglobin in meat animals varies extensively, because it depends on is dependent upon animal species, muscle fibre type, degree of exercise, age, sex, and diet. However, all of them have a molecular weight of around 16,800 kDa. This protein consists of two essential parts: a heme-group and a protein moiety called globin. The heme-complex is attached to globin by chelation of histidine (Xiong 2004, Hui 2006)

### 3.1.7.2.2. *Myofibrillar Proteins*

Myofibrillar proteins comprise around 55-60 wt. % of total protein in muscle, being the structural proteins that make up the myofibrils. Myofibrillar proteins can be divided into three subgroups:

- a) The major contractile proteins, including myosin and actin, which are responsible for muscle contraction and are the backbone of the myofibril. Particularly myosin, have been extensively studied. At the fibril level, the architecture of the myofibril is a determinant of myofibril swelling, hydration, and protein extraction. At the individual protein level, however, the conformation, shape, and size of the protein molecules have remarkable effects on their functionalities.
- b) Regulatory proteins, including tropomyosin, the troponin complex, and several other minor proteins, which are involved in the initiation and control of contraction.
- c) Cytoskeletal or scaffold proteins, including titin or connection, nebulin, desmin, which, provide structural support and may function in keeping the myofibril in alignment.

In food processing myofibrillar proteins play a major structural and techno-functional role. Thus, they are responsible for the formation of thermally induced cohesive structures and the firm texture of meat products. The techno-functional behaviour of myofibrillar proteins is manifested by their

ability to bind water, to produce three-dimensional, viscoelastic gel matrices via protein-protein interactions, as well as to form cohesive and strong membranes on the surface of fat globules, in emulsion systems, or flexible films around the air/water interface. As a result, myofibrillar proteins can lead to the formation of certain structural components (e.g., gels and emulsions) (Xiong 2004).

### 3.1.7.2.3. *Stromal Proteins*

The interstitial space of muscle cells contains three extracellular proteins: collagen, reticulin and elastin. Collectively, these proteins are called stromal proteins or connective tissue proteins since they make up tissues connecting the muscle cells. The extracellular proteins around the muscle fibres consist mainly of fine reticular and collagenous fibrils, which constitute the endomysium layer, as well as perimysium, which surround fibre bundles, and epimysium, which encases the whole muscle. Elastin is mainly associated with blood vessels, capillaries, and nerve systems. Therefore, only small amounts of elastin are generally found in meat. Other minor proteins belonging to the stromal protein group are also those insoluble proteins that are constituents of membranes in many intracellular organelles. However, compared to connective tissue proteins, the contribution of membrane proteins to meat quality seems to be negligible (Xiong 2004).

### 3.1.7.3. **Techno-functional properties of muscle proteins**

In meat processing, protein functionality is usually described in terms of hydration, surface properties, binding, and rheological behaviour. Thus, the ability to bind water, to solubilize or disperse in solution, and to form gels and emulsions are some of the most important techno-functional properties of muscle proteins in meat processing.

### 3.1.7.3.1. *Water Retention*

The ability of meat and meat products to retain moisture before, during, and after processing or cooking plays a crucial role in consumer acceptance of the product and is usually described in terms of water-holding capacity. Physico-chemically, the water in meat is present in either the bound or the free state. The bound water is tightly associated with proteins through charged groups and dipolar sites on the protein surface.

### 3.1.7.3.2. *Solubility*

Solubility of proteins is quite important for the manufacture of processed muscle foods. This is because most techno-functional properties of muscle proteins are related to protein solubility, and, in fact, some are achieved only when the proteins are in a highly soluble state. This is because most functional properties of muscle proteins are related to protein solubility, and, in fact, some are achieved only when the proteins are in a highly soluble state.

Solubility of muscle proteins is a function of protein structures, the structure of myofibrils, pH, concentration (ionic strength) of salt added to meat, temperature, time of mixing meat with salt... Sarcoplasmic proteins are naturally soluble in muscle. However, solubilisation of myofibrillar proteins generally requires relatively high ionic strength ( $I > 0.4 \text{ M}$ ). Thus, protein solubility is highly dependent on the ionic strength of the extraction buffer. Extraction of myofibrillar proteins begin at an ionic strength close to  $0.5 \text{ M}$ , and it reaches a maximum at ionic strength  $1.0 \text{ M}$ . Thus, an increase in salt (NaCl) concentration to above  $0.5 \text{ M}$  (approximately 2% salt in meat), is widely used in processed meats (Xiong 2004).

### 3.1.7.3.3. *Viscosity of protein solutions*

Rheological properties, as related to flow and deformation, are important functional attributes of muscle proteins. The rheological behaviour of a

protein suspension in muscle foods is often described in terms of viscosity. This is because the rheological properties of the aqueous protein phase can influence texture and stability.

Proteins are charged polymers capable of binding water and causing fibre swelling by the uptake of water and loosening of the polypeptide matrix. As a consequence of swelling process, a protein increases its effective hydrodynamic volume, and, therefore, increases the resistance to shear.

Finally, the myosin structure (the large length-to-diameter ratio of the rod portion), makes myosin highly viscous in salt solution. Because of its great viscosity and abundance in muscle, myosin is the major contributor to the rheological properties of the aqueous extract in salted meat (Xiong 2004).

#### **3.1.7.3.4. *Gelation***

Gelation of proteins is a thermodynamic process that occurs widely in food processing using muscle proteins. A gel has been referred to as a continuous network of macroscopic dimensions immersed in a liquid medium and exhibiting non steady state flow. The importance of protein gelation to muscle foods has been demonstrated. Thus, myofibrillar proteins at the junction of meat particles were responsible for the meat binding and texture of cooked sausage products (Xiong 2004).

#### **3.1.7.3.5. *Emulsification***

Emulsions from muscle proteins are stabilized through two mechanisms. The first mechanism is physical entrapment of fat globules within the protein matrix formed largely via protein-protein interactions. In the second mechanism, fat globules are stabilized by an interfacial protein film (membrane) that surrounds them. The interfacial film is interactive in the sense that it interacts with the viscoelastic continuous phase to further enhance the emulsion stability.

In meat emulsions, salt-soluble proteins play the most critical role in forming interfacial films that encapsulate fat particles or oil droplets. The emulsifying capacity of different muscle proteins was found to follow the order of myosin > actomyosin > sarcoplasmic proteins > actin (Xiong 2004).

### *3.1.7.3.6. Foaming*

Foaming of protein solutions is fairly common. Difficulties arise when the foam volume expands to the capacity of the container and proteins become denatured as a result of foam formation. The behaviour of proteins at the air/liquid interface is extremely important because the formation of a protein-based flexible, cohesive film around air bubbles is essential for foaming capacity and foam stability. In fact, there is a relationship between the molecular flexibility of proteins, film properties, and foam stability. Flexible, disordered proteins are more surface-active than extensively cross-linked, stable, and compact globular proteins (Xiong 2004).

## 3.2. Rheology

### 3.2.1. Definition

The term "rheology" is originated from the Greek: "rheos" meaning "the river", "flowing", "streaming". Thus, rheology is literally "the science of flow". More specifically, rheology is the science of flow and deformation of matter and describes the interrelation between force, deformation and time. Therefore, it is a branch of physics since these variables come from the field of mechanics. However, rheological experiments do not merely show information about the flow behaviour of liquids, but also about the deformation behaviour of solids (Mezger 2014).

### 3.2.2. Flow laws

Isaac Newton was the first to express the basic law of viscosity describing the flow behaviour of an ideal liquid. Thus, Newton postulated that an ideal (Newtonian) fluid is a fluid in which the viscous stresses arising from its flow, at every point, are linearly proportional to the local strain rate. The constant of proportionality in Newton's Law is the viscosity of the fluid. EQ. (3.2-1) illustrates this behaviour:

$$\tau = \eta \cdot \dot{\gamma} \quad (3.2-1)$$

where  $\tau$  represents the stress,  $\eta$  the viscosity and  $\dot{\gamma}$  the strain rate

Usually, a simple shear experiment, in which a fluid is confined between two plates (Figure 3.2-1) is used to define some fundamental rheological parameters (Two Plates Model). The upper plate with the (shear) area  $A$  is set in motion by the (shear) force  $F$  and the resulting velocity  $v_{max}$  is measured. The lower plate is stationary ( $v = 0$ ). The gap size ( $y_1$  or  $y_2$ ) is the distance between the plates, and the liquid sample is sheared within this gap. It is assumed that the following shear conditions are met:

- 1) The sample adheres to both plates and does not slide or slip along them.
- 2) There are laminar flow conditions.

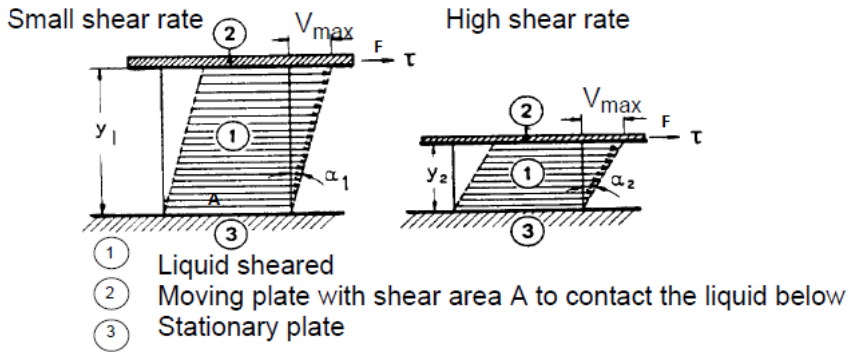


Figure 3.2-1: Two-pate model representation

### 3.2.3. Shear stress

A force applied tangentially to an area being the interface between the upper plate and the liquid underneath, leads to a flow in the liquid layer. Shear stress ( $\tau$ ) precisely arises from the application of this tangential force ( $F$ ) to the shear surface area ( $A$ ), as the ratio between both variables:

$$\tau = \frac{F}{A} \quad (3.2-2)$$

### 3.2.4. Shear rate

The shear stress ( $\tau$ ) causes the liquid to flow in a special pattern. A maximum flow speed is found at the upper boundary. The speed drops across the gap size ( $y$ ) down to 0 ( $v_{min} = 0$ ) at the lower boundary contacting the stationary plate. Laminar flow means that infinitesimally thin liquid layers slide on top of each other, similar to the cards in a deck of cards. Thus, one laminar layer is then displaced with respect to the adjacent ones by a fraction of the total displacement encountered in the liquid between both plates. The speed



drop across the gap size is named “shear rate” ( $\dot{\gamma}$ ) and it may be mathematically defined by a differential function of the fluid velocity ( $v$ ), as follows:

$$\dot{\gamma} = \frac{dv}{dy} \quad (3.2-3)$$

In addition, the shear rate may be defined as the time-derivative of the strain caused by the shear stress acting on the liquid layer:

$$\dot{\gamma} = \frac{d\gamma}{dt} \quad (3.2-4)$$

Therefore, EQ. (3.2-3) and EQ. (3.2-5) may be combined to give a more general expression of Newton:

$$\tau = \eta \cdot \frac{dv}{dy} = \eta \cdot \dot{\gamma} \quad (3.2-5)$$

### 3.2.5. Dynamic viscosity

From EQ. (3.2-1), the dynamic viscosity can be readily written as follows:

$$\eta = \frac{\tau}{\dot{\gamma}} \quad (3.2-6)$$

For ideal-viscous fluids measured at a constant temperature, the value of the ratio of the shear stress ( $\tau$ ) to the corresponding shear rate  $\dot{\gamma}$  is a material constant ( $\eta$ ) (Newtonian fluids).

### 3.2.6. Non-Newtonian liquids. Non-ideal liquids

There are several kind of fluids which do not exhibit the ideal Newtonian behaviour where  $\eta$  is not constant. Various types of common flow behaviour can be observed in Figure 3.2-2.

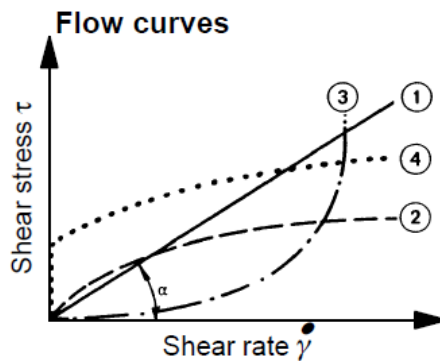


Figure 3.2-2: Behaviour of different fluids: Newtonian (1), Pseudoplastic or Shear-thinning (2), Dilatant or Shear thickening (3) and Pseudoplastic or Shear-thinning fluid with a yield point (4).

### 3.2.6.1. Pseudoplastic fluids

Many liquids show drastic viscosity decreases when the shear rate is increased from low to high levels. This means that for a given force more mass can be made to flow or the energy can be reduced to sustain a given flow rate (phenomena desirable in industrial processes).

This behaviour is related to their internal structure. Many liquid products that seem homogeneous are in fact composed of several ingredients that may possess irregular shapes or may interact with each other. Other liquids may consist of polymer solutions with long entangled and looping molecular chains. At rest, all of these materials will maintain an irregular internal order and correspondingly they are characterized by a sizable internal resistance against flow (and as a consequence high viscosity). With increasing shear rates, matchstick-like particles suspended in the liquid will be turned lengthwise in the direction of the flow. Chain-type molecules in a melt or in a solution can disentangle, stretch and orient themselves parallel to the driving force. Particle or molecular alignments allow particles and molecules to slip past each other more easily. Spherical particles may be deformed to oval-shaped particles (smaller in diameter but longer). Moreover, there are several

other possible explanations for this behaviour, e. g. solvent layers may be stripped from dissolved molecules or from particles, which means, that the intermolecular interactions causing resistance to flow become reduced. Finally, for most liquid materials the shear-thinning effect is reversible (Mezger 2014) .

### 3.2.6.2. Dilatant fluids

Fluids are liquids which under certain conditions of stress or shear rate increase their viscosity whenever shear rate increases. Thus, the resistance to flow increase and may become so high that make impossible to pump out the fluid.

Dilatant flow behaviour is relatively common in highly concentrated suspensions. The particles are densely packed and the amount of liquid is just sufficient to fill the space between the particles. At rest or at low flowrate the liquid medium fully lubricates the particle surfaces and thus allows an easy positional change of particles when forces are applied (this suspension behaves as a liquid at low shear rates). At higher shear rates, particles will wedge others, causing general volume increases. Since the liquid is no longer sufficient to fill all voids and to keep the particle surfaces fully lubricated, the solution becomes more viscous. However, dilatant fluids are rare and this flow behaviour most likely complicates production conditions (Schramm 2000).

### 3.2.6.3. Yield point

A sample with a yield point begins to flow only if the external forces  $F_{\text{ext}}$  acting on the material are larger than the internal structural forces  $F_{\text{int}}$ . Below the yield point the material shows elastic behaviour, exhibiting under load only a very small degree of deformation that does not remain after removing the load. Thus, When  $F_{\text{ext}} < F_{\text{int}}$  the material is only deformed to a small degree. The sample does not begin to flow before  $F_{\text{ext}} > F_{\text{int}}$ . Finally, the yield point is

also referred to as yield stress or yield value (Schramm 2000). There is a wide range of materials which appear to show this kind of behaviour, however Barnes (2000) stated that there is as much happening in terms of flow below as above the 'yield stress'. Thus, Barnes showed a number of examples of such liquids, where the viscosity falls many orders of magnitude over a narrow range of shear stress, and indeed when approaching this critical stress region from regions of high stress it appears that the viscosity goes to infinity. However, careful and patient measurement below this stress shows that the viscosity is still finite, and eventually levels off to a constant, but very high value at low stresses. Fluids exhibiting such behaviour were named "very shear-thinning" or "yield stress" fluids and the critical stress was denoted as "apparent yield stress" (Barnes 2000).

#### **3.2.6.4. Thixotropic fluids**

Thixotropy is the change of viscosity with time of shearing, and is generally viewed as a troublesome property that one could well do without. In fact, thixotropy could be better seen as the result of a high degree of shear thinning, and comes about whenever a shear-induced change in microstructure takes time to occur.

Microstructure is brought to a new equilibrium by competition between, on the one hand the processes of tearing apart by stress during shearing, and on the other hand build-up due to flow and Brownian motion induced collision, over a time that can be minutes. Then, when the flow ceases, the Brownian motion (the only force left) is able to slowly move the elements of the microstructure around to more favourable positions and thus rebuild the structure: this can take many hours to complete. The whole process is completely reversible.

Thixotropy is a function of time and shear rate, and therefore cannot be properly accounted for in experiments where both these variables are changed simultaneously. As a consequence, the best experiments to properly measure thixotropy are those where the sample to be tested is sheared at a given shear rate until equilibrium is obtained (Barnes 2000).

### 3.2.7. Elastic Behaviour

Nowadays instruments allow to characterize elastic behaviour in a range of very low deformations, and therefore without any destruction of the structure of materials to be tested.

In order to define further rheological parameters, Two Plates Model will be used. This model is plotted in Figure 3.2-3, where shear strain is defined as follows:

$$\gamma = \frac{s}{h} \quad (3.2-7)$$

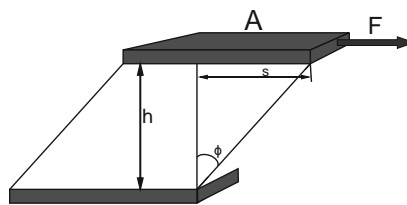


Figure 3.2-3: Shear deformation of a material using the Two Plates Model.

#### 3.2.7.1. Shear modulus

When measuring an ideal-elastic solid at a constant temperature, the ratio of the shear stress and the corresponding deformation is constant if the measurement takes place within the reversible elastic deformation range

(called linear viscoelastic range). This value is referred to as the shear modulus and reveals information about the rigidity of a material. EQ. (3.2-8) defines the shear modulus (G):

$$G = \frac{\tau}{\gamma} \quad (3.2-8)$$

where  $\tau$  is the shear stress and  $\gamma$  is the shear strain.

However, this behaviour is not followed by real fluids, many of which may exhibit viscoelastic behaviour.

### 3.2.8. Viscoelastic fluids

Viscoelastic materials show viscous and elastic behaviour simultaneously. The viscous portion of the viscoelastic response behaves according to Newton's law, while the elastic portion behaves according to Hooke's law. The simplest models that may be used to describe the linear viscoelastic behaviour of viscoelastic materials are the Maxwell and The Kelvin-Voigt models.

#### 3.2.8.1. The Maxwell model

The behaviour of a viscoelastic liquid can be illustrated using the combination of a spring and a dashpot in serial connection (Figure 3.2-4). Both components can be deflected independently of each other. The spring model according to Hooke and the dashpot model according to Newton (Mezger 2014).

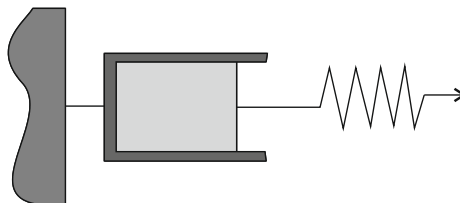


Figure 3.2-4: Kelvin Model. Serial connection of dashpot and spring

Some stages can be observed in this model:

- 1) Before the load phase: Both components of the model are not deformed.
- 2) As soon as a force is applied, only the spring shows an immediate deformation until it reaches a constant deflection value which is proportional to the constant value of the acting force. Therefore, immediately after the beginning of the load phase it is only the spring which is deformed.
- 3) Then, under the still acting constant force also the piston of the dashpot is beginning to move and it is moving on as long as the force is applied. After a certain period of time under load, both components show a certain extent of deformation which corresponds to the degree of the force.
- 4) Finally, when the load is removed, the spring recoils elastically, it moves back immediately and completely. The distance travelled by the dashpot however, remains unchanged.

Figure 3.2-5 shows the deformation behaviour of a viscoelastic liquid whose behaviour is in accordance to Maxwell model.

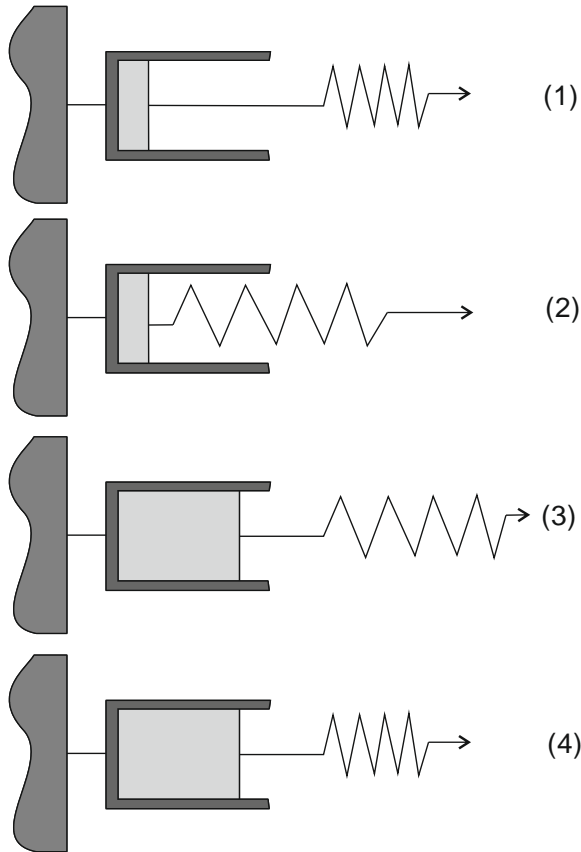


Figure 3.2-5: Deformation behaviour of a viscoelastic liquid according to the Maxwell model

In this model, there are two assumptions. The first one is that the total deformation is the sum of the single deformations applied to the two model components, thus the total deformation is defined according to EQ. (3.2-9).

$$\gamma = \gamma_{viscous} + \gamma_{elastic} \quad (3.2-9)$$

The second one is related to the shear stress and said that the same shear stress is acting on both components, it is shown in EQ (3.2-10).

$$\tau = \tau_{viscous} = \tau_{elastic} \quad (3.2-10)$$

In terms of ideality, Newton's law applies to the viscous element Hooke's law applies to the elastic element:



$$\eta = \frac{\tau_{viscous}}{\dot{\gamma}_{viscous}} \quad (3.2-11)$$

$$G = \frac{\tau_{elastic}}{\gamma_{elastic}} \quad (3.2-12)$$

### 3.2.8.2. The Kelvin-Voigt model

The behaviour of a viscoelastic solid can be illustrated using the combination of a spring and a dashpot in parallel connection (instead of serial connection). Both components are connected by a rigid frame. Figure 3.2-6 represents this model:

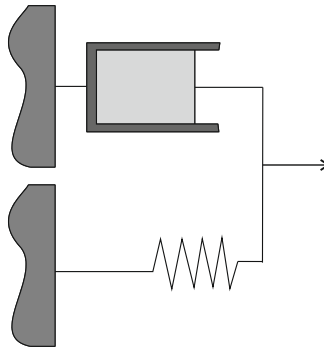


Figure 3.2-6: The Kelvin-Voigt model. A spring and a dashpot in parallel connection

Some stages can be observed in this model:

- 1) Before the load phase: Both components of the model are non-deformed.
- 2) During the load phase: Deformation is increasing steadily as long as the constant force is applied. The two components can only be deformed together (both simultaneously and to the same extent), because they are connected by the rigid frame.

- 3) When the load is removed: The spring immediately aims to jump back to its initial shape and this driving force is causing both components to reach their initial position, which is not reached.

Figure 3.2-7 shows the deformation behaviour of a viscoelastic liquid whose behaviour is in accordance to Kelvin-Voigt model.

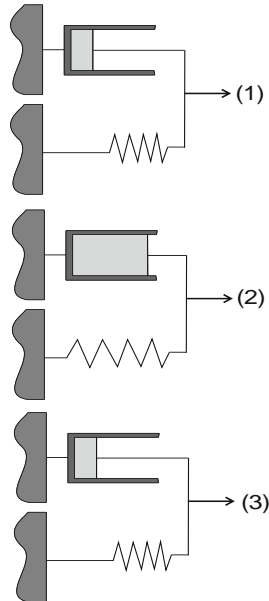


Figure 3.2-7: Deformation behaviour of a viscoelastic liquid according to Kelvin-Voigt model

This model also has some considerations:

After a load cycle, the sample shows delayed but complete re-formation. This is a reversible deformation process since the form of the sample is the same at the end of the test. Therefore, the material behaves essentially like a solid and is referred to as a viscoelastic solid or Kelvin-Voigt solid.

In this case, as reflects EQ. (3.2-13), the total shear stress applied will be distributed on both components:

$$\tau = \tau_{viscous} + \tau_{elastic} \quad (3.2-13)$$

However, both components undergo the same deformation:

$$\gamma = \gamma_{viscous} = \gamma_{elastic} \quad (3.2-14)$$

As previously mentioned, Newton's law applies to the viscous element and Hooke's law applies to the elastic element (Mezger 2014).

### 3.2.9. Viscoelastic tests

There are several ways of measuring linear viscoelastic response. However, creep and oscillatory tests are the most frequently used.

#### 3.2.9.1. Creep tests

Creep properties are very important in studying certain practical situations where high stresses and long times are involved (suspension bridges or pressurised nuclear reactor vessels). This kind of stress-controlled test was later used for softer materials.

Figure 3.2-8 shows the typical behaviour of a fluid in a creep test.

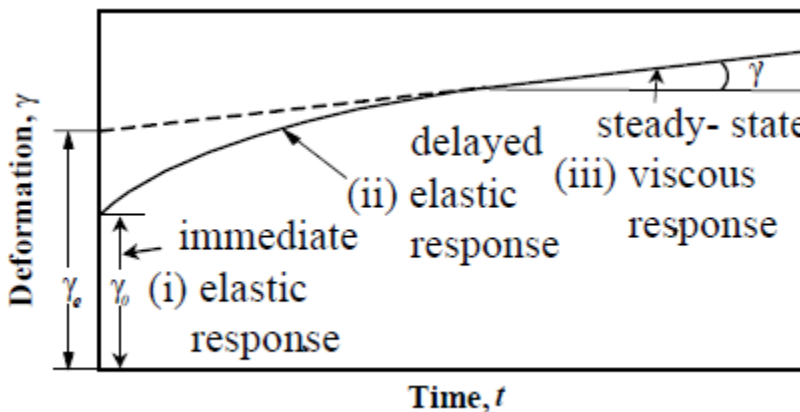


Figure 3.2-8: Creep test example

Initially, there is an initial elastic response. Thereafter there is a so-called delayed elastic response where the deformation rate becomes slower and slower, ending up as a very slow but steady-state deformation at the longest times. This curve describes the creep response of most structured liquids and gels.

### 3.2.9.1.1. *Models for creep test*

In general, in a creep test, a simple elastic solid (a spring) shows an immediate response to give a constant deformation (strain). On the other hand, a simple Newtonian liquid (a dashpot) would show an ever-increasing strain, which displayed on a graph of strain against time would be a straight line starting at the origin, with the slope giving the shear rate  $\dot{\gamma}$ .

#### *Maxwell Model*

Thus, according to Maxwell model, the behaviour can be described by the EQ. (3.2-15).

$$\gamma = \tau \left( \frac{1}{G} + \frac{t}{\eta} \right) \quad (3.2-15)$$

where, as defined previously, the strain is given by  $\gamma$ , the modulus by  $G$ , the time by  $t$  and the viscosity by  $\eta$ .

Thus, at very short times, is characterised by an immediate elastic response, ( $\gamma = \tau/G$ ) and at very long times, when  $t \gg \eta/G$ , by simple viscous behaviour,  $\gamma = \sigma t/\eta$ . Here  $\eta/G$  is called the relaxation time  $\lambda$ .

#### *Kelvin-Voigt model*

If a creep test is performed on a Kelvin-Voigt model, the strain gradually builds up to a constant value as described by EQ. (3.2-16), which is the solution of the model for the creep test.

$$\gamma = \frac{\tau}{G} [1 - e^{-t/\lambda'}] \quad (3.2-16)$$

Here,  $\lambda'$  is called the retardation time, since it characterises the retarded response of the model, and its value is again given by  $\eta/G$ . At very short times, the response is viscous, and  $\gamma \sim t \cdot \tau/\eta$ .

### 3.2.9.1.2. Models for relaxation tests

Relaxation tests consist on the application of a constant strain, and the monitoring of the consequent stress, which then decays away with time.

#### *Maxwell Model*

Thus, according to Maxwell model, the strain and the shear rate is as follows:

$$\gamma = \gamma_{el} + \gamma_{vis} \quad (3.2-17)$$

$$\dot{\gamma} = \dot{\gamma}_{el} + \dot{\gamma}_{vis} \quad (3.2-18)$$

After multiplying both equation sides by  $\mu$ , we can obtain:

$$\mu\dot{\gamma} = \mu\dot{\gamma}_{el} + \tau \quad (3.2-19)$$

Taking into account that  $\dot{\gamma}_{el} = G^{-1} \cdot d\tau/dt$ , EQ. (3.2-19) can be expressed as follows:

$$\tau = \dot{\gamma} - \lambda \frac{d\tau}{dt} \quad (3.2-20)$$

#### *Kelvin-Voigt Model*

Thus, according to Kelvin-Voigt model, the stress applied is as follows:

$$\tau = \tau_{el} + \tau_{vis} \quad (3.2-21)$$

Introducing EQ. (3.2-11) and EQ. (3.2-12) in EQ (3.2-21), we can obtain the following expression:

$$\tau = G \cdot \gamma + \mu \dot{\gamma} \tag{3.2-22}$$

After dividing both equation sides by G, we can obtain:

$$\frac{\tau}{G} = \gamma + \lambda' \frac{d\gamma}{dt} \tag{3.2-23}$$

### 3.2.9.2. Oscillatory tests

Oscillatory tests are used to examine all kinds of viscoelastic materials, from low-viscosity liquids to polymer solutions, and even rigid solids. This mode of testing is also referred to as "dynamic mechanical analysis" (DMA).

To explain oscillatory tests, the Two Plates Model is used again. The bottom plate is stationary. When the wheel or disk is turning, the upper plate with the (shear) area is moved back and forth by the (shear) force. Figure 3.2-9 represents this movement:

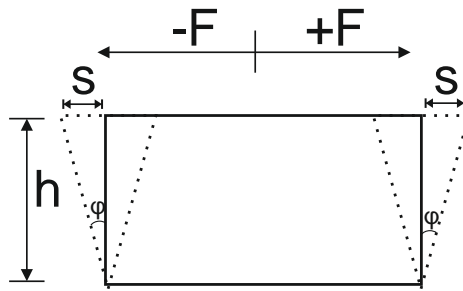


Figure 3.2-9: Oscillatory tests for a fluid between two parallel plates

where  $F$  is the shear force,  $S$  the deflection path,  $\phi$  the deflection angle and  $h$  the shear gap.

Thus, instead of applying a constant stress leading to a steady-state flow, samples are subjected to oscillating stresses or oscillating strains. The stress may be applied as a sinusoidal time function (EQ. 3.2-24):

$$\tau = \tau_0 \cdot \sin(\omega t) \quad (3.2-24)$$

where  $\tau$  is the stress applied, which is a sinusoidal function of the maximum stress applied ( $\tau_0$ ), as well as, the frequency ( $\omega$ ) and time ( $t$ ).

### 3.2.9.2.1. Theoretical aspects of dynamic testing

#### *The Hookean Spring in oscillatory movement*

Figure 3.2-10 represents the movement of a wheel connected to the spring model.

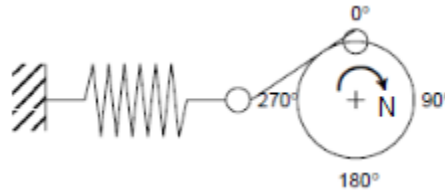


Figure 3.2-10: Spring subjected to an oscillatory movement

The spring extends to a maximum strain ( $\gamma_0$ ) and contracts to its original length with a frequency equal to the angular velocity of the wheel ( $\omega$ ) and then the strain and the stress can be written as a function of time as follows:

$$\gamma = \gamma_0 \cdot \sin(\omega t) \quad (3.2-25)$$

Thus, the stress function is defined by EQ. (3.2-26):

$$\tau = G\gamma_0 \cdot \sin(\omega t) \quad (3.2-26)$$

For this case strain and stress are in-phase with each other. That is, upon deformation, the maximum stress and the maximum strain occur at the same instant in time.

#### *The newtonian dashpot model in oscillatory movement*

Figure 3.2-11 represents the movement of a wheel connected to the dashpot model:

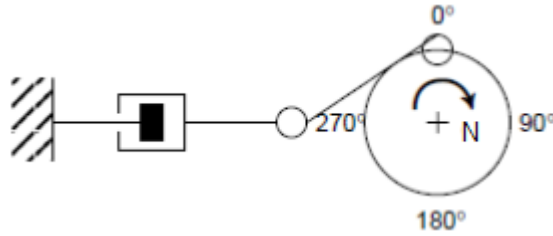


Figure 3.2-11: Dashpot model in an oscillatory movement

Consequently, if the spring is exchanged by a dashpot and the piston is subjected to a similar crankshaft action, the following equations apply:

$$\dot{\gamma} = \frac{d\gamma}{dt} = \omega \cdot \dot{\gamma} \cdot \cos(\omega t) \quad (3.2-27)$$

Substituting this into the dashpot equation:

$$\tau = \eta \cdot \frac{d\gamma}{dt} = \eta \cdot \omega \cdot \gamma_0 \cdot \cos(\omega t) \quad (3.2-28)$$

For the dashpot the response of  $\tau$  is  $90^\circ$  out of phase to the strain. This can also be expressed by defining a phase shift angle  $\delta = 90^\circ$  by which the assigned strain is trailing the measured stress.

The above equation EQ. (3.2-28) can then be rewritten:

$$\tau = \eta \cdot \omega \cdot \gamma_0 \cdot \cos(\omega t) = \eta \cdot \omega \cdot \gamma_0 \cdot \sin(\omega t + \delta) \quad (3.2-29)$$

According to this equation, in-phase stress response to an applied strain is called “elastic”. A  $90^\circ$  out-of-phase stress response is called “viscous”.

If a phase shift angle is within the limits of  $0 < \delta < 90^\circ$  is called “visco-elastic”.

#### *The Maxwell model in oscillatory movement*

Figure 3.2-12 represents the movement of a wheel connected to the Maxwell model:



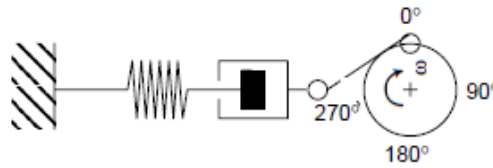


Figure 3.2-12: Maxwell model in an oscillatory movement

The stresses in each element are equal and the total strain is the sum of the strains in both the dashpot and the spring.

The equation of state for the model is EQ. (3.2-30):

$$\frac{1}{G} \cdot \left( \frac{d\tau}{dt} \right) + \frac{\tau}{\eta} = \frac{d\gamma}{dt} \quad (3.2-30)$$

Introducing the sinusoidal function, we can obtain EQ. (3.2-31).

$$\frac{1}{G} \cdot \left( \frac{d\tau}{dt} \right) + \frac{\tau}{\eta} = \omega \cdot \gamma_0 \cdot \cos(\omega t) \quad (3.2-31)$$

The stress response to the sinusoidal strain consists of two parts which contribute the elastic sin-wave function with  $\varphi = 0^\circ$  and the viscous cosine-wave-function with  $\varphi = 90^\circ$

*The Kelvin-Voigt model in oscillatory movement*

Figure 3.2-13 represents the movement of a wheel connected to the Kelvin-Voigt model:

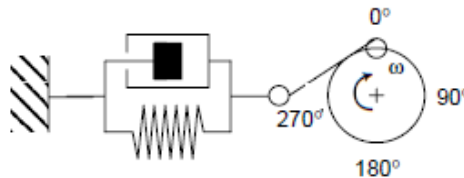


Figure 3.2-13: Kelvin-Voigt model in an oscillatory movement

This model combines a dashpot and spring in parallel. The total stress is the sum of the stresses of both elements, while the strains are equal.

The equation of state for the model is EQ. (3.2-32).

$$\tau = G \cdot \gamma + \eta \cdot \frac{d\gamma}{dt} \quad (3.2-32)$$

Introducing the sinusoidal function, we can obtain EQ. (3.2-33).

$$\tau = G \cdot \gamma_0 \cdot \sin(\omega t) + \eta \cdot \omega \cdot \gamma_0 \cdot \cos(\omega t) \quad (3.2-33)$$

The stress response in this two-element-model is given by two elements being elastic when  $\delta = 0$ , and being viscous when  $\delta = 90^\circ$ .

### *Real viscoelastic samples*

Real viscoelastic samples are more complex than either the Kelvin-Voigt solid or the Maxwell liquid. Their phase shift angle is positioned between  $0 < \delta < 90^\circ$ .  $G$  and  $\delta$  are again frequency dependent:

It is common to introduce the term Complex Modulus ( $G^*$ ) which is defined as EQ. (3.2-34) indicates:

$$G^* = \frac{\tau_0}{\gamma_0} \quad (3.2-34)$$

$G^*$  represents the total resistance of a substance against the applied strain. It is quite important to note that for real viscoelastic materials both the complex modulus ( $G^*$ ) and the phase angle ( $\gamma$ ) are frequency dependent.

Complex numbers can be used to express the complex modulus in two other parameters. Thus, Complex modulus ( $G^*$ ) can be defined as EQ (3.2-35) shows:

$$G^* = G' + iG'' = \frac{\tau_0(t)}{\gamma_E(t)} \quad (3.2-35)$$

where the real part of the complex function is the elastic component,  $G'$ , and the imaginary part corresponds to the viscous component,  $G''$ . As a consequence, the complex modulus  $G^*$  ( $|G^*|$ ) results from the combination of both parts:

$$|G^*| = \sqrt{G'^2 + G''^2} \quad (3.2-36)$$

Thus,  $G'$  and  $G''$  may be expressed in terms of the measured quantities ( $\tau_0$  and  $\gamma_0$ ) and the phase angle between them ( $\delta$ ):

$$G' = G^* \cdot \cos \delta = \frac{\tau_0}{\gamma_0} \cdot \cos \delta \quad (3.2-37)$$

$$G'' = G^* \sin \delta = \frac{\tau_0}{\gamma_0} \cdot \sin \delta \quad (3.2-38)$$

If a substance is purely viscous then the phase shift angle  $\delta$  is  $90^\circ$ :  $G' = 0$  and  $G'' = G^*$ . On the contrary, if the substance is purely elastic then the phase shift angle  $\delta$  is zero:  $G' = G^*$  and  $G'' = 0$  (Schramm 2000).

It is also useful to define the  $\tan \delta$  EQ. (3.2-39).

$$\tan \delta = \frac{G''}{G'} \quad (3.2-39)$$

$G'$  is known as the storage modulus.  $G'$  is a measure of the deformation energy stored by the sample during the shear process. After the load is removed, this energy is completely available, now acting as the driving force for the reformation process which partially or completely compensates the previously obtained deformation of the structure. Materials which are storing to be whole deformation energy are showing completely reversible deformation behaviour since they are occurring finally with an unchanged shape after a load cycle. Thus,  $G'$  represents the elastic behaviour of a material.

On the other hand,  $G''$  is known as the loss modulus.  $G''$  is a measure of the stress energy used by the sample during the shear process and therefore, it is eventually lost by transformation into heat. Energy losing materials show irreversible deformation behaviour since they occur with a change of shape after a load cycle. Thus,  $G''$  represents the viscous behaviour of a material (Mezger 2006).

Alternatively to the complex modulus  $G^*$  one can define a complex viscosity, as EQ. (3.2-40) indicates:

$$\eta^* = \frac{G^*}{i\omega} = \frac{\tau_0}{\gamma_0\omega} \quad (3.2-40)$$

The complex viscosity ( $\eta^*$ ) describes the total resistance to a dynamic shear. It can again be broken into the two components of the storage viscosity  $\eta'$  (the elastic component) and the dynamic viscosity  $\eta''$  (the viscous component).

### 3.2.10. The oscillatory response of real systems

The most general response for  $G'$  and  $G''$  of real samples (for structured systems) is shown in Figure 3.1-1. The exact values of the moduli and their position in the frequency domain will vary, however, this figure indicates the overall qualitative behaviour. A number of specific regions can often be differentiated, namely:

- a) The viscous or terminal region, where  $G'$  predominates and viscous (flow) behaviour prevails. All materials have such a region, even solids (because they creep at long times), but the frequency where this is seen is often so low that most oscillatory instruments cannot detect this part of the curve.

- b) The transition-to-flow region is so called because, when viewed from higher frequencies (where elastic behaviour dominates and  $G' > G''$ ), the loss modulus  $G''$ , describing viscous or flow behaviour, becomes significant. The point where the two moduli cross over is sometimes noted, and for a Maxwell model, this crossover frequency is given by the inverse of the relaxation time.
- c) The rubbery or plateau region is where elastic behaviour dominates. While in many cases we see what appears to be a flat plateau, there is always a slight increase of  $G'$  with frequency, but it can be as small as a few percent increase in modulus per decade increase in frequency. The value of  $G''$  is of course always lower than that of  $G'$ , but sometimes it can be considerably lower.

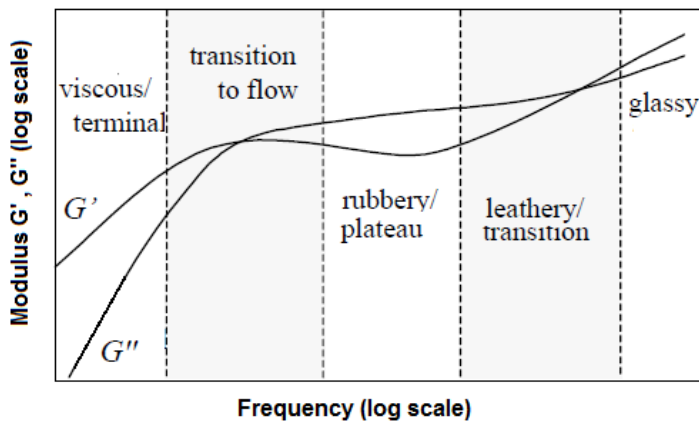


Figure 3.2-14: Regions in the viscoelastic spectrum of non-Newtonian liquids.

- d) A leathery or higher transition crossover region is also seen, where, due to high-frequency relaxation and dissipation mechanisms, the value of  $G''$  again rises, this time faster than  $G'$ . Once more at  $G' = G''$ , a crossover frequency can be defined, from which another characteristic time can be obtained.

## *Background. Interfacial Assessment*

- e) At the highest frequencies usually encountered in this form of testing, a glassy region is seen, where  $G''$  again predominates and continues to rise faster than  $G'$ .

### 3.3. Interfacial Assessment

The interface of a system is the boundary between two adjacent phases, being the interfacial tension the most important characteristic of this region. Thus, molecules at the end of a continuous phase are subjected to a net inward force which is imbalanced and, as a consequence, an excess of free energy appears. However, in terms of thermodynamics, interfaces not only have an excess energy but also an excess entropy. It is because of the entropic contribution that the temperature dependence plays an important role (Lyklema 2000).

#### 3.3.1. Interfacial tension and adsorption

As it was above mentioned, an interface between two phases contains an excess of energy and this energy is proportional to the boundary area. One of the most important consequence is that the interface will be as small as it could be possible. This force is attractive and acts in the plane of the interface. If this force appears in the interface between two liquids or a liquid-air interface, can be measured, the force per unit length is  $\gamma$  and Figure 3.3-1 shows how it can be measure using a Wilhelmy plate:

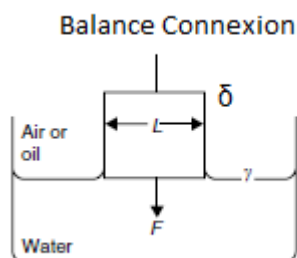


Figure 3.3-1: Representation of the measure of interfacial tension, using a Wilhelmy plate.

The attractive force ( $F$ ) generated in the interface is measured using a balance and the interfacial tension ( $\gamma$ ), which depends on the composition of both phases and temperature, is given by the following equation:

$$F = 2\gamma \cdot (L + \delta) \quad (3.3-1)$$

where  $L$  and  $\delta$  are the length and thickness of the Wilhelmy plate, respectively.

Thus, when a surfactant or a molecule that exhibit interfacial activity is adsorbed at the interface, the interfacial tension of the solvent changes according to the following equation that defines the interfacial pressure:

$$\Pi = (\gamma_0 - \gamma) \quad (3.3-2)$$

where  $\gamma_0$  is the interfacial tension of the pure solvent and  $\gamma$  is the interfacial tension in the presence of surface active agent molecules.

Molecules in a solution that is in contact with an interface can accumulate and adsorbed at this interface, forming a monolayer. It is important to remark that any substance showing surface activity is adsorbed because that gives a lower surface free energy and hence a lower surface tension, always leading to a positive value of the interfacial pressure ( $\Pi$ ). It is known that the decrease in  $\gamma$  depends on the surfactant concentration left in solution after equilibrium has been reached. The lower the value of this concentration, at which a given decrease in  $\gamma$  is obtained, the higher the surface activity of the agent.

The rate of adsorption of a surface active agent depends primarily on its concentration. The adsorption of any surface active agent at the interface involves different stages, the first of which is generally assumed to be its transport to the interface by diffusion. This stage may be followed by subsequent stages of penetration and rearrangement.



### **3.3.2. Surfactants**

Molecules which have an interfacial activity are known as surfactants. Generally, it is accepted there are two main types of surfactant: small amphiphilic molecules and polymers.

#### **3.3.2.1. Amphiphiles**

Amphiphiles are molecules that show a hydrophobic and hydrophilic side in the same chain. Usually, hydrophobic (lipophilic) part of a small-molecule amphiphile is an aliphatic chain. Most of amphiphilic substances are not highly soluble neither in water nor in oil and they suffer the smallest repulsive interaction from these solvents when they are partly in a hydrophilic environment (water) and partly in a hydrophobic one (oil). In solution, they tend to associate and form micelles to minimize repulsive interaction with solvent, this takes place above a critical micellization concentration (CMC).

One of the most important parameter is the HLB index, which is defined as the hydrophile-lipophile balance. It is defined that a value of 7 means that the substance has the same solubility in water and in oil and smaller values imply better solubility in oil.

The relation between HLB value and solubility is useful, because it relates to the suitability of the surfactant as an emulsifier. Thus, surfactants with HLB  $>7$  are generally suitable for making foams and O/W emulsions, and those with HLB  $<7$  are suitable for W/O emulsions.

Initially, the HLB value of a surfactant was determined from its solubility in water divided by its solubility in oil. Currently, HLB numbers have been derived for a range of chemical groups (e.g. polar groups of a surfactant have a positive value and the hydrophobic groups have a negative value) the sum of these values plus 7 gives the HLB index. For instance the HLB index for the

monostereate glycerol is 3.8, however this index reach up to 15 for the Tween 20® (Dickinson and McClements 1995).

### **3.3.2.2. Polymers**

Several synthetic or natural polymers can be used as surfactants. As regards natural polymers, proteins are the most important (although polysaccharides also can exhibit some surface activity, results have to be taken carefully, since most polysaccharides contain a small amount of protein that may be responsible for this attribute). Proteins are surfactants in food technology. The mode of adsorption of proteins varies, but, it always seems to involve a change in conformation. For instance, most globular proteins appear to retain an approximately globular conformation at interfaces, though not the native one. On the other hand, proteins with little secondary structure, such as gelatine and caseins, tend to adsorb more like a linear polymer. Forms intermediate between those mentioned also occur (Damodaran, Parkin et al. 2007).

### **3.3.3. Proteins adsorption**

As it was mentioned previously, proteins are large complex amphipathic molecules, which contain combinations of ionic, polar and non-polar regions. This makes them surface-active and strongly interacting with many other food components. Adsorption that takes place at fluid-fluid interfaces in food emulsions or foams is an 'unnatural' behaviour for any protein insofar as the protein is typically not in its native state. Nevertheless, this is a functional behaviour found for many proteins.

Although the surface activity of proteins is important, the reduction of surface or interfacial tension cannot in itself explain the stability of emulsions and foams. The essential stabilizing function of proteins is that they enable the

fluid interface to resist tangential stresses from the adjoining flowing liquids (Damodaran, Parkin et al. 2007).

### **3.3.3.1. Adsorbed layers at solid surfaces**

The strength of the interactions between a protein and an impenetrable surface depends on the conformational structure which protein adopts, as well as on the chemical nature of the surface. The complex, and substantially non-reversible, nature of protein adsorption at solid surfaces suggests there is not one single driving force which determine the free energy of the adsorption process.

Thus, proteins tend to adsorb more extensively and less reversibly at hydrophobic surfaces than at hydrophilic surfaces. With increasing degree of hydrophobicity of the surface, the ease of exchange of adsorbed protein molecules with the bulk aqueous phase is generally reduced. This difference can be attributed to a greater degree of unfolding at hydrophobic surfaces following protein adsorption, which leads to the development of strong interfacial hydrophobic interactions and associated displacement of neighbouring water molecules from the unfavourable environment of the surface. In contrast, electrostatic protein-surface interactions tend to be more important at hydrophilic surfaces, especially for 'hard' proteins, which may undergo very little changes in configurational structure upon adsorption. The extent of globular protein unfolding upon adsorption is dependent on the protein structure. The effective thickness of the globular protein monolayer is often close to the known size of the native protein molecule in solution. Depending on surface coverage and molecular shape, however, some differences may be expected in the interfacial orientation.

The degree of saturation in the adsorbed layer has a considerable influence on the degree of conformational change. The lower is the adsorbed

amount, the more space that the protein molecule has to spread out at the surface, and hence the greater the opportunity for unfolding to minimize the configurational free energy following adsorption. Early adsorbing proteins tend to exhibit a large loss of enzymatic activity, and are poorly exchangeable with the bulk phase after adsorption. Late adsorbing proteins tend to retain more enzymatic activity due to less unfolding and more participation in loosely held multilayers.

The maximum adsorbed amount is determined by the rate of unfolding at the surface in relation to the rate of adsorption. Fast adsorption gives less time for protein molecules to spread out at the surface, and consequently the area occupied per molecule is lower and the adsorbed amount is higher.

### **3.3.3.2. Adsorbed layers at fluid interfaces**

Almost everything described previously for protein adsorption at solid surface is applicable when proteins are adsorbed at fluid-fluid interfaces. However, there are some differences. In particular, related to how protein molecules can penetrate further into the non-aqueous phase and can move more freely, on a liquid surface.

Processes involving diffusion, reorientation and conformational reorganization will occur faster at air-water and oil-water interfaces than on solid substrates. In addition, another important difference is that in fluid-fluid interfaces is possible to perform additional experimental studies on the surface equation of state and on the surface rheological behaviour.

Analytical surface equations of state developed for small-molecule adsorbed layers are unable to represent fully the properties of protein systems. However, some simple formula can capture most of the essential features of the behaviour. Nearly all protein adsorption studies are characterized by extremely non-ideal behaviour. The non-ideality arises from

a combination of enthalpic and entropic contributions to the surface free energy as a result of complex intermolecular interactions and intramolecular rearrangements. Frumkin (1925) described a fairly simple equation that can account for both enthalpic and entropic terms:

$$\frac{\Pi\omega_1}{RT} - \ln(1 - \theta) - (1 - S^{-1})\theta - \frac{H}{RT}\theta^2 \quad (3.3-3)$$

where  $S$  is the ratio ( $\omega_1/\omega_2$ ) of the solvent molar area ( $\omega_1$ ) to the protein molar area ( $\omega_2$ ),  $H$  is the enthalpy of mixing of a regular solution,  $R$  is the gas constant,  $T$  is the temperature and  $\theta$  is the fractional surface coverage which may be expressed as  $\theta = \omega_2\Gamma$ , in terms of the surface load ( $\Gamma$ ).

The first term is the surface pressure of an ideal surface mixture of equal-sized adsorbed molecules. The second term (linear in  $\theta$ ) allows for the non-ideal surface entropy of mixing of large and small adsorbed molecules (for  $S \ll 1$ ). This term has the effect of greatly reducing the value of  $\Pi$ , especially at low values of  $\theta$ . The third term (proportional to  $\theta^2$ ) is related to intermolecular interactions in the adsorbed layer. For the normal case of net attractive protein-protein interactions ( $H > 0$ ), the combination of substantial enthalpy and entropy contributions reproduces the very strong deviation from ideality typically observed at low surface coverage.

However, this equation breaks down at high surface coverage ( $\theta \rightarrow 1$ ) when  $\theta$  is predicted to strongly diverge, whereas in practice  $\Pi$  reaches a saturation value corresponding to monolayer collapse and possible onset of multilayer formation. The theory breaks down because it is based on a two-dimensional model of the adsorbed layer, whereas the real system is three-dimensional.

Regardless of the restriction of the two-dimensional model, other refinements can in principle be made to account for protein aggregation and

reorientation in the adsorbed layer. In particular, a more realistic allowance for unfolding of protein molecules in the adsorbed layer can be made by replacing the single state of the adsorbed protein by a distribution of states with different values of the molar area  $\omega_2$ . However, such complex models have the disadvantage of increasing the number of adjustable parameters without providing a fully rigorous statistical mechanical description of the system under consideration (Dickinson and McClements 1995).

### **3.3.3.3. Simulation model of a globular protein adsorbed layer**

A computer simulation model is available in which an adsorbed monolayer of globular protein molecules at a fluid–fluid interface is represented as a quasi-two-dimensional network of cross-linked rigid spherical particles (Wijmans and Dickinson 1998).

The approach is motivated by the similarity in rheological properties between a globular protein adsorbed film and an extremely thin layer of bulk heat-set protein gel. The monolayer network structures produced by the model are qualitatively similar to those generated in two-dimensional simulations of aggregated particle gels formed from irreversibly bonding Brownian particles. However, the Brownian dynamics algorithm used to simulate the adsorbed layer properties is actually closer in detail to that used to simulate three-dimensional aggregated particle gel networks. The model neglects specific effects of changes in intramolecular interactions during or after adsorption, whilst accounting for associative intermolecular interactions between adsorbed particles through the formation of strong flexible bonds. Confinement of the particles to the interface is achieved with a steep potential well of finite width in the  $z$ -direction (perpendicular to the interface). Although particles are strongly adsorbed, they still have some freedom to distribute themselves around their equilibrium positions at  $Z=0$ . For this reason, the

model of the layer is not completely two-dimensional (Wijmans and Dickinson 1998).

### **3.3.3.4. Competitive adsorption**

Some of the complexity of protein adsorption is partly due to the potential for competitive adsorption between proteins which are present.

In mixtures involving globular proteins, the irreversibility of the adsorption events prevents equilibrium from ever being achieved. Although more easily denaturable (“soft”) proteins are expected to have greater surface affinity and exchangeability than more stable (“hard”) proteins, a useful rule of thumb is that the adsorbed layer will be dominated by the protein that presents itself first to the interface.

In cases where both proteins are presented together in roughly equal amounts, the extent of dominance of individual components will depend on the residence times of individual protein molecules at the interface in relation to their rates of unfolding. Thus, the competition to occupy sites at the interface may prevent ‘early’ adsorbed species from ever achieving the ‘irreversible state’, in which case an initially adsorbing molecule may be displaced.

The finiteness of the time required to achieve the irreversible state is a key point because it allows for multiple collisions of potentially competing molecules to take place before any chance of replacement becomes impossible.

The protein interfacial composition at any given bulk protein composition ratio appears to be affected largely by the relative rates of arrival of the components at the interface and the molecular areas available to them at the time of arrival. In this sense the accumulation of protein molecules at the fluid-fluid interface from the mixed solution is not a thermodynamically-controlled

competitive adsorption process. This means that the composition of the interface cannot be predicted from any simple thermodynamic model

When small-molecule surfactants are present in protein-containing systems, the adsorption of the protein is affected by the binding of surfactant to both the protein and the fluid interface. In addition to the preferential binding of surfactant to the surface at high bulk concentrations, surfactant binding to hydrophobic sites on the protein may also reduce its surface affinity. Therefore the protein can be removed from the interface as a consequence of two distinct mechanisms:

- 1) The solubilisation mechanism: desorption of protein arises as a result of solubilisation into the aqueous phase in the form of a protein-surfactant complex.
- 2) The replacement mechanism: displacement of protein arises because surfactant lowers the interfacial free energy more effectively than does protein (or protein-surfactant complex).

Ionic surfactants usually bind strongly to proteins, such that competitive adsorption involving charged amphiphiles can be regarded as proceeding mainly by the solubilisation mechanism. With more weakly interacting non-ionic surfactants, however, the replacement mechanism can be regarded as (Wijmans and Dickinson 1998).

### **3.3.4. Interfacial Measurements**

#### **3.3.4.1. Surface pressure-area**

The Langmuir adsorption model is the most common model used to quantify the amount of amphiphilic compounds adsorbed. This adsorption is a function of partial pressure or concentration and temperature. For the sake of simplicity, this model considers the adsorption of an ideal gas onto an



idealized surface. Thus, when a monolayer is fabricated at the gas-liquid or liquid-liquid interface, the film is named Langmuir film (Toth 2002).

A useful method to characterise the Langmuir film is by obtaining the surface pressure/molecular area isotherms, measured by the Langmuir method. The measurement system consists of a plate fitted with two mobile barriers, and a device which is able to measure surface tension (e.g. Wilhelmy plate). Figure 3.3-2 illustrates the device measurement:

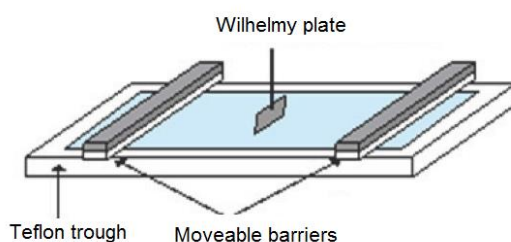


Figure 3.3-2: Langmuir trough device

Thus, the experiment consists of measuring the surface tension as a function of the mean molecular area perpendicular on the monolayer as it is compressed by the two barriers.

Figure 3.3-3 shows a typical pressure-molecular area curve for an amphiphilic monolayer adsorbed at the interface obtained when the barriers are moved towards each other. The different phases occurring over the adsorption isotherm are also represented in this figure.

At the beginning, when the barriers are at their greatest distance from each other, the monolayer is in the gaseous phase where the hydrophobic groups are completely separated. Further compression (from right to left) forces the monolayer molecules into the liquid phase that causes a slight elevation of the surface pressure, starting with the so-called “lift-off” point. Further compression squeezes the amphiphilic molecules into a solid, which

gives a steep rise in the surface tension. By further increasing the compression, the layer collapses into a many-layered structure (Toth 2002).

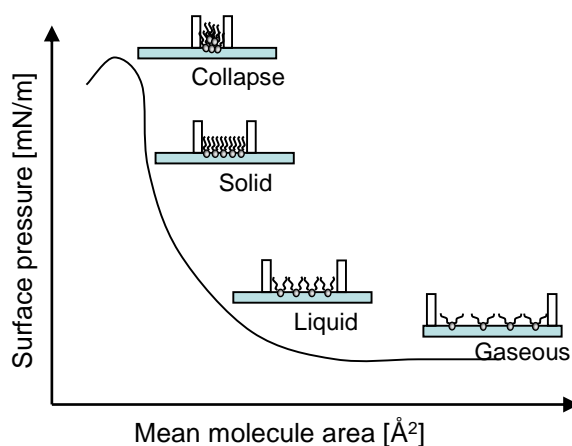


Figure 3.3-3: Surface pressure Vs. Molecular area for an amphiphilic molecule

#### 3.3.4.2. Dilatational Droplet Tension

When a drop of a fluid is in contact with other fluid, the drop exhibits a combination of effects coming from the surface tension (which tends to form a spherical drop) and the gravitational force (which tends to elongate the drop). In this way, the asymmetric drop can be expressed by using the Laplace equation:

$$\frac{1}{x} \frac{d(x \sin \theta)}{dx} = \frac{2}{b} - cz \quad (3.3-4)$$

Where  $x$  and  $z$  are the cartesian coordinates,  $b$  is the radius of curvature,  $\theta$  is the tangent angle and  $c$  is a constant related to the Capilar number, which is defined as :  $c=g \cdot \Delta\rho/\gamma$ , where  $g$  is the gravity acceleration,  $\Delta\rho$  is the difference of density between both studied fluids and  $\gamma$  the surface tension.

### 3.3.4.3. Interfacial Shear Rheology

Two different kinds of interfacial rheological measurements can be distinguished by applying shear or dilatational deformations to a fluid-fluid interface.

When the interface is sheared, both the area and the amount of surfactant in the interface remain constant and then it is possible to measure the required shear force applied to the plane of the interface. For most systems, shear rate thinning occurs and the observed viscosity is an apparent interfacial viscosity. For instance, values for globular proteins usually show a high experimental uncertainty, since the monolayer can yield or rupture and the measured “viscosity” will greatly depend on the rupture pattern.

On the other hand, if the interfacial area is enlarged by dilatational deformation, leaving its shape unaltered, an increase in interfacial tension takes place, because the molar amount of adsorbed material per unit surface area (surface load,  $\Gamma$ ) is decreased. This is usually expressed in the surface dilatational modulus, defined as follows:

$$E_{SD} = \frac{d\gamma}{d \ln A} \quad (3.3-5)$$

where  $A$  is the surface area.

For proteins  $E_{SD}$  may be large and less dependent on time, because proteins adsorb more or less irreversibly. However, the concentration of protein at the interface has a large effect. In addition, changes in protein conformation upon adsorption and dilation can also affect the modulus.

Surface rheological parameters of protein layers depend on pH, ionic strength, solvent quality, temperature. However, moduli and viscosities are usually at their maximum values near the isoelectric pH. In any case, the measurement of  $E_{SD}$  is difficult and so is the interpretation of the results

obtained from dilatational rheological measurements (Damodaran, Parkin et al. 2007).

## 3.4. Products from protein

### 3.4.1. Emulsions

Emulsions are disperse systems consisting of two immiscible liquids. One of the phases (called the internal or disperse phase) is dispersed in the form of small droplets in a liquid medium (called the continuous phase). According to the hydrophobicity, some classes may be distinguished: oil-in-water (O/W), water-in-oil (W/O), and oil-in-oil (O/O). To disperse two immiscible liquids, it is needed a third component, namely, the emulsifier. The choice of the emulsifier is crucial in the formation of the emulsion and its long-term stability (Tadros 2013).

Classification according to system structure:

1. O/W and W/O macroemulsions: Droplet size range of 0.1–5  $\mu\text{m}$  with an average of 1–2  $\mu\text{m}$ . They are kinetically stable.
2. Nanoemulsions: Droplet size range of 20–100 nm. Similar to macroemulsions, they are only kinetically stable.
3. Micellar emulsions or microemulsions: these usually have the size range of 5–50 nm. They are thermodynamically stable.
4. Double and multiple emulsions: these are emulsions-of-emulsions, W/O/W, and O/W/O systems.
5. Mixed emulsions: these are systems consisting of two different disperse droplets that do not mix in a continuous medium.

#### 3.4.1.1. Methods of Emulsification

Several procedures may be applied for emulsion preparation, including: simple pipe flow devices (low agitation energy); static mixers and general

stirrers (low to medium energy); high-speed mixers colloid mills and high-pressure homogenizers (high energy); and ultrasound generators.

All methods involve liquid flow; unbounded and strongly confined flow. In the unbounded flow, any droplets are surrounded by a large amount of flowing liquid. The forces can be frictional (mostly viscous) or inertial. Viscous forces cause shear stresses to act on the interface between the droplets and the continuous phase, and the shear stresses can be generated by laminar flow or turbulent flow.

In bounded flow, other relations hold. If the smallest dimension of the part of the device in which the droplets are disrupted is comparable to droplet size, other relations hold (the flow is always laminar). A different regime prevails if the droplets are directly injected through a narrow capillary into the continuous phase (injection regime).

### 3.4.1.1.1. *Role of Surfactants in Emulsion Formation*

Surfactants decrease the interfacial tension  $\gamma$ , and this causes a reduction in droplet size. The latter decrease with decrease in  $\gamma$ . For laminar flow, the droplet diameter is proportional to  $\gamma$ . In contrast, for a turbulent regime, the droplet diameter is proportional to  $\gamma^{3/5}$ .

The amount of surfactant required to produce the smallest drop size will depend on its activity in the bulk that determines the reduction in  $\gamma$ , as given by the Gibbs adsorption equation,

$$-d\gamma = RT\Gamma da \quad (3.4-1)$$

where  $R$  is the gas constant,  $T$  is the absolute temperature, and  $\Gamma$  is the surface excess or surface load previously defined (number of moles adsorbed per unit area of the interface).

Thus,  $\Gamma$  increases with increase in surfactant concentration and eventually it reaches a plateau value when saturation adsorption occurs.

During emulsification, an increase in the interfacial area “A” takes place and this causes a reduction in  $\gamma$ . The equilibrium is restored by adsorption of surfactant from the bulk, but this process (Tadros 2013).

### 3.4.1.2. Emulsion breakdown

According to Janssen & Meijer (1995) the strain and rupture of the drop during the emulsification is controlled by a local capilar number, which establish the relationship between the shear stress ( $\tau$ ), and the interfacial tension ( $\gamma / R$ ) or Laplace Pressure ( $2 \gamma / R$ ), which tends to prevent the drop strain (EQ. 3.4-2).

$$Ca = \frac{\tau R}{\gamma} = \frac{\eta_c \dot{\gamma} R}{\gamma} \quad (3.4-2)$$

where  $\eta_c$  is the viscosity of the continuous phase,  $\dot{\gamma}$  is the shear rate,  $\gamma$  the interfacial tension and  $R$  the droplet diameter.

As a consequence, there is a critical value for the capilar number ( $Ca_{crit}$ ) that depends on the viscosity ratio of disperse and continuous phases, above which shear forces overcome surface tension and breakup of droplets occurs ( $Ca > Ca_{crit}$ ).

Macroemulsions are kinetically stable. As a consequence, there are several process which induce the emulsion breakdown, Figure 3.4-1 summarises that:

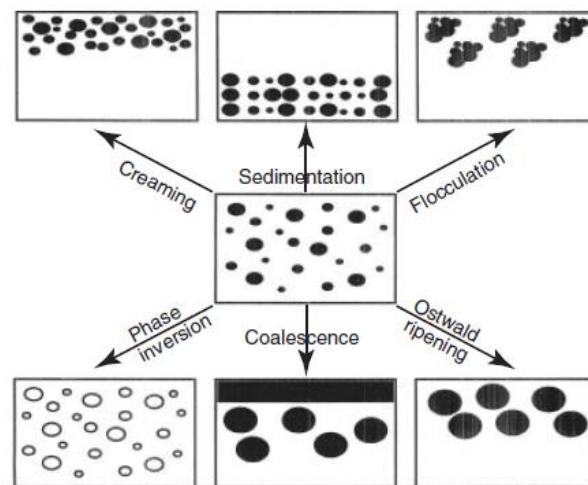


Figure 3.4-1: Emulsion breakdown process

The physical phenomena involved in each breakdown process are not simple, and it requires analysis of the various surface forces involved. In addition these processes may take place simultaneously or consecutively and this complicates the analysis. Model emulsions, with monodisperse droplets, cannot be easily produced (Tadros 2013).

### 3.4.1.2.1. *Creaming and Sedimentation*

This process is a result from external forces (usually gravitational). Thus, when these forces exceed the thermal motion of the droplets (Brownian motion), a concentration gradient builds up in the system with the larger droplets moving faster to the top or to the bottom (depending on the density of both phases). In the limiting cases, the droplets may form a close-packed array at the top or bottom of the system with the remainder of the volume occupied by the continuous liquid phase.

### 3.4.1.2.2. *Flocculation*

This process refers to aggregation of droplets (without any change in primary droplet size) into larger units. It is the result of the van der Waals



attraction that is universal with all disperse systems. Flocculation occurs when there is not enough repulsion (e.g. electrostatic) to keep the droplets apart to distances where the van der Waals attraction is weak.

### 3.4.1.2.3. *Ostwald Ripening*

This is a result of the finite solubility of both liquid phases. Liquids that are referred to as being immiscible often have mutual solubility that are not negligible. In this case, the smallest droplets will have larger solubility in the continuous phase. Over time, the smaller droplets disappear and their molecules diffuse to the bulk and become deposited on the larger droplets. As a result, the droplet size distribution shifts to slightly larger values.

### 3.4.1.2.4. *Coalescence*

This refers to the process of thinning and disruption of the liquid film between the droplets with the result of fusion of two or more droplets into larger ones. The limiting case for coalescence is the complete separation of the emulsion into two liquid phases. The driving force for coalescence is the surface or film fluctuations which results in close approach of the droplets whereby the van der Waals forces are strong, thus preventing their separation.

### 3.4.1.2.5. *Phase Inversion*

This refers to the process through which there will be an exchange between the disperse phase and the medium. For instance, an O/W emulsion may with time or change of conditions invert to a W/O emulsion. In many cases, phase inversion passes through a transition state whereby multiple emulsions are produced.

The above mentioned are the most typical process of emulsion destabilization mechanisms. These process could take place alone or in combination of some of them (Tadros 2013).

### **3.4.1.3. Stabilization of systems**

#### **3.4.1.3.1. Prevention of Creaming or Sedimentation**

Several strategies for preventing emulsion destabilization induced by gravitational forces are possible. An obviously way to prevent these phenomena is matching density of oil and aqueous phases. However, this method is not practical. Density matching is not always possible to know and it would only occur at one temperature.

Other way could be by the reduction of droplet size: As the gravity force is proportional to  $R^3$ , and then if  $R$  is reduced by a factor of 10, the gravity force is reduced by 1,000. Below a certain droplet size, the Brownian diffusion may exceed gravity and creaming or sedimentation is prevented. Thus, this is the principle of formulation of the above mentioned thermodynamically stable nanoemulsions

The use of “thickeners” is also possible. These are high-molecular-weight polymers, natural, or synthetic such as Xanthan gum, hydroxyethyl cellulose, alginates, carragenans and many others.

Controlled flocculation may also prevent creaming or sedimentation to some extent. Weak flocculation can occur by adding small amounts of electrolyte, such that a secondary minimum could appear in the free energy curve. The same applied for sterically stabilized emulsions. In practice this is not an easy alternative since droplet size should be simultaneously controlled.

Finally, depletion flocculation may also be considered a way of favouring emulsion stability. This is obtained by addition of “free” polymer in the continuous phase. At a critical concentration, or volume fraction of free polymer weak flocculation occurs because the free polymer coils become “squeezed out” from between the droplets (Tadros 2013).

### *3.4.1.3.2. Prevention of flocculation*

There are several alternatives to prevent flocculation of droplets, where the first one is obtaining charge-stabilized emulsions, for example by using ionic surfactants. The most important criterion is to make the free energy barrier ( $G_{\max}$ ) as high as possible. This may be achieved mainly by three conditions: high surface or zeta potential, low electrolyte concentration, and low valence of ions.

Other way to reduce flocculation is by sterically stabilized emulsions. Four criteria are necessary in this case:

- 1) Complete coverage of the droplets by the stabilizing chains.
- 2) Firm attachment (strong anchoring) of the chains to the droplets. This requires the chains to be insoluble in the medium and soluble in the oil. However, this is incompatible with stabilization that requires a chain that is soluble in the medium and strongly solvated by its molecules.
- 3) Thick adsorbed layers: the adsorbed layer thickness should be in the range of 5–10 nm.
- 4) The stabilizing chain should be maintained in good solvent conditions under all conditions of temperature changes on storage.

### *3.4.1.3.3. Prevention of coalescence*

There are two mechanisms in order to prevent the coalescence: increasing repulsion both electrostatic and steric and dampening of the fluctuation by enhancing the Gibbs elasticity. In general, smaller droplets are less susceptible to surface fluctuations and hence coalescence is reduced.

There are two main methods which may be applied to achieve the above effects:

- 1) Use of mixed surfactant films: In many cases using mixed surfactants can reduce coalescence
- 2) Formation of lamellar liquid crystalline phases at the O/W interface:

As a result of multilayer structures, the potential drop is shifted to longer distances thus reducing the van der Waals attraction.

#### **3.4.1.4. Food emulsions**

Everything above described about emulsions is applicable to food emulsions, the only difference is that now the system is very complex, and proteins are usually used as emulsifiers instead of surfactants.

Thus, at similar bulk concentrations (w/v), low molecular mass surfactants decrease the surface tension to a greater extent than the macromolecular surfactants. This difference is mainly related to differences in orientation and configuration of these surfactants at an interface. Although low molecular mass surfactants are more effective than proteins in reducing the interfacial tension, surfactant-based foams and emulsions are generally more unstable than those processed using proteins.

This is because proteins, in addition to lowering interfacial tension, can form a continuous viscoelastic membrane-like film around oil droplets or air cells via non-covalent intermolecular interactions and via covalent disulphide cross-linking. Consequently, in foods, which contain both low molecular and macromolecular surfactants, the stability of colloiddally dispersed phases is primarily dependent on protein films adsorbed at the interfaces. However, practical observations indicate that all proteins are not equally surface active, even though all are amphiphilic and a majority of them contain similar percentages of polar and nonpolar amino acid residues (Tadros 2013).

The differences found in the surface activities of various proteins must be related to differences in their conformation and the susceptibility of those conformations to unfold at interfaces. Intuitively, the molecular factors that influence surface activity of proteins must be related to flexibility, conformational stability at interfaces, rapid adaptability of the conformation to changes in its environment, and to the distribution pattern of hydrophilic and hydrophobic residues in its primary structure, as well as on its folded surface.

In addition, apart from the intrinsic molecular factors, the surface activity of a protein will be also dictated by several extrinsic factors such as pH, ionic strength, and temperature (Damodaran 1997).

### 3.4.1.5. Emulsion characterisation

#### 3.4.1.5.1. Rheology of emulsions

Emulsions generally show a rheological behaviour fitting into the category of complex fluids. However, they differ from other complex fluids in three main aspects:

- 1) The mobile liquid/liquid interface that contains surfactant or polymer layers.
- 2) The dispersed-phase viscosity relative to that of the medium has an effect on the rheology of the emulsion.
- 3) The deformable nature of the dispersed-phase droplets.

Consequently, we can difference between interfacial and bulk rheology.

### 3.4.1.5.2. Interfacial Rheology

#### *Mixed Surfactant Films*

According to the data available, there seems to be a relationship between the use of a mixture of surfactants and the enhancement of the stability of the emulsion. This could be due to the increase of interfacial dilatational elasticity ESD for the mixed film when compared to that one containing a single surfactant. However, other factors such as thinning of the film between emulsion droplets can also play a major role.

#### *Protein Films*

The viscoelastic properties of protein films at the O/W interface also correlates well with the stability of emulsion drops against coalescence.

Some viscoelastic measurements can be carried out using creep-recovery tests. The stability of the emulsion was assessed by measuring the residence time  $t$  of several oil droplets at a planar O/W interface containing the adsorbed protein. Thus, Biswas and Haydon (1963) derived a relationship between coalescence time ( $\tau$ ) and interfacial parameters such as surface viscosity ( $\eta_s$ ), instantaneous modulus ( $G_0$ ), and adsorbed film thickness ( $h$ ) (EQ. 3.4-3).

$$\tau = \eta_s \cdot \left[ 3C' \frac{h^2}{A} - \frac{1}{G_0} - \phi(t) \right] \quad (3.4-3)$$

where  $3C'$  is a critical deformation factor,  $A$  is the Hamaker constant (Van der Waals body-body interaction) and  $\phi(t)$  is the elastic deformation per unit stress.

The equation analysis shows that viscoelasticity is necessary (eg.  $\tau$  increases with increasing  $\eta_s$ ) but not sufficient to ensure stability against coalescence. Film thickness seems to be the most important factor, such that to ensure stability of an emulsion  $h$  must be large enough.

### 3.4.1.5.3. Bulk rheology

#### *Diluted emulsions*

For highly viscous oil droplets dispersed in low viscosity media such as water, dilute O/W emulsions (volume fraction  $\phi \leq 0.01$ ) of non-interacting droplets behave as “hard spheres”. In this case, the relative viscosity ( $\eta_r$ ) is given by the Einstein equation (3.4-4):

$$\eta_r = 1 + [\eta]\phi \quad (3.4-4)$$

where  $[\eta]$  is the intrinsic viscosity (2.5 for hard spheres).

For droplets with a viscosity comparable to that of the medium, the transmission of tangential stress across the O/W interface, from the continuous phase to the dispersed phase, causes liquid circulation inside the droplets. Energy dissipation is less than that for hard spheres and the relative viscosity is lower than that predicted by the Einstein equation.

Thus, for an emulsion with viscosity  $\eta_i$  for the disperse phase and  $\eta_o$  for the continuous phase, the intrinsic viscosity can be defined as show EQ. (3.4-5).

$$\eta = 2.5 \left( \frac{\eta_i + 0.4\eta_o}{\eta_i + \eta_o} \right) \quad (3.4-5)$$

When  $\eta_i \gg \eta_o$ , the droplets behave as rigid spheres and  $\eta$  approaches the limit value of 2.5. In contrast if  $\eta_i \ll \eta_o$  (e.g. in foams),  $[\eta] = 1$ .

If the volume fraction of droplets exceeds the Einstein limit, ( $\phi > 0.01$ ), it must take into account the effect of Brownian motion and interparticle interactions.

The smaller the emulsion droplets, the more important the contribution of Brownian motion and colloidal interactions. Brownian diffusion tends to randomize the position of colloidal particles, leading to the formation of

temporary doublets, triplets, and so on. The hydrodynamic interactions are of longer range than the colloidal interactions, and they come into play at relatively low volume fractions ( $\phi > 0.01$ ) resulting in ordering of the particles into layers and tending to destroy the temporary aggregates caused by the Brownian diffusion. This explains the shear thinning behaviour of emulsions at high shear rates.

For the volume fraction range  $0.01 < \phi < 0.2$ , Batchelor (1977) derived the following expression for a dispersion of hydrodynamically interacting hard spheres:

$$\eta_r = 1 + 2.5\phi + 6.2\phi^2 + v\phi^3 \quad (3.4-6)$$

Where the first part corresponds to the Einstein limit (EQ. 3.4-4) while the third term accounts for hydrodynamic (two-body) interactions and the fourth term relates to multibody interactions.

#### *Concentrated emulsions*

Considering the rheology of concentrated emulsions, an expression for the fourth term in  $\phi^3$  of EQ. (3.4-8) should be provided. Unfortunately, there is no theoretical rigorous treatment of this term and only semiempirical equations for intermediate volume fractions are available (Phan-Thien and Tanner 1999, Pal 2000).

Two models were proposed by Pal (2001):

$$\eta_r \left[ \frac{2\eta_r + 5\lambda}{2 + 5\lambda} \right]^{1/2} = e^{\left[ \frac{2.5\phi}{1 - \phi/\phi^*} \right]} \quad (3.4-7)$$

$$\eta_r \left[ \frac{2\eta_r + 5\lambda}{2 + 5\lambda} \right]^{1/2} = [1 - \phi/\phi^*]^{2.5\phi^*} \quad (3.4-8)$$



where  $\lambda$  is the ratio of viscosities of disperse drops and continuous medium and  $\phi^*$  is the limit of closest packing of drops in free space.

An increase in the concentration of drops in emulsions results not only in an increase in viscosity at low shear rates but also in the appearance of strong non-Newtonian effects leading to a shear rate dependence of the apparent viscosity. A remarkable transition from an almost Newtonian behaviour at low stresses to an anomalous flow with pronounced non-Newtonian effects may also take place (Tadros 2013).

### *3.4.1.5.4. Microscopy*

The human eye is able to resolve objects that are greater than 0.1 mm. Many of the structural components in food emulsions (such as droplets, surfactant micelles, fat crystals, gas bubbles or protein aggregates) are smaller than this limit and cannot be distinguished by humans.

Several techniques are available to provide information about the structure, dimensions, and organization of the components within food emulsions, for example, optical microscopy, electron microscopy (SEM) or atomic force microscopy (AFM). These techniques have the ability to provide relevant information about complex systems in the form of “images” (McClements 2004).

#### *Conventional optical microscopy*

The optical microscope is one of the most valuable tools for observing the microstructure of emulsions. The optical microscope contains several lenses that direct light through the specimen and magnify the resulting image. The resolution is determined by the wavelength of light used and the mechanical design of the instrument, being the theoretical limit of resolution of an optical microscope about 0.2  $\mu\text{m}$ . Nevertheless, it provides useful information about the size distribution of droplets in emulsions that contain larger droplets, and

can often be used to distinguish between flocculation and coalescence, which is sometimes difficult using instrumental particle sizing techniques based on light scattering (McClements 2004)

### *Laser Scanning Confocal Microscopy*

Laser Scanning Confocal Microscopy (LSCM) can provide extremely useful information about the microstructure of food emulsions. This technique has the advantage that provides higher clarity images than conventional optical microscopy, and often allows the generation of three-dimensional images of structures without the need to physically sectioning the specimen. The LSCM focuses an extremely narrow laser beam at a particular point in the specimen being analysed and a detector measures the intensity of the resulting fluorescence signal. 3D images can be obtained by focusing the laser beam at different vertical depths. The observation of the microstructure of multicomponent systems is often facilitated by using the natural fluorescence of certain components (such as proteins) or by using fluorescent dyes (McClements 2004).

### *Scanning Electron Microscopy*

Scanning Electron Microscopy (SEM) is widely used to examine the microstructure of food emulsions, especially those that contain structural components that are smaller than the lower limit of resolution of optical microscopes. This technique can provide relevant information about the concentration, dimensions, and spatial distribution, whereas microstructure is not significantly altered by the sample

Electron microscopes use electron beams, instead of light beams, to provide information about the structure of materials. These beams are directed through the microscope using a series of magnetic fields, instead of optical lenses, which used optical microscope. Electron beams have much

smaller wavelengths than light and so they can be used to examine much smaller objects (about 0.2 nm)

### *Static light scattering*

Droplet size analysis instruments that use static light scattering (also called laser diffraction) are based on the principle that a beam of light is directed through an emulsion, the laser is scattered by the droplets in a well-defined manner. A measurement of the extent of light scattering by an emulsion can be used to determine the droplet size distribution and concentration by using a mathematical model to relate the measured data to the particle characteristics.

## **3.4.2. Food Gels**

### **3.4.2.1. Definition**

A food gel can be considered as a high moisture three-dimensional polymeric network that resists flow under pressure and is able to retain their distinct structural shape. Generally, a gel is a continuous network of interconnected particles or assorted macromolecules dispersed in a continuous liquid phase. The gelation is the phenomenon which involves the association or crosslinking of the polymer chains to form a three-dimensional network that immobilizes water within it.

Food hydrocolloids are usually the most frequently used gelling agents in food products. A wide range of polysaccharides and proteins are nowadays available as food hydrocolloids derived from natural sources. Polysaccharides are incorporated because of their ability to control stability and texture of foods, as well as for their role in encapsulation and controlled release of active agents (flavours, functional ingredients, etc.) (Banerjee and Bhattacharya 2012).

In food gels the liquid is invariably water and the molecular network consists of proteins or polysaccharides or a combination of both. The properties of the gel are the net results of the complex interactions between the water and the molecular network. The water, as a solvent, has influence in the nature and magnitude of the intermolecular forces that maintain the integrity of the polymer network. The polymer network holds the water, preventing it from flowing away.

Unfortunately the complexity of these interactions, responsible for the useful functional properties of gels, makes it very difficult to predict quantitatively their physical properties, even for pure proteins or polysaccharides. In addition, food hydrocolloids are rarely pure and are often used with other ingredients that increase the degree of complexity of food systems. For this reason, their physical properties must generally be treated empirically (Damodaran 1997).

### **3.4.2.2. Protein gelation**

Heat--induced gelation, pH-induced gelation or high pressure gelation are techniques widely used for the gelation of globular proteins and proceed through a series of transitions, such as denaturation (unfolding) of native proteins, aggregation of unfolded molecules, strand formation from aggregates, and association of strands into a network (Banerjee and Bhattacharya 2012).

#### **3.4.2.2.1. *Heat-induced gelation***

Heat-induced gelation is probably the most important and common method to obtain gels. Gelation involves different steps from protein denaturation to formation of protein aggregates and association of aggregates to form a three-dimensional network:

- The first step always consists of protein denaturation involving unfolding (at least partially) or dissociation of the molecules induced by thermal energy. As a consequence, some of the hydrophobic groups, which remained buried in the protein core under native configuration, become exposed to the aqueous phase above some temperature.
- The second step takes place through hydrophobically driven protein-protein interactions that lead to the association and aggregation of unfolded molecules to form complexes of higher molecular weight. In this stage, disulphide (-S-S-) bonds may also play an important role in combination with hydrophobic interactions.
- Random association of aggregates to form a three-dimensional structure which extends to the whole system has been suggested as a third step. Meanwhile the continuous phase is entrapped within the network (Clark, Kavanagh et al. 2001).

The reaction rate can be typically determined either by the unfolding or by the aggregation reaction, depending on the ratio of the reaction rates of the single steps (Banerjee and Bhattacharya 2012). Several variables, depending either on protein nature and composition or on environmental factors, such as pH or ionic strength may exert an important influence on protein-protein and protein-solvent interactions and as a result on these reaction rates, thus conditioning the type of gel network formed.

Essentially, proteins can aggregate in two ways. One is by random aggregation which can lead to heterogeneous particulate network structures. The other is by linear aggregation that gives rise to fine stranded (string of beads) network structures. Many proteins (e.g. globular proteins) can form either type of gel network depending on the balance of forces. The

intermolecular interactions are generally controlled by both attractive hydrophobic and repulsive electrostatic interactions, although other interactions such as disulphide bridging and hydrogen bonding would also contribute to the final gel strength

### *3.4.2.2.2. High-pressure gelation*

High pressure offers an additional degree of freedom in modifying functional properties of molecules, because high pressure can be applied as a single process or in combination with others, in particular with increased temperatures. In general, high pressure favours reactions, which lead to a reduction of the overall volume of the system. Pressure causes water to dissociate (Banerjee and Bhattacharya 2012).

### *3.4.2.2.3. pH-induced gelation*

Changes in pH due to the addition of acids or microbial fermentation change the net charge of the molecule and therefore modify the attractive and repulsive forces between molecules as well as the interactions between molecules and solvent. In addition, the solubility of salts changes with pH which may contribute to gel formation. The mechanism of acid gel formation could be explained by the fractal aggregation theory (Banerjee and Bhattacharya 2012).

### **3.4.2.3. Physicochemical properties of protein gels**

To form a gel, the food material must contain large molecules capable of forming cross-links in three dimensions. Proteins have many advantages for this purpose due to their chemical composition and reactivity. Compared with carbohydrates, they are able to form a wider range of cross-links and they have a higher nutritional value. However, these advantages have to be balanced against the increased cost of some proteins and the fact that

generally much higher concentrations are required to form a protein gel than a carbohydrate gel.

For gel production, some of the most important properties are their flexibility, their ability to denature and give extended chains, and, their ability to form extensive networks by cross-linking (Damodaran 1997).

### 3.4.2.3.1. *Protein interactions*

Physical characteristics of gels result directly from a continuous molecular network spanning the volume of the gel. Gelation occurs when the conditions are such that the molecules are induced to aggregate in some way. As previously discussed, regardless of the gel-inducing agent used (heat, pressure or chemical additive), the molecules partly unfold, exposing previously hidden reactive groups. These groups can then react intermolecularly to form a continuous network.

The stability of protein structures arises from a combination of covalent bonds, particularly disulphide bonds, with non-covalent, intermolecular connections provided by hydrogen and electrostatic bonds and hydrophobic effects. Some of the non-covalent bonds are relatively weak although collectively they confer great strength.

For maximum stability, all possible bonds will be formed. Electrostatic bonds may be stronger than other non-covalent bonds, but their existence is determined by the pH and salt concentration. Hydrogen bonds and hydrophobic forces depend very much on the unique nature of water as a solvent. Because water is both a hydrogen bond donor and a hydrogen bond acceptor, liquid water itself is a continuous molecular network but an exceedingly transient one, continuously reforming and regrouping. No other liquid is held together by such strong and directional intermolecular forces. In aqueous solution, nonpolar molecules, or molecules carrying nonpolar groups,

are surrounded by an ordered or structured layer of water molecules. When these nonpolar molecules approach each other some of the ordered water molecules are squeezed out, and the molecular rearrangements that this entails provide the thermodynamic driving force for hydrophobic interaction.

The main covalent cross-links that join protein chains are the disulphide bonds of cysteine residues. These interactions stabilize the structure of many proteins. They have great strength but are broken by sulfhydryl-containing compounds and some other reducing agents and by oxidizing agents such as peroxides. They are formed readily by the mild oxidation of sulfhydryl groups. The ability of these disulphide bonds to undergo sulfhydryl-disulphide interchanges confers flexibility on protein structures.

Finally, the last important contribution is achieved by means of the Maillard reactions (Ellis 1959). Maillard reactions are a complex series of reactions between amino and carbonyl compounds. They take typically place when proteins are heated with reducing sugars, and as a consequence, covalent cross-links are formed which may substantially contribute to the gel network.

### *3.4.2.3.2. Denaturation and Formation of Extended Protein Chains*

Partial or complete denaturation is required for gelation. During denaturation, proteins undergo unfolding of their three-dimensional structures to give extended chains but without rupture of covalent bonds.

Denaturation, or partial denaturation, exposes at least some of the hydrophobic parts of the molecule to the solvent. Thus, regions of the molecule originally involved in maintaining the stability of the native form become available for intermolecular bonding and a network will form. Complete denaturation of the protein is not often necessary for gelation; in



fact, a completely denatured protein usually forms an insoluble precipitate because of extensive hydrogen bonding or hydrophobic interactions between unfolded chains

During denaturation by heat, the protein concentration may be important, high concentrations are more likely to give precipitates, and low concentrations are likely to give gels. Gelling occurs especially at the boundary between aggregation and solubility (Damodaran 1997).

### *3.4.2.3.3. Opacity/transparency*

Protein gels are usually opaque. Opaque gels are formed when fluctuations in polymer density approach macroscopic size and effectively scatter light. Such networks are characterized by regions of high polymer concentration separated by regions nearly devoid of polymer.

Transparent gels, on the other hand, have an almost homogeneous network. In some protein gel systems there can be a transition from transparency to opacity. This transition can be addressed by a model proposed by Hegg (1982) for the gelation of globular proteins. According to this model, linear aggregates are formed at pH values far from the isoelectric point and low ionic strength and the system remain at the sol state. A reduction of electrostatic repulsions leads to formation of fine stranded transparent gels. However, a further reduction, obtained at high ionic strength or at pH values close to the isoelectric point, gives rise to a heterogeneous particulate network of random aggregates leading to a turbid gel.

### *3.4.2.3.4. Thermal reversibility*

Thermal-induced protein gels are almost invariably irreversible. Thus, if a gel forms when the protein solution is heated, cooling or further heating does not reverse the process. Gelatine is the most notable exception, since it form cold-set thermoreversible gels.

### *3.4.2.3.5. Rheological properties*

A gel is a semi-solid material. Consequently it has rigidity but readily deforms under application of a stress. When we apply a force to an elastic solid, the shape changes and the deformation is proportional to the applied force. When this force is removed, the material springs back to its original shape and most of the energy used in producing the deformation is recovered.

The rheological response of a gel to a deformation provides fairly relevant information about the characteristics of the gel. However, it is important to distinguish between those rheological measurements performed under small deformations and those made with large deformations since they provide very different classes of information about the nature of the gel (Mezger 2006).

Measurements with large deformations are easy to perform with relatively simple devices, and hence they are the most frequently reported type of gel measurements. However, small deformation tests required the development of suitable measuring technology to achieve such small deformations, either under dynamic or static conditions, in order to obtain dynamic viscoelastic properties or the elastic modulus. Current rheometers are capable of measuring ultra-low deformation or deformation rates, however its development did not take place until recently (i.e. commercial controlled-stress rheometers started to be available in the mid-1980s).

From a rheological point of view gels are complex materials that are complex to measure. Thus, as previously mentioned, gelation arises either from chemical cross-linking, by way of covalent reactions, or from physical cross-linking, through polymer-polymer interactions. Moreover, the macromolecular substances responsible for network formation in food systems are primarily polysaccharides and proteins, which are present in small amounts. In fact, the unifying property among these foods is that

compositionally they are mostly fluids but rheologically they respond as viscoelastic solids with a high degree of elasticity. In addition, they usually fracture rather than flow when deformed. This property is inherent in sensory biting and mastication of foods so it is important to relate the fracture character of gels to their sensory texture. There are several methods for determining fracture properties of foods based on uniaxial compression, uniaxial tension, or torsion. However, the uniaxial compression is the most commonly used method

Traditionally, single point measurements have been used to characterize gel systems. However, these single point measurements, often based on rupture tests, are not representative of the overall mechanical behaviour of gels. To evaluate the rheological properties of gels many considerations should be taken into account (e. g. composition)

There are several classifications which may be used for gels. First of all, biopolymer gels can be classified based on the level of order of the macromolecule, both before and during the network formation: gels formed from disordered biopolymers (carrageenan, pectin, starch, gelatine) or gel networks that involve specific interactions between denser and less flexible particles, such as thermally denatured globular proteins and aggregated proteins from enzymatic or chemical action. Other classification is based on the macroscopic behaviour of gelled system. Thus, true gels are a consequence of the development of the three dimensional networks, and weak gels are characterized by a tenuous gel-like network that is easily broken when submitted to a high enough stress.

Stress-strain tests are useful in studying the behaviour of food gels and generally can be categorized as two types: small-strain and large-strain testing.

In small-strain testing the strain must be low enough to avoid any unrecoverable structural change (e.g. SAOS tests). On the other hand, large-strain testing refers to deforming a sample above to the point of permanent structural change. This later group of tests often yields information that correlates with sensory evaluation (Schramm 2000).

### *Small-strain testing. Oscillatory test*

Since gels exhibit viscoelastic behaviour, dynamic rheological tests to evaluate properties of gel systems are widely used for studying the characteristics of gels as well as gelation and melting. Figure 3.4-2 illustrates the change in modulus when the gel transforms its liquid-like structure to gel-like structure.

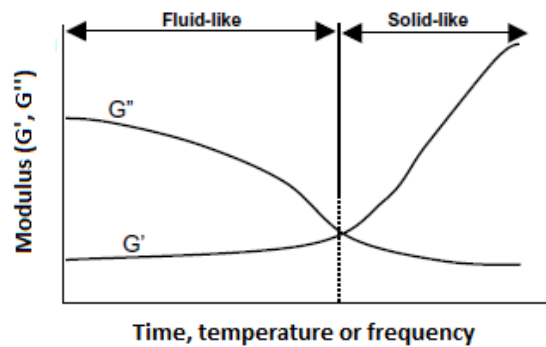


Figure 3.4-2: Viscoelastic response of a material

If  $G'$  is much greater than  $G''$ , the material will behave more like a solid; that is, the deformations will be essentially elastic. However, if  $G''$  is much greater than  $G'$ , the energy used to deform the material is dissipated viscously and the material exhibits liquid-like behaviour.

Three types of dynamic tests are usually used to obtain useful properties of gels, gelation, and melting:

- 1) Frequency sweep studies in which  $G'$  and  $G''$  are determined as a function of frequency, at fixed temperatures.
- 2) Temperature sweep tests in which  $G'$  and  $G''$  are determined as a function of temperature at fixed frequency.
- 3) Time sweep in which  $G'$  and  $G''$  are determined as a function of time at fixed frequency and temperature.

### *Kinetics of Gelation*

Measurement of gelation kinetics requires a method for following the development of the gel network without significantly affecting the process by mechanical disturbance.

The most widely used technique to study gelation kinetics, arisen after the development of controlled-stress rheometers, involves formation of the gel between the plates of an oscillatory rheometer (Hermansson 1986). With this type of instrument, provided that conditions are chosen appropriately, it is possible to monitor the evolution of the linear viscoelastic functions over the gelation process (Damodaran 1997).

In fact, nowadays the most universally accepted definition of the gel point comes from the determination of linear viscoelasticity properties associated to the development of a self-similar structure of the so-called critical gel (Winter 1987). Materials at the gel point exhibit a distinct rheological behaviour where the following power law equation holds for linear viscoelastic functions:

$$G'(\omega) = k_1 \cdot \omega^n \quad (3.4-9)$$

$$G''(\omega) = k_2 \cdot \omega^n \quad (3.4-10)$$

where  $n$  is the relaxation exponent and  $k_1, k_2$  are constants related to this exponent and to the gel stiffness. As a consequence, the loss tangent is frequency independent at the critical gel. In practice, the gel point has been widely determined as the point at which  $\tan(\delta)$  is not a function of frequency.

### 3.4.2.3.6. *Gel Strength*

Many different instruments are available for measuring gel strength. Some simply results that provide empirical tests cannot be related to fundamental rheological quantities. However, there are other tests that can measure well-defined parameters such as shear modulus or rupture strength. A typical test measures the force applied for the gel versus displacement.

In any case, as previously mentioned, modern rheometers are the most extended devices used to characterize gels. Moreover, among the different measurement techniques that rheometers can perform, SAOS measurements of viscoelastic properties using parallel plates or cone-plate geometries are preferred, since they allow monitoring the change in structure over gelation, which is based on the assumption that the material's behaviour is linear. Gel strength can then be related to linear viscoelastic functions ( $G'$ ,  $G''$ ,  $\tan \delta$ , etc).

### 3.4.2.3.7. *Water holding capacity (WHC)*

Mainly, there are two causes which contribute to the water holding capacity of a material: the polarity (including surface charges) and the capillarity, which is the most important. For this functional property, myofibrillar proteins are the most important. Thus, water is able to be held mainly in the holes between actin and myosin filaments.

### 3.4.2.3.8. *Microscopy*

Microscopy techniques are widely used for the characterisation of the protein microstructure. Optical microscopy may be used, however LSCM and

SEM, described above, are some of the most useful techniques for the visualization of gel microstructure.

### **3.4.2.4. Nutritional properties**

#### **3.4.2.4.1. *Antioxidant properties of food gels***

Free radicals are generated through normal reactions within the body during respiration in aerobic organisms. The presence of these potentially toxic products can give rise to several diseases. Air pollutants and oxidants in tobacco can typically cause some harmful reactions in skin or can be absorbed to blood circulation, exerting some adverse effects. Additionally, UV radiation can be a producer of a variety of oxidants.

The free radicals, which are physiologically produced, can provide a protection against infections. According to the free radical theory of ageing developed by Denham Harman, organisms age when free radicals accumulate in cells and cause harm over time. In this way, reactive species can cause damage in proteins, and mutations in DNA, oxidation of membrane phospholipids and modification in low density lipoproteins (LDL). Thus, antioxidant compounds can remove reactive species through enzymatic and non-enzymatic antioxidants. However, in certain circumstances the endogenous immune system fails to protect the body against reactive radicals on its own.

This brings about the need for synthetic and natural antioxidants, which can prevent oxidative stress and its deleterious effects. Synthetic antioxidants are cost-effective and efficient but display some toxic and hazardous effects. In the areas of human nutrition, and biochemistry, natural antioxidants from food resources have been the focus of growing interest for their potential health benefits with little or no side effects (Sarmadi and Ismail 2010).

### *Antioxidative peptides in food products*

Several peptides from protein ingredients have been found to possess antioxidant ability. Antioxidant peptides from foods contain 5-16 amino acid residues and are considered to be safe and healthy compounds with low molecular weight, low cost, high activity and easy absorption. They have some advantages in comparison to enzymatic antioxidants; that is, with simpler structure they have more stability in different situation and no hazardous immunoreaction. In addition, they present nutritional and functional properties beside their antioxidant activity. There are two different forms of antioxidant activity: either as hydrolysates of precursor proteins or as bioactive peptides. Hydrolysate is a mixture that is mainly composed of peptides and amino acids which are produced through protein hydrolysis by enzyme, acid or alkali treatment

The exact mechanism underlying the antioxidant activity of peptides has not fully been understood, yet various studies have displayed that they are inhibitors of lipid peroxidation, scavengers of free radicals and chelators of transition metal ions. Antioxidative properties of the peptides are more related to their composition, structure, and hydrophobicity. Tyr, Trp, Met, Lys, Cys, and His are examples of amino acids that cause antioxidant activity. Amino acids with aromatic residues can donate protons to electron deficient radicals. This property improves the radical-scavenging properties of the amino acid residues. It is proposed that the antioxidative activity of His-containing peptides is in relation with the hydrogen-donating, lipid peroxy radical trapping and/or the metal ion-chelating ability of the imidazole group. In addition, SH group in cysteine has an independently crucial antioxidant activity due to its direct interaction with radicals. Nevertheless, protein linkage conformation and structural features of the peptides have been claimed to influence antioxidant ability (Sarmadi and Ismail 2010).



### **3.4.3. Bioplastics**

The bioplastics industry is a strongly growing part of the plastics industry. With a global production capacity around 1.7 million tonnes per year in 2014, the volume in the market is still small compared to the overall plastics volume of 320 million tonnes/year. However, according to recent estimations, the share of bioplastics will increase up to 7.8 million tonnes of bioplastics (2-3 percent of plastics market) in 2019 (Plastics-Europe 2008).

According to European-bioplastic Association, the term bioplastic encompasses a whole family of materials which have some differences with conventional plastics because they are bio-based, biodegradable, or both. Thus, two kinds of bioplastic materials can be distinguish according to this definition:

- Bio-based materials, in which the material or product is derived from biomass, which can stem from either plant or animal sources.
- Biodegradable polymeric materials, where the term biodegradable refers to a chemical process during which micro-organisms, which are available in the environment, convert materials into natural substances. Obviously, the process of biodegradation depends on the surrounding environmental conditions (moisture, temperature, light, O<sub>2</sub>), and on the material itself. Biodegradability is an inherent property of certain bioplastic materials that can benefit specific applications (Plastics-Europe 2008)

#### **3.4.3.1. Materials used in the bioplastic manufacturing**

Usually, a bioplastic material (of the biodegradable group) consists of a polymeric network formed by a biodegradable macromolecular substance (in this case is a protein) and a plasticiser.

### *3.4.3.1.1. Natural raw-materials*

In recent years there has been a great interest to utilize renewable biomass in order to manufacture consumer goods which exhibit high-quality, cost-competitive and biodegradable, reducing the consumption and the dependence on petrochemical feedstock and diminishing environmental pollution (Rosentrater and Otieno 2006, Felix, Martin-Alfonso et al. 2014).

Mainly, proteins and polysaccharides have been postulated as renewable biomass to manufacture biopolymers for many years (De Graaf 2000, Hernandez-Izquierdo and Krochta 2008). Polysaccharides are naturally extended, and are widely used for food industry. These compounds have been also used for bioplastics (e.g. starch and chitosan are good examples of polysaccharides used for this purpose). As regards proteins, they are a renewable, biodegradable resource with great potential to improve the quality and stability of a large range of food products by using a number of processing techniques (Romero, Cordobes et al. 2008, Jayasundera, Adhikari et al. 2009, Erni, Windhab et al. 2011). For a long time, proteins have been used to produce edible materials, but understanding of the precise physical and chemical mechanisms of protein interactions, they can be used to produce stable bioplastic materials (Hernandez-Izquierdo and Krochta 2008, Balaguer, Gomez-Estaca et al. 2011).

### *3.4.3.1.2. Plasticisers*

Plasticizers are generally added to improve the processability of the protein network, as well as in order to modify the properties of the final structure, decreasing the glass transition and the brittleness. Usually, plasticizers consist of compounds which exhibit low-molecular weight, low volatility and that interact with the polymer chains producing swelling (Hernandez-Izquierdo and Krochta 2008).

This type of compounds is widely used in polymer industries as additives. The primary role of such substances is to improve the flexibility and processability of polymers by lowering the second order transition temperature, the glass transition temperature ( $T_g$ ). The council of the IUPAC (International Union of Pure and Applied Chemistry) defined a plasticizer as “a substance or material incorporated in a material (usually a plastic or elastomer) to increase its flexibility, workability, or distensibility”.

These substances reduce the tension of deformation, hardness, density, viscosity and electrostatic charge of a biopolymer, at the same time as increasing the polymer chain flexibility, resistance to fracture and dielectric constant. Other properties are also affected, such as degree of crystallinity, optical clarity, electric conductivity, fire behaviour and resistance to biological degradation (Vieira, da Silva et al. 2011).

There are many plasticizer for protein-based bioplastics, such as: 1,4-Butanediol, DATEM<sup>a</sup>, Dibutyl, Glycerol, Lactic acid, Octanoic, Palmitic acid, Sorbitol, Sucrose and Water (Hernandez-Izquierdo and Krochta 2008).

For this study, Glycerol has been the chosen plasticizer. This is a widely used bioplastic, exhibiting hydrophilic properties with a low molecular weight, and high boiling point. Its high plasticizing effect has been attributed to the ease with which glycerol can insert and position itself within the 3-dimensional biopolymer network (di Gioia and Guilbert 1999).

### 3.4.3.2. **Methods for protein-based bioplastics manufacturing**

#### 3.4.3.2.1. *General approach*

Proteins offer a large range of possible physical and chemical interactions. This dual character is given because proteins can participate in non-covalent interactions such as ionic, hydrogen, and van der Waals bonding

or in chemical reactions through covalent linkage (peptide and disulphide bonds).

Usually, the formation of the protein network is divided in two main stages: Plasticization and protein interactions (Hernandez-Izquierdo and Krochta 2008).

The plasticizing effect of small polar molecules has been described in terms of insertion and positioning within the 3-dimensional protein network. Mainly, there are four theories to explain this process:

- 1) The lubricity theory, where the plasticizer is acting as a lubricant to facilitate mobility of the chain molecules.
- 2) The gel theory, which considers the disruption of polymer-polymer interactions (weak physical interactions).
- 3) The free volume theory, which considers that the plasticizer increases the free volume and mobility of polymer chains (used to understand the effect of plasticizers in lowering the glass transition temperature).
- 4) The coiled spring theory, which explains plasticizing effects from the point of view of tangled-macromolecules.

However, the various possible ways in which proteins may interact during thermoplastic processing are unclear. Thus, the reactivity of proteins depends on their physicochemical environment as well as on the thermomechanical treatment used (Hernandez-Izquierdo and Krochta 2008).

### **3.4.3.2.2. *Solvent casting***

For the formation of protein films or coatings, the protein has to be first dissolved in a proper solvent, which sometimes requires heating or pH

adjustment, as well as the addition of some compounds which could improve film-forming or other properties

Subsequently, the mixture is heated above the lipid melting point and then homogenized. Degassing is an important step to eliminate bubble formation in the final film or coating. Finally, the protein film or coating is formed by applying the prepared formulation to the desired casting or product surface and allowing the solvent to evaporate. Providing heated air at low humidity and high velocity increases drying rates (Krochta 2002).

### *3.4.3.2.3. Thermo-mechanical processing*

#### *Compression moulding*

Compression moulding technique use the combination of high temperatures, high pressures, short times, and low moisture contents in order to the transform the protein-plasticizer blends into viscoelastic melts. Then, the protein-based bioplastics are formed by cooling, increasing hydrogen, ionic, hydrophobic, and covalent interactions (Hernandez-Izquierdo and Krochta 2008). The use of higher compression moulding temperatures typically promotes a more extensive protein denaturation, and as a consequence higher cross-linking.

Compression moulding can result in the formation of protein-based films or materials whose mechanical and barrier properties are dependent on the formulation and processing conditions used. This technology is suitable for investigating the thermoplastic properties of plasticized proteins as well as the properties of the resulting films and materials (Hernandez-Izquierdo and Krochta 2008).

### *Extrusion*

Extrusion is one of the most important polymer processing techniques in use nowadays, and consequently it is quite interesting to assess bioplastic formation through this technique. Therefore, extrusion of bioplastics would increase their commercial potential, offering several advantages over other techniques.

An extruder is able to apply high-temperature in a short-time, where the raw materials are continuously introduced into a hopper, conveyed by a screw, and pushed through a die of a desired shape. This process can involve any or all of the following operations: heating, cooling, feeding, conveying, compressing, shearing, reacting, mixing...

The extruder barrel can be subdivided into 3 processing zones:

- 1) The feeding zone.
- 2) The kneading zone.
- 3) The heating zone.

Controllable or process variables include screw speed, screw configuration, screw length-diameter ratio (L/D), barrel temperature profile, moisture addition, feed rates, and die size/shape, among others.

### *Injection moulding*

Injection moulding is one of the most frequently used polymer processing techniques to obtain a wide range of plastic materials. However, this technique has not been used much to process biopolymers (Felix, Martin-Alfonso et al. 2014), The process entails the injection of melted polymer into a closed mould, which is normally cooled to facilitate rapid solidification, to produce discrete products. The moulds can be single or family moulds. The

machines are rated by their clamping force and shot capacity. As for the case of protein-based bioplastics, the biopolymer is heated in a pre-injection stage at a higher temperature than the  $T_g$  of the dough-like material, favouring the mobility of protein chains. Subsequently, the dough-like material is injected into the mould cavity which is heated in order to favour the crosslinking reactions. Finally, the bioplastic material is cooled. This type of processing is different from the regular procedure used for thermoplastic polymers because of the specific behaviour exhibited by protein-based materials which is intermediate between thermoplastic and thermoset polymers (Felix, Martin-Alfonso et al. 2014, Martin-Alfonso, Felix et al. 2014).

### **3.4.3.3. Properties of the protein bioplastics**

There are many properties that can be attributed to this kind of materials, the importance of which depend on their application. Some of the most relevant are summarised below:

#### **3.4.3.3.1. Barrier properties**

The main advantage of edible films and coatings is generally based on their potential to provide some combination of moisture, oxygen, flavour, aroma or even colour for a food or drug, with a resulting increase in quality and shelf life (Krochta 2002). Thus, the permeability properties of edible films to these substances are of interest.

Permeability is defined as a steady-state property that describes the extent to which a permeating substance dissolves and then the rate at which the permeant diffuses through a film. To achieve this, usually the driving force is related to the difference in concentration of both sides of the film.

The polar character of proteins determines the barrier properties of protein films and causes the high permeability to polar substances, such as water vapour, and low permeability to non-polar substances.

The challenge is to use the appropriate protein and plasticiser in order to obtain desirable barrier properties, while achieving other essential properties such as film flexibility, strength, and solubility (Krochta 2002).

### *Water vapour permeability (WVP)*

Protein films have quite high WVP compared to edible waxes. Thus, protein film exhibits WVP values two to four orders of magnitude greater than that of Low-density polyethylene (LDPE). Usually, higher plasticizer concentration involve an increase of WVP (Krochta 2002).

### *Oxygen permeability (OP)*

At low to intermediate relative humidity, protein films have values of oxygen permeability that are lower than those of the polyethylene-based plastics (which are not good oxygen barriers), and are comparable to as polyesters. The low OP of protein films would appear to make them useful for coatings and pouches for oxygen-sensitive products (Krochta 2002).

### *3.4.3.3.2. Thermal properties*

Thermal transitions of the films should be investigated in order to predict protein-based package behaviour under different end-use conditions. Thus, differential scanning calorimetry and dynamic mechanical thermal analysis have been the most common thermal analysis techniques used in determining the glass transition temperatures of protein-based films. These techniques are going to be explained further, but now it is possible to say that during DMTA testing, as temperature increased, moisture was lost from the films, resulting in higher transition temperatures. Therefore, DSC was considered to be a more reliable technique in determining the  $T_g$  values of protein sheets containing moisture (Krochta 2002).



#### 3.4.3.3.3. *Microstructural properties*

The microstructural characteristics of protein-based films are a function of the formulations and processing conditions used to manufacture the films. It is possible to use different techniques such as AFM, SEM or even confocal Microscopy in order to obtain images illustrating the bioplastic microstructure.

#### 3.4.3.3.4. *Viscoelastic behaviour.*

Viscoelastic behaviour of polymers can be analysed by dynamic mechanical thermal analysis (DMTA).

Typically, this technique consists in the application of a sinusoidal bending stress to a material and the resultant sinusoidal strain is measured, allowing one to determine viscoelastic parameters such as storage modulus, loss modulus and  $\tan \delta$ . Most DMA measurements are made using a single frequency and constant deformation (strain) amplitude while varying temperature.

The task of evaluating new materials and projecting their performance for specific applications is a challenging one for engineers and designers. Often, materials are supplied with short-term test information, which has to be used to project long-term, high-temperature performance. DMTA tests continuously monitors material modulus with temperature and, hence, provides a better indication of long-term, elevated temperature performance. Predicting the changes in viscoelastic properties that occur as a result of plasticization and processing conditions is essential for process design, evaluation, quality control, and stability of the product. In order to detect and measure the temperatures at which the amorphous domains of proteins reach the free-flow state, methods such as DMTA can be used. DMTA is also used to relate structural and viscoelastic properties to changes in temperature,

frequency and/or deformation. In addition, DMTA is even capable of detecting glass transitions as an alternative to DSC, especially when changes in heat capacity are too small (Hernandez-Izquierdo and Krochta 2008).

#### 3.4.3.3.5. *Differential Scanning Calorimetry*

Differential Scanning Calorimetry (DSC) has been used to characterize protein interactions. This technique is widely used to characterize the thermal transitions of a polymer. Protein and protein-plasticizer thermal transitions detected by DSC include the glass transition temperature ( $T_g$ ), melting, crystallization, thermal denaturation, aggregation, and protein degradation.

#### 3.4.3.3.6. *Tensile measurements*

In this assay the device measures load or force and displacement (or extension). The stress ( $\sigma$ ) is related to force ( $F$ ) and the specimen cross-sectional area ( $A$ ) by  $\sigma = F/A$ ; and extension ( $\Delta L$ ) and specimen gauge length ( $L$ ) to strain ( $\epsilon$ ) by  $\epsilon = \Delta L/L$ . Another parameter is the Poisson's ratio,  $\nu$ , which indicates the change in the specimen cross-section as a result of axial strain and is expressed as a ratio of lateral strain to axial strain EQ. (3.4-11):

$$\nu = -\frac{\frac{\Delta w}{w}}{\frac{\Delta L}{L}} \quad (3.4-11)$$

where  $w$  is the specimen width

In addition, tensile parameter of Young's modulus (elastic modulus,  $E$ ), the yield strength, the tensile strength and the maximum elongation can be extracted from the stress-strain curves.

Figure 3.4-3 shows a typical representation of a stress-strain curve:

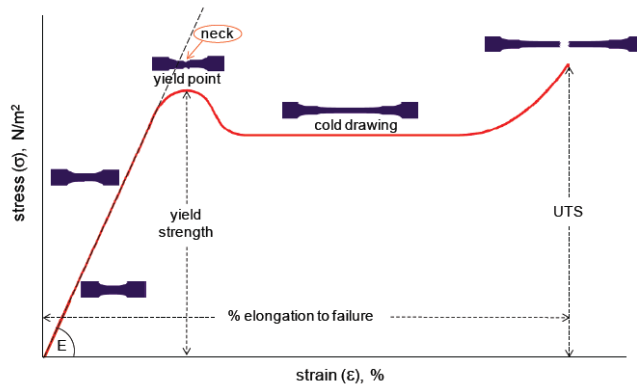


Figure 3.4-3: Representation of a typical polymer stress-strain curve

In the elastic region, the strain is small and there is a linear relationship between stress and strain where Hooke's law holds, and material can instantly revert back to its original form when unloaded. Young's modulus ( $E = \sigma / \epsilon$ ) is determined by using the stress and strain data extracted from this elastic region. Beyond the elastic region and up to approximately the yield point, there is a non-linear viscoelastic region within which the material can recover to its original form over time.

Above the yield point, the material begins to deform plastically, (the material will undergo permanent deformation) and therefore, upon the release of load only the elastic portion of the strain will be recovered and plastic deformation will not be recovered. In addition, at the yield point the material begins to neck, and as a consequence, the specimen cross-sectional area undergoes a significant reduction, such that further elongation causes a fall in load and, in nominal stress (engineering stress). Note that the engineering stress is calculated by dividing the load with the initial cross-sectional area of the specimen and it should be distinguished from the true stress, which is calculated by using the actual cross-section of the specimen during the test. Accordingly, the true stress does not decrease at

necking/yielding but either remains approximately constant or rises less steeply with increasing strain, depending on the extent of cold drawing.

Cold drawing succeeds the yield point where material undergoes permanent deformation as a result of molecular slippage. Continuing extension of the narrow portion of the dumbbell specimen is achieved during drawing by causing the shoulders of the neck to travel along the specimen as it reduces from the initial cross-section to the drawn cross-section. At further elongations, the slope of the stress-strain curve increases again, due to “strain hardening”/“molecular orientation”, and finally material failures (Akay 2012).

This type of curve is very useful since allows to classify the material. For instance, Figure 3.4-4 compares four different plastic materials:

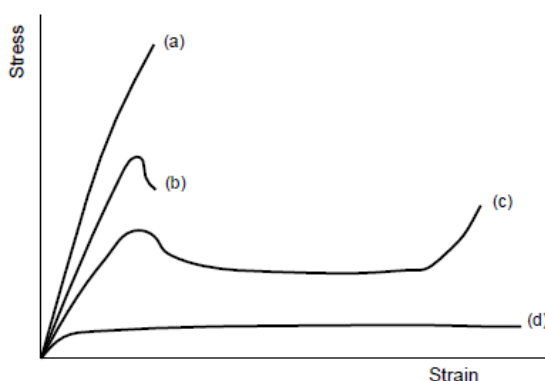


Figure 3.4-4: comparison between different curves stress-strain

Thus we can say that (a) is a low ductility polymer, (b) is a ductile polymer, (c) is a ductile polymer capable of cold drawing, and (d) is a polymer with long-range elasticity (Akay 2012).

### 3.4.3.4. Applications of protein bioplastics

The main goal of biodegradable bioplastics is to achieve the replacement of existing synthetic, non-biodegradable products for these others at the

lowest cost possible. Other goals may be also found for specific applications. For instance, edible films and coatings aim for improving food quality and shelf life by reducing the effect of moisture, oxygen, migration, etc., protecting food from microbes, maintaining food product integrity, and enhancing product appearance. However, this must be related to the cost of coating materials and to the cost of the coating process.

Certain new edible film and coating materials made from proteins are targeted for replacing materials currently used in existing applications. However, compared to the large number of studies performed on film formation and properties, a relatively small number of application studies have been performed. For this reason, information available is generally lacking on approaches to coating foods, as well as the resulting effectiveness of edible films and coatings in food systems. This makes it very difficult for food processors to decide on the “value-added” merit of an edible film or coating relative to the additional cost involved (Krochta 2002).


### **3.4.3.5. Composite materials**

A composite compound is a material made by combining two or more materials, and frequently they have very different properties. The two materials work together to give the composite unique properties. However, within the composite you can easily tell the different materials apart as they do not dissolve or blend into each other.

Natural composites exist in both animals and plants from the early beginnings. Thus, wood is a composite which is made from long cellulose fibres (a polymer) held together by a much weaker substance called lignin. The two weak substances (lignin and cellulose) together form a much stronger structure.

Nowadays, human have synthesized this kind of compounds. The first modern composite material was fibreglass. It is still widely used today for boat hulls, sports equipment, building panels and many car bodies. The matrix is a plastic and the reinforcement is glass that has been made into fine thread. On its own, the glass is very strong but brittle and it will break if bent sharply. The plastic matrix holds the glass fibres together and also protects them from damage by sharing out the forces acting on them.

Some advanced composites are now made using carbon fibres instead of glass. These materials are lighter and stronger than fibreglass but more expensive to produce. They are used in aircraft structures and expensive sports equipment. Carbon nanotubes have also been used successfully to make new composites.



*A Alberto y Antonio*

*Por ayudarme a crecer junto a ellos,  
Por ser una pieza clave en mi formación como investigador, por todas esas  
horas de trabajo que hemos pasado juntos.*







## 4. Materials and Methods

---



## 4.1. Materials

### 4.1.1. Crayfish powder

The CF meat was separated from the shell by grinding and sieving and supplied as CF pulp by ALFOCAN (Isla Mayor, Sevilla, Spain). Figure 4.1-1 shows the process followed to obtain different protein fractions from crayfish (CF) meat. CF pulp was kept frozen until its use. After thawing at 4°C, CF pulp was homogenized and subjected to centrifugation at 15,000 x g for 15 minutes in a Centromix II-BL (Selecta, Spain), obtaining three different phases: a heavy phase, CF1P (c.a. 20 wt. %), an intermediate phase (CF2P) which is the aqueous phase (c.a. 70 wt. %) and a light phase, CF3P (c.a. 10 wt. %). The CF2P was the selected phase because it is the water soluble protein fraction and it represents the highest protein content. Finally, the intermediate phase (CF2) was freeze-dried in a BETA 1-8 LD Plus Series (CHRIST, Germany) to obtain a powder-fraction rich in proteins. This phase will be named CF2L.

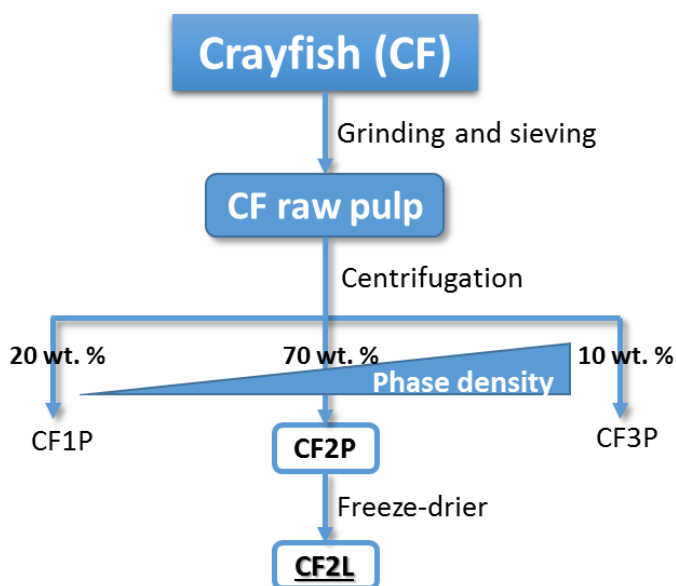


Figure 4.1-1 : Diagram of the procedure carried out in order to obtain the CF2L protein concentrate.

The protein content of the CF2L was determined in quadruplicate as % N x 6.25 using a LECO CHNS-932 nitrogen micro analyser (Leco Corporation, St. Joseph, MI, USA) from Microanalysis service (CITIUS, University of Seville). In the same way, lipid, moisture and ash contents were determined according to A.O.A.C. (2000). Table 4.1-1 shows the elemental characterisation of CF2L system:

<b>Component</b>	<b>wt. %</b>
<b>Protein</b>	78.6 ± 0.5
<b>Moisture</b>	6.8 ± 0.1
<b>Lipid</b>	5.1 ± 0.3
<b>Ash</b>	9.5 ± 0.6

*Table 4.1-1: Elemental characterisation of CF2L system*

First of all, it is remarkable the high protein percentage (ca. 80 wt. %). Hence, according to Pearson classification (1983), it must be considered as a protein concentrate. Furthermore, this system contents up to 5 wt. % of lipids despite centrifugation stage was carried out. That means that this stage is not able to a complete organic and aqueous phases separation, or in the manual procedure of separating both phases a certain amount of organic phase was adjoined together to aqueous phase.

All systems studied have in common this protein concentrate, however for each product (emulsion, gel or bioplastic) some modifications have been considered: for emulsions a polysaccharide (a gum) have been used to provide stability. In addition, for gels three hydrolysed systems have been obtained at three different degree of hydrolysis and for bioplastics with a low-value crayfish flour have been evaluated in order to be cost-competitive with synthetic polymers.

### 4.1.2. Materials for Emulsions

The oil-in-water emulsions consist of a continuous phase of distillate water and dispersed phase of high oleic oil. To provide stability, apart from the initial crayfish protein concentrate (CF2L), a polysaccharide (xanthan gum) was used in order to improve the system stability. Gums have a high influence on the structural characteristics of food products, modifying the texture and the organoleptic properties, even being present at concentrations lower than 1 wt. %. For this reason, gums are nowadays widely used for fat replacement in many low-calorie products (Williams and Phillips 2003). Xanthan gum was discovered in the 1950s and nowadays have widely application in the food industry, where was introduced in the early 1970s. This gum is obtained from the genus *Xanthomonas* by aerobic fermentation

Figure 4.1-2 shows the primary structure of the Xanthan gum (XG):

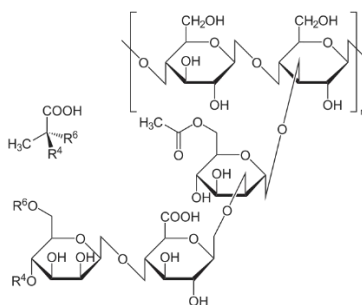


Figure 4.1-2: Primary structure of xanthan gum

. The xanthan gum is an anionic molecule which has a (1,4)-β-D-glucopyranose backbone and a trisaccharide side chain on every other glucose residue linked through the C3 position. The side chain consists of two mannopyranosyl residues linked on either side to a glucopyranosyl uronic acid group. The inner mannose residue which is connected to the backbone may be acetylated while the terminal mannose residue may be pyruvated. The

molecular mass of the xanthan molecules is very high ( $> 3 \times 10^6$ ) and is soluble in water to give highly viscous solutions (Williams and Phillips 2003).

Xanthan gum is widely used nowadays for emulsion stabilisation, one of this advantages is its stability at low pH, as well as its ability to slow down the separation of the oil-and-water phases. In addition, it is a rheological modifier, exhibiting pronounced shear thinning characteristics (Williams and Phillips 2003).

### 4.1.3. Materials for gels

Apart from the above mentioned crayfish flour obtained by using freeze-drying process, three different hydrolysates were obtained. The hydrolysis was carried out at 50°C using trypsin as proteolytic enzyme. After hydrolysis, enzyme was deactivated by heating for 15 min at 90°C. The degree of hydrolysis was determined by Formol titration (Taylor 1957), which uses formaldehyde to react with terminal amino groups. Figure 4.1-3 shows the kinetic of CF2L hydrolysis carried out:

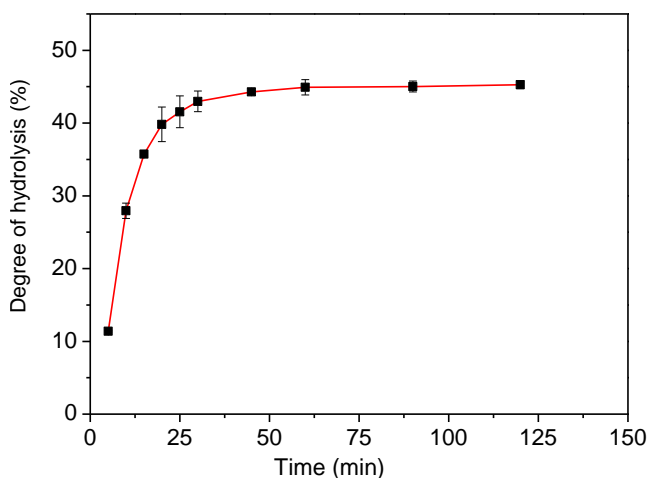


Figure 4.1-3: Kinetic of CF2L hydrolysis

This figure shows a fast increase in the degree of hydrolysis at the beginning of the enzymatic process, followed by a plateau zone at the end of it. This enzymatic behaviour is typical, since follows a Michaelis-Menten kinetics (Dowd and Riggs 1965). Three different systems, which correspond to three different hydrolysis times, were selected. The hydrolysis times selected were 5, 25 and 120 min, obtaining systems with  $11 \pm 1$ ,  $31 \pm 1$  and  $45 \pm 2$  degree of hydrolysis (%), respectively.

### **4.1.4. Materials for Bioplastics**

Apart from the common protein concentrate, the others polymers used were a low-cost protein concentrate obtained from crayfish, and a biodegradable polymer called polycaprolactone (PCL).

First of all, the low cost protein concentrate was selected to be cost competitive because plastic industry is nowadays very well developed. This selected powder is an industrial by-product that nowadays is used for animal feed and may suppose a cost competitive bioplastic source.

PCL (monomer showed in Figure 4.1-4) is classified as a polyester from fossil source, which has been widely used as the polymer matrix in the development of new materials. It is highly flexible, biodegradable, biocompatible and easy to process (Wu 2003, Filipczak, Wozniak et al. 2006). PCL can be blended with a variety of other polymers to improve their properties (Iannace, Deluca et al. 1990). In fact, blending a natural polymer with polyester is an interesting way to reduce costs and to improve the biodegradability of the resulting polymer blends (Corradini, Mattoso et al. 2004).

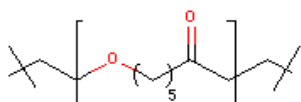


Figure 4.1-4: Monomer of Polycaprolactone (PCL)

This synthetic polymer has been used in order to produce a composite material which may improve the mechanical properties of the bioplastic made using protein concentrate alone.

Finally, the effect of using different additives was evaluated. These additives are: sodium sulphite (SS) or bisulphite (BS) as reducing agents, urea (U) as denaturing agent and L-cysteine (LC) as crosslinking agent

Additives such as reducing agents may be helpful in order to reduce the average molecular weight of protein aggregates, thus facilitating both mixing and moulding processes. The effect of adding a denaturing agent can be useful since an open protein have expose more hydrophobic groups which may induce more interactions in the crosslinking stage. As for the use crosslinking agent it is justified because it could improve the feasibility of crosslinking between different protein chains.

As it was mentioned in background section, plasticisers are essential in bioplastic polymers, since they reduce the glass transition temperature and provide mobility to polymeric chains (Irissin-Mangata, Bauduin et al. 2001). Hence, glycerol, which is a polar plasticiser (molecule showed in Figure 4.1-5) is among the most commonly used plasticizers for biopolymer-based biodegradable materials (Krochta 2002).

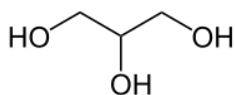


Figure 4.1-5: Glycerol molecule



## **4.2. Methods**

Since this study evolves the development of three products which exhibit quite different mechanical and structural properties, there are a wide variety of analytical methods. For this reason this section has been divided in methods which are common for protein characterisation and those methods which have been performed specifically for each product (emulsion, gel and bioplastic).

### **4.2.1. pH-adjustment of proteins dispersions**

The pH value was adjusted by using buffers at different pH values, controlling the ionic strength at 0.05 M with NaCl. To prepare the buffers, weak acids or basis were used. Thus, phosphoric acid, citric acid, benzoic acid, acetic acid, carbonic acid, sodium phosphate, TRIS, ethanolamine and methylamine were used at 10 mM for buffers at pH 2, 3, 4, 5, 6, 7, 8, 9 and 10, respectively.

### **4.2.2. Protein characterisation**

#### **4.2.2.1. pH- Value**

The pH value was determined with a pH 25+ device (Crison, Italy). The electrode used was selected according to the medium measured. For protein dispersions the 50 series was used, and for the dough-like material of the bioplastic, the semi-solid sensor of the 25 series.

#### **4.2.2.2. Protein content**

The protein content of products was determined in quadruplicate as % N x 6.25 using a LECO CHNS-932 nitrogen micro-analyser (Leco Corporation, St. Joseph, MI, USA), showed in Figure 4.2-1 (Etheridge, Pesti et al. 1998).



Figure 4.2-1: LECO CHNS-932 nitrogen micro-analyser

#### 4.2.2.3. Lipid content

Bottles, lids, and samples were placed in an oven at 105°C overnight to ensure that all of them are dried until stable weight. About 3 g of sample ( $W_1$ ) were weighted and wrapped in paper filter. Sample wrapped in paper filter were transferred into Soxhlet device, which is filled up petroleum ether about 250 ml into the bottle and took it on the heating mantle.

Soxhlet device was connected and turn on the water to cool them and then switch on the heating mantle. The sample was heated about 14 h, finishing the liquid extraction.

Now, sample wrapped in paper filter is soaked. To remove the petroleum ether, sample was incubated inside the bottle at 80-90°C until solvent is completely evaporated and bottle is completely dry. After drying, sample was transferred to the bottle with partially covered lid to the desiccator to cooler. Finally, sample was reweighed ( $W_2$ ) (A.O.A.C. 2000).

The lipid content calculation was made according to EQ. (4.2-1).

$$\text{Lipid content (\%)} = \frac{(W_1 - W_2)}{W_1} \quad (4.2-1)$$

#### 4.2.2.4. Moisture content

First of all, empty dishes and lids were dried in the oven at 105°C for 3 h and transfer to desiccator to cool. After cooled, the empty dish and lid were weighed.

About 3 g of sample ( $W_1$ ) were deposited in the dish, and the sample was spread to the uniformity. Then, the dishes with sample were place in the oven, and dried over night at 105°C. After this drying stage, dishes were transferred with partially covered lid to the desiccator to cool. After cooled, he dish, the lid and its dried sample were reweighed ( $W_2$ ) (A.O.A.C. 2000).

The calculation was made according to EQ. (4.2-2).

$$\text{Moisture content (\%)} = \frac{(W_1 - W_2)}{W_1} \quad (4.2-2)$$

#### 4.2.2.5. Ash content

Initially, crucibles were cleaned and dried for at least 2 h at 100°C in oven and kept in a desiccator. Subsequently, they were cooled and weighed, recording the tare weight to the nearest 0.0001 g. From 1.5 to 2.0 g of sample test were put into the crucible, recording the weight of crucible and test portion. After heating at 105°C for 2 h and keeping in a desiccator, samples were cooled weigh, recording weight. Subsequently, samples were subjected to heating for 5 h at 550°C (A.O.A.C. 2000). Samples were kept in a desiccator, cooled at room temperature and weight. EQ. (4.2-3) shows the expression of ash content:

$$\text{Ash content (\%)} = \frac{(S - S_c)}{S} \cdot 100 \quad (4.2-3)$$

where  $S$  is the initial sample weight and  $S_c$  is the sample weight after being subjected to calcination.

#### **4.2.2.6. Protein solubility**

Aqueous dispersions at 1 mg/mL were prepared and the pH of different aliquots was adjusted to alkaline pH with 6 M NaOH, and to acid pH with 6 M HCl. Samples were homogenized and, after that, centrifuged for 15 min at  $15,000 \times g$ . The total protein content was determined in quadruplicate by the procedure of Lowry modified (Markwell, Haas et al. 1978).

This method consist on a mixture of protein power at 0.1 mg/ml incubated at room temperature for 20 min with 3 mL of buffer A (2 wt. %  $\text{Na}_2\text{CO}_3$ , 0.4 wt. % NaOH, 0.4 wt. % sodium potassium tartrate, 1 wt. % Sodium Dodecyl Sulphate (SDS) and 0.4%  $\text{CuSO}_4$ ). Subsequently, Folin-Ciocalteu reagent 1:1 diluted is added and incubated for 45 min. Absorbance at 660 nm wavelength was measured in a Genesys-20 spectrophotometer (Thermo Scientific, USA) in 1 cm length cuvettes, using Bovine Serum Albumin (BSA) as standard.

#### **4.2.2.7. Surface hydrophobicity**

Surface hydrophobicity ( $H_0$ ) of soluble proteins in protein extracts (pH 8.0) was measured according to Kato and Nakai (1980), using the fluorescent probe 1-anilino-8-naphtalene-sulfonate (ANS).

Protein extracts were diluted with pH 0.05 M phosphate buffer (pH 8.0) to obtain protein concentrations ranging from 5 to 0.005 mg/mL. Then, 40  $\mu\text{L}$  of ANS (8.0 mM in the same buffer) were added to 2 mL of sample. Fluorescence intensity (FI) was measured with a Tucan Infinite 200 PRO Microplate Reader (Tecan Group Ltd, Männedorf, Switzerland), at wavelengths of 365 nm (excitation) and 484 nm (emission). The initial slope of fluorescence intensity versus protein concentration was used as an index of protein hydrophobicity ( $H_0$ ).

#### **4.2.2.8. Free and total sulfhydryl**

Free and total sulfhydryl groups of protein samples were determined using the method developed by Beveridge et al. (1974) and Thannhauser et al. (1984), respectively.

Samples were suspended (10 mg/mL) in 0.086 mol/L Tris-HCl, 0.09 mol/L glycine, 4 mmol/L EDTA, 8 mol/L urea, pH 8.0 buffer. Dispersions were stirred at 25°C for 10 min at 500 rpm in a thermomixer and centrifuged at 15,000 x g (10 min, 10°C). The supernatant was incubated with Ellman's reagent (4mg DTNB/mL methanol) and 1 mL NTSB was used in the case of the total sulfhydryls.

Absorbance at 412 nm was measured in a genesys-20 spectrophotometer (Thermo Scientific, USA). The molar extinction coefficient of NTB (13,600 L/mol·cm) was used. Protein concentration of extracts was determined by a modification of Lowry method (Markwell, Haas et al. 1978).

#### **4.2.2.9. Differential scanning calorimetry**

Protein samples were subjected to Differential Scanning Calorimetry (DSC) by means of a Q-20 DSC calorimeter (TA Instruments, USA) (Figure 4.2-2), using 5 to 10 mg samples. Tests were performed at 10 °C/min heating rate between -30 and 180 °C, using hermetically sealed aluminium pans. The sample environment was purged with a nitrogen flow of 50 mL/min.



*Figure 4.2-2: DSC Q 20 calorimeter*

#### 4.2.2.10. High performance liquid chromatography (HPLC)

Crayfish protein concentrate (CF2L) was dissolved in 6.0 M hydrochloric acid and then were incubated in an oven at 110°C for 24 h. After hydrolysis process, pH was adjusted to 7 using 6M NaOH and samples were filtered through a Whatman glass microfibre filter (GF/C). Finally, samples were diluted (1:500) by adding bidistilled water (Weiss, Manneberg et al. 1998).

Reverse phase HPLC by precolumn fluorescence derivatization with o-phthaldialdehyde (SIL-9A Auto Injector, LC-9A Liquid Chromatograph, RF-530 Fluorescence HPLC Monitor, all parts from Shimadzu Corporation, Japan) (Figure 4.2-3) was performed using a NovaPak C18 cartridge (Waters, Milford, MA, USA) by the method of Lindroth and Mopper (1979). Glycine/arginine and methionine/tryptophan were determined together, as their peaks merged. The analysis was performed once on each sample. By this procedure, it is only possible the detection to: Alanine (Ala), Aspartic acid (Asp), Glutamic acid (Glu), Histidine (His), Serine (Ser), Glycine (Gly), Arginine (Arg), Threonine (Thr), Tyrosine (Tyr), Methionine (Met), Valine (Val), Phenylalanine (Phe), Isoleucine (Ile), Leucine (Leu), Lysine (Lys). The other amino acids were not included in the results because they are completely destroyed by acid hydrolysis or cannot be directly determined from acid hydrolysed samples (Fountoulakis and Lahm 1998).



Figure 4.2-3: LC-9A Liquid Chromatograph

#### **4.2.2.11. Water imbibing capacity (WIC)**

WIC of CF2L protein concentrate was determined by using a modification of the Baumann apparatus (Torgersen and Toledo 1977). This device consists of a funnel connected to a horizontal capillary (shown in Figure 4.2-4). Sample (50 mg) was dusted on a wetted filter paper which was fastened to a glass filter placed on top of the funnel filled with water. The apparatus was kept at 20 °C. The uptake of water by the sample at equilibrium was read in the graduated capillary and expressed as millilitres of water imbibed per gram of isolated. Determinations were performed at least in triplicate.



*Figure 4.2-4: Baumann apparatus*

### **4.2.3. Specific methods**

#### **4.2.3.1. Emulsions performing**

Initially, an interfacial O/W characterisation was carried out by means of droplet pendant in order to determine protein content, as well as to predict the emulsion stability.

Transient interfacial pressure and interfacial dilatational measurements were carried out using a pendant drop tensiometer from CAM200 (KSV, Finland) (Figure 4.2-5). A single batch of commercial n-hexadecane oil was used to measure oil–water kinetic adsorption. The n-hexadecane oil was purified by elution on a silica column to extract the polar lipids.

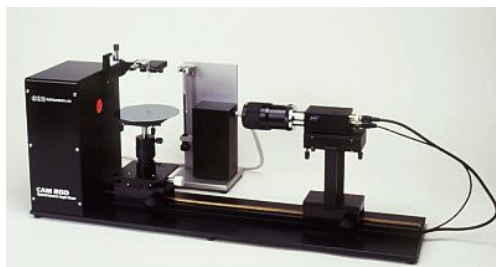


Figure 4.2-5: CAM 2000 device

An axisymmetric drop was formed at the tip of the needle of a syringe whose verticality was controlled by a computer. The drop profile was digitized and analysed through a CCD camera coupled to a video image profile digitizer board connected to a computer. The image was continuously visualized on a video monitor. Drop profiles were processed according to the Laplace equation as was described by Castellani, Al-Assaf et al. (2010).

Surface tension kinetics and sinusoidal area fluctuation experiments were carried out independently. Surface tension kinetics was performed for two concentrations (1 and 2 g/L) and two pH values (2.0 and 8.0). In addition, the viscoelastic moduli of protein adsorption layers were determined at 10% strain amplitude under equilibrium at 0.126 rad/s and non-equilibrium conditions at different frequencies (ranging from 0.031 to 0.314 rad/s) once the pseudo-steady state was achieved after 30,000 s (results obtained experimentally).

All the experiments were carried out, at least in duplicate, using an optical glass cuvette (8 ml), containing the oil phase, which was thermostated at  $20.0 \pm 0.1$  °C.

As for the experimental procedure, first of all, Xanthan Gum (XG) stock solution was prepared by dissolving 3wt. % XG powder in water. Then, high mechanical agitation was applied overnight and after that, the evaporated water was added to keep constant the gum concentration. Finally, 0.1 wt. %



$\text{NaN}_3$  was added to preserve the gum dispersion. The stock solution was diluted to prepare the rest of XG solutions (for the final concentration of 0.06, 0.12, 0.25 and 0.5 wt. % XG in emulsions). Systems were kept refrigerated at 5 °C for at least 48 h to ensure the complete polysaccharide hydration.

The final concentration of high oleic sunflower oil was 50 wt. %. The emulsions were prepared by gradually blending sunflower oil with the proportional aqueous CF2L protein dispersion (at each pH value) using a high-shear mixer (Ultraturrax T-50). Both phases were mixed for 2 min at 5,000 rpm (pre-emulsion). Subsequently, the pre-emulsions were passed through a high-pressure valve homogenizer once at 200 KPa (Avestin, Germany, Figure 4.2-7).

As for the selection of the number of emulsifying stages, the pre-emulsion containing 3% CF2L and 50% high-oleic sunflower oil, prepared at pH 5.0, was passed through a high-pressure valve homogenizer up to three times at 200 KPa.

Figure 4.2-6 shows influence of passing the emulsion through the high pressure homogeniser.

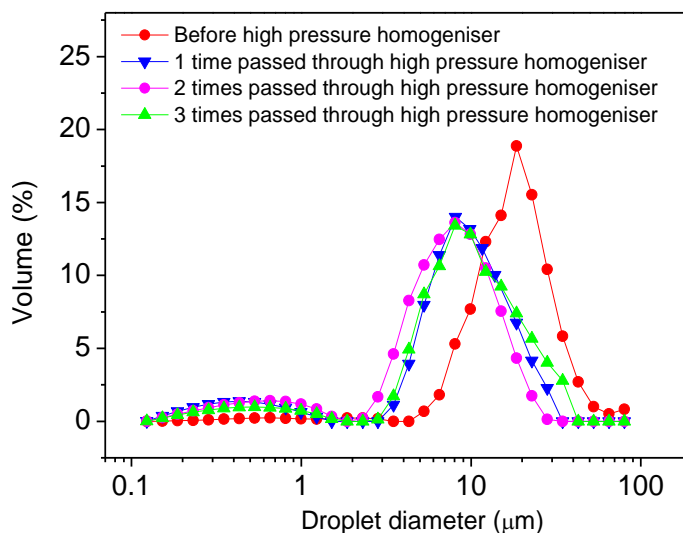


Figure 4.2-6: Evolution of the droplet diameter of high oleic emulsions before and after being threated through the high pressure homogeniser at pH 5.

A remarkable reduction in droplet sizes takes place after submitting the pre-emulsion to 1 stage high pressure homogenising. Further processing yields a moderate enhancement after the second stage that seems to be reversed after the third stage. In any case, both effects are moderate such that a procedure consisting of a single high-pressure homogenising stage has been selected for all the emulsions studied.

Subsequently, diluted emulsions were prepared by diluting concentrated emulsions with XG solutions. The concentrated emulsion and XG gum solutions were mixed manually using a spatula (final emulsion). Final emulsion contained 50 wt% high-oleic sunflower oil, 47 wt% aqueous CF2L protein dispersion (2 or 3 wt% CF2L) and different amounts of XG, obtaining a final XG concentration of: 0.06 wt. %, 0.12 wt. %, 0.25 wt. % and 0.5 wt. %. Three pH values were also studied (3, 5 and 8).



Figure 4.2-7: Avestin high pressure homogeniser

#### 4.2.3.2. Emulsion characterisation

##### 4.2.3.2.1. Droplet size distribution measurements

The droplet size distributions (DSD) were determined with the particle size analyser of laser diffraction Mastersizer X (Malvern, Worcestershire, United Kingdom) (Figure 4.2-8).



Figure 4.2-8: Mastersizer X apparatus

To avoid the measure of flocculated drops, sodium dodecyl sulphate (SDS) was added to the measured dispersion and stirred at the same time.

The mean droplet diameter was expressed as a Sauter diameter ( $D_{[3,2]}$ ) was calculated according to EQ. (4.2-4). Sauter diameter is defined as the diameter whose ratio of volume to surface area is the same as that of the entire droplet sample.

$$D_{[M,N]} = \left[ \frac{\int D^M n(D) dD}{\int D^N n(D) dD} \right]^{\frac{1}{M-N}} \quad (4.2-4)$$

Where  $M$  and  $N$  acquire the value of 3 and 2 ( $D [3,2]$ ), respectively, for Sauter diameter. The values of 4 and 3, for  $M$  and  $N$ , respectively, for the mean volumetric droplet size ( $D [4,3]$ ). Then the upside term is referred to the volumetric size and the downside is referred to the area.

From DSD, uniformity parameter also was obtained. The uniformity ratio is an index of polydispersity of the different droplet sizes and is defined by the following expression:

$$U = \frac{\sum V_i |d(v, 0,5) - d_i|}{d(v, 0,5) \sum V_i} \quad (4.2-5)$$

where  $d(v,0,5)$  is the median for the distribution, and  $V_i$  is the volume of droplets with a diameter  $d_i$ .

Eventually, the flocculation index (EQ.4.2-6) was defined in order to elucidate the typically flocculation process which takes place in food emulsions where p roteins are used as emulsifier.

$$Flocculation\ index = \frac{|D[4,3] - D[4,3]_{SDS}|}{D[4,3]} \quad (4.2-6)$$

Where  $D [4,3]$  is de mean volumetric droplet size and  $D [4,3]_{SDS}$  is the mean volumetric droplet size when SDS is added in the sample bath.

#### 4.2.3.2.2. *Rheological characterization*

The Thermo Scientific Haake MARS II rheometer (Figure 4.2-9) was used for all rheological measurements. Stress sweeps at a frequency of 0.62, 6.20 and 12.52 rad/s were performed for all systems studied to estimate the dynamic linear viscoelastic range. Frequency sweep tests (from 0.06 to 100

rad/s) were performed selecting a stress within the linear range. Flow curves experiments were performed for all emulsions in the range of 1-60 Pa.



*Figure 4.2-9: Mars II rheometer*

#### **4.2.3.2.3. Physical stability**

Backscattered light measurements were carried out with Turbiscan Lab Expert (L'Union, France) (Figure 4.2-10). These measurements were used in order to study the destabilization of the emulsions and were carried out for 60 days to study the stability of the emulsions and to determine the predominant mechanism of destabilization in each case as well as the kinetics of the destabilization processes.



*Figure 4.2-10: Turbiscan expert Lab apparatus*

Backscattering measurements consist on the application of a light source on the tube where the sample is contained, obtaining the backscattering and the transmittance as a function of the tube length.

#### 4.2.3.2.4. *Confocal laser scanning microscopy (CLSM)*

CLSM allows the tridimensional observation of samples, avoiding the structural changes. The microscopy used was LEICA TCS SP2 (Heidelberg, Alemania). The lens used was x100, and the de Argon laser. The exciting wavelength was 488 nm and the emission was within 520 and 687 nm. Autofluorescent compound was not need because proteins are autofluorescent itself.

#### 4.2.3.3. **Gel performing**

CF2L dispersions at 12 wt. % protein concentration were submitted at thermal gelation at three different pH values. The concentration of CF2L was selected since previous results showed that an increase of protein concentration does not involve an increase in gel strength (data not shown). Protein dispersions where subjected to an initial thermal ramp from room temperature to 90 °C at 5 °C/min. Then, the temperature was kept constant for 30 min, and subsequently cooled from 90 °C to 25 °C at 5 °C/min.

#### 4.2.3.4. **Gel characterisation**

##### 4.2.3.4.1. *Temperature ramp test*

Simulation of gelation process for different protein dispersions were performed in a controlled-stress rheometer (Kinexus Ultra +) from Malvern Instruments (Malvern, Worcestershire, United Kingdom), showed in Figure 4.2-11. Previously, stress sweep tests were performed in order to establish the linear viscoelasticity range for different regions. In fact, all tests were carried out at a stress clearly lower than the critical value. The gelation process was simulated through heating in situ in the rheometer with three different stages:

(i) The first step consisted of a temperature ramp carried out at constant heating rate (5 °C/min) from 20 °C to 90 °C; (ii) After the first step, a isothermal oscillation was performed at 90 °C for 30 min; (iii) Subsequently, a temperature ramp was carried out at constant heating rate (5 °C/min) from 90 °C to 20 °C. All stages were performed at constant frequency (6.28 rad/s). The geometry used was cone-plate geometry (50 mm, 2 °).



Figure 4.2-11: Kinexus Ultra + controlled-stress rheometer

#### 4.2.3.4.2. Frequency sweep tests

Frequency sweep tests (0.06 - 64 s<sup>-1</sup>) were carried out in order to obtain mechanical spectra. These measurements were performed in a controlled-stress rheometer (Kinexus Ultra +) from Malvern Instruments (Malvern, Worcestershire, United Kingdom), showed Figure 4.2-11. The geometry used was cone-plate geometry (50 mm, 2°). All rheological tests were carried out at 20 °C. All gels studied were subjected to the same thermorheological history (30 min at room temperature) before performing any rheological test.

#### 4.2.3.4.3. Protein interactions

Solubility of CF2L gels in a number of selected solutions was carried out in order to determine ionic bonds, hydrogen bonds, hydrophobic interactions and disulphide bonds according to the method of Gomez-Guillen et al. (1997). The selected solutions were as follows: 0.05 mol/L NaCl (SA), 0.6 mol/L NaCl

(SB), 0.6 mol/L NaCl + 1.5 mol/L urea (SC), 0.6 mol/L NaCl + 8 mol/L urea (SD) and 0.6 mol/L NaCl + 8 mol/L urea + 0.5 mol/L  $\beta$ -mercaptoethanol (SE) solutions.

Ionic bonds were the result of the difference between protein solubilized in SB buffer and protein solubilized in SA buffer; hydrogen bonds was the difference between protein solubilized in SC buffer and protein solubilized in SB buffer; hydrophobic interactions was the difference between protein solubilized in SD buffer and protein solubilized in SC buffer and, finally, disulphide bonds was the difference between protein solubilized in SE buffer and protein solubilized in SD buffer. The protein concentration was determined using a modification of Lowry method (Markwell, Haas et al. 1978).

#### 4.2.3.4.4. *Water holding capacity (WHC)*

Portions of gel (0.3-1.3 g) were equilibrated at room temperature and placed on a nylon plain membrane (5.0-mm pores, Micronsep, New York, N.Y., U.S.A.) maintained in the middle position of a centrifuge tube. Water loss was determined by weighing before ( $W_1$ ) and after centrifugation ( $W_2$ ) at  $120 \times g$  for 5 min at 5 °C (Queguiner, Dumay et al. 1989). WHC was expressed as the percentage of the initial water remaining in the gel after centrifugation EQ. (4.2-7).

$$WHC (\%) = \frac{(W_1 - W_2)}{W_1} \cdot 100 \quad (4.2-7)$$

#### 4.2.3.4.5. *Bio-active properties*

##### *2,2-diphenyl-1-picrylhydrazyl (DPPH) Assay*

The DPPH assay was performed as described by Brand-Williams et al. (1995) with some modifications (Kikuzaki, Hisamoto et al. 2002, Stratil, Klejdus et al. 2006, Nenadis, Lazaridou et al. 2007). Thus, the day before analysis, 0.1



mM ethanolic DPPH\* working solution was prepared and kept on a magnetic stirrer overnight at 4°C. The day after, a series of 0-750 µM methanolic working solutions of Propyl Gallate and gel solutions at 10 wt. % in methanol were prepared.

An aliquot of DPPH\* solution (2.9 mL) was well mixed with 0.1 mL of a sample or methanol (blank). After 20 min of incubation at room temperature, the absorbance at 515 nm was recorded in a Genesys-20 spectrophotometer (Thermo Scientific, USA), in 1 cm length cuvettes. Water was used as a blank. Finally, results were expressed as equivalent activity of the gel, compared to the antioxidant activity of the reference (Propyl Gallate, PG).

### *2,2'-Azino-bis(3-ethylbenzothiazoline-6-sulfonic acid) diammonium salt (ABTS) Assay.*

The ABTS assay was performed as described by Nenadis et al. (2004) with a few modifications: ethanol was replaced with methanol and the amount of sample added to the activated ABTS (ABTS<sup>•+</sup>) solution was 200 µL. As a consequence, for the analysis, a series of 0-55 µM working solutions of Propyl Gallate and gels at 1 wt. % were prepared from stock gels. To prepare ABTS<sup>•+</sup> solution, the previous night, 440 µl 140 mM K<sub>2</sub>S<sub>2</sub>O<sub>8</sub> was added to 25 ml 7 mM ABTS, as well as stirred and cooled overnight. The ABTS<sup>•+</sup> reaction mixture was dilute with methanol until the absorbance is 0.75 ± 0.05 at 734 nm wavelength using water as reference.

Series of dilutions from the Propyl Gallate (PG) stock solution and methanol with concentrations 10 µM, 20 µM, 30 µM, 40 µM and 50 µM were made. These solutions constitute the standard and the blank. After that, 2 ml ABTS<sup>•+</sup> diluted were mixed with 200 µl extract/standard solutions/blank (80% methanol). Samples were incubated for about 6 minutes at room temperature and absorbance was read at 734 nm with water as reference by means of

Genesys-20 spectrophotometer (Thermo Scientific, USA), using 1 cm length cuvettes. To compare the antioxidant activities, the absolute values for each antioxidant and each assay were recalculated into PG equivalents.

### *Folin-Ciocalteu (FC) Assay*

The FC assay was performed as described by Singleton et al. (1999) with some modifications (Miliauskas, Venskutonis et al. 2004, Nenadis, Lazaridou et al. 2007). Thus, a series of 0-4 mM working solutions of Propyl Gallate (PG) and suitable gel solutions were prepared. Deionized water (10 mL), antioxidant solution (1 mL), and 2.0 M Folin-Ciocalteu phenol reagent (1 mL) were transferred to a 20 mL volumetric flask. The reaction mixture was mixed by shaking, and after 3 min, 2 mL of 20% Na<sub>2</sub>CO<sub>3</sub> solution (20 g/L) was added. The volume was brought up with deionized water. The absorption at 725 nm was read after 1 h of incubation at room temperature in a Genesys-20 spectrophotometer (Thermo Scientific, USA), using 1 cm length cuvettes. Water was used as a reference. Results were expressed as equivalent activity of the gel compared to the reference compound (PG).

### *TCA-soluble peptides*

Autolysis was measured by the method of Miller and Spinelli (1982) for ground fish with the following modifications: 3 g samples were incubated both at 5 °C and 90 °C for 30 min and the reactions stopped by the adding of 27 mL 5% trichloroacetic acid (TCA). Aliquots of the resulting TCA supernatants were monitored at 280 nm with an Ultrospec 2000 from Pharma Biotech (Parker, United Kingdom).

#### **4.2.3.5. Bioplastic manufacturing**

##### **4.2.3.5.1. Mixing stage**

Different blends were manufactured by means of a thermomechanical procedure which includes two stages:

- 1) In the first stage, blends were mixed in a two-blade counter-rotating batch mixer Haake Polylab QC (ThermoHaake, Germany), showed in Figure 4.2-12. The operation mode was at constant temperature (25 °C, air cooling) and 50 rpm for 60 min. Torque and sample temperature were monitored during mixing process.
- 2) After this first stage, the second stage consists on the analysis of both profiles torque and temperature, selecting a suitable time mixing, which depends on profile characteristics. Thus, protein/plasticiser blends have to be well mixed, but cross-linking reactions must be avoided. Then, a new mixture was performed using the time selected.



*Figure 4.2-12: Mixing apparatus: Haake Polylab QC*

##### **4.2.3.5.2. Injection stage**

The biocomposite blends obtained after the second mixing stage were processed by injection moulding using a MiniJet Piston Injection Moulding System II (Thermo Haake, Germany) (Figure 4.2-13) to obtain biocomposites specimens. Three stages are considered over this process:

- 1) The pre-injection stage.
- 2) The injection itself.
- 3) The packing stage.

For all stages temperature and time must be selected. In contrast, pressure only can be selected for the second and the third stage. Thus, the values for the processing parameters at the pre-injection cylinder are selected to ensure a blend viscosity low enough to facilitate its injection into the mould. The parameters for the injection stage were selected to ensure that the mould was completely filled, as well as to promote cross-linking. The packing stage parameters (right after injection) are selected since no further enhancement has been noticed by increasing the time, the temperature or the pressure. In addition, exposition to high temperature for a long time typically leads to protein degradation (i.e. via Maillard-type reactions) (Ellis 1959).



Figure 4.2-13: Haake Mini Jet II, injection moulding apparatus

### 4.2.3.6. Bioplastic characterisation

#### 4.2.3.6.1. Dynamic Mechanical Temperature Analysis

Viscoelasticity for rigid bioplastic materials were carried out by means of a RSA3 (TA Instruments, New Castle, USA) (Figure 4.2-14) which is connected to a chiller that leads to decrease the temperature. 1 mm rectangular probes

were used and measured in dual cantilever bending tool. All the experiments were carried out at constant frequency (6.28 rad/s) and strain (between 0.01 and 0.3%, within the linear viscoelastic region). The selected heating rate was 3 °C/min, from -20 to 140 °C. All the samples were coated with Dow Corning high vacuum grease to avoid water loss.



Figure 4.2-14: RSA III rheometer

### 4.2.3.6.2. Tensile strength measurements

Tensile tests were performed by using the Insight 10 kN Electromechanical Testing System (MTS, Eden Prairie, MN, USA) (Figure 4.2-15), according to ISO 527-2:2012 (2012) for Tensile Properties of Plastics.



Figure 4.2-15: MTS insight 10kN apparatus

Tensile stress and elongation at break were evaluated from at least three duplicates for each product using type 5B (Figure 4.2-16) probes and an extensional rate of 10 mm/min at room temperature.

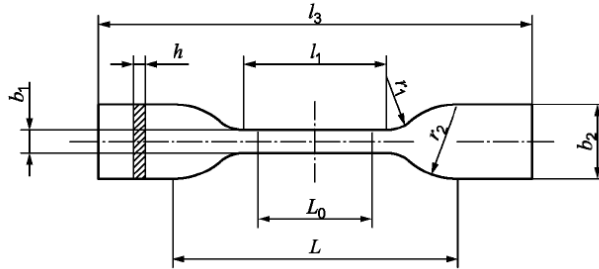


Figure 4.2-16: Probe 5B (ISO 527-2:2012)

#### 4.2.3.6.3. Water uptake capacity

Water uptake of bioplastics was determined following the ASTM D570 norm (2001) using at least three 60×10×1 mm specimens. Probes were previously dried in an oven at 50 °C for 5 h, after that the weight ( $W_1$ ) was noted. Then, probes were immersed in distillate water for 2 h or 24 h at room temperature and noted the weigh again ( $W_2$  and  $W_3$ , respectively). Finally, probes were dried in an oven at 50 °C overnight and reweight ( $W_4$ ). Water uptake 2 h was calculated as indicates EQ. (4.2-8), water uptake 24 h was calculated as indicated EQ. (4.2-9) and soluble matter loss as defined EQ. (4.2-10).

$$\text{Water uptake (2h)(\%)} = \frac{W_1 - W_2}{W_1} \cdot 100 \quad (4.2-8)$$

$$\text{Water uptake (24h)(\%)} = \frac{W_1 - W_3}{W_1} \cdot 100 \quad (4.2-9)$$

$$\text{Soluble matter loss(\%)} = \frac{W_1 - W_4}{W_1} \cdot 100 \quad (4.2-10)$$

#### 4.2.3.6.4. X-Ray diffraction (XRD)


XRD studies of the probes were carried out using a D8 Discover (BRUKE, Massachusetts, USA) (Figure 4.2-17) at 45 kV and 100 mA. The device was equipped with Cu K $\alpha$  radiation ( $\lambda = 0.1516$  nm) in order to visualise different crystalline phases (which belong to PCL) that may indicate systems whose microstructure could be different.



*Figure 4.2-17: D8 Discover apparatus*







*A aquellos que no están*

*Por haber marcado mi vida y ayudarme a ser como soy,  
Por los que vengan, y llenen de felicidad cada pequeño momento, cada  
instante de mi vida.*





## 5. Results





## 5.1. Protein Characterisation

### 5.1.1.1. Amino acid characterisation

Figure 5.1-1 shows the amino acid profile for CF2L protein concentrate. Glutamic acid was the most abundant amino acid found, followed by alanine and aspartic acid (without considering glycine and arginine which appear merged into a single peak). The proportion of essential/total amino acids in CF2L was around 0.75. As not all amino acids were detected by the method used, this value is not accurate. However, since the value is well above 33.9% recommended by FAO (1985), the nutritional value can be regarded as high.

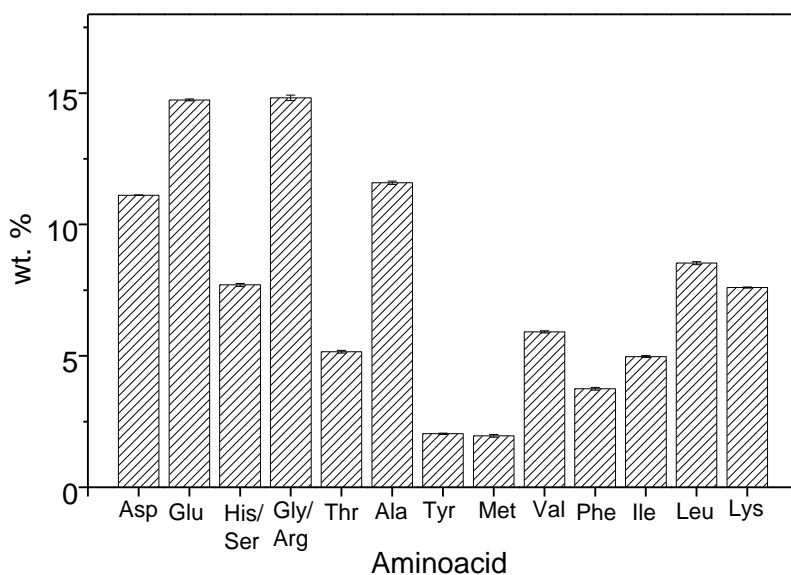


Figure 5.1-1: Amino acid profile of CF2L protein concentrate obtained from HPLC.

The CF2L protein concentrate contains a significant amount of the essential amino acids (adding up to 43 wt. % of total amino acid content). All essentials are present except Tryptophan (Trp), which could not be determined by the analytical procedure used. The adult daily requirement for essential amino acids given by WHO/FAO/UNU (1985) has been used as

reference protein for discussion of nutritional quality. The sulphur-amino acids, Met and Cys, are nutritionally essential. In CF2L fraction, Met is one of the least abundant amino acid in the sample and Cys could not be determined through the performed HPLC analysis. Therefore, it is not possible to predict the crosslinking potential, based on cysteine content, however this will be discussed later, based on sulfhydryl content.

Nevertheless, the second limiting amino acid in the maintenance requirement after the sulphur amino acids, Thr, can be found in a sufficient amount in this protein concentrate. These results are consistent with results reported by other authors, who have found similar results for crab (Vilaso-Martinez, Lopez-Hernandez et al. 2007) and crayfish protein (Cremades, Parrado et al. 2003), respectively.

Finally, FAO's report (1985) pointed out the requirement for lysine. This amino acid had received most attention, given its nutritional importance as the likely limiting amino acid in cereals. CF2L protein is an excellent source of lysine since lysine is the fifth most abundant amino acid. Therefore, it can be concluded that CF2L concentrate has a high nutritional quality.

### 5.1.1.2. Protein solubility

Figure 5.1-2 shows the values of CF2L solubility in water as a function of pH values. As may be observed, high protein solubility values were generally obtained for CF2L, showing similar solubility profile to that one previously obtained for the spray-dried crayfish pulp (Cremades, Parrado et al. 2003). Minimum solubility was found at pH around 5, which is most probably related to the proximity of the isoelectric point, (IEP) (Petursson, Decker et al. 2004).

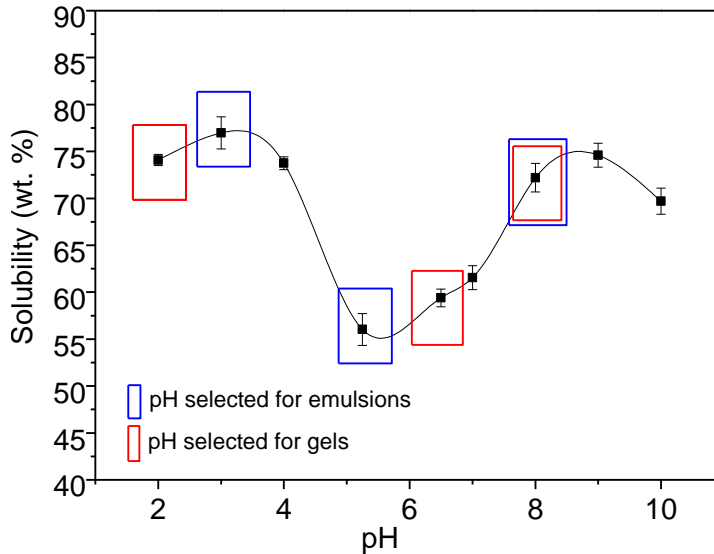
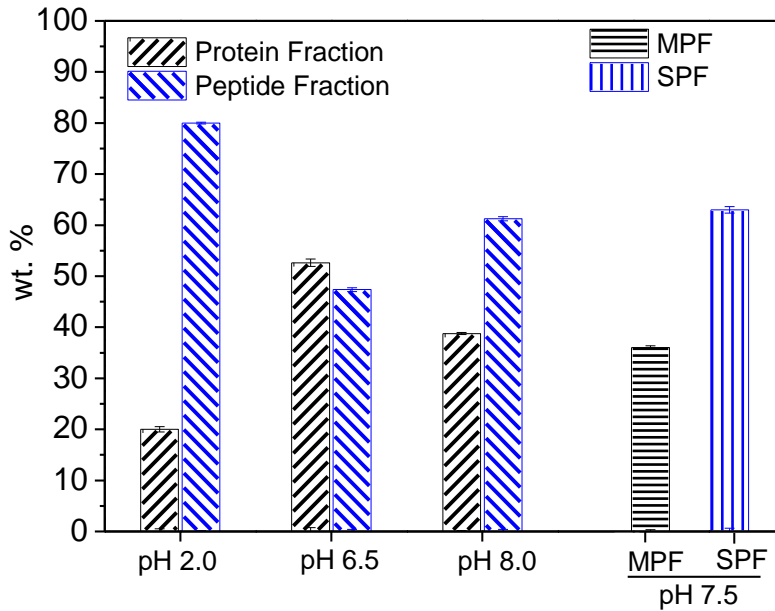


Figure 5.1-2: Protein solubility as a function of pH values.

Figure 5.1-3 shows the balance of soluble protein vs. peptides at three selected pH values (2.0, 6.5 and 8.0), as well as the proportion of both the myofibrillar protein fraction (MFP) and the sarcoplasmic protein fraction (SPF) at pH 7.5. This graph reveals that the amount of proteins remains higher than the amount of peptides only when pH is close to the isoelectric point (IEP), although the difference is moderate. However, far from the IEP, CF protein is predominantly in the form of peptides. The high level of soluble peptides at pH 2.0 may be a consequence of acid hydrolysis (Lehninger, Nelson et al. 2005).

At pH 7.5, pH selected according to the method of Hashimoto et al. (1979) for the determination of sarcoplasmic and myofibrillar protein fractions, the sarcoplasmic protein fraction (SPF) is higher than the myofibrillar protein fraction (MFP) in CF2L protein concentrate. However, MFP still contributes ca. 35% of total protein. Myofibrillar proteins have been reported to be the main

responsible for the texture and gel-structure in food products obtained by heating (Ramirez-Suarez, Addo et al. 2005, Liu, Bao et al. 2014).



*Figure 5.1-3: Protein solubility as a function of molecular size (differentiating between protein and peptide) at three different pH values or protein fraction: myofibrillar (MFP) or sarcoplasmic (SFP) at pH 7.0.*

The amount of free sulfhydryl groups is  $18 \pm 1 \mu\text{mol/g}$  protein while the total disulphide bonds reaches values up to  $2240 \pm 20 \mu\text{mol/g}$  protein. Both values are about twice the sulphide content of albumen protein concentrate (Martin-Alfonso, Felix et al. 2014). However, the amount of S-S bonds is lower than the value reported for legume proteins (Tang 2008) and must be related to the presence of Cys, up to 3 wt. %. Moreover, these data show that the amount of -SH group is very low compared to the total sulphide content. These results suggest that a high amount of S-S bonds is naturally present in CF protein since no crosslinking formation is expected during protein manipulation as freeze drying was used to obtain the protein concentrate.



However, the relatively high content of free sulfhydryls obtained from CF2L as compared to other proteins would also yield a higher density of crosslinking by forming sulphide bonds (Buonocore, Del Nobile et al. 2003).

As for surface hydrophobicity ( $H_0$ ), the result obtained was  $12 \pm 2$ , which is extremely low as compared to other proteins such as albumen, soy or zein, all of them obtained by spray-drying (Ortiz, Puppo et al. 2004, Chen and Zhong 2014, Martin-Alfonso, Felix et al. 2014). This low value of surface hydrophobicity could indicate a low degree of denaturation. In fact, proteins obtained by freeze-drying are less denatured than protein obtained by spray-drying (Ezhilarasi, Indrani et al. 2013). It is worth mentioning that this limited denaturation of CF2L makes this protein fraction a potential candidate for many applications involving both physical and chemical interactions.

Table 5.1-1 summarises a comparison for the chemical composition of all systems studied:

	CF2L	CF2LH <sub>5</sub>	CF2LH <sub>25</sub>	CF2LH <sub>120</sub>
Protein Content (wt. %)	78.6 ± 0.5	72.6 ± 0.4	70.8 ± 0.3	70.0 ± 0.2
Moisture (wt. %)	6.8 ± 0.1	7.3 ± 0.1	8.6 ± 0.6	8.5 ± 0.1
Lipid content (wt. %)	5.1 ± 0.3	3.8 ± 0.3	1.5 ± 0.1	3.4 ± 0.2
Ashes content (wt. %)	9.5 ± 0.6	16.4 ± 0.8	18.1 ± 0.2	17.55 ± 0.5
Free Sulfhydryl (μmol/g prot)	18 ± 1	9 ± 1	10 ± 1	10 ± 1
Disulph. bonds (μmol/g prot)	2240 ± 40	2175 ± 50	2380 ± 60	2150 ± 50
Surface hydrophobicity ( $H_0$ )	13 ± 1	13 ± 1	26 ± 1	21 ± 1
WIC (mL/g)	0.57 ± 0.02	0.34 ± 0.02	0.35 ± 0.03	0.35 ± 0.03
Degree of Hydrolysis (%)	0	11 ± 1	31 ± 1	45 ± 2

*Table 5.1-1: Physicochemical characterisation of all systems studied*

All hydrolysate systems exhibit lower protein content. This is a clearly consequence of the hydrolysis process, and probably it is related to the pH adjustment during the hydrolysis process and the moisture content. In addition, the pH adjustment may be also responsible for the increase in ash content, which is around two times the initial ash content of CF2L system.

CF2L system contents up to 5 wt. % of lipids, these results are similar to other found previously and could be attributed to a high content of phospholipids (Chalamaiah, Kumar et al. 2012). However, any of the hydrolysate exhibits lower lipid content as a consequence of the hydrolysis process carried out.

As regards sulfhydryl content, there are not significant differences in disulphide bonds for any of the systems studied. The total disulphide bonds in these systems is about twice the value corresponding to albumen protein concentrate (Martin-Alfonso, Felix et al. 2014), being the ovalbumin protein considerate as a protein rich in S-S and –SH groups (Mine, Li-Chan et al. 2010). However, these results show that the total sulphide content in these systems is lower than the typical content found in legume proteins (Tang 2008).

A comparison between total disulphide bonds and free sulfhydryl groups shows that the amount of -SH groups is very low. Since the extraction procedure carried out is known to preserve protein structure fairly well, this small amount of –SH groups cannot be attributed to protein aggregation or denaturation. As a result, it should be related to native S-S interactions. Probably, the cause of this chemical property is related to protein conformation, which is held after freeze-dried procedure. Finally, it is worth mentioning that hydrolysates exhibit a lower content of free sulfhydryl, which is clearly influenced by the hydrolysis procedure carried out. Level of free sulfhydryl would suggest that a desirable density of crosslinking could be

achieved by forming S-S bonds during the gelling stage (Buonocore, Del Nobile et al. 2003).

Values of surface hydrophobicity ( $H_0$ ) suggest that after a certain degree of hydrolysis, the protein surface hydrophobicity increase significantly. An increase of  $H_0$  when a protein is hydrolysed was previously found by Zheng et al. (2015). This parameter is important in protein gelation, since apart from SS bonds, the non-covalent interactions (particularly the hydrophobic interactions) are quite important for the protein aggregation stage (Cabra, Vazquez-Contreras et al. 2008). The increase in  $H_0$  after hydrolysis suggests that the process involves exposition on some hydrophobic sites previously buried at the protein core, however aggregation might not be promoted since it depends on other factors (Zheng, Wang et al. 2015).

Water imbibing capacity (WIC) of all systems is very low compared to other protein systems such as soy or wheat protein concentrates (Sorgentini, Wagner et al. 1991). These results may be related to the high solubility of these protein systems, since the insoluble protein fraction usually contributes to increase WIC, as a consequence of its high denatured state (Wagner and Anon 1990).



## 5.2. Crayfish-based high oleic/water emulsions

### 5.2.1. Selection of emulsification conditions

High oleic oil-in-water emulsions were prepared according to the procedure described in the section 4.2.3.1. However the optimal CF2L concentration have to be previously selected.

First of all, interfacial oil/water tensions were determined for protein-adsorbed interfacial layers at several protein concentrations (0.5, 1.0, 1.5, 2.0, 2.5, 3.0, 3.5, 4.0 and 5.0 wt. %) and at three pH values (3, 5 and 8) in order to select the most suitable CF2L concentration for each pH. Table 5.2-1 exhibits results from interfacial measurements (measured by using a Wilhelmy plate).

[C] (wt. %)	Surface tension (mN/m)		
	pH 3	pH 5	pH 8
0.5	9.2 ± 0.3	12.1 ± 0.3	11.4 ± 0.5
1.0	7.6 ± 0.2	9.0 ± 0.5	9.7 ± 0.3
1.5	7.5 ± 0.2	5.2 ± 0.3	9.6 ± 0.2
2.0	6.4 ± 0.1	3.4 ± 0.2	8.2 ± 0.3
2.5	6.3 ± 0.2	2.7 ± 0.3	7.9 ± 0.3
3.0	6.3 ± 0.1	2.0 ± 0.2	8.2 ± 0.2
3.5	6.4 ± 0.3	1.9 ± 0.2	8.1 ± 0.2
4.0	6.2 ± 0.2	2.0 ± 0.3	8.3 ± 0.3
5.0	6.3 ± 0.2	2.0 ± 0.1	8.2 ± 0.2

*Table 5.2-1: Results from interfacial measurements at three different pH values and several protein concentrations (0.5, 1.0, 1.5, 2.0, 2.5, 3.0, 3.5, 4.0 and 5.0)*

In view of these results, a protein concentration higher than the saturation concentration was selected for each pH value (2 wt. % for pH 3.0, 3 wt. % for pH 5.0 and 2 wt. % for pH 8.0). As may be observed in this table, the

interfacial tension requires higher protein concentration to reach the equilibrium at pH 5.0, leading to a lower value for interface saturation. This may be related to the low protein surface charge found at this pH, since it is close to the IEP of the CF2L protein. However, it has to be taken into account that the concentration of water soluble protein at which the equilibrium is reached turns out to be similar for the three pH values, although is slightly higher at pH 5.0.

However, to confirm that the selected protein concentration was optimal, emulsions containing different protein concentrations were prepared according to the procedure described in the experimental section. Figure 5.2-1 shows the DSD profiles obtained for these emulsions.

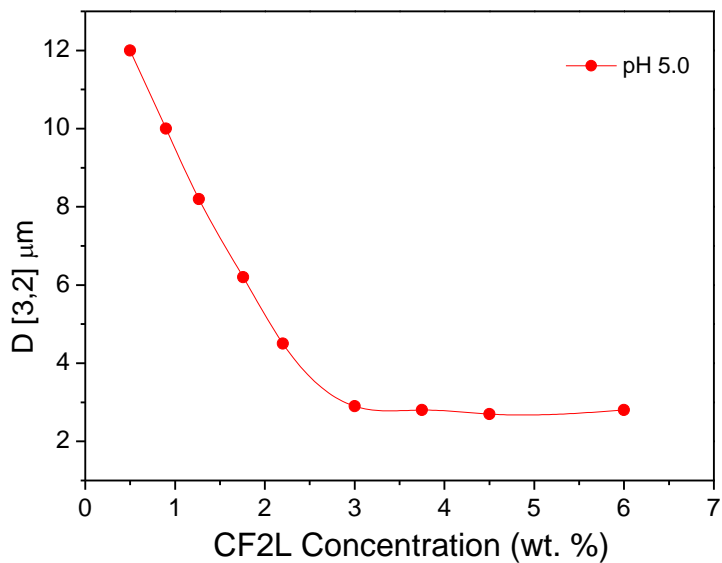


Figure 5.2-1: Influence of concentration on  $D [3,2]$  diameter for emulsions at pH 5.0.

As may be observed, an evolution towards smaller sizes takes initially place. However, differences in DSD profiles are becoming smaller as protein concentration increases. No further differences may be noticed after reaching

3 wt. % CF2L, which is consistent with the results found for the interfacial tension values.

### 5.2.2. Interfacial characterisation

#### 5.2.2.1. Adsorption kinetics

The adsorption kinetics of CF2L protein at a fluid-fluid interface was monitored by measuring changes in interfacial pressure ( $\pi$ ) or interfacial dilatational modulus ( $E'$ ) over time. Figure 5.2-2 shows the transient interfacial pressure response for the adsorption kinetics of CF2L at the high oleic sunflower-oil/water interface, at the selected emulsification concentration as a function of pH (3, 5 and 8).

Regardless of the pH value, protein adsorption is characterized by a rapid increase in surface pressure, which is followed by a slower evolution and a tendency to reach a constant value ( $\Pi_{eq}$ ). All systems reached the same value of interfacial pressure. These results indicate that all systems have similar interfacial equilibrium activity and can be compared in terms of emulsion ability. The adsorption kinetics can be discussed in a well-known simplified model, where the occurrence of different stages was postulated. In the first stage, a fast protein diffusion from the bulk to the interface takes place. This stage is followed by a slower one, where protein molecules penetrate through the interfacial layer. Finally, conformational rearrangements of proteins at the interface seem to take place in the last stage and the overall adsorption rate slows down.

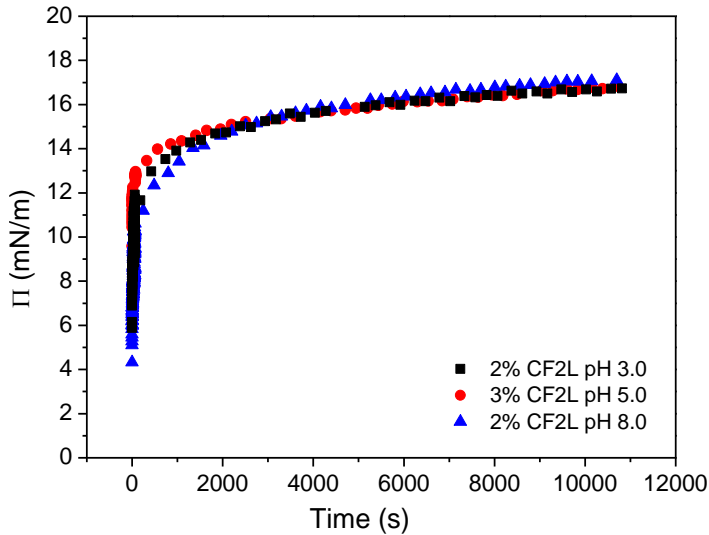


Figure 5.2-2 : Surface pressure over protein adsorption at fluid-fluid interface

During the first step, where diffusion is the rate-controlling step of the adsorption process, a modified form of the Ward and Tordai equation (Ward and Tordai 1946) can be used to correlate easily the change in the surface pressure as a function of time (EQ. 5.2-1):

$$\Pi = \frac{2}{\sqrt{\pi}} c_0 \kappa T [D \cdot t]^{1/2} \tag{5.2-1}$$

where  $c_0$  is the protein concentration in the bulk phase,  $\kappa$  is the Boltzmann constant,  $T$  is the absolute temperature, and  $D$  is the diffusion coefficient.

Thus, from the slope of the plot of  $\Pi$  vs.  $t^{1/2}$  it is possible to deduce the diffusion rate ( $k_D = \frac{2}{\sqrt{\pi}} c_0 \kappa T D^{1/2}$ ) of protein towards the interface, as reported by Rodríguez Patino, Rodríguez Niño, & Carrera Sánchez (2007).

After this first stage, adsorption kinetics becomes slower, since an energy barrier exists and the process starts to be controlled by the proper adsorption (the transition from the subsurface layer to the interface) where desorption



and blocking function, considering the steric hindrances, must be taken into account (Noskov and Mikhailovskaya 2013). To quantify the kinetics, a first-order phenomenological equation can be used to fit the evolution of surface pressure with time (EQ. 5.2-2):

$$\ln \frac{\Pi_f - \Pi(t)}{\Pi_f - \Pi_0} = -k_A \cdot t \quad (5.2-2)$$

where  $\Pi_f$ ,  $\Pi(t)$  and  $\Pi_0$  are the surface pressures at the final adsorption time, at any time (t), and at the initial time (0), respectively, and  $k_A$  is the first-order constant that can be associated to the above described process (Rodriguez Patino, Rodriguez Nino et al. 1999, Pérez, Sánchez et al. 2009). The values of  $k_D$  and  $k_A$  parameters are shown in Table 5.2-2.

System	$k_D \times 10^3$	$k_A \times 10^4$
2% CF2L pH 3	$1.19 \pm 0.04$	$-2.99 \pm 0.03$
3% CF2L pH 5	$1.35 \pm 0.02$	$-2.40 \pm 0.05$
2% CF2L pH 8	$1.09 \pm 0.02$	$-2.91 \pm 0.01$

*Table 5.2-2: Kinetic parameters from protein adsorption*

The data obtained for the diffusion rate ( $k_D$ ) should be take into account with caution since this stage is relatively fast at the concentrations studied, as a consequence, a limited number of data points are available to fit EQ. (5.2-1). However, the trend is clear and several replicates always show that the highest values for  $k_D$  correspond to the pH 5.0, which according to the value reported by Puppo & Añón (1998) is close to the isoelectric point (IEP) (4.5) and, as a consequence, protein molecules have low surface charge.

In the second stage, the first-order is the rate-controlled, the maximum value corresponds to acid pH, and it is very similar to the value obtained for the alkaline pH. However, it is quite different to that one found for the pH

close to the isoelectric point. This fact may be relate with the absence of net charge found in the IEP, exhibiting the protein the ability to migrate to the non-polar phase.

### 5.2.2.2. Interfacial dilatational rheology measurements

Figure 5.2-3 shows the apparent dilatational moduli (Fuller and Vermant 2012, Sagis, Humblet-Hua et al. 2014, Verwijlen, Imperiali et al. 2014) ( $E'_{ap}$  and  $E''_{ap}$ ) for CF2L protein system at different pH values (2.0, 5.0 and 8.0) obtained during protein adsorption.

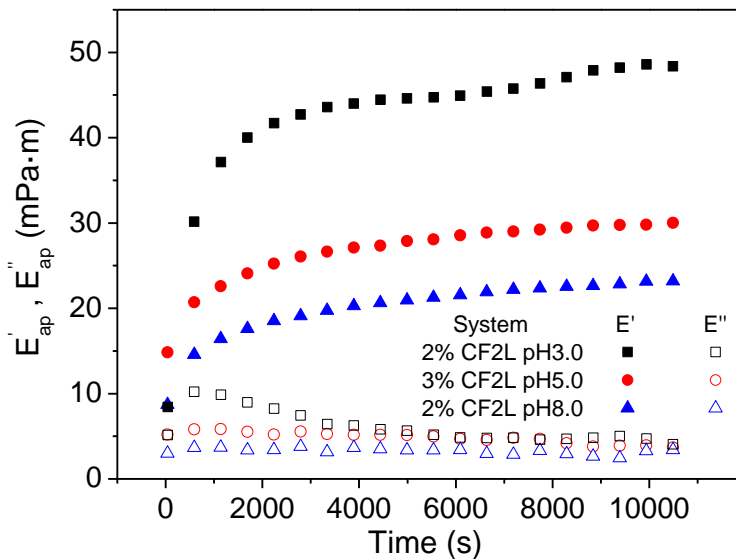


Figure 5.2-3: Elastic and viscous moduli ( $E'$  and  $E''$ , respectively) for protein adsorption.

As may be observed,  $E'_{ap}$  undergoes an increase over adsorption time that tend to reach an equilibrium value after a long time. In contrast,  $E''_{ap}$  is not time-dependent or even shows a slight decrease. This evolution of the apparent linear viscoelastic functions may be regarded as the result of a

gelation of the interface as the amount of protein adsorbed is growing. Similar evolution of the dilatational moduli was previously found for crayfish protein isolate (Romero, Beaumal et al. 2011), for potato protein isolate (Romero, Beaumal et al. 2011) and for rice protein concentrate (Romero, Beaumal et al. 2012). Moreover, dilatational properties show a strong influence on pH. Thus, the adsorption (rheo)kinetics obtained at pH 3.0 shows a faster initial evolution towards much higher values than those corresponding to pH 5.0 and 8.0. In addition, this figure also shows that the slowest (rheo)kinetics behaviour is obtained at pH 8.0.

Figure 5.2-4 shows the apparent moduli ( $E'_{ap}$  and  $E''_{ap}$ ) for CF2L protein system as a function of frequency from interfacial dilatational rheology at equilibrium. The values of the apparent interfacial dilatational viscoelastic properties have been plotted as a function of the oscillation frequency.

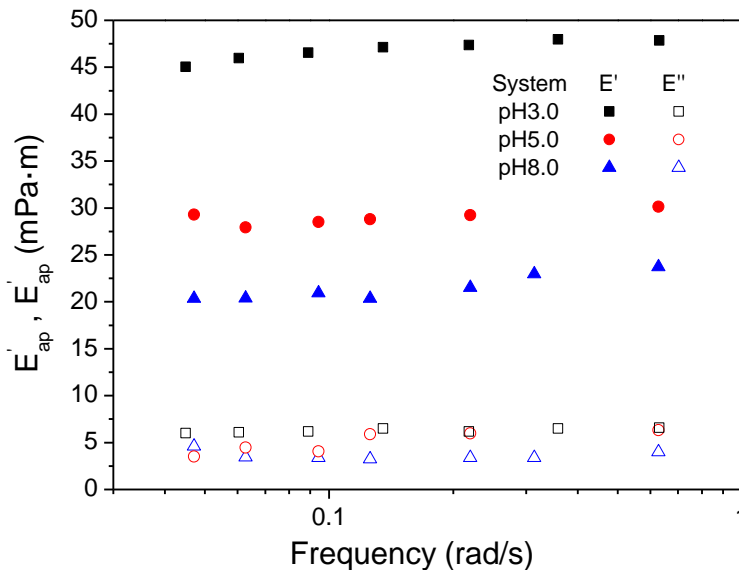


Figure 5.2-4: Mechanical spectra for proteins adsorbed at fluid-fluid interface at different pH values (3, 5 and 8)

The interfacial dilatational mechanical spectra obtained put forward the occurrence of a strong elastic response, which may correspond to a gel-like behaviour. However, although dilatational measurements are considered to be helpful tools for long-term stability, they do not to elucidate the nature of the protein interactions at a complex fluid-fluid interface (Sagis and Fischer 2014). In any case, this figure shows that an increase in pH yields a reduction in  $E'$  values. Furthermore,  $\tan \delta$  was calculated at 0.1 rad/s and results obtained were 0.17, 0.20 and 0.21 for pH 3.0, 5.0 and 8.0, respectively.

A comparison between these values obtained and other interfacial small amplitude oscillatory dilatational properties obtained previously reflects a similar elastic response. For instance,  $\tan \delta$  obtained for interfacial rice film was ca. 0.1 at pH 2.0 and 8.0 (Romero, Beaumal et al. 2012); for potato protein  $\tan \delta$  was even ca. 0.6 at pH 2.0 and 0.1 at pH 8.0 (Romero, Beaumal et al. 2011); for crayfish protein isolate-adsorbed layers were ca. 0.2 and 0.13 at pH 2.0 and 8 respectively (Romero, Beaumal et al. 2011).  $\tan \delta$  obtained for CF2L concentrate have the same order of magnitude which indicate the remarkably elastic response, at the concentration studied here, is a consequence of strong interactions at an interface or densely packed interface with denatured protein molecules (Freer, Yim et al. 2004, Erni, Windhab et al. 2011).

Figure 5.2-5a shows a plot relating the norm of the apparent complex dilatational modulus and interfacial pressure for different proteins at pH 2.0, 3.0, 5.0 or 8.0, whereas the slope of each  $E^*$ - $\Pi$  line is plotted vs.  $\Pi$  in Figure 5.2-5b. The protein derivatives included in both figures at both pH values are crayfish protein isolate, CFPI, (Romero, Beaumal et al. 2011), as well as two other fractions (CFS and CFH), potato protein isolate, PPI (Romero, Beaumal et al. 2011), rice protein concentrate, RPC (Romero, Beaumal et al. 2012), and the protein derivative CF2L. As may be seen, the lowest interfacial pressure values correspond to CF2L, while CFPI shows the highest values. As a general

response, this figure shows that an increase in time leads to an increase in both interfacial pressure and complex modulus. However, the behaviour is strongly dependent on the protein system and also may depend on concentration and pH.

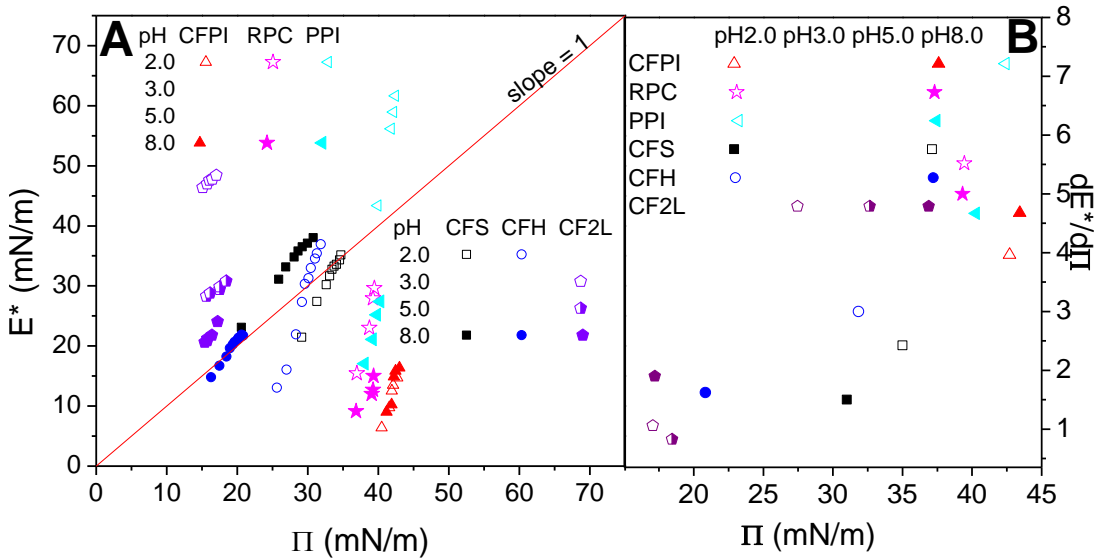


Figure 5.2-5: Relationship between the apparent dilatational viscoelastic response and interfacial pressure for CF2L compared to different protein systems (Crayfish Protein Isolates (CFPI, CFS, and CFH), Rice Protein Concentrate, RPC and Potato Protein Isolate): (A) Complex dilatational modulus; (B) Derivative of the complex modulus with respect to interface pressure.

CF2L-adsorbed layer at pH 3.0 shows a nearly ideal behaviour with a slope not far from unity, in agreement with the theory of Lucassen et al. (1975), and this behaviour corresponds to a low level of protein interactions. CF2L also shows a lower slope at pH 5.0, which indicates poorer viscoelastic properties compared to the ideal case of non-interacting molecules (negative interactions). At pH 8.0, the CF2L slope is significantly higher deviating even further from the ideal behaviour, where molecular interactions increase as the amount of protein at the interface (and interfacial pressure) increases. Other globular proteins (PPI and RPC) show even more pronounced non-ideal

responses, particularly PPI at pH 2.0, as previously reported (Romero, Beaumal et al. 2011).

### 5.2.3. Emulsion characterisation

#### 5.2.3.1. Droplet size distribution (DSD)

Figure 5.2-6 shows the DSD profiles as a function of pH for the emulsions containing an intermediate concentration of XG (0.25 wt. %), prepared according to the procedure described in experimental section.

All the emulsions exhibit a bimodal DSD profile where the peak of small droplets (ranging from 0.1 to 0.8  $\mu\text{m}$  for pH 3.0 and 8.0, and from 0.6 to 3 for pH 5.0) is fairly smooth.

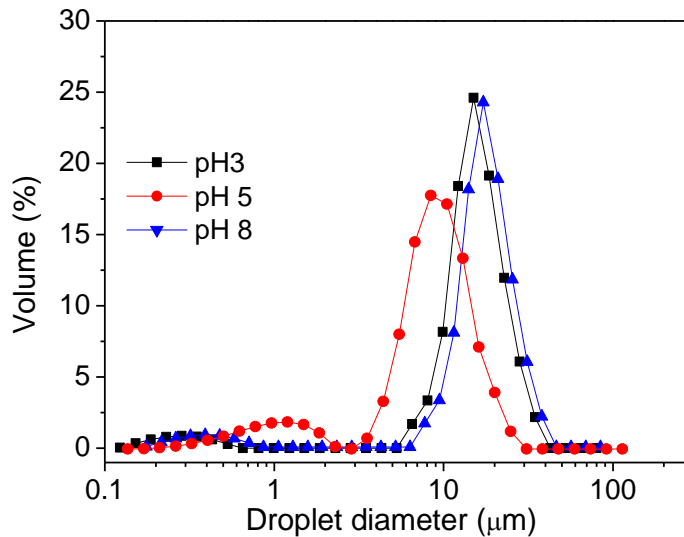


Figure 5.2-6: Droplet size distribution for emulsions made at pH 3.0, 5.0 and 8.0 at 0.25 wt. % XG concentration after adding SDS.

The location of the second peak, which corresponds to the largest amount of oil droplets, is pH-dependent, showing significant differences for the three pH values studied. Thus, while the smallest value of this second peak

corresponds to pH 5.0 (at ca. 9  $\mu\text{m}$ ), the highest is located at ca. 15  $\mu\text{m}$  at pH 3.0 and 8.0. These data are in accordance with the smaller interfacial tension found at pH 5.0, as may be observed in Table 5.2-1. In addition, it may be also considered that the protein concentration used in the emulsification carried out at pH 5.0 is higher than at any other pH value. A lower interfacial tension facilitates the formation of smaller droplets, whereas a higher protein concentration allows stabilising a higher oil droplets surface. Both factors contribute to the formation of an emulsion displaying smaller size and narrower DSD at pH 5.0. Thus, the reduction in interfacial tension is widely considered as a key factor in the emulsification process (Huang, Kakuda et al. 2001). However, protein concentration is also important in order to allow formation of a protective barrier around the new oil/water interfaces formed during emulsification (Sanchez, Berjano et al. 2001).

Figure 5.2-7 shows the DSD profiles for CF2L-based emulsions containing XG at pH 3.0, as a function of ageing time (Figure 5.2-7a) and as a function of XG concentration after seven days (Figure 5.2-7b).

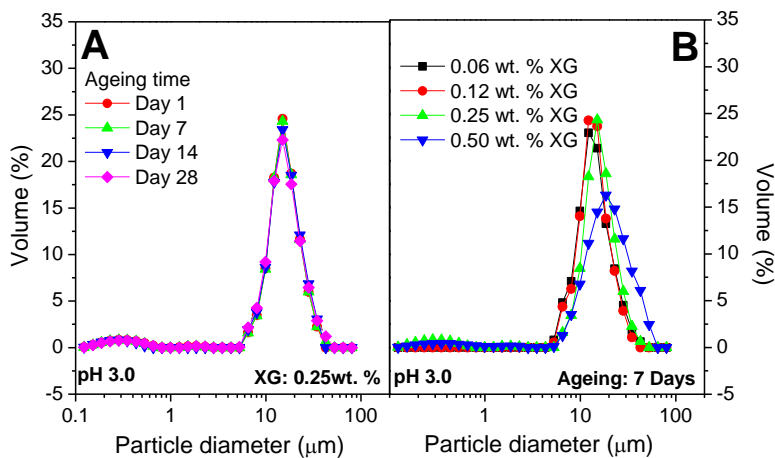


Figure 5.2-7: DSD profiles obtained for emulsions after adding SDS at constant pH and XG concentration (3.0 and 0.25 wt. %, respectively) during the ageing (A) and DSD profiles for emulsions on the seventh day of ageing at different XG concentration and pH 3.0 (B).

All the profiles shown in Figure 5.2-7a reflect the occurrence of a bimodal volumetric DSD with a smooth peak at ca. 0.3  $\mu\text{m}$  and a main peak at ca. 15  $\mu\text{m}$ . As may be observed, emulsion droplets under these conditions are fairly stable since no significant difference in size can be noticed over one month.

DSD profiles obtained at constant ageing time (7 days) show a shift from a unimodal distribution (showing only the longest peak) to the above-mentioned bimodal DSD with increasing XG content. The second peak is displaced towards higher sizes (from ca. 12 to 18  $\mu\text{m}$ ) as XG concentration is raised. It may be noticed that the increase in XG concentration also involves a wider DSD distribution, which is more apparent at 0.5 wt. % XG. Both effects can be explained in terms of coalescence caused by depletion flocculation phenomenon among oil droplets, which in turn is induced by an excess of polysaccharide. The addition of non-adsorbing macromolecules to protein-stabilized emulsions has been reported to cause flocculation by a depletion mechanism (Sanchez, Berjano et al. 2001, Romero, Cordobés et al. 2008). Although this mechanism has been reported to be reversible (Cao, Dickinson et al. 1990), a fast evolution onto irreversible coalescence seems to take place over time. As a matter of fact, addition of SDS surfactant at pH 3.0 does not yield significant differences on DSD profiles for any of the emulsion studied over ageing time (data not shown). The only effect detected has been a slight evolution of DSD profiles from 1 to 7 days ageing time taking place for emulsions containing 0.5 wt. % XG, either with or without SDS. This effect may be attributed to the above-mentioned fast evolution from depleted floccules to coalesced droplets.

Figure 5.2-8 shows the DSD profiles for emulsions containing XG at pH 5.0, as a function of ageing time in absence of surfactant (Figure 5.2-8a) and in the presence of SDS (Figure 5.2-8b). As may be observed, the evolution of DSD profiles over time is quite different compared to that one found at pH 3.0



(in the presence of SDS). In the present case (at pH 5.0), a dramatic evolution in the DSD profile takes place either for SDS-free emulsions or for emulsions deflocculated with SDS. As may be observed in Figure 5.2-8a, there is a marked evolution over ageing time towards larger droplet sizes within the range between 1 and 14 days after emulsification. This evolution might be caused by flocculation since the emulsion evolves from an initial bimodal DSD profile to unimodal distributions after ageing for the first day. However, coalescence may also play an important role. An unexpected exception to this behaviour is found for the emulsions aged for 28 days, where the peak apparently moves back to lower sizes. This is most probably due to a marked coalescence effect that provokes shifting of the main peak to very large sizes, exceeding the experimental size window.

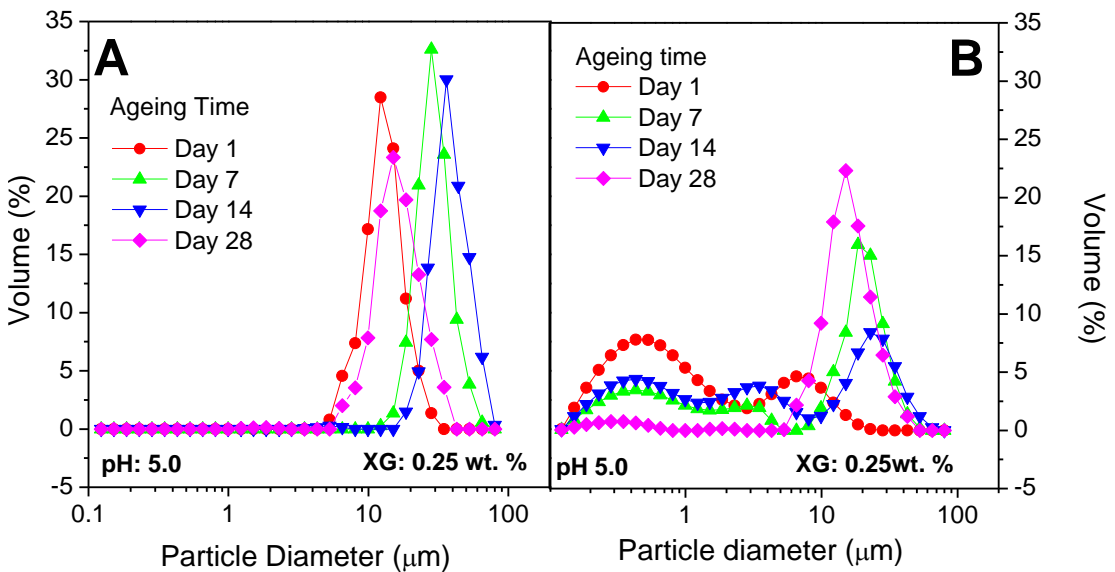


Figure 5.2-8: DSD profiles for emulsions at constant pH and XG concentration (5.0 and 0.25 wt. %, respectively) during the ageing for systems without SDS (A) and with SDS (B).

The evolution of DSD profiles after addition of SDS may be analysed in order to distinguish between flocculation and coalescence (Figure 5.2-8b). The

addition of SDS at the first day after emulsification puts forward a strong deflocculation effect, since a remarkable reduction in size and frequency may be noted for the largest peak, as well as the onset of another peak at much smaller sizes. No apparent coalescence effect seems to take place since the size of the larger peak does not undergo any significant evolution before and after adding SDS.

A different evolution is clearly observed 7 days after emulsification where the large peak is displaced towards larger sizes, whereas the small peak expands to a high extent. The former effect is due to droplet coalescence while the later must be associated to deflocculation of larger drops (emulsions without SDS shows a peak at ca. 30  $\mu\text{m}$ ). Similar effect occurs 14 days after emulsification, with a slight displacement of the second peak to larger sizes. Both results suggest that flocculation is progressively leading to coalescence as ageing time becomes longer (Tcholakova, Denkov et al. 2006). The same tendency should be expected to occur after 28 days. However, as described previously (Figure 5.2-8a), coalescence becomes so relevant that drop size exceeds the experimental size window.

In any case (before or after adding SDS), the overall evolution observed at pH 5.0 suggests that phase separation is taking place at some point over time. However, this event should be confirmed by carrying out further stability measurements.

Figure 5.2-9 exhibits DSD profiles for emulsions at pH 5.0 and different XG concentration at the same ageing time (14 days), either before (Figure 5.2-9a) or after addition of SDS (Figure 5.2-9b). In absence of the surfactant, all the SDS profiles are rather coincident, at least so it seems, being characterised by a single mode at ca. 30  $\mu\text{m}$ . However, the emulsion containing 0.5 wt. % XG shows a slightly wider polydisperse distribution. This

effect might be related to some depletion flocculation caused by the excess of XG.

After addition of SDS, the behaviour is completely different. When the XG content is low the difference between the profile without and with SDS reveals the occurrence of coalescence and also some flocculation. However, when XG is increased the coalescence effect is being progressively reduced while flocculation is becoming more relevant, thus leading to the enhancement of small-size peaks. This means that the above-mentioned lack of dependence on XG concentration shown for DSD profiles in absence of surfactant was not truly real. Thus, the same DSD profile may come from a predominant droplet coalescence process (at low XG content) or from a predominant flocculation mechanism (at higher XG content). It may be noticed that the coalescence effect seems to disappear at the highest XG concentration.

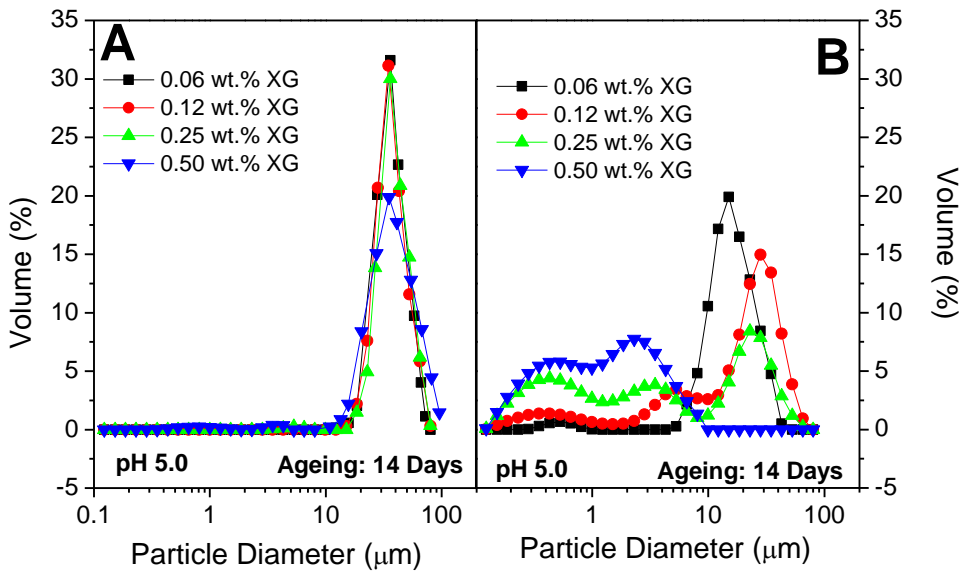


Figure 5.2-9: DSD profiles for emulsions on the fourteen day of ageing at different XG concentration and pH 5.0, without SDS (A) and with SDS (B).

As a result, it may be stated that the increase in XG tends to slow down the effect of droplet coalescence, which is particularly evident at 0.50 wt. % XG. This effect is shown at different ageing times (results not shown).

Figure 5.2-10 shows the DSD profiles for emulsions containing XG at pH 8.0, as a function of ageing time in absence of SDS surfactant (Figure 5.2-10a) and in the presence of SDS (Figure 5.2-10b). As may be observed in Figure 5.2-10a, a dramatic evolution of DSD takes place towards higher sizes seven days after emulsification. This increase in droplet size can be related to either flocculation or coalescence phenomenon.

A comparison with those DSD obtained after addition of SDS (Figure 5.2-10b) is accomplished in order to discriminate between both phenomena. This comparison evidences that after one day, flocculation is scarcely noticed and droplets remain almost unaltered since the end of the emulsification process.

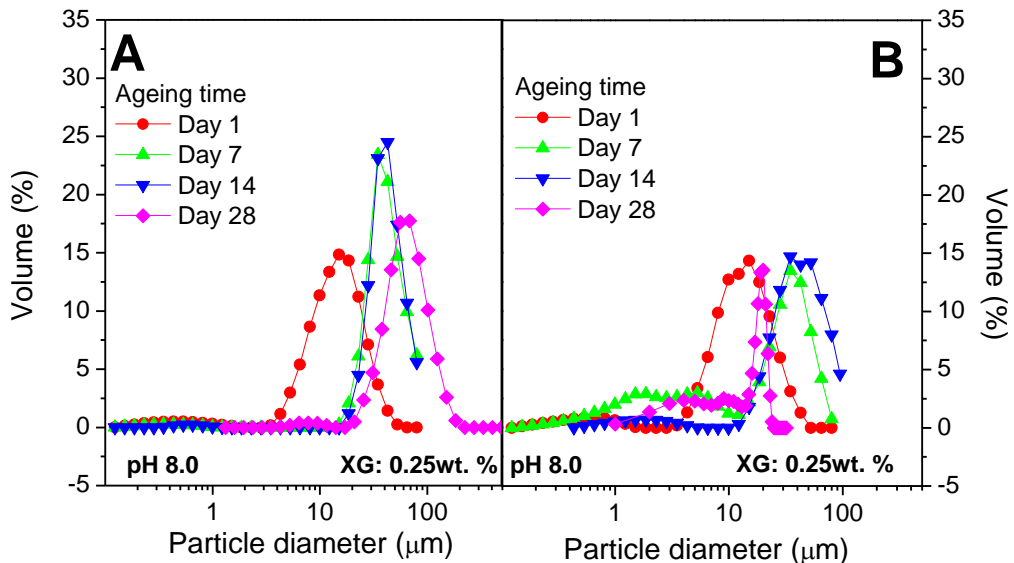


Figure 5.2-10: DSD profiles for emulsions at constant pH and XG concentration (8 and 0.25 wt. %, respectively) during the ageing for systems without SDS (A) and with SDS (B).

However after one week both, flocculation and coalescence take place. The displacement of the peak found in Figure 5.2-10a is caused not only by flocculation, which justify the peak found at lower sizes in Figure 5.2-9b, but also by coalescence, since this second peak is only little reduced after adding SDS. This trend is also found after 14 days, but coalescence becomes more noticeable. After 28 days, the response is very different, probably because extended coalescence and phase separation is eventually taking place.

Finally, Figure 5.2-11 exhibits DSD profiles for systems at pH 8.0 and different XG concentration on the seventh day of ageing either, before or after adding SDS (Figure 5.2-10a and Figure 5.2-11b, respectively). As may be observed in Figure 5.2-11a, similar DSD profiles are obtained regardless of XG concentration. As for DSD profiles obtained after adding SDS, once again, the increase in XG leads to a shift in the destabilisation mechanism from coalescence to flocculation, which may be inferred from the development of the short peak at the expense of the large one.

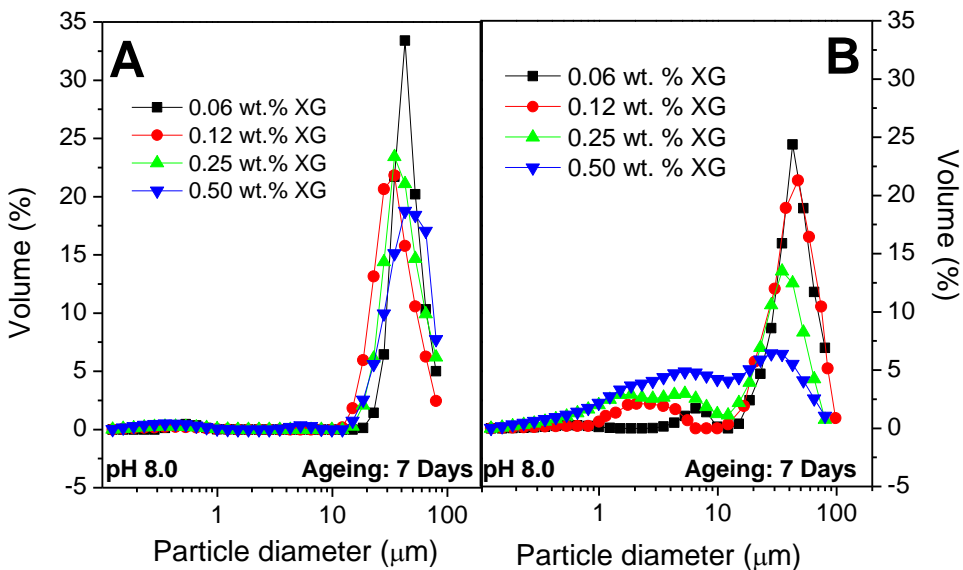


Figure 5.2-11: DSD profiles for emulsions on the seventh day of ageing at different XG concentration and pH 8.0 ageing, without SDS (A) and with SDS (B).

## Results

Two parameters (D [4,3] and Uniformity index) have been obtained from DSD measurements. Figure 5.2-12 shows the change in D [4,3], after adding SDS, as a function of ageing time. This graph summarises the results discussed above. Thus, at pH 3.0, no noticeable increase in D [4,3] takes place over time, however when XG concentration is 0.5 wt. %, emulsions exhibit a higher droplet size in the overall ageing time. This phenomenon was attributed to depletion flocculation, which initially induces a fast coalescence. In fact, this effect seems to be slightly developed at 0.25 wt. % XG.

On the other hand, droplet size shows a strong influence on ageing time for emulsions prepared at pH 5.0 and 8.0, caused by coalescence. The increase in XG attenuates this effect to a great extent. In fact at pH 8.0 no evolution in D [4,3] is noticed within 60 days ageing. At pH 5.0, the droplet sizes are always smaller than those observed for pH 8.0, at the same XG content. This may be related to both, the lower interfacial tension found at pH 5.0 and the larger amount of protein available for stabilising interfaces.

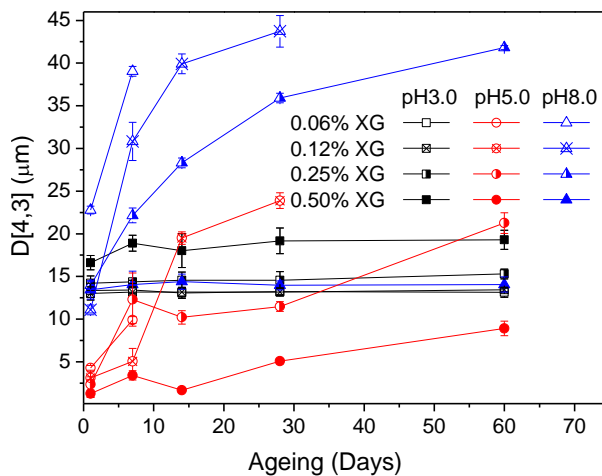


Figure 5.2-12: Evolution of D[4,3] for all systems over the ageing time (60 days) at three different pH values (3, 5 and 8) and four gum concentration (0.06, 0.12, 0.25 and 0.5 wt. %)

## Results

The uniformity parameter has been plotted in Figure 5.2-13 as a function of pH, XG concentration and ageing time. This parameter is a useful tool to determine the polydispersity of the sample, where low values are desirable. The smallest uniformity values were found for CF2L protein emulsions at pH 3.0, for all XG concentration in the overall ageing time studied, coinciding with highly stable unflocculated unimodal distributions. Emulsions prepared at pH 8.0 with low XG concentration also yield U values lower than 0.5 corresponding to unimodal distributions. However in this case the effect is linked to large droplets, being a consequence of an extensive coalescence such that early phase separation takes place. The rest of systems show U values higher than 0.8 corresponding to broad bimodal (and even trimodal) dispersions coming from significantly flocculated emulsions.

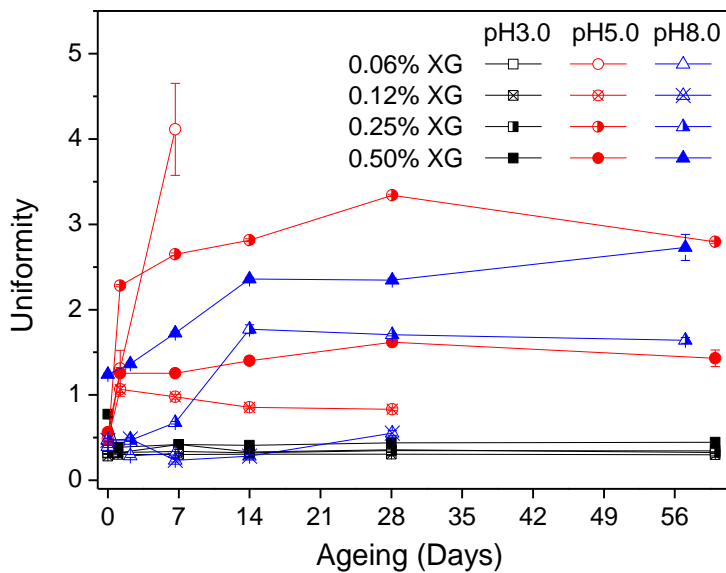


Figure 5.2-13: Evolution uniformity parameter for all systems over the ageing time (60 days) at three different pH values (3.0, 5.0 and 8.0) and four gum concentration (0.06, 0.12, 0.25 and 0.50 wt. %)

### 5.2.3.2. Rheological characterisation

#### 5.2.3.2.1. Rheological properties of the continuous phase

In order to determine the nature of the viscoelastic behaviour found for CF2L-based emulsions, a previous rheological characterisation of the continuous phase was carried out. Figure 5.2-14 shows mechanical spectra (Figure 5.2-14a) and flow curves (Figure 5.2-14b) for solutions containing 0.25 wt.% XG at the selected pH values (3.0, 5.0 and 8.0).

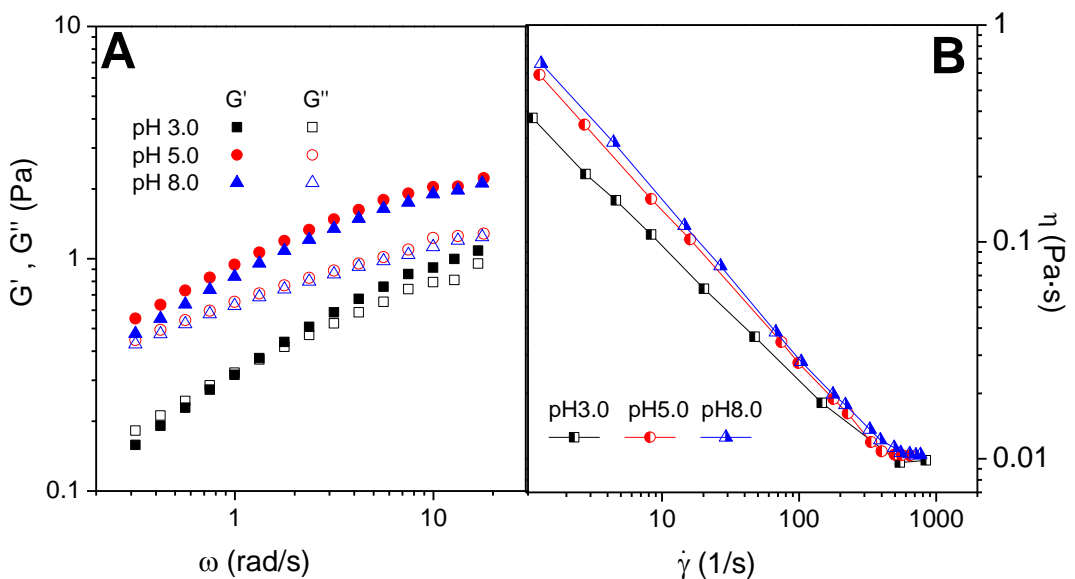


Figure 5.2-14: Viscoelastic characterisation for XG solution at 0.25 wt. % at different pH values (3.0, 5.0 and 8.0) carried out by means of oscillatory frequency sweep test (A) and flow curve (B).

Mechanical spectra plotted in Figure 5.2-14a for XG dispersions at different pH values show the behaviour of a highly associated polymeric material in solution, generally exhibiting weak “gel-like” behaviour (Rocheffort and Middleman 1987). The viscoelastic response found is pH-dependent, in spite of  $G'$  was always higher than  $G''$ , however a cross point at lower frequencies than studied is suggested at pH 5.0 and 8.0. On the contrary, the XG dispersion at pH 3.0 shows a crossover point with a shift from a



predominant viscous behaviour at low frequencies to a dominant elastic behaviour at high frequencies.

Flow curves in Figure 5.2-14b for XG dispersions show a rather shear-sensitive power-law behaviour with a tendency to reach a high shear Newtonian viscosity. Again, the responses for pH 5.0 and 8.0 are quite similar and the consistency shown by the dispersion at pH 3.0 is lower. In any case, shear forces tend to overcome this difference.

### 5.2.3.2.2. *Linear viscoelastic properties of emulsions*

Dynamic frequency sweep tests were carried out for all the emulsions studied to determine the frequency dependence of storage and loss moduli, well within the linear viscoelastic range (LVR). The mechanical spectra obtained have been plotted in Figure 5.2-15, as a function of pH, for selected emulsions at 0.25 wt. % XG concentration. Some selected parameters from mechanical spectra have been summarised in Tables: 5.2-3, 5.2-4 and 5.2-5 for all the emulsions studied.

CF2L-based emulsions exhibit a gel-like behaviour where  $G'$  is above  $G''$ , regardless of the pH value for the continuous phase, showing a moderate dependence on frequency. This behaviour corresponds to the plateau region of the mechanical spectrum and has been previously found for food emulsions using a polysaccharide as stabiliser, being attributed to the formation of a polysaccharide gel network (Tasneem, Siddique et al. 2014). Occurrence of a plateau zone has been related to the development of macromolecular entanglements either in polymer melt rheology (Fetters, Lohse et al. 1994) or in concentrated polymer solutions (Nandan, Kandpal et al. 2004). Other food emulsions (Quintana, Califano et al. 2002, Bengoechea, Cordobes et al. 2006, Romero, Cordobés et al. 2008) or aqueous dispersions of protein-

polysaccharide systems (Aguilar, Batista et al. 2011) also showed this entanglement region.

As may be seen in Figure 5.2-15, an increase in pH leads to a progressive weakening of the gel-like network of the emulsion. This effect may be attributed to modifications in the interactions among protein side chains and polysaccharide molecules. At low pH, positive charges are predominant at protein surfaces, which surround oil droplets, leading to attractive interactions with the carboxyl groups of XG dispersed in the continuous phase. Therefore, electrostatic interactions tend to reinforce emulsion network structures. Similar results were reported for O/W emulsions stabilised by potato protein isolate and chitosan (CH), at pH higher than the IEP, also resulting in attractive electrostatic interactions (Calero, Munoz et al. 2013). These authors described how CH strands were linked to protein segments located at the oil droplet surfaces and how, in this way, oil droplets were trapped into the CH network that is formed at the continuous phase. This rheological behaviour is directly related to the above-described stability found for DSD profiles at pH 3.

However, after increasing pH up to a value close to the IEP no further attractive electrostatic interactions take place, which results in an apparent reduction of the emulsion viscoelastic properties. On the other hand, a further increase in pH leads to occurrence of repulsive electrostatic interactions among protein and polysaccharide molecules, as protein surfaces are negatively charged, eventually leading to a weakening of the emulsion gel-like network.

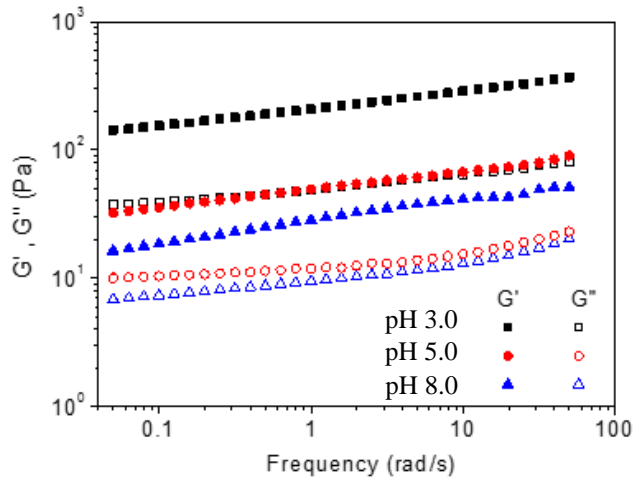


Figure 5.2-15: Mechanical spectra for systems at 0.25 wt. % XG concentration and pH 3.0, 5.0 and 8.0

Table 5.2-3 shows the values for the elastic modulus obtained at 1.5 rad/s ( $G'_{1.5}$ ) for all emulsions studied. As can be observed, an increase in gum concentration always involves an increase in  $G'_{1.5}$ . However this increase is more relevant for the system at pH 3.0. Thus, the gel strength found for this protein emulsions can be attributed not only to the polysaccharide network but also to the interaction protein polysaccharide, which depends on pH value. The structure, which causes the gel strength, has been previously attributed to the presence of polysaccharides, as a consequence of the formation of a highly flocculated droplet network (Kontogiorgos, Biliaderis et al. 2004). DSD results obtained before and after adding SDS confirm this effect at pH 5.0 and 8.0. However, these results also indicate that no significant flocculation takes place at pH 3.0. Therefore, the gel strength obtained at pH 3.0, which is the strongest of all, is a consequence of the above-mentioned electrostatic attractive interactions among protein and polysaccharide molecules.

$G'_{1.5}$  (Pa s)

System		Day 1	Day 7	Day 14	Day 30	Day 60
<b>pH3.0</b> <b>2% CF2L</b>	0.06% XG	6.8±0.2	7.8±0.2	8.7±0.2	9.0±0.2	13.5±0.3
	0.12% XG	36.4±0.5	28.9±0.5	22.1±0.3	19.4±0.5	14.6±0.4
	0.25% XG	188 ± 2	188 ± 1	162 ± 2	149 ± 1	154 ± 2
	0.50% XG	221 ± 1	199 ± 1	190 ± 1	172 ± 1	149 ± 1
<b>pH5.0</b> <b>3% CF2L</b>	0.06% XG	7.6±0.1	2.2±0.1	-	-	-
	0.12% XG	12.5±0.3	7.1±0.1	6.0±0.2	7.0±0.2	-
	0.25% XG	52.5±0.3	36.9±0.3	33.4±0.3	28.9±0.3	0.2±0.1
	0.50% XG	122 ± 2	78.9±0.3	89.6±0.5	92.6±0.4	68.1±0.3
<b>pH8.0</b> <b>2% CF2L</b>	0.06% XG	1.2±0.1	1.6±0.1	-	-	-
	0.12% XG	8.8±0.2	8.5±0.2	8.8±0.2	7.3±0.5	-
	0.25% XG	31.0±0.3	31.6±0.3	25.1±0.1	20.0±0.4	13.8±0.7
	0.50% XG	116 ± 1	83.4±0.3	63.6±0.5	59.3±0.3	59.3±0.8

*Table 5.2-3:  $G'$  values at 1.5 rad/s for all systems over the ageing time (60 days) at three different pH values (3.0, 5.0 and 8.0) and four gum concentration (0.06, 0.12, 0.25 and 0.5 wt. %)*

As for the ageing time, a decrease of  $G'$  was found for all the systems studied over the elapsed time. Thus, after two months a 15 % reduction in  $G'$  took place for all the systems, except for 0.5 and 0.25 at pH 3.0. Emulsions prepared at this pH are also more stable according to DSD measurements.

Table 5.2-4 collects results obtained from  $\tan \delta$  at 1.5 rad/s for all the emulsions studied over 2 months. As can be observed,  $\tan \delta_{1.5}$  decreases when the concentration of XG increases. These results support the key role of the polysaccharide in the formation of the gel-like network, either through formation of extensive flocculation (at pH 5.0 and 8.0) or through complexation with protein, favoured at pH 3.0. Ageing time induce some significant differences at pH 3.0 and 5.0, but not at pH 8.0. However, the increase in XG content tends to overcome this evolution of  $\tan \delta_{1.5}$  over time.

System		Tan $\delta_{1.5}$				
		Day 1	Day 7	Day 14	Day 30	Day 60
<b>pH3.0</b> <b>2% CF2L</b>	0.06% XG	0.56±0.05	0.56±0.02	0.53±0.02	0.49±0.02	0.54±0.02
	0.12% XG	0.42±0.02	0.45±0.03	0.46±0.02	0.49±0.01	0.50±0.03
	0.25% XG	0.30±0.03	0.31±0.01	0.34±0.01	0.39±0.02	0.38±0.01
	0.50% XG	0.23±0.02	0.24±0.01	0.25±0.03	0.25±0.03	0.26±0.02
<b>pH5.0</b> <b>3% CF2L</b>	0.06% XG	0.43±0.05	0.66±0.03	-	-	-
	0.12% XG	0.39±0.02	0.53±0.02	0.54±0.02	0.60±0.02	-
	0.25% XG	0.23±0.01	0.27±0.01	0.30±0.01	0.32±0.01	0.36±0.02
	0.50% XG	0.20±0.02	0.24±0.01	0.23±0.01	0.23±0.03	0.22±0.01
<b>pH8.0</b> <b>2% CF2L</b>	0.06% XG	0.73±0.03	0.71±0.03	-	-	-
	0.12% XG	0.40±0.01	0.41±0.01	0.41±0.01	0.43±0.02	-
	0.25% XG	0.32±0.01	0.32±0.02	0.30±0.02	0.30±0.01	0.31±0.02
	0.50% XG	0.24±0.02	0.22±0.02	0.23±0.02	0.23±0.03	0.23±0.02

Table 5.2-4: Tan  $\delta$  values at 1.5 rad/s for all systems over the ageing time (60 days) at three different pH values (3.0, 5.0 and 8.0) and four gum concentrations (0.06, 0.12, 0.25 and 0.5 wt. %)

The values for the slope of  $G'$  obtained after linear fitting against  $\omega$  ( $n' = \frac{d(\log G')}{d(\log \omega)}$ ) are included in Table 5.2-5 for all the emulsion studied over 60 days.

These results indicate that an increase of gum concentration leads always to an apparent reduction in the frequency dependence for  $G'$ , which is associated to an enhancement in the gel-like character of the material and has been previously related to an increase in emulsion stability (Tadros 2013). This behaviour is in agreement with above-described observations.

System		n'				
		Day 1	Day 7	Day 14	Day 30	Day 60
pH3.0 2% CF2L	0.06% XG	0.25 ± 0.02	0.25 ± 0.02	0.25 ± 0.02	0.25 ± 0.02	0.25 ± 0.02
	0.12% XG	0.23 ± 0.02	0.23 ± 0.02	0.23 ± 0.02	0.23 ± 0.02	0.23 ± 0.02
	0.25% XG	0.17 ± 0.03	0.17 ± 0.04	0.19 ± 0.02	0.23 ± 0.02	0.23 ± 0.02
	0.50% XG	0.14 ± 0.01	0.14 ± 0.01	0.14 ± 0.01	0.14 ± 0.01	0.14 ± 0.01
pH5.0 3% CF2L	0.06% XG	0.08 ± 0.03	0.30 ± 0.03	-	-	-
	0.12% XG	0.20 ± 0.02	0.33 ± 0.02	0.33 ± 0.02	0.33 ± 0.02	-
	0.25% XG	0.13 ± 0.02	0.17 ± 0.02	0.17 ± 0.02	0.19 ± 0.02	0.19 ± 0.02
	0.50% XG	0.12 ± 0.02	0.12 ± 0.02	0.12 ± 0.02	0.12 ± 0.02	0.12 ± 0.02
pH8.0 2% CF2L	0.06% XG	0.39 ± 0.03	0.31 ± 0.03	-	-	-
	0.12% XG	0.22 ± 0.02	0.22 ± 0.02	0.22 ± 0.02	0.25 ± 0.02	-
	0.25% XG	0.20 ± 0.02	0.20 ± 0.02	0.20 ± 0.02	0.19 ± 0.02	0.19 ± 0.02
	0.50% XG	0.14 ± 0.02	0.14 ± 0.02	0.14 ± 0.02	0.13 ± 0.02	0.13 ± 0.02

Table 5.2-5: G' slope (n') values for all systems over the ageing time (60 days) at three different pH values (3.0, 5.0 and 8.0) and four gum concentration (0.06, 0.12, 0.25 and 0.5 wt. %)

### 5.2.3.2.3. Flow properties of emulsions

Figure 5.2-16 shows the flow curves of emulsions at 0.25% of XG concentration one day after emulsion preparation.

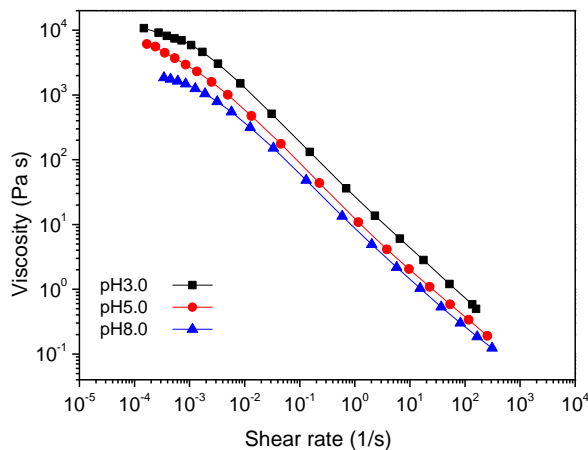


Figure 5.2-16: Flow curves for systems at 0.25 wt. % of XG concentration at different pH values (3.0, 5.0 and 8.0)

All steady state flow curves exhibit a very shear-thinning behaviour as may be deduced from the flow index values shown in Tables 5.2-6 and 5.2-7. A tendency towards a low shear Newtonian region is also noted. These flow curves can be fitted fairly well to the Cross model (EQ. 5.2-3,  $R^2 > 0.99$ ).

$$\eta = \eta_{\infty} + \frac{(\eta_0 - \eta_{\infty})}{\left[1 + \frac{\dot{\gamma}}{\dot{\gamma}_c}\right]^{1-n}} \quad (5.2-3)$$

Where  $\eta_{\infty}$  and  $\eta_0$  are the viscosities at infinite and zero shear rates, respectively.  $\dot{\gamma}_c$  is the critical shear rate for the onset of the non-Newtonian region, and n is the flow index.

Where  $\eta_{\infty}$  and  $\eta_0$  are the viscosities at infinite and zero shear rates, respectively. Parameter  $\dot{\gamma}_c$  is the critical shear rate for the onset of the non-Newtonian region, and n is the flow index.

Table 5.2-6 shows the results from the mathematical fitting to the Cross model.

System	$\eta_0$	$\dot{\gamma}_c \times 10^4$	n
<b>CF2L pH 3.0</b>	12,389±20	9.0±0.2	0.14±0.01
<b>CF2L pH 5.0</b>	6,543±49	9.5±0.2	0.13±0.02
<b>CF2L pH 8.0</b>	2,540±35	12.2±0.3	0.17±0.02

*Table 5.2-6: Parameters obtained from fitting flow curves to Cross model*

An increase in pH leads to an apparent decrease in the low shear viscosity,  $\eta_0$ , as well as an increase in  $\dot{\gamma}_c$ . However, the pH does not induce any significant difference on the flow index. Although  $\eta_0$  is the result of an extrapolation obtained through fitting to the Cross model, its evolution is consistent with that one found for other linear viscoelastic parameters such as  $G'_{1.5}$ . High values for the emulsion viscosity at zero shear rate has been

related to a kinetic stabilising effect, slowing down some destabilisation phenomena such as coalescence and creaming (Amine, Dreher et al. 2014). This increase in stability is consistent with the reduction in the evolution of DSD measurements over ageing time found at pH 3.0. The increase in  $\dot{\gamma}_c$  also reflects the tendency of increasing pH to produce a weakening of the emulsion.

Table 5.2-7 collects the values of the flow index obtained for all the emulsions studied over ageing time. As can be observed, an increase in gum concentration always leads to a decrease in the flow index, however this parameter is not affected by the ageing time, excepting at pH 5.0 and 8.0 for the lowest XG content, which are also the emulsions showing faster destabilisation. At low XG concentration the flow index is markedly affected by pH. However, this effect vanishes after increasing XG concentration above 0.12 wt. %, in spite of the strong differences found for the flow and viscoelastic properties, as well as for the DSD profiles. This behaviour suggests that the shear-thinning behaviour, which reflects the emulsion sensibility to shear, is governed by the polysaccharide.

**Flow index (n)**

System		Day 1	Day 7	Day 14	Day 30	Day 60
<b>pH3.0</b> <b>2% CF2L</b>	0.06% XG	0.33 ± 0.01	0.33 ± 0.01	0.33 ± 0.01	0.33 ± 0.01	0.33 ± 0.01
	0.12% XG	0.25 ± 0.02	0.25 ± 0.02	0.25 ± 0.02	0.25 ± 0.02	0.23 ± 0.02
	0.25% XG	0.20 ± 0.01	0.20 ± 0.01	0.20 ± 0.01	0.20 ± 0.01	0.20 ± 0.01
	0.50% XG	0.11 ± 0.01	0.11 ± 0.01	0.11 ± 0.01	0.11 ± 0.01	0.11 ± 0.01
<b>pH5.0</b> <b>3% CF2L</b>	0.06% XG	0.58 ± 0.02	0.49 ± 0.02	-	-	-
	0.12% XG	0.30 ± 0.01	0.30 ± 0.01	0.30 ± 0.01	0.30 ± 0.01	-
	0.25% XG	0.19 ± 0.01	0.19 ± 0.01	0.19 ± 0.01	0.19 ± 0.01	0.19 ± 0.01
	0.50% XG	0.13 ± 0.01	0.13 ± 0.01	0.13 ± 0.01	0.13 ± 0.01	0.13 ± 0.01
<b>pH8.0</b> <b>2% CF2L</b>	0.06% XG	0.55 ± 0.01	0.44 ± 0.03	-	-	-
	0.12% XG	0.32 ± 0.01	0.32 ± 0.01	0.32 ± 0.01	0.32 ± 0.01	-
	0.25% XG	0.19 ± 0.01	0.19 ± 0.01	0.19 ± 0.01	0.19 ± 0.01	0.19 ± 0.01
	0.50% XG	0.12 ± 0.01	0.12 ± 0.01	0.12 ± 0.01	0.12 ± 0.01	0.12 ± 0.01

*Table 5.2-7: Flow index (n) for all emulsions*



## Results

In the same way, Table 5.2-8 shows the shear viscosity at 0.1 s<sup>-1</sup> shear rate ( $\eta_{0.1}$ ) for all the emulsions studied over ageing time. As can be expected, the increase in gum concentration involves an increase in viscosity, which is more noticeable for systems at pH 3.0. Ageing time generally produce a reduction in this parameter viscosity. These results are in accordance with G' <sub>1.5</sub> values shown in Table 5.2-3.

System		Viscosity (Pa s)				
		Day 1	Day 7	Day 14	Day 30	Day 60
<b>pH3.0</b> <b>2% CF2L</b>	0.06% XG	13.4±0.3	10.3±0.7	12.7±0.5	8.1±3.1	14.2±0.7
	0.12% XG	61.2±0.7	51.1±0.9	42.8±0.7	42.0±0.9	39.2±0.8
	0.25% XG	293.9±0.8	192.7±1.5	165.2±0.9	108.1±1.1	124.4±0.5
	0.50% XG	1724.7±0.7	1781.4±0.9	1621.1±1.9	1551.2±2.1	657.5±0.8
<b>pH5.0</b> <b>3% CF2L</b>	0.06% XG	7.3±0.5	2.2±0.9	-	-	-
	0.12% XG	26.4±0.6	15.5±0.4	12.9±0.7	15.8±1.3	-
	0.25% XG	135.8±0.8	96.7±0.5	69.5±0.5	74.8±0.4	55.2±0.5
	0.50% XG	1010.1±1.3	395.90.7	378.1±0.8	350.6±0.9	309.6±0.8
<b>pH8.0</b> <b>2% CF2L</b>	0.06% XG	0.9±0.1	3.0±0.2	-	-	-
	0.12% XG	13.9±0.3	23.3±0.5	23.7±0.4	20.1±0.5	-
	0.25% XG	80.3±0.4	78.9±0.8	54.0±0.7	57.8±0.6	59.8±1.1
	0.50% XG	735.5±1.7	484.2±1.1	515.6±1.9	409.5±0.6	434.9±1.9

*Table 5.2-8: Shear viscosity at 0.1 s<sup>-1</sup> shear rate for all emulsions studied over the ageing time (60 days) at three different pH values (3.0, 5.0 and 8.0) and four different XG concentration (0.06, 0.12, 0.25 and 0.5 wt. %)*

From the above discussed results, it may be deduced that steady flow properties of these emulsions, similarly to linear viscoelastic properties, seem to be governed by protein-polysaccharide interactions that in turn depend on pH. Those interactions also seem to control the destabilization of the emulsions studied.

### 5.2.3.3. Light scattering measurements

Consecutively to emulsification process, and as a part of the stability study, light scattering diffraction was measured, reflecting both short and long-term stability in the emulsions containing 0.25 wt. % XG. Back Scattering (BS) measurements were performed in order to determine the destabilization mechanism of CF2L emulsions. Figure 5.3-17 shows BS profiles for emulsions prepared at 0.25 wt. % XG and pH 3.0, as a function of time. At pH 3.0, emulsions do not seem to be affected by coalescence, however some creaming may be detected in a small proportion, at long term.

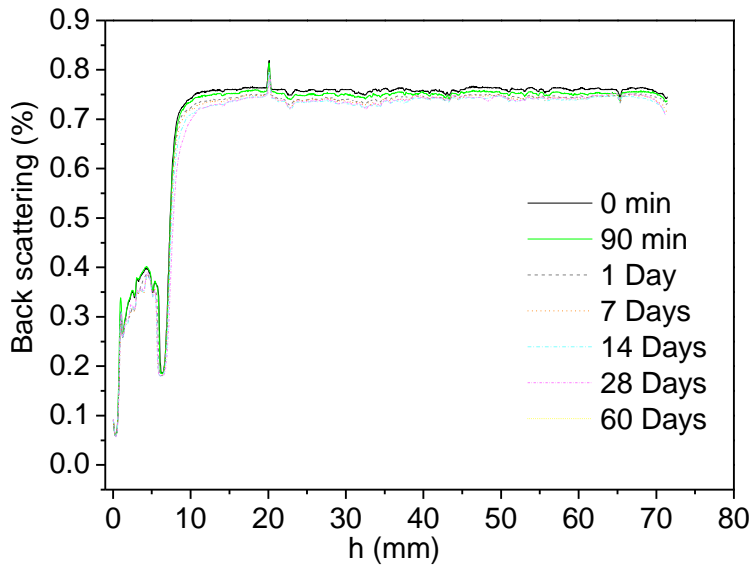


Figure 5.2-17: Evolution of backscattering results obtained at 20°C for emulsion at pH 3.0 and 0.25 wt. %.

However, Back Scattering (BS) measurements were also performed in order to determine the destabilization mechanism of CF2L emulsions at pH values 5.0 and 8.0 (Figure 5.2-18 and Figure 5.2-19, respectively). These graphs

exhibit quite different emulsion behaviour. As may be observed, the back scattering decreases homogeneously in the overall tube length, which indicates occurrence of marked coalescence/flocculation phenomena.

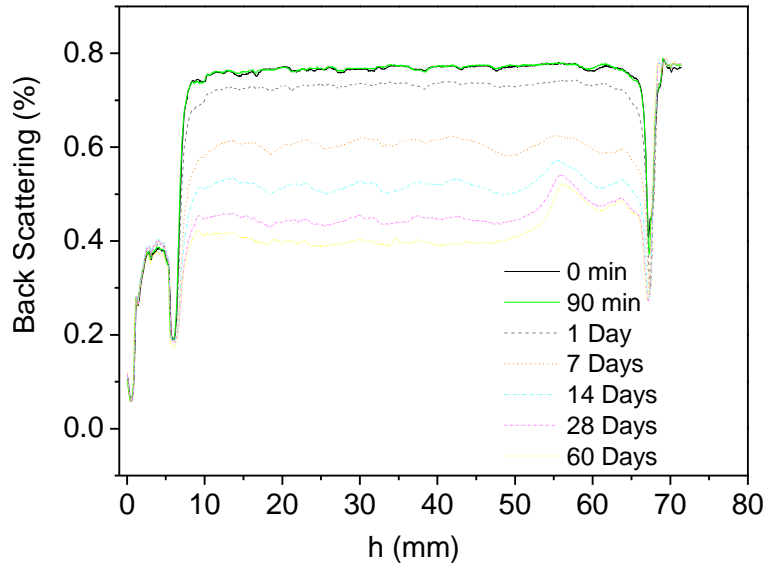


Figure 5.2-18: Evolution of backscattering results obtained at 20°C for emulsion at pH 5.0 and 0.25 wt. %.

These results are in accordance with DSD measurements, which detected both, coalescence and flocculation phenomena. However, the determination of creaming process in *BS* measurements cannot be determined in this measurement, since the presence of the above mentioned destabilisation phenomena probably mask this process.

In addition, a peak at the top side can be observed. This peak is related to oiling-off and become rather pronounced for system at pH 8.0. The difference of emulsion viscosity can explain the different ratio of oiling off.

Both emulsions have the same destabilization process, however emulsion at pH 8.0 has lower viscosity. Big drops coming from coalescence at pH 8.0 are able to rise faster than those formed at pH 5.0.

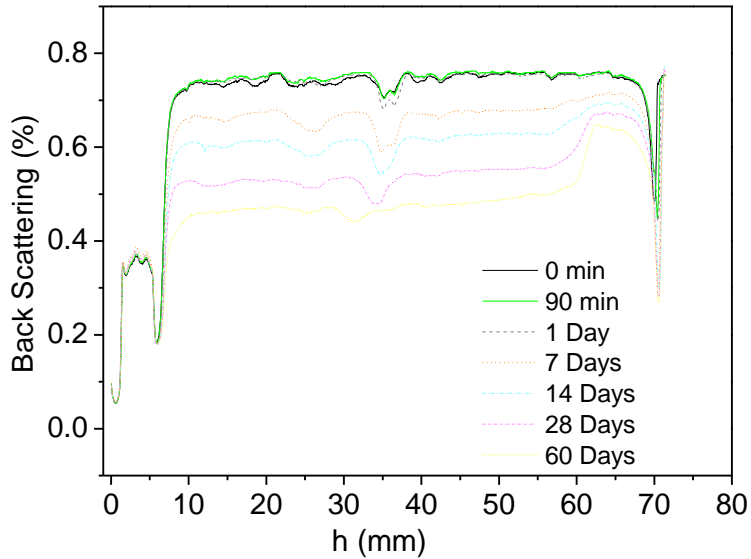


Figure 5.2-19: Evolution of backscattering results obtained at 20°C for emulsion at pH 8.0 and 0.25 wt. %.

Figure 5.2-20 shows the evolution of the relative Back Scattering ( $\Delta BS$ ) as a function of time obtained within the middle part of the tube.  $\Delta BS$  is defined as follows (EQ. 5.2-4):

$$\Delta BS = BS_0 - BS_t \quad (5.2-4)$$

where  $BS_0$  and  $BS_t$  are the mean values for the  $BS$  profile obtained at the initial time and time  $t$ , respectively.

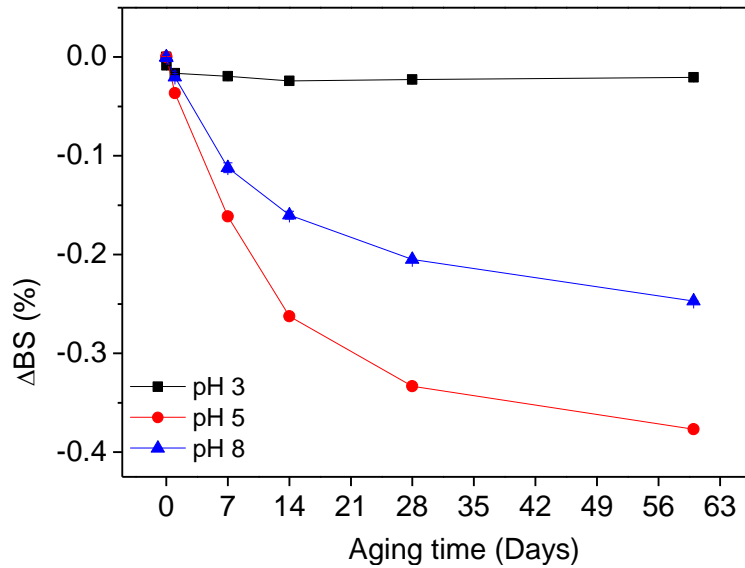


Figure 5.2-20:  $\Delta$ BS for emulsions at 0.25 wt. % XG concentration at pH 3.0, 5.0 and 8.0 at the middle of the tube length

Figure 5.2-20 summarises the results from Figure 5.2-17, Figure 5.2-18 and Figure 5.2-19. CF2L-based high oleic emulsions at pH 3.0 do not suffer any significant coalescence destabilisation in the studied ageing. On the other hand,  $\Delta$ BS values decrease dramatically at pH 5.0 and 8.0, as a consequence of the coalescence process, which is more noticeable at pH 5.0.

#### 5.2.3.4. Optical measurements

Figure 5.2-21 shows the confocal laser scanning microscopy (CLSM) images for CF2L-based high oleic and low-oil content emulsions. Pictures were taken for emulsions containing 0.25 wt. % XG, at the three pH values studied and also at different ageing time (1, 7 and 14 days).

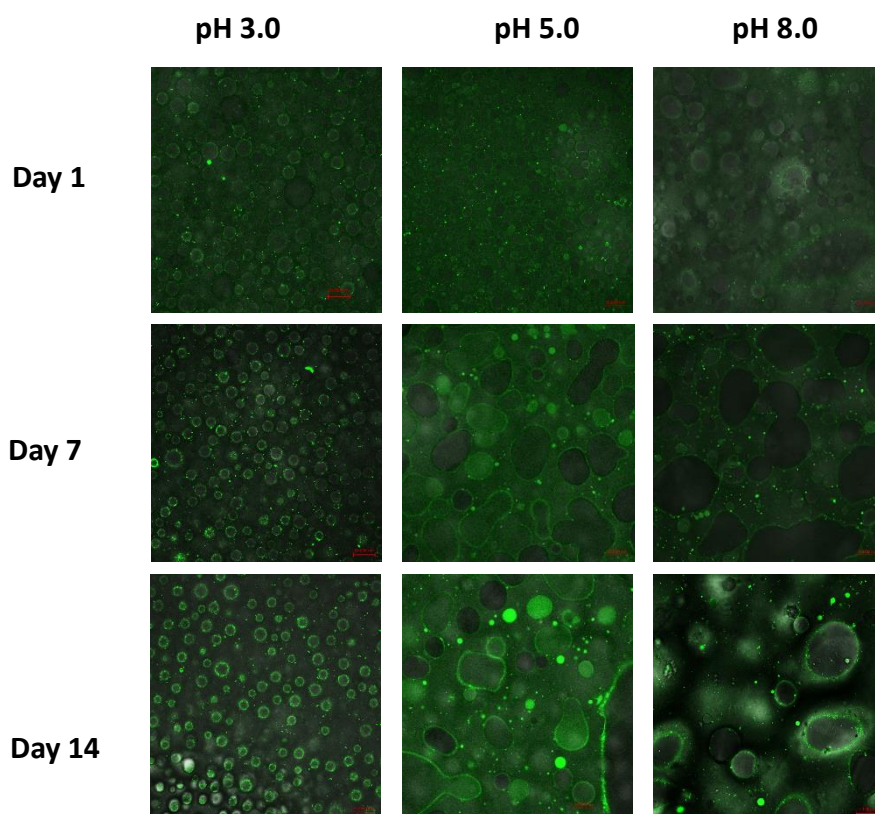


Figure 5.2-21: Confocal microscopy for emulsions made at pH 3.0, 5.0 and 8.0 over 14 days

Since proteins exhibit auto-fluorescence, a high light intensity corresponds to the presence of protein. CLSM images illustrate how protein is preferentially located at the oil/water interfaces, although some small aggregates may be also detected.

As may be observed, at the beginning, the smallest drops are found in the emulsion at pH 5.0. However after the first week emulsion droplets at pH 5.0 and 8.0 are increased dramatically their sizes, being the consequence of coalescence. Only droplets at pH 3.0 hold their initial size, being more stable over the selected ageing time (14 days). The presence of protein aggregates

seems to be more apparent at pH 5.0 and 8.0, where coalescence is relevant, as less protein is necessary to cover the reduced interfacial area.

These pictures also confirm results shown in previous sections. Thus, oil/water interfaces seem to be better defined at pH 3.0. These results are in accordance with DSD and interfacial rheology data. The lower interfacial equilibrium tension at pH 5.0 allows the formation of smaller drops, however the stronger interface found at pH 3.0 favours the stability of the systems. Emulsions after 1 day at pH 8.0 exhibits an inhomogeneous DSD, characterised by a soft interface.





## 5.3. Antioxidant Crayfish Gels

### 5.3.1. CF2L-based protein gels

Gels from CF2L dispersions were obtained according to the procedure described in section 4.2.3.3. Taking into account the solubility curve, three pH values were selected: a neutral pH (6.5), relatively close to the isoelectric point, an acid pH (2.0) and an alkaline pH (8.0), both of the later pH values being far from the IEP.

#### 5.3.1.1. Viscoelastic characterisation

##### 5.3.1.1.1. Gel formation

Figure 5.3-1 shows the evolution of SAOS viscoelastic properties (the storage modulus,  $G'$  and the loss modulus,  $G''$ ) of CF2L dispersions at constant protein concentration (12 wt. %) for three different pH values (2.0, 6.5 and 8.0) over the thermal gelation process.

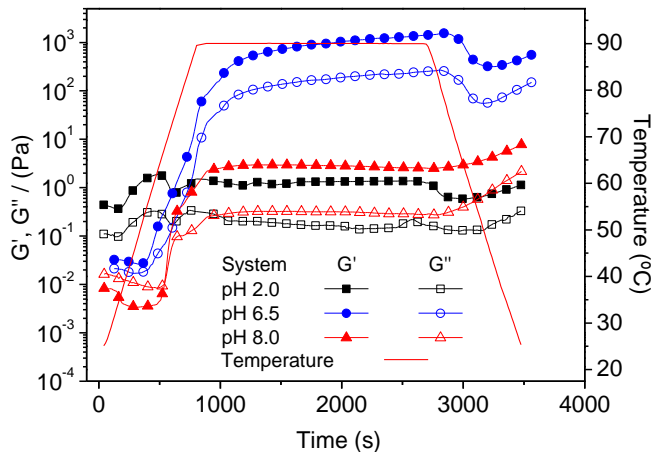


Figure 5.3-1: Temperature ramp tests performed at constant frequency, 6.3 rad/s, and constant heating rate, 5 °C/min, for CF2L dispersions (12 wt. %) at three different pH values (2.0, 6.5 and 8.0) followed by a isothermal step (90 °C, 30 min) and a cooling step (rate: 5 °C/min).

The SAOS profiles for all the pH values show a different evolution depending on the stage of the thermal cycle applied:

i) The first heating stage, performed at constant heating rate, begins with a smooth decrease in  $G'$  and  $G''$ , taking place at temperature lower than 45 °C. Over these first several hundreds of seconds, the increase in temperature leads to an increase in mobility of the protein chains, due to thermal agitation, where physical interactions (i.e. hydrogen bonds) are typically reduced. However, protein aggregation has also been reported at temperatures below 50 °C (Ramos, Pereira et al. 2014). In fact, this behaviour has been previously found for crayfish protein and was attributed to the aggregation of the globular head regions of myofibrillar protein molecules (Romero, Bengoechea et al. 2009). This aggregation depends on the oxidation of sulfhydryl groups, which shows considerable reduction in the early temperature range of 30-50 °C (Acton and Dick 1988, Sano, Ohno et al. 1994). Other authors have also found a minimum in  $G'$  in this temperature region. The increase in  $G'$  with increasing temperature above the minimum was attributed to denaturation of myosin chains, suggesting that  $\alpha$ -helices in the tail segments began to unfold around 30-40°C (Yoon, Gunasekaran et al. 2004, Kim, Yongsawatdigul et al. 2005, Romero, Bengoechea et al. 2009). Moreover, in this temperature range,  $G'$  is above  $G''$  at pH 2.0 and 6.5, whereas  $G'$  is below  $G''$  at pH 8.0, which suggests that physical interactions are initially weaker at this pH value.

Subsequently, in all systems, above 60°C a strong increase in both moduli ( $G'$  and  $G''$ ) takes place as the temperature increases. This effect may be related on one hand to protein aggregation and association of aggregates to form gel network structures (Cordobes, Partal et al. 2004) and on the other to structural changes of the helical rod segments of myosin proteins which promote the network formation through sulphide-bonds of protein segments (Acton and Dick 1988).

ii) During the second heating stage, performed at constant temperature, no apparent increase in the moduli could be noticed, neither at pH 2.0 nor at pH 8.0, whereas  $G'$  and  $G''$  still undergo a moderate increase at pH 6.5. These results indicate that formation of disulphide-bonds of the helical rod segments of myosin is counterbalanced at pH 2.0 and 8.0 by electrostatic repulsion between protein chains, whereas it is favoured at pH 6.5, at which the protein surface charges are much weaker due to its proximity to the IEP.

iii) Finally, during the third stage, performed at constant cooling rate, an increase in both viscoelastic moduli occurs, although it may be preceded by a smooth decrease in viscoelastic properties. During this cooling stage, physical interactions (i.e. hydrogen bonding) are responsible for this increase in mechanical moduli. These interactions may be important in the stabilization of the protein system. In addition, hydrogen bonds may also contribute to immobilize water into the hydrogel network (Lanier, Carvajal et al. 2005).

### 5.3.1.1.2. *Gel characterisation*

#### *Mechanical spectra of gels*

Figure 5.3-2 shows the evolution of SAOS viscoelastic properties (the storage modulus,  $G'$ , and the loss modulus,  $G''$ ) of CFL2.0 dispersions at constant protein concentration (12 wt. %) for three different pH values (2.0, 6.5 and 8.0) as a function of frequency.

The mechanical spectra indicate that all the systems exhibit gel-like behaviour, where  $G'$  is higher than  $G''$ , both functions showing a slight dependence on frequency. The evolution of linear viscoelastic properties for CFL2 gels with increasing pH is quite similar to that found for the thermal processing.

Two different gel strength behaviours were observed: At pH 6.5, the system exhibits an almost parallel evolution within the whole frequency

range, which denotes the occurrence of a strong gel (showing the lowest  $\tan \delta$  values, around 0.2 in the overall interval). This behaviour may be attributed to the absence of net charge observed close to the IEP, which means that at this pH value, electrostatic repulsions could not be taken into account as a destabilizing phenomenon. On the contrary, at low pH (pH 2), the CF2L-gel behaviour is closer to that of a typical weak gel, where  $\tan \delta$  values is not constant over the frequency interval studied, increasing its value at high frequency (from 0.2 to 0.45). This low gel-strength exhibited at pH 2.0 may be related to the remarkable increase of the relative amount of peptide fraction found in section 5.1.1.2 most probably being a consequence of acid hydrolysis. Finally, although the gel at pH 8.0 also exhibits strong gel behaviour,  $\tan \delta$  at high frequency rise up to 0.36, exhibiting an intermediate gel-like structure between those found at pH 6.5 and 2.0.

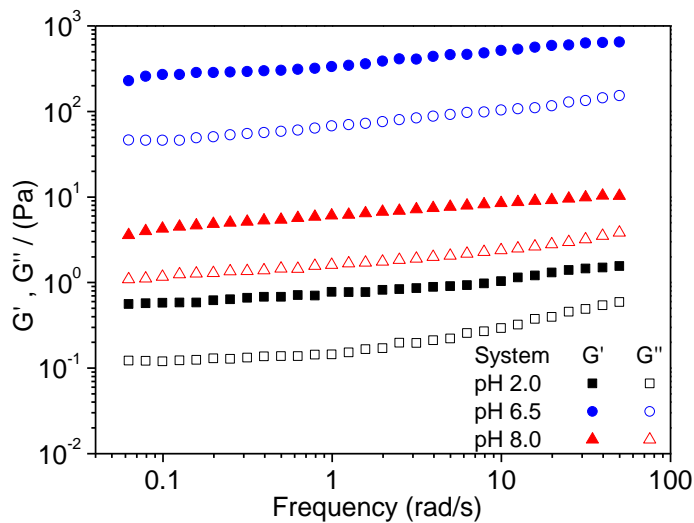
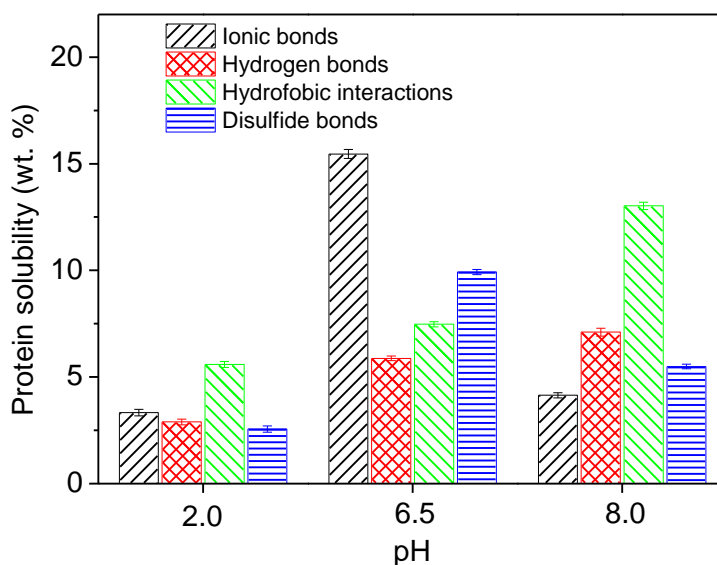


Figure 5.3-2: Evolution of linear viscoelastic properties for CF2L protein system gels as a function of frequency (from 0.06 to 50 rad/s) performed at three different pH values (2.0, 6.5 and 8.0)

### *Protein interactions*

The gel structure has been evaluated by quantifying the interactions among different protein chains present in gels (Figure 5.3-3):



*Figure 5.3-3: Effect of pH on interactions nature: Ionic bonds, hydrogen bonds, hydrophobic interactions and disulphide bonds*

As may be observed in this picture, interactions depend strongly on pH values. Ionic bonds, hydrogen bonds, hydrophobic interactions and disulphide bonds are highly involved in the formation of the gel network (Careche, Alvarez et al. 1995, Cofrades, Carballo et al. 1996, Gomez-Guillen, Montero et al. 1998). Thus, at acid pH, interactions are low and, as a result, the gel is weak. These results are consistent with the above mentioned results for the viscoelastic properties (low  $G'$  and  $G''$  values).

At pH close to the IEP (pH 6.5), ionic interactions are the most important in absolute terms, which suggests that interactive forces are active, in spite of their weakness. This effect is probably related to the absence of repulsive

electrostatic interactions as a consequence of the proximity to the IEP. However, it does not suffice to explain the gel strength, taking place at this pH. This remarkable gel strength found in the rheological study is probably attributed to disulphide bonds which are the main responsible for the gel strength (Lanier, Carvajal et al. 2004).

Finally, at alkaline pH (pH 8.0), hydrophobic interactions are the most important interactions, in spite of the large number of disulphide bonds, compared to pH 2.0. These hydrophobic interactions were usually considered as the most important bonds in surimi gels (Gomez-Guillen, Borderias et al. 1997, Liu, Zhao et al. 2011). As explained above, they arise as a consequence of the exposure of protected polar groups taking place after heat-induced unfolding of native proteins (Lanier, Carvajal et al. 2005) .

All these results indicate that disulphide bonds show the greatest effect on gel strength. However, formation of disulphide bonds seems to be counterbalanced by repulsive interactions taking place as a result of charged protein surfaces (far from the IEP). Ionic interactions, being particularly relevant at the IEP, act avoiding repulsive electrostatic interactions, thus contributing to facilitate formation of S-S bonds. Hydrophobic interactions, typically enhanced over thermal heating, as well as hydrogen bonds, play an important role at the cooling stage, both contributing to reinforce the gel network structures. Thus,  $G'$  and  $G''$  profiles undergo a noticeable increase upon cooling at pH 8.0, where hydrophobic interactions are relevant.

### *Water holding capacity*

The water holding capacity (WHC) was determined for each gel for three different pH values (Figure 5.3-4).

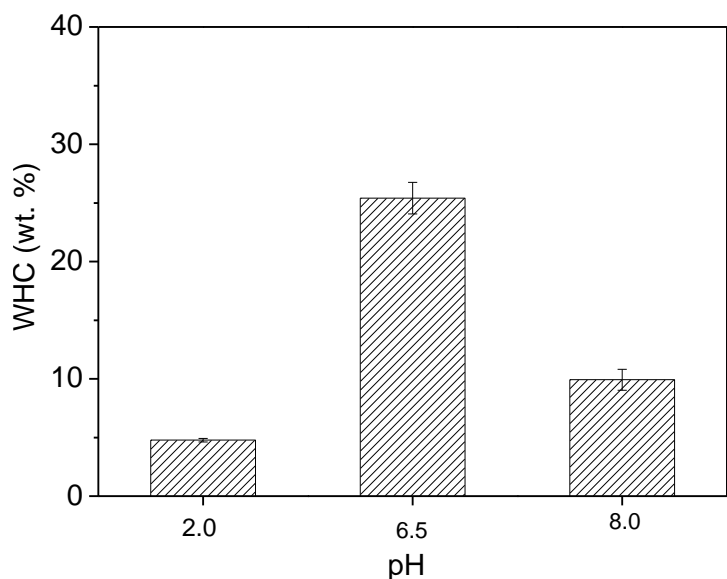


Figure 5.3-4: Water holding capacity of gels performed at three different pH values (2.0, 6.5 and 8.0).

Water holding capacity (WHC) usually reflects the strength of a protein gel network. Proteins generally build a continuous three-dimensional network during thermal gelation and retain water in its network. The results from WHC tests are in agreement with those obtained from linear viscoelasticity and interactions measurements, all of them reflecting different aspects of gel strength. In this sense, the gel with the highest value of WHC is the gel made at pH 6.5. This corresponds to the gel showing higher viscoelastic moduli (higher  $G'$  and  $G''$  and lower  $\tan \delta$ ) and higher amount of total interactions, particularly disulphide bonds.

#### *Bioactivity characterisation*

Figure 5.3-5 shows the antioxidant activity of the gels formed at different pH values compared to the reference (Propyl Gallate, PG) measured according to three different methods: DPPH, Folin–Ciocalteu and ABTS. These methods

are widely used in the food and nutraceutical industries to determine the antioxidant capacities of foods, beverages and nutraceutical products (Slizyte, Mozuraityte et al. 2009).

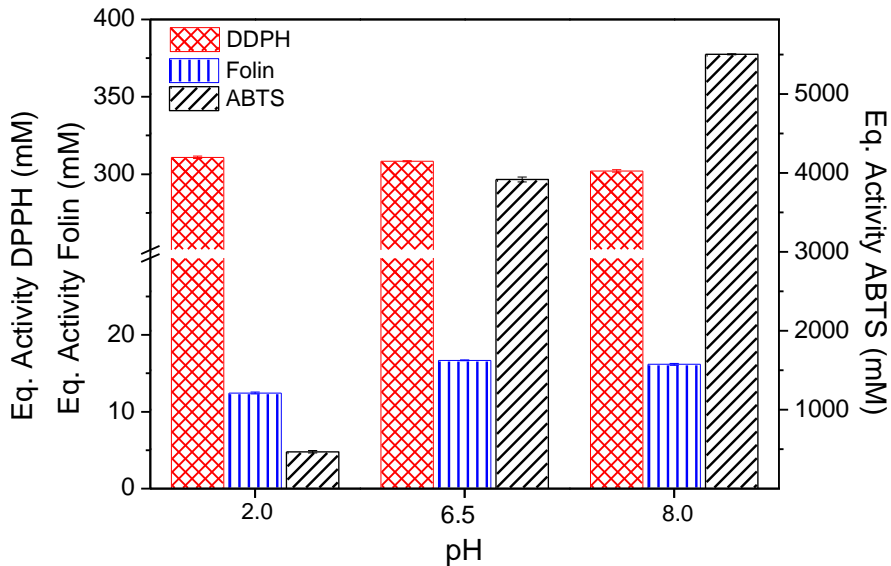


*Figure 5.3-5: Antioxidant activity of CF2L gels at three different pH values (2.0, 6.5 and 8.0) behind three different compounds: ABTS, DPPH and Folin-Ciocalteu, compared to the activity of the reference compound (Propyl Gallate, PG).*

The DPPH method is based on the reduction of DPPH and takes place when some substrate is able to donate a hydrogen group, which leads to the formation of the non-radical form DPPH-H (Blois, 1958). All the gels show a similar radical scavenging activity, having the same activity as c.a. 310 mM of PG equivalent. Most of the studies on DPPH scavenging activity have been focused on different vegetable oils, grapes and wines (Arranz, Cert et al. 2008, Espinoza, Olea-Azar et al. 2009, Spatafora, Barbagallo et al. 2013), even some researchers have found this property for proteins such as egg yolk and fish proteins, which can scavenge free radicals (Sakanaka, Tachibana et al. 2005, Elias, Kellerby et al. 2008, Kristinova, Mozuraityte et al. 2009).



ABTS assay is based on the ability of antioxidant compounds to decolorize the ABTS radical cation, denoted as  $ABTS^{*\cdot}$ , which is blue in methanol solution and has a maximum absorbance at 734 nm (Walker and Everette 2009). Figure 5.3-5 shows that these gels have a high ABTS antioxidant ability. In contrast to DPPH, the pH has a remarkable effect, exhibiting an activity between 500 and 5500 mM PG equivalent. This strong dependence on pH cannot be justified on the basis of protein interactions, since the trend followed by the ABTS assay is not in accordance to the gel interactions and rheology measurements. Thus, whereas gels exhibit a higher ABTS activity when an increase in pH values takes place, structural characterisation showed that stronger interactions (and as a consequence higher gel strength) occurred at pH 6.5. This pH effect is also contradictory for other authors, Floch et al. (2007) found the highest activity in soil at low pH values. However, Lemanska et al. (2001), found the same pH effect for hydroxyflavones, which means that the ABTS assay is strongly dependent on the nature of the protein studied.

The FC reagent was initially used as a colorimetric method for the analysis of the proteins. Due to its activity towards tyrosine (containing a phenol group) (Folin and Ciocalteu 1927, Markwell, Haas et al. 1978), Singleton et al. (1999) made extensive use of this phenol affinity in order to determine the total phenols in wine (Singleton, Orthofer et al. 1999, Huang, Kakuda et al. 2001). Now the FC reagent is used to determine antioxidant activity of proteins (Kristinova, Mozuraityte et al. 2009). The FC assay is based on the oxidation of phenol compounds in alkaline (carbonate) solution giving a coloured product with a maximum absorbance ( $\lambda_{max}$ ) at 765 nm (Apak, Gueclue et al. 2007). As may be observed in Figure 5.3-5, all gels show a FC antioxidant activity with a slight increase if the pH value rises from 2.0 to 8.0. This antioxidant activity is quite different from the ABTS radical cation assay, which also was sensitive to phenol compounds. This difference may be

explained because the FC reagent is not capable to measure lipophilic antioxidants due to the high affinity of the FC chromophore towards water (Berker, Olgun et al. 2013).

Despite the different behaviour of protein gels, many studies have been reported showing this effect that depends on the active agent and the type of assay (DDPH, ABTS, FC) (Wojdylo, Oszmianski et al. 2007, Wootton-Beard, Moran et al. 2011).

TCA-soluble peptides can be observed in Figure 5.3-6. The amount of TCA-soluble peptide was determined before and after the gelation process in order to determine the protease activity during the gelation step. This fact can be important because the characteristic texture of fresh fish or food product may be modified (Miller and Spinelli 1982, Greene and Babbitt 1990). A slight increase in TCA-soluble peptides was observed at 20°C concomitant with an increase in pH. This means that an increase in pH values gives an increase in the number of amino acids and small peptides in the bulk solution. Subsequently, after the gelation process, TCA-soluble peptides do not increase in any of the gels and there is therefore no proteolytic activity as a consequence of the thermal procedure. A decrease of TCA-soluble peptides was found at pH 6.5 after gelation process. This fact confirms structural results found previously in the functional characterisation. In this way, at this pH, the gel not only exhibits better mechanical properties (higher gel strength and higher WHC), but the gel is also able to hold more free amino acids and short peptides.

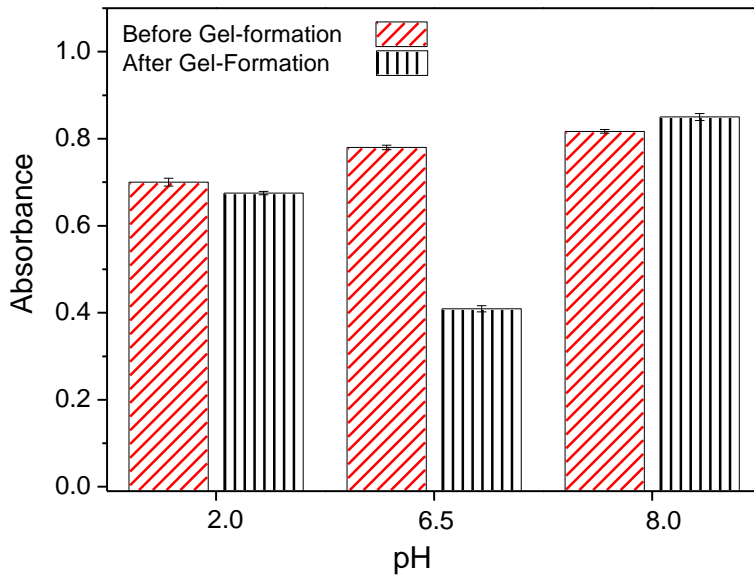


Figure 5.3-6: Proteolytic activity measured at two different wave-length (280 and 562 nm) in gels, evaluated at three different pH values (2.0, 6.5 and 8.0), before and after gelation process.

### 5.3.2. CF2L-Protein hydrolysate gels

CF2L system was hydrolysate according to the method described in section 4.1.3. After the kinetic study, different hydrolysates, based on their degree of hydrolysis, were selected. The hydrolysis time were: 5, 25, 120 min, and the systems obtained were named as: CF2L<sub>5</sub>, CF2L<sub>25</sub>, and CF2L<sub>120</sub>.

#### 5.3.2.1. Gel Characterisation

##### 5.3.2.1.1. Viscoelastic characterisation

###### *Gel formation*

Below are three figures that show the evolution of  $G'$  and  $G''$  obtained for all the systems studied over the gelation process at pH 2.0 (Figure 5.3-7), 6.5 (Figure 5.3-8) and 8.0 (Figure 5.3-9). All the dispersions evaluated contained 12 wt. % protein.

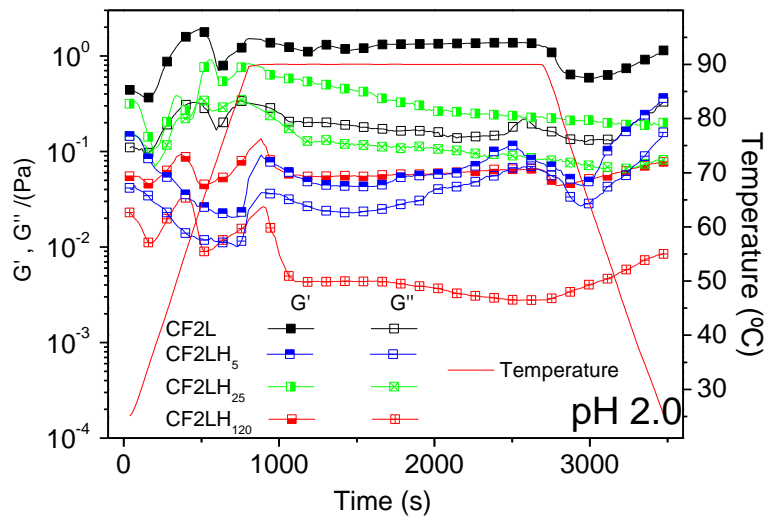


Figure 5.3-7: Temperature ramp tests performed at constant frequency, 6.3 rad/s for proteins dispersions: CF2L, CF2LH<sub>5</sub>, CF2LH<sub>25</sub> and CF2LH<sub>120</sub> at 12 wt. % and pH 2. An initial heating step (5°C/min from 25 to 90°C) was followed by an isothermal step (90°C, 30 min) and a cooling step (rate: 5°C/min from 90 to 25°C).

As may be seen in Figure 5.3-7, none of the systems studied at pH 2.0, neither CF2L nor the hydrolysates, exhibit any gelling potential within the gelling conditions studied, since the highest  $G'$  achieved is around 1 Pa. Hence, at this pH no strong interactions between protein chains were found, and very weak gel-like products were obtained. In fact, they behave as high viscous liquids which cannot keep its shape.

Regarding the degree of hydrolyses, only CF2L and CF2L<sub>5</sub> exhibit a slight thermal-induced reinforcing potential, where the system after heating stage is a bit more structured than at the beginning. It seems that the hydrolysis inhibits the cross-linking and interaction potentials of CF2L proteins derivatives at pH 2.0 (Jin, Wu et al. 2014).

Figure 5.3-8 shows the gelation process for all the system studied at pH 6.5. At this pH value the evolution over the thermal cycle is quite different and the gelation profile is more similar to other typical protein gelation processes (Romero, Cordobes et al. 2009). As described in the previous section where the gelation was described for CF2L protein-based gels, the behaviour is characterised by a first stage below 45°C where a smooth decrease in  $G'$  and  $G''$  takes place. Firstly, an increase in temperature involves an increase in mobility of the protein chains, due to the thermal agitation (electrostatic and hydrogen bonds interactions are reduced), and as consequence the viscoelastic properties of the dispersions decrease. At this moment, positive interactions are not significant. This protein behaviour has been previously attributed to the oxidation of sulfhydryl groups, which show considerable reduction in the early temperature range of 30-50°C (Acton and Dick 1988, Sano, Ohno et al. 1994).

Above 60°C, an increase in temperature value involves a remarkable increase in both modulus ( $G'$  and  $G''$ ). This effect can be a consequence of structural changes of the helical rod segments of myosin proteins which

promote the network formation through sulphide-bonds of these segments. (Acton and Dick 1988).

Finally, at the cooling stage, a slight decrease followed by an increase of both moduli ( $G'$  and  $G''$ ) takes place. Physical interactions (e. g. hydrogen bonds, hydrophobic interactions...) have been postulated to be able to increase both mechanical moduli. These interactions are important in the stabilization of the protein system. (Lanier, Carvajal et al. 2005).

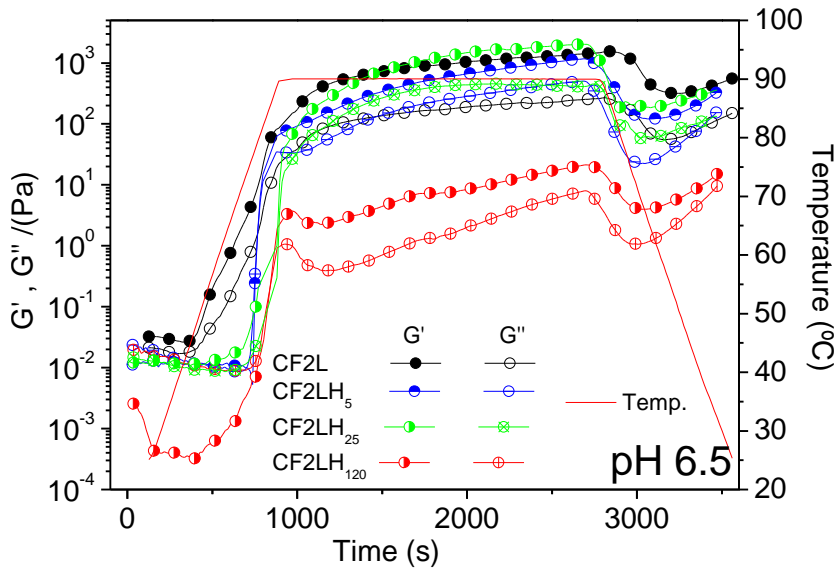


Figure 5.3-8: Temperature ramp tests performed at constant frequency, .63 rad/s for proteins dispersions: CF2L, CF2LH<sub>5</sub>, CF2LH<sub>25</sub> and CF2LH<sub>120</sub> at 12 wt. % and pH 6.5. An initial heating step (5°C/min from 25 to 90°C) was followed by an isothermal step (90°C, 30 min) and a cooling step (rate: 5°C/min from 90 to 25°C).

It is worth mentioning that all the systems except CF2LH<sub>120</sub> protein hydrolysate exhibit similar evolution of the viscoelastic functions over protein cross-linking. The maximum  $G'$  value obtained for CF2L, CF2LH<sub>5</sub> and CF2LH<sub>25</sub> is around 1,000 Pa, without any significant difference among these systems. In contrast, CF2LH<sub>120</sub> system cannot achieve the same level of gel strength.

Previously, Jin et al. (2014) found that the gel ability is restricted by the degree of protein hydrolysis. Hydrolysis tends to decrease gelation properties, because it reduces the molecular weight, although increases the hydrophobicity of the protein chains (Jin, Wu et al. 2014). However, a proper degree of hydrolysis may increase the effective hydrophobicity of certain globular proteins by means of the exposure of buried non-polar residues (Creusot and Gruppen 2007). On this basis, CF2LH<sub>120</sub> seems to have an excessive degree of hydrolysis and CF2LH<sub>5</sub> and CF2LH<sub>25</sub>.

Finally, Figure 5.3-9 shows the gelation process for all the systems studied at pH 8.0.

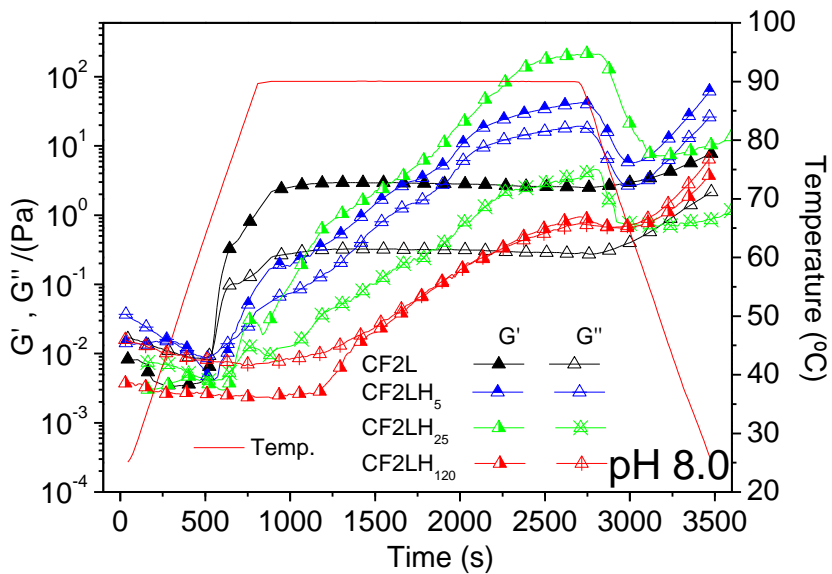


Figure 5.3-9: Temperature ramp tests performed at constant frequency, .6.3 rad/s for proteins dispersions: CF2L, CF2LH<sub>5</sub>, CF2LH<sub>25</sub> and CF2LH<sub>120</sub> at 12 wt. % and pH 6.5. An initial heating step (5°C/min from 25 to 90°C) was followed by an isothermal step (90°C, 30 min) and a cooling step (rate: 5°C/min from 90 to 25°C).

At this pH value the protein hydrolysates exhibit an intermediate behaviour between pH 2.0 and pH 6.5. Thus, at this pH, the initial decrease in

both moduli ( $G'$  and  $G''$ ) take place below  $45^\circ$ . A further increase in gel strength takes also place. However, in this case, the evolution is delayed to higher temperatures, being much slower than at pH 6.5, depending on the degree of hydrolysis. These results suggest that heat-induced chemical interactions do not become important until hydrophobically driven aggregates have not developed to a certain extent, which seems to be responsible for the delay in the gel development. The cooling stage brings about again the contribution of physical interactions (i.e. hydrogen bonds). Once again CF2LH<sub>120</sub> is the system that exhibits the lowest gel ability, as a consequence of the above-mentioned excess in the degree of hydrolysis. Interestingly, an enhancement in the final viscoelastic properties can be observed for CF2LH<sub>5</sub> and CF2LH<sub>25</sub> protein hydrolysates as compared to the original CF2L protein system. It is noticeable that at the end of the experiment CF2LH<sub>5</sub> is the system with the highest elastic modulus, however the gel system with the lowest  $\tan \delta$  (ratio  $G''/G'$ ) is the CF2LH<sub>25</sub> system, reflecting the highest solid character.

### *Mechanical spectra of gels*

Figure 5.3-10 shows the mechanical spectra by means of frequency sweep tests for all the systems studied after the gelation process at pH 2.0. In accordance with the results obtained after applying the thermal cycle (Figure 5.3-7) all the systems show a fairly weak gel-like behaviour, particularly the hydrolysate with the highest degree of hydrolysis that tend to reach a crossover point at high frequency.



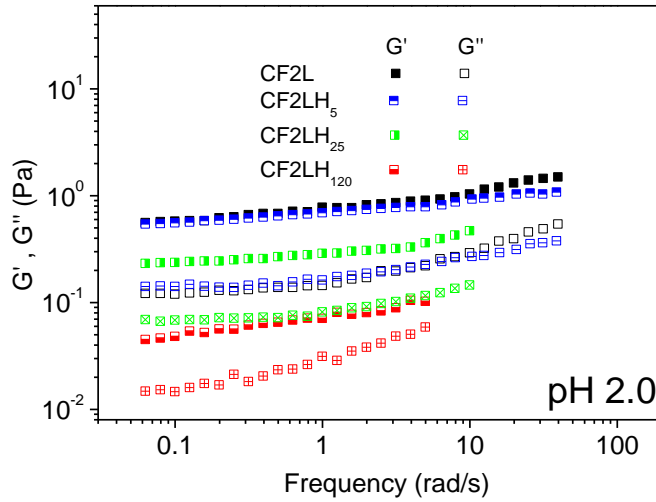


Figure 5.3-10: Evolution of linear viscoelastic properties for CF2L, CF2LH<sub>5</sub>, CF2LH<sub>25</sub> and CF2LH<sub>120</sub> gels as a function of frequency (from 0.06 to 50 rad/s) at pH 2.0

Figure 5.3-11 shows the mechanical spectra for all the systems studied at pH 6.5.

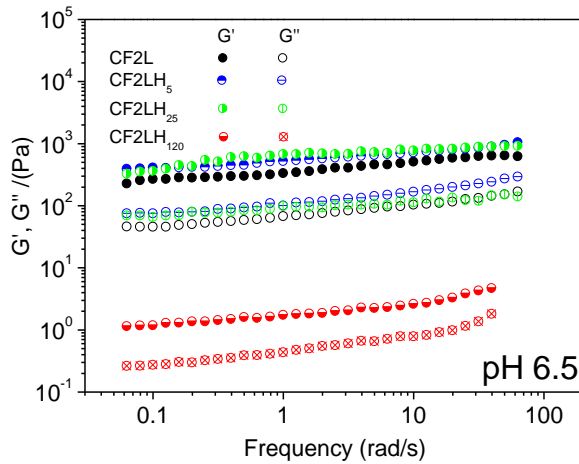


Figure 5.3-11: Evolution of linear viscoelastic properties for CF2L, CF2LH<sub>5</sub>, CF2LH<sub>25</sub> and CF2LH<sub>120</sub> gels as a function of frequency (from 0.06 to 50 rad/s) at pH 6.5

In this case, CF2L, CF2LH<sub>5</sub> and CF2LH<sub>25</sub> show mechanical spectra reflecting a relatively strong gel-like behaviour, where both storage and loss moduli are only slight frequency dependent (Damodaran 1997). On the other hand, CF2LH<sub>120</sub> system exhibits much weaker gel-like behaviour with low  $G'$  and  $G''$  values, as corresponds to its high degree of hydrolysis.

Finally, Figure 5.3-12 shows the mechanical spectra for all the systems studied at pH 8.0.

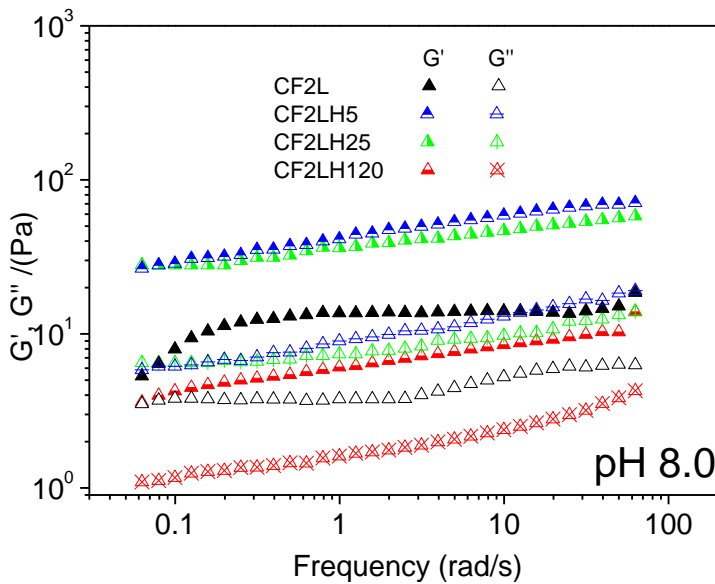


Figure 5.3-12: Evolution of linear viscoelastic properties for CF2L, CF2LH<sub>5</sub>, CF2LH<sub>25</sub> and CF2LH<sub>120</sub> gels as a function of frequency (from 0.06 to 50 rad/s) at pH 8.0

This figure confirms the intermediate behaviour between pH 6.5 and 2, found for the temperature ramp tests. The above-mentioned enhancement produced by a moderate increase in the degree of hydrolysis is now fairly apparent. Thus, CF2LH<sub>5</sub> and CF2LH<sub>25</sub> exhibit higher values for  $G'$  and  $G''$  than those corresponding to the protein dispersion CF2L. It is also noticeable that  $\tan \delta$  for both systems are the lowest in any case, being this parameter related to the gel stability (Damodaran, Parkin et al. 2007).

With regards to CF2L system, it seems to have the lowest frequency-dependence, which may indicate an acceptable gel strength, however at low frequency,  $G'$  goes down which indicates certain gel weakness.

### 5.3.2.1.2. *Protein interactions*

Figure 5.3-13 shows protein interactions (ionic bonds, hydrogen bonds, hydrophobic interactions and disulphide bonds) for all the systems studied (CF2L, CF2LH<sub>5</sub>, CF2LH<sub>25</sub>, CF2LH<sub>120</sub>) at pH 2.0. At this pH, there are not any remarkable interactions between proteins chains, being all different interactions in a short extend. These results could be expected from rheological measurements, since that revealed the formation of a weak gel, caused by the absence of strong interactions. Among them, hydrophobic interactions were the most important for all systems at this pH value.

CF2LH<sub>25</sub> is the system that exhibits the lowest ionic interactions and hydrogen bonds. These results are in consonance with the results observed in the temperature ramp tests, since these interactions take place in the cooling stage, being this system the only one which does not shows any thermal-induced enhancement in viscoelastic properties.

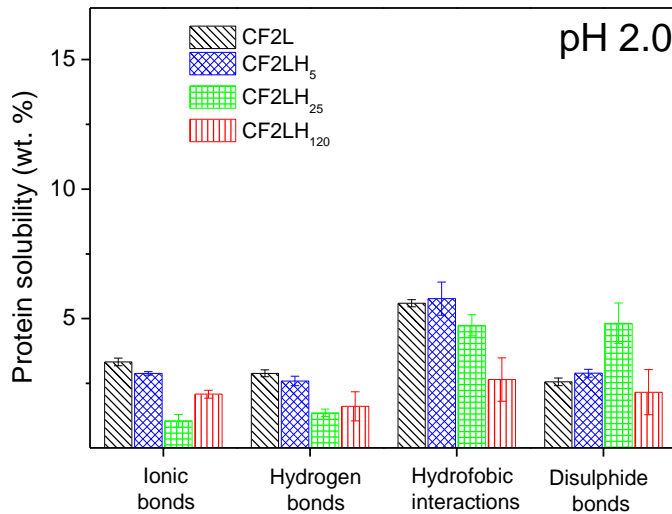


Figure 5.3-13: Protein interactions for all the systems studied (CF2L, CF2L5, CF2L25 and CF2L120) at pH 2.

Figure 5.3-14 shows protein interactions for all the systems studied at pH 6.5. At this pH, interactions are clearly higher than at pH 2.0, where non-specific ionic interactions are the most important. This fact is related to its proximity to the isoelectric point discussed in the previous section, which is around 5. This fact is related to the closeness of the isoelectric point discussed in the previous section, which is around 5. Although ionic interactions are not responsible for strong gel interactions, the equal number of charges inhibit protein repulsions at this pH (Gomez-Guillen, Borderias et al. 1997).

Specific disulphide bonds are also relevant at this pH for all systems. This type of specific chemical interactions takes place above 65 °C (Acton and Dick 1988), and is related to the increase of both moduli found in temperature ramp test. Disulphide bonds decrease with the degree of hydrolysis, however these systems are able to form a strong gel (except for CF2LH<sub>120</sub>) since they still maintain a high level of hydrophobic interactions and hydrogen bonds.

In consonance with the viscoelastic, CF2LH<sub>120</sub> system is the gel showing the lowest interactions. It only has noticeable ionic interactions, which may be related with the small protein size. The small size of CF2LH<sub>120</sub> chains may allow them to reorganise easily in order to facilitate electrostatic interactions.

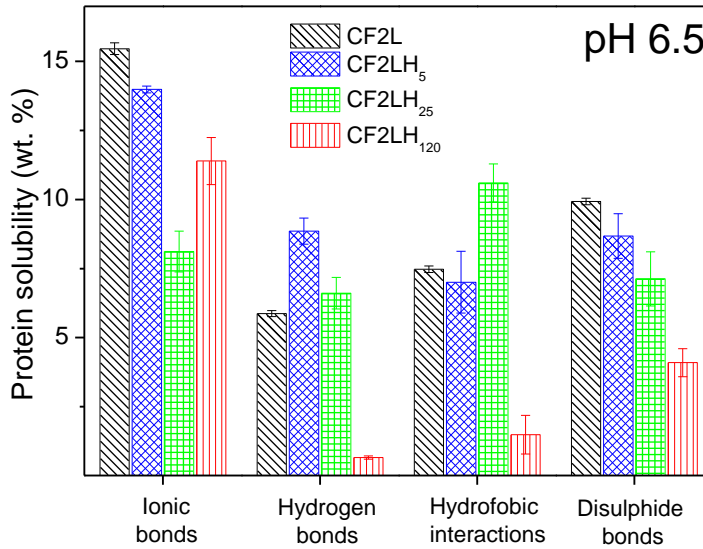


Figure 5.3-14: Protein interactions for all the systems studied (CF2L, CF2L<sub>5</sub>, CF2L<sub>25</sub> and CF2L<sub>120</sub>) at pH 6.5.

Finally, Figure 5.3-15 shows protein interactions for all systems at pH 8.0. At this pH, protein systems exhibit intermediate interactions between pH 2.0 and pH 6.5. Far from isoelectric point, any system exhibits remarkable ionic interactions, and they are similar to that one found at pH 2.0.

Protein interactions can be related to thermal profile obtained through temperature ramp test. Hence, CF2L exhibits a moderate increase of both moduli (characterised by a fast initial increased followed by a constant value). This result may be related with the moderate disulphide bonds found at this pH value. By contrary, CF2LH<sub>5</sub> and CF2LH<sub>25</sub> show a constant increase of both

moduli during the heating stage, which is related to higher values of disulphide bonds found.

Again, CF2LH<sub>120</sub> is the system that exhibit lowest  $G'$  and  $G''$  moduli and higher  $\tan \delta$ , which is the ratio  $G''/G'$  (denoting a marked liquid character). It is noticeable that interactions for this system found at pH 8.0 are similar to those found at pH 6.5, this result is in accordance to the comparable moduli obtained at pH 6.5 and 8.0.

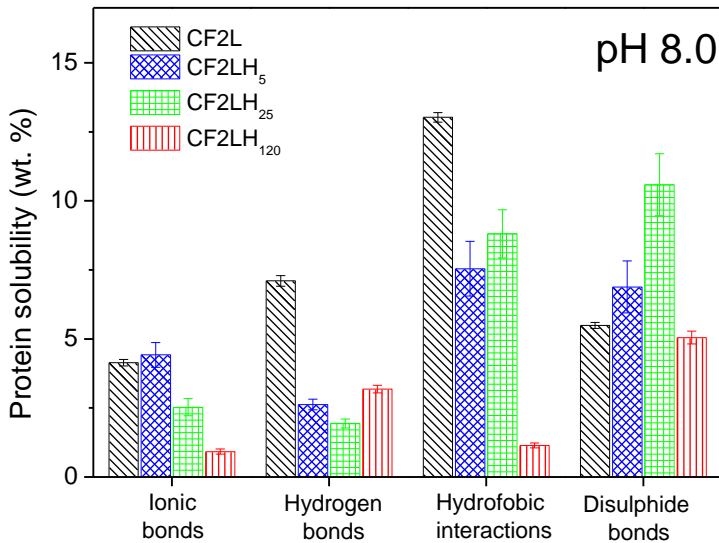


Figure 5.3-15: Protein interactions for all the systems studied (CF2L, CF2L<sub>5</sub>, CF2L<sub>25</sub> and CF2L<sub>120</sub>) at pH 8.0.

### 5.3.2.1.3. Water holding capacity

Figure 5.3-16 shows the water holding capacity (WHC) for all the systems. WHC is a very important property of food gels because the separation of liquid from the gel network can involve physical modifications (e.g. shrinking or alterations in the palatability of the product) due to the moisture reduction (Mao, Tang et al. 2001).

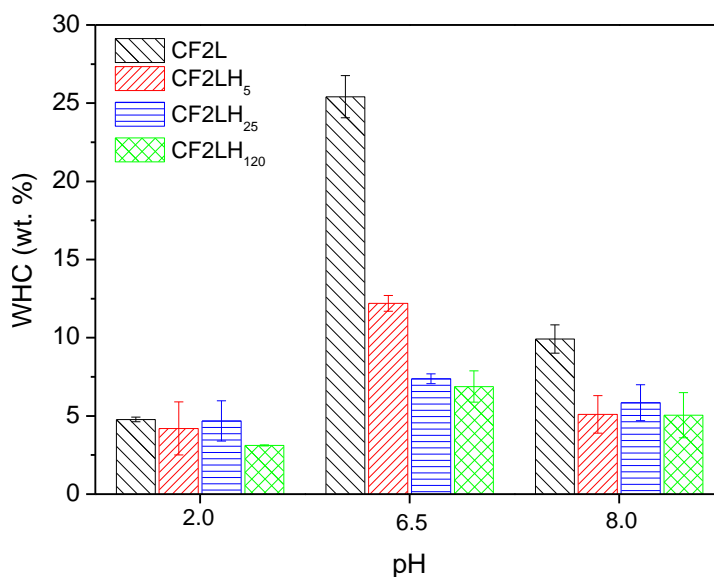


Figure 5.3-16: Water holding capacity (WHC) for all the systems studied (CF2L, CF2L<sub>5</sub>, CF2L<sub>25</sub> and CF2L<sub>120</sub>) at three different pH values (2.0, 6.5 and 8.0).

WHC results are rather consistent with those obtained from SAOS measurements. Thus, systems at pH 6.5 exhibit the highest values for WHC, although this effect tends to decline and even lose its significance as hydrolysis proceeds. At neutral pH CF2L is the system which holds water in a larger extent, decreasing the WHC with the degree of hydrolysis. This behaviour can be related to the fact that globular CF2L protein is able to develop a gel network that is able to keep water in clusters better than hydrolysate systems, which have lost their globular conformation (Nieto-Nieto, Wang et al. 2014). This behaviour also can be found at pH 8.0, however at this pH, WHC is quite lower, which is related to their lower viscoelastic properties (as a result of lower protein interactions).

Finally, at pH 2.0 the lowest values for WHC are typically obtained, as corresponds to the weakness of their interactions and of the gel-like network developed.

5.3.2.1.4. Bio-Active Characterisation

Figure 5.3-17 shows the antioxidant activity of all studied gels made at pH 2.0 and measured with three different methods: DPPH, Folin-Ciocaltau and ABTS. Results were expressed as mM Eq. of PG.

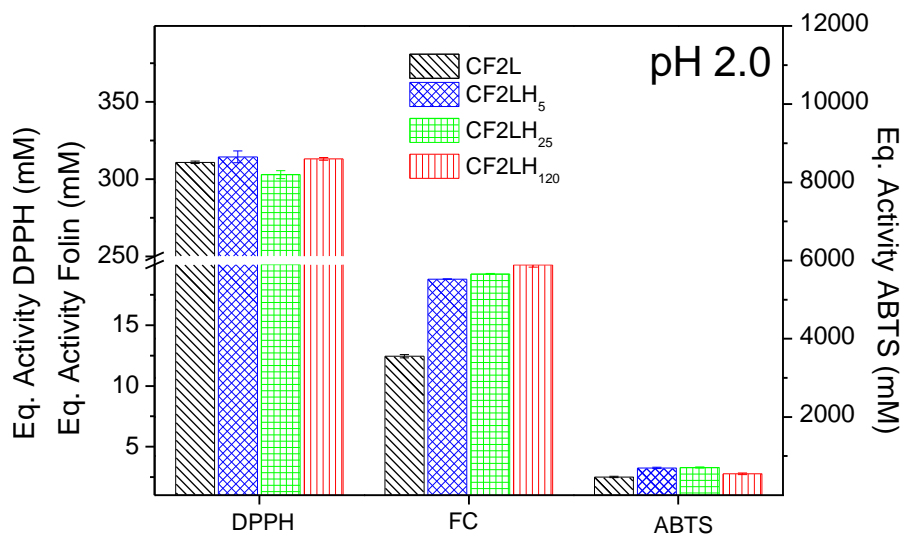


Figure 5.3-17: Antioxidant activity of all the systems studied (CF2L, CF2L<sub>5</sub>, CF2L<sub>25</sub> and CF2L<sub>120</sub>) at pH 2.0 behind three different compounds: DPPH, FC and ABTS. Antioxidant activity was expressed as equivalent activity of PG.

According to this plot, at pH 2.0, the maximum antioxidant activity is obtained for ABTS, followed by DPPH and FC reagent (note the difference in scale for ABTS). The ability of proteins to interact with free radicals has been studied previously. These studies have usually used a free radical generator, and the determination is based on the ability of the protein to quench the radical species produced. The protein antioxidant ability seems to be related to chemical mechanisms such as electron/hydrogen donation, radical quenching, and metal ion chelation (Kong and Xiong 2006).



Kong and Xiong (2006) obtained lower values of ABTS activity using (TEAC) as a reference compound. Despite results cannot be compared, since the reference compound is different, CF2L system and their hydrolysates exhibit a higher antioxidant activity. However at pH 2.0 we could not found any clear dependence on the degree of hydrolysis, in contrast with the results found by these authors. In our case, a moderate hydrolysis seems to enhance ABTS activity.

As for DPPH antioxidant activity, this is a free-radical compound that has been widely used to test the free-radical scavenging ability of different system, from phenolic compounds (Espinoza, Olea-Azar et al. 2009) to protein systems (Sakanaka, Tachibana et al. 2005). DPPH activity is related to the ability of the protein to scavenge free radicals or reduce  $\text{Fe}^{3+}$  (Ryan, Ross et al. 2011). At pH 2.0, the DPPH exhibit an important activity against DPPH, however we could not found any dependence on the degree of hydrolysis.

Finally, antioxidant activity against FC reagent also was evaluated. Initially, FC reagent was used for the determination of the proteins (Folin and Ciocalteu 1927). Many years later, Singleton et al. (Singleton, Orthofer et al. 1999) made extensive use of this phenol affinity in order to determine the total phenols in wine. Eventually, FC reagent is also used to determinate antioxidant activity of proteins, where, in the same way that DPPH, FC antioxidant activity is related to the ability to donate an electron (Kristinova, Mozuraityte et al. 2009). For all systems at pH 2.0, FC activity is the lowest. However, this antioxidant activity undergoes a significant increase with the degree of hydrolysis. As previously mentioned, these low values found may be explained because FC reagent is not capable to measure lipophilic antioxidants due to the high affinity of the FC chromophore toward water (Berker, Olgun et al. 2013).

## Results

Antioxidant activity at pH 6.5 is shown in Figure 5.3-18. Once again, the maximum antioxidant activity at this pH value is obtained for ABTS, which rises up to 7,000 mM Eq. of PG. Moreover, the ABTS activity depends on the degree of hydrolysis. Hence, an increase in the degree of hydrolysis involves an increase in antioxidant activity. This effect also was found by Kong and Xiong (2006) for potato protein. However in this study, a decrease of antioxidant activity was found when a high level of protein hydrolysis takes place.

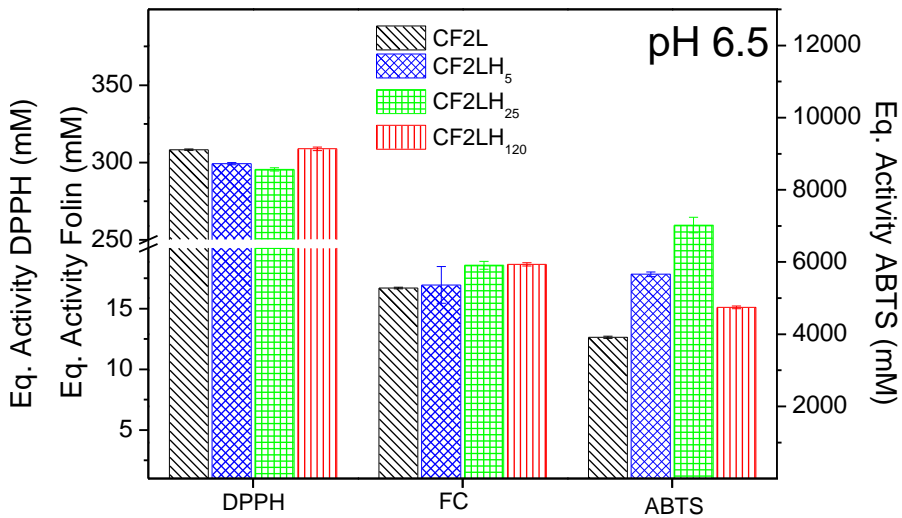


Figure 5.3-18: Antioxidant activity of all the systems studied (CF2L, CF2L<sub>5</sub>, CF2L<sub>25</sub> and CF2L<sub>120</sub>) at pH 6.5 behind three different compounds: DPPH, FC and ABTS.

Antioxidant activity was expressed as equivalent activity of PG.

As for DPPH, similar behaviour to pH 2.0 was found. There are not significant differences for any protein system and DPPH radical scavenging is around 300 mM eq. of PG. However, in this case DPPH activity seems to undergo a decrease when the degree of hydrolysis is moderate.

## Results

Finally, for FC reagent, the antioxidant activity is the lowest, in consonance with pH 2.0, however at pH 6.5 no significant differences among protein and protein hydrolysates were found.

Figure 5.3-19 shows antioxidant activity at pH 8.0. At this pH value, the same sequence of antioxidant activities was found, being maximum for ABTS once again, where the antioxidant activity rises up to 11,000 mM Eq. of PG. Similar evolution of results from the ABTS assay with the degree of hydrolysis where also found at alkaline pH. Thus, a maximum ABTS activity at intermediate degree of hydrolysis (CF2LH<sub>25</sub> in this case) is apparent at pH 8.

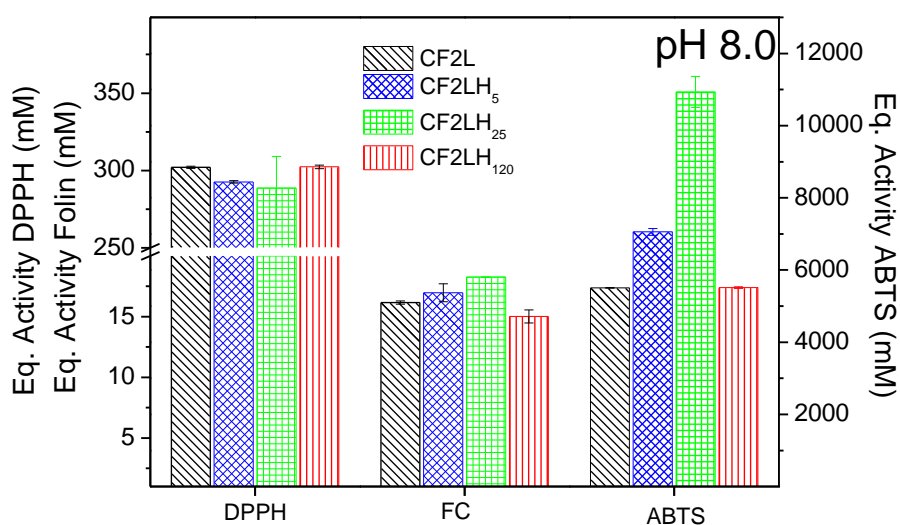


Figure 5.3-19: Antioxidant activity of all the systems studied (CF2L, CF2L<sub>5</sub>, CF2L<sub>25</sub> and CF2L<sub>120</sub>) at pH 8.0 behind three different compounds: DPPH, FC and ABTS. Antioxidant activity was expressed as equivalent activity of PG.

As for DPPH, similar behaviour was found at pH 6.5 and 8.0 and there are not significant differences for any protein system, neither protein concentrate (CF2L), nor protein hydrolysates (CF2LH<sub>5</sub>, CF2LH<sub>25</sub>, and CF2LH<sub>120</sub>). These results

confirm that DPPH measurements are not dependent on pH or on the hydrolysis degree.

Finally, at pH 8.0 the lowest antioxidant activity was found for FC reagent. The degree of hydrolysis seems to favour FC activity in some extent at this pH, except for its highest value (i.e. CF2LH<sub>120</sub>)

It is worth pointing out that the different behaviour of protein systems could be striking because it depends on the method used. In fact, many studies have been reported that the antioxidant activity depends on the nature of the reference compound (DDPH, ABTS, FC) (Wojdylo, Oszmianski et al. 2007, Wootton-Beard, Moran et al. 2011, Boulanouar, Abdelaziz et al. 2013). In any case, regardless of the pH studied and the different reference compounds used, there seems to be a general tendency of increasing antioxidant activity with the degree of hydrolysis, even though is not always significantly detected. An excessively high degree of hydrolysis seems to lose this ability.

Figure 5.3-20 shows TCA-soluble peptides (free-amino acids and short peptides) before and after thermal processing. The proteolytic activity of enzymes, which are capable of breaking the chemical bonds of the muscle fibres during the cooking step, has been widely studied. This enzymatic process may be important since it can modify the characteristic texture of fresh fish or food products (Miller and Spinelli 1982, Greene and Babbitt 1990)

The determination of TCA-soluble peptides has been carried out by means of measuring the absorbance of TCA-soluble peptide solution before and after gelation process at 280 nm. First of all, it can be observed significant differences between non-hydrolysate system (CF2L) and hydrolysates systems (CF2LH<sub>5</sub>, CF2LH<sub>25</sub> and CF2LH<sub>120</sub>). These results could be expected since they can be a consequence of the hydrolysis carried out. This means that an

increase in pH values gives raise an increase in the number of amino acids and small peptides in the bulk solution.

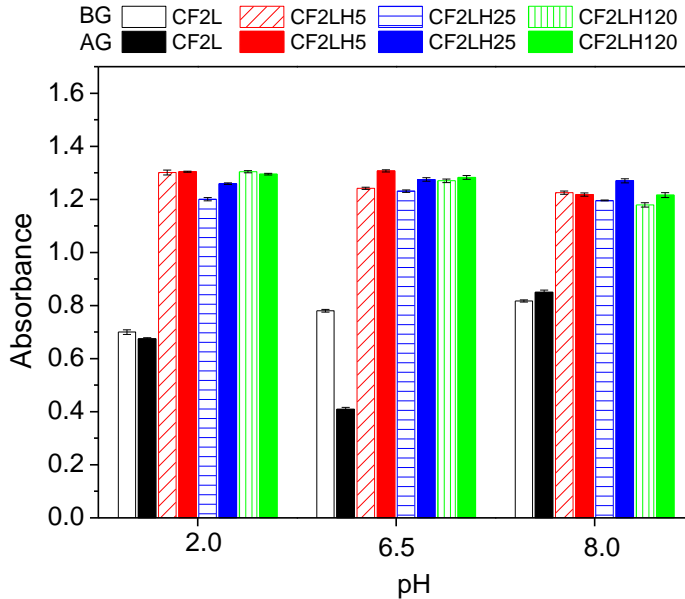


Figure 5.3-20: Proteolytic activity measured at 280 nm in all the systems studied (CF2L, CF2L<sub>5</sub>, CF2L<sub>25</sub> and CF2L<sub>120</sub>), evaluated at three different pH values (2.0, 6.5 and 8.0), before and after gelation process.

For CF2L system, a slight increase of TCA-soluble peptides at 20°C can be observed when an increase of pH takes place. Finally, after gelation process, TCA-soluble peptides do not increase in any case, for this reason we can discard proteolytic activity as a consequence of the thermal procedure followed.

Regarding to hydrolysates systems, we could not found any pH dependence of TCA-soluble proteins on pH or hydrolysates systems, neither before gelation nor after gelation. Thus, proteolytic activity was not found in any system, and it is not pH-dependent.

Finally, it is remarkable the decrease of TCA-soluble peptides found at pH 6.5 after gelation process for CF2L system. Hence, at this pH, the gel not only

## *Results*

exhibit better mechanical properties (higher gel strength and high WHC), but also the gel is able to hold in a greater extend free amino acids and short peptides in its structure. This can be related to the highest values of WHC found for CF2L system at pH 6.5.

## 5.4. Crayfish-based bioplastics

An industrial low cost surplus obtained from crayfish (CF) (dried in a rotary furnace) was used in this section due to the restricted availability of CF2L protein concentrate, along with the high raw material required for protein-based bioplastics manufacturing. This way of proceeding allows us to study the optimisation of CF-based bioplastic.

Eventually, at the end of this section, results were compared with CF2L-bioplastics processed by using the protocol obtained from CF-based bioplastics.

The first stage for all protein-based bioplastics is to select the ration protein/plasticizer. This election is usually made based on the processability of the dough-like material obtained.

Figure 5.4-1 shows both torque and temperature profiles as a function of mixing time for blends obtained at different CF/GL ratios, as well as their visual appearance after mixing.

These results put forward the remarkable dependence of these parameters on the CF/GL ratio. Thus, a rapid increase in torque up to a maximum value takes place for the system having less amount of plasticizer, denoted as 80/20, which represents the CF/GL weight ratio. This evolution is readily followed by an asymptotic decrease towards a plateau value. In contrast, the system 70/30 shows a moderate growth in torque showing no maximum value but a slow tendency to the plateau value. The profile of the 60/40 system shows only a slightly initial increase in torque, being dominated by a constant torque value over mixing time. In general, the temperature evolution is very similar to the torque profile where an increase takes place excepting for the lowest CF/GL ratio. Both increases in torque and

## Results

temperature may be attributed to shear-induced exothermic reactions developed during the mixing process.

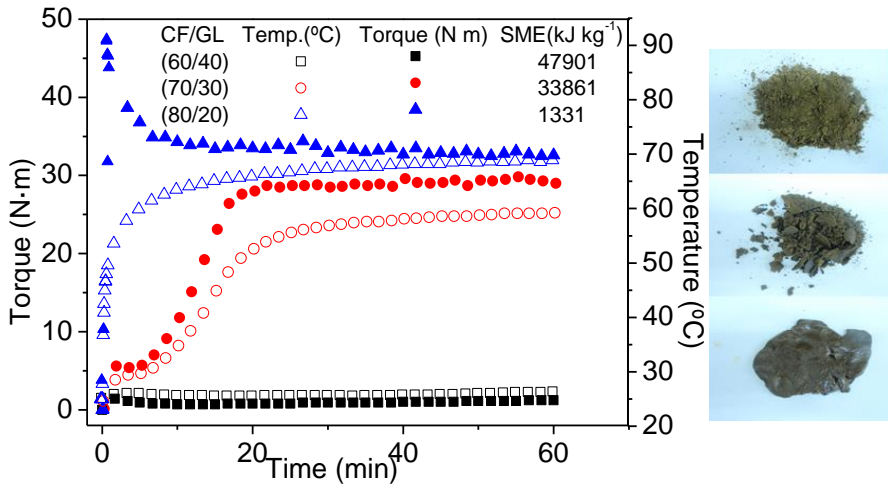


Figure 5.4-1: Images, SME and evolution with time of mixing torque and temperature for systems CF/GL (80/20, 70/30 and 60/40).

As a consequence of the above-mentioned differences in torque profile, the specific mechanical energy (SME) employed for mixing is also quite different. This characteristic parameter of mixing may be defined as follows EQ. (5.4-1). (Redl, Morel et al. 1999):

$$SME = \frac{\omega}{m} \int_0^{t_{mix}} M(t) dt \quad (5.4-1)$$

where  $\omega$  (in rad/s) is the mixing speed,  $m$  (in g) the sample mass,  $M(t)$  (in Nm) the torque and  $t_{mix}$  (in s) the mixing time. The values for the SME for these three systems are included in Figure 5.4-1. A remarkable increase in this parameter can be observed with the CF/GL ratio. This effect takes also place at the higher concentrations in spite of the fact that the plateau torque values are relatively close.



From the visual appearance observed in Figure 5.4-1, the 80/20 system does not seem to contain enough amount of plasticizer to obtain an easy-to-handle material, giving rise to a granulated powder instead of a homogeneous dough-like blend. This is evidenced by the fact that this is the system displaying the highest torque values, which correspond to the highest rheological consistency. On the other hand, the highest amount of glycerol in the 60/40 system provides a neat dough-like appearance to the blend. This is also consistent with the lowest torque values obtained (associated to a lower consistency) after the mixing process. The 70/30 blend shows intermediate appearance between both limits although it is closer to the most concentrated protein-based blend. In the present study, the system 80/20 has been discarded because the high energy required for mixing. Moreover, this system has proven to be hard to inject (results not shown). On the other hand, systems containing a low protein/glycerol ratio may be injected easily but the final bioplastic materials tend to exude the excess of glycerol. Exudation is a well-known phenomenon described in the polymer/plasticiser literature and should be avoided in order to prevent contamination of the surrounding materials (e.g. in food packaging) (Rahman and Brazel 2004). This seems to be the case for the 60/40 system. As a result, the 70/30 system is selected as the most suitable to obtain a homogeneous and easily injectable CF/GL blend.

In order to compare and evaluate the effect of chemical agents and synthetic polymer on crayfish-based bioplastic materials, a dual strategy was followed. On the one hand the presence of sodium sulphite (SS) or bisulphite (BS) as reducing agents, urea (U) as denaturing agent and L-cysteine (LC) as crosslinking agent were analysed as chemical modifiers. On the other hand, a polyester from fossil source, which has been widely used as the polymer matrix in the development of new materials, which is highly flexible,

biodegradable, biocompatible and easy to process, was used (polycaprolactone, PCL).

### 5.4.1. Crayfish-bioplastic with chemical modifiers

#### 5.4.1.1. Blends characterisation

##### 5.4.1.1.1. Preparation of blends by thermoplastic mixing

Figure 5.4-2 shows the evolution of torque as a function of time for different 70/30 CF/GL blends prepared using SS as reducing agent, U as denaturing agent, or LC as crosslinking promoter at different concentrations (3 and 30 mg/g protein for SS and U and 1 and 3 mg/g for LC).

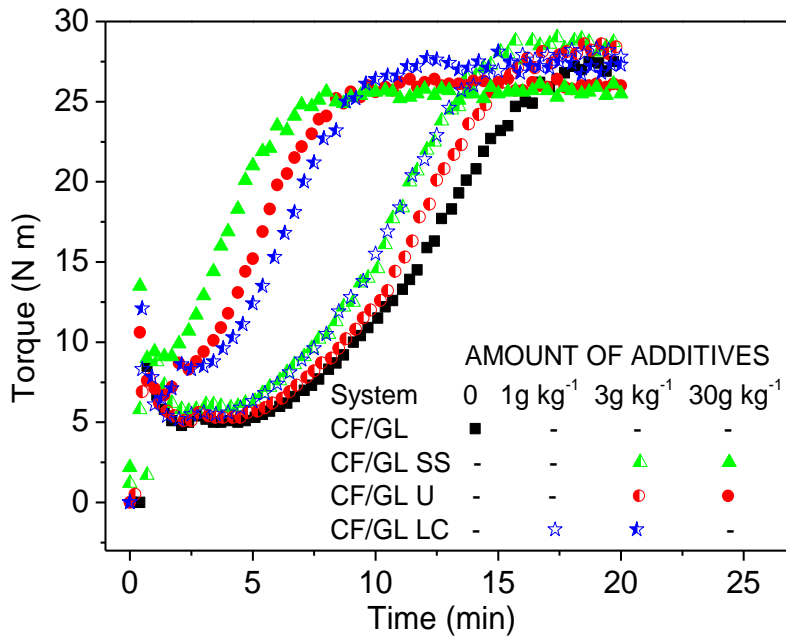


Figure 5.4-2: Evolution with time of mixing torque for additive-containing system (SS, U and LC).

These results generally show that any of the additives used induces an anticipation of the torque profile, particularly at the highest additive concentrations. No differences in the torque profile are noticed at the two different concentrations of BS (data not shown). The highest amount of additive (corresponding to SS or U) also yields lower torque plateau values, which may be considered beneficial for the processability of blends, for example under injection moulding. Temperature-time profiles show the same type of evolution for all the additives and concentrations in spite of that an air stream was used as a cooling fluid. No differences are found in the final values for the highest SS or U content in this case. The only difference found between temperature and torque profiles is that the former undergo a further delay in time, which may be related to the air-cooling effect.

It may be also noted that the system is not still properly mixed at times shorter than that one corresponding to the maximum torque. Therefore, as a general rule, the mixing time range for subsequent blend processing is selected once the plateau torque value is reached such that a good homogeneity degree is assured.

Another interesting parameter to compare different mixing processes is the relative energy input (REI), which is defined as follows (5.4-2).

$$REI (\%) = \frac{SME_{min}(a, c)}{SME_{min}(0)} \cdot 100 \quad (5.4-2)$$

where  $SME_{min}(0)$  and  $SME_{min}(a, c)$  are the SME values at which torque reaches 95% of the maximum value for the profile of the additive free blend and additive at concentration  $c$ , respectively. Therefore, REI is an index of the reduction in energy input relative to that one required for mixing the additive free blend.

The values of  $SME_{20}$  and REI parameters are shown in Figure 3.1-1 for these additives. The  $SME$  values for BS are also included in this figure.  $SME_{20}$  is the specific mechanical energy supplied, as defined in EQ. (5.4-2), after mixing for 20 min. As may be observed in this graph, an increase in additive concentration always leads to an apparent increase in  $SME_{20}$  parameter, as a consequence of the above-mentioned anticipation of the torque profile. If the same additive concentration is used, this increase is particularly remarkable for LC and, in any case, is only moderate when BS is used.

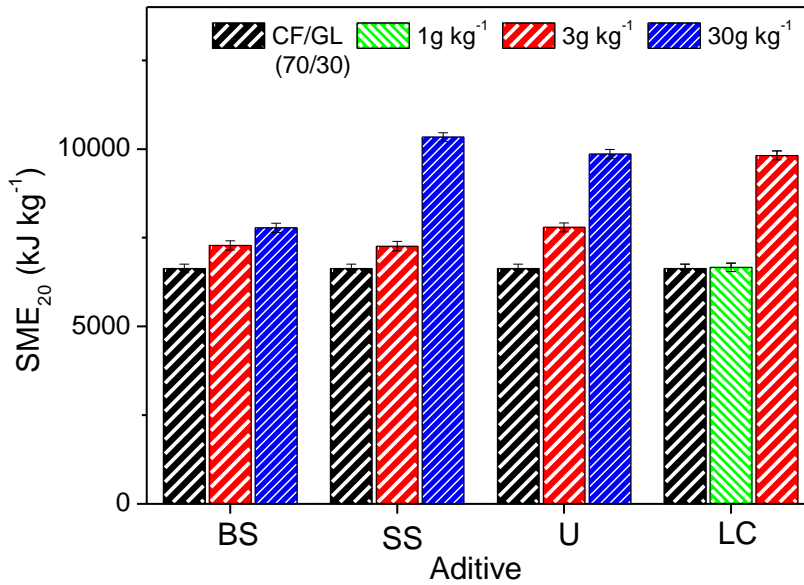


Figure 5.4-3: Specific mechanical energy (SME) employed for mixing at 20 minutes

The values of REI parameters are shown in Figure 5.4-4 for these additives.

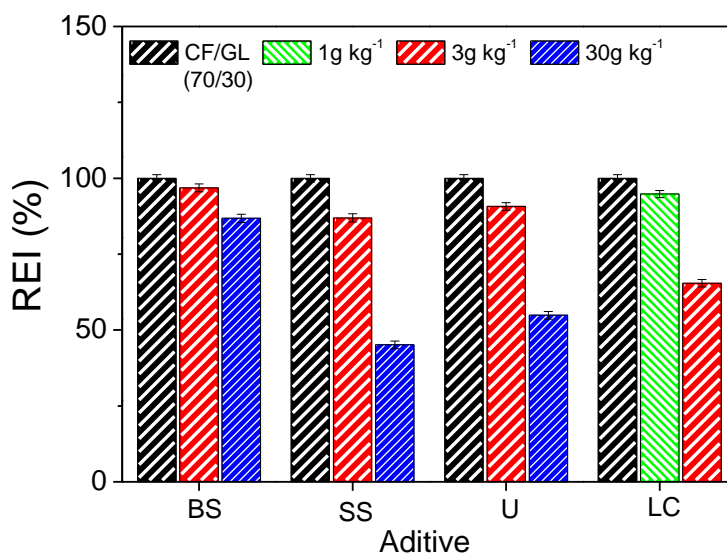


Figure 5.4-4: Reduction energy index (REI) for each system.

The results obtained with parameter REI confirm the relevant effect of the addition of LC at constant additive concentration. Thus, estimation tendencies from the results obtained indicate that the additive/protein ratio required to achieve a 50% REI would be 33 mg/g for U and 27 mg/g for SS, whereas a ratio as low as 4.4 mg/g would be required by using LC.

#### 5.4.1.1.2. Rheological characterisation of blends

Figure 5.4-5 shows the dependence of linear viscoelastic functions on temperature for different blends containing 3 mg additive per g CF protein. The additive free (CF/GL) blend is also displayed in this figure.

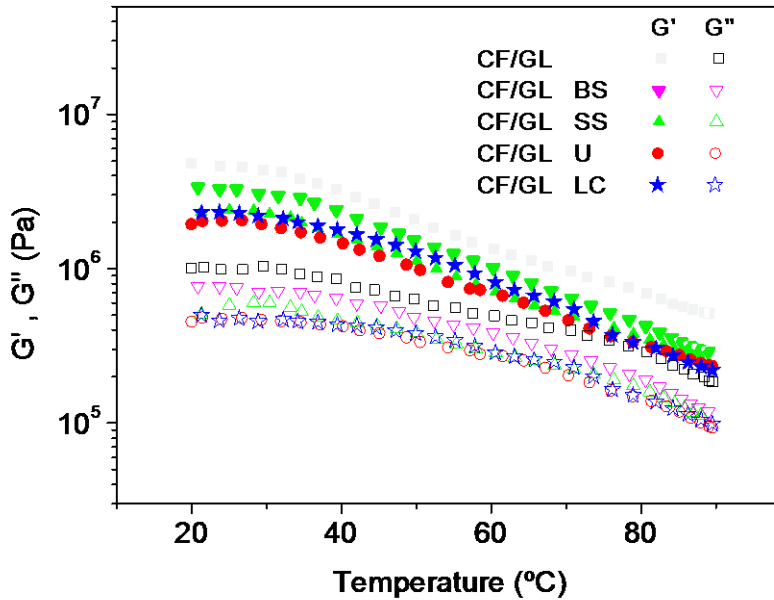


Figure 5.4-5: Storage and loss modulus ( $G'$  and  $G''$ ) for different blends containing additives at 3 mg/g and reference (CF/GL).

All the additives studied induce a reduction in  $G'$  and  $G''$  in the experimental temperature range studied. Once again the additive showing the poorest effect is BS. The other three additives do not show any apparent difference for  $G'$  or  $G''$  (Figure 5.4-5). In contrast to some protein such as gluten, CF does not show extensive cross-links, such that processing is not influenced by the addition of SS to a high extent. This seems to be also the case for U and LC. Thus, as reported by Verbeek and Van den Berg (2010), U plays the role of a plasticizer at concentration as low as that one used in this study, not showing any crosslinking effect. LC does not seem either to produce any noticeable crosslinking, under the experimental conditions for the temperature ramp.

As for  $\tan \delta$  profiles, in Figure 5.4-6  $\tan \delta$  is plotted for all systems.

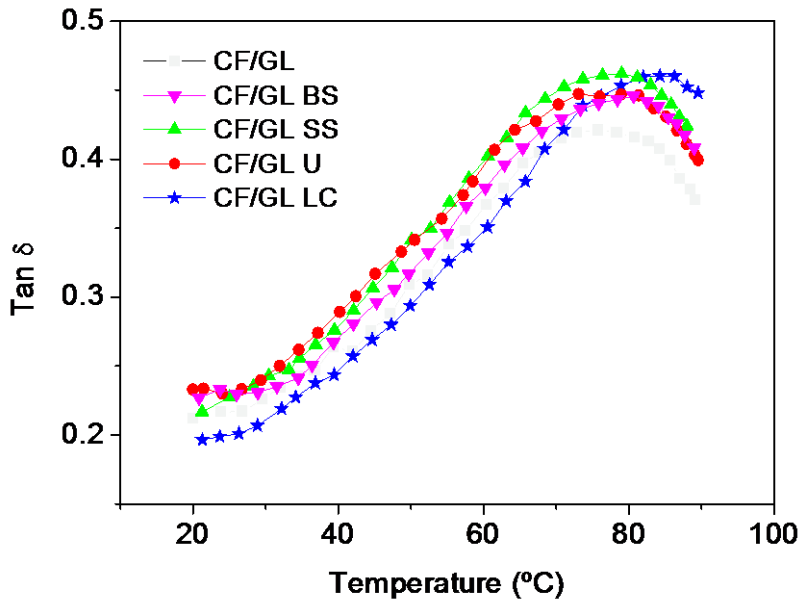


Figure 5.4-6: loss tangent for different blends containing additives at 3 mg/g and reference (CF/GL).

All of them show a similar elastic-dominant behaviour characterized by the presence of a broad distribution showing a maximum value. This maximum has been also found at 70 °C by DSC measurements for the CF/GL system (results shown in the next section), being associated to a glass-like transition of the protein fraction. Most of additive-containing blends show this smooth thermal induced glass transition in the same temperature range than the additive free system (70-83 °C). However, a shift in this event towards higher values (80-87 °C) takes place when LC is used as additive, although it is not detected by the  $G'$  thermal profile. This effect might be a consequence of the participation of some shear-induced crosslinking events taking place over the mixing stage for this system. In fact both torque and temperature profiles showed the fastest kinetics at the same additive concentration. In any case, this effect seems to be rather moderate.

As a consequence, the addition of any of the additives used leads to a potential enhancement of the moulding processability of CF/GL blends, where rheological properties are regarded as the key factor. In other words, additives contribute to facilitate injection of CF-based blends. Similar results were found by Pallos et al. (2006) for thermoformed wheat glutted modified by reducing agents and additives.

### 5.4.1.2. Injection moulding process

Table 5.4-1 shows the conditions selected for the injection moulding process for each of the blends studied.

	T (°C)	Pressure (MPa)	Time (s)
Pre-injection cylinder	60	0.1	100 (*)
Injection	60 - 100	0.1-50	<1
Packing stage	100 or 130	50	20
	100 or 130	20	200 (*)

*Table 5.4-1: Injection moulding parameters.*

Processing parameters for the pre-injection cylinder are selected taking into account that the elastic properties of CF/GL blends should be reduced to some extent (typically  $G'$  should be in the order of  $1 \cdot 10^6$  Pa or below). On the other hand, temperature should not be excessively increased in order to prevent thermal-induced protein crosslinking effects before the injection stage. For the same reason, the residence time in the cylinder should not be long. Under such premises the parameters selected for the first stage has been 60 °C and 100 s.

As for the mould processing conditions, the temperature has to be high enough to ensure the normal development of thermal and pressure-induced protein crosslinking reactions. On the other hand, exposition to high temperatures for a long time typically leads to protein degradation (i.e. via

*(\*)For a system containing L-cysteine, 130 °C and 600 s were also used.*



Maillard-type reactions). Therefore, 100 °C and 20 s have been selected as the moulding temperature and time, respectively. The injection pressure selected in this case has been 50 MPa. Once the blend has been injected into the mould, a further stage is performed at the same temperature for a residence time long enough (10 s) to allow for the development of protein crosslinking to achieve the final network structure. The residence time selected has been 200 s since no further enhancement has been noted by increasing this period.

### 5.4.1.3. Characterization of bioplastic probes

#### 5.4.1.3.1. *Dynamic Mechanical Temperature Analysis*

Figure 3.1-1 shows the values of the elastic modulus,  $E'$ , as a function of temperature (from -30 to 140 °C) obtained from DMA measurements for additive-free CF/GL specimens and CF/GL probes containing 3 mg/g additive. This figure compares the influence of different additives (BS, SS, U and LC) for specimens moulded at 100 °C for 200 s.

As may be observed in this Figure, all the specimens show similar profiles for  $E'$ , undergoing a remarkable decrease with increasing temperature that tends to reach a plateau value at high temperature that in some cases evolves to an eventual increase in  $E'$ , indicating a certain thermosetting potential. DMA profiles for the additive-free, U and BS specimens do not display any significant difference, in spite of the effect observed on the viscoelastic properties of their corresponding blends Figure 5.4-5. SS containing specimens show lower  $E'$  values at low temperature but higher values in the high temperature region as compared to the reference (additive-free) system. This system also evolves in a more gradual way than the other bioplastic specimens, particularly at high temperature showing no thermosetting potential region. This behaviour may be associated to the ability of SS to impair disulphide bridges. Thus, the results obtained after application of the Beveridge et al. (1974) procedure indicate that the concentration of free

sulphydryl groups in CF is raised from  $19 \pm 3 \mu\text{mol/g}$  to  $300 \pm 17 \mu\text{mol/g}$  after addition of 3 mg SS/g protein.

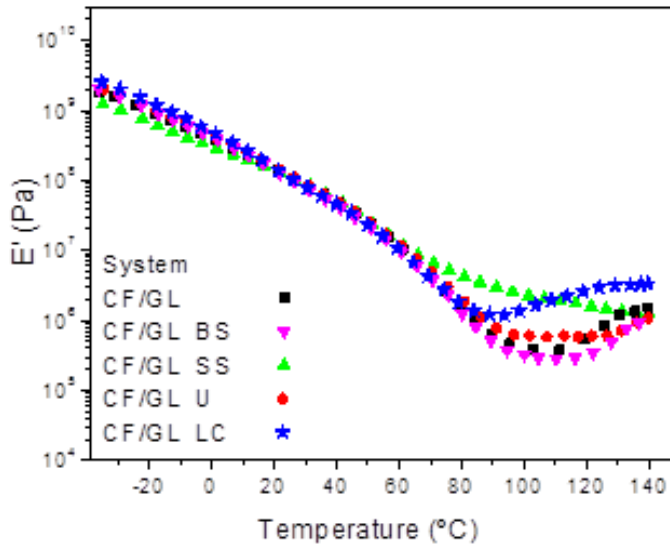


Figure 5.4-7: DMA temperature ramp measurements performed at constant frequency (6.28 rad/s) and heating rate (5 °C/min) for different CF/GL and additive-containing probes: storage ( $E'$ ).

As for LC specimens, they show a rather similar DMA profile at low and medium temperature but also shows an apparent increase in  $E'$  at high temperature, which reveals that this system still exhibits a marked remnant thermosetting potential for further processing. In order to explore this potential LC-containing specimens were processed using different moulding conditions, increasing either the residence time in the mould (up to 600 s) or the moulding temperature (up to 130 °C).

DMA results for these new LC-containing specimens are shown in Figure 5.4-8:

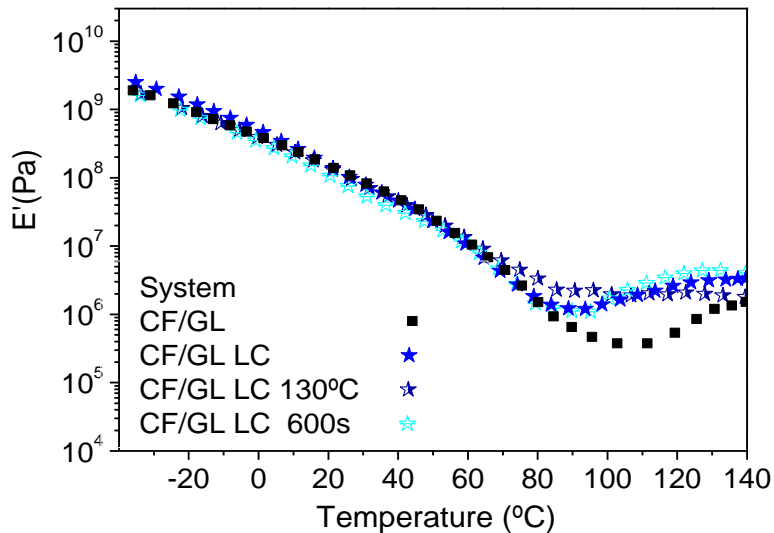


Figure 5.4-8: Values of the elastic modulus,  $E'$ , as a function of temperature (from -30 to 140 °C) obtained from DMA measurements for additive-free CF/GL specimens and LC containing probes moulded at 100 °C for 200 s, as well as the effect of different moulding conditions for LC containing specimens.

As may be observed, the increase in moulding time does not lead to any noticeable change in the DMA profile, which suggests that the time selected for the former specimens is long enough to complete the crosslinking stage. On the other hand, an increase in moulding temperature leads to plateau value for  $E'$  in the high-temperature region. However, this change in moulding conditions does not drive any particular enhancement in the viscoelastic bending properties below 60 °C. This behaviour is somehow unexpected since occurrence of the above-mentioned thermosetting potential typically involves an enhancement of mechanical properties (Jerez, Partal et al. 2007, Gomez-Martinez, Partal et al. 2009, Zarate-Ramirez, Martinez et al. 2011).

#### 5.4.1.3.2. Uniaxial tensile strength measurements

Figure 5.4-9 displays the results of stress-strain curves obtained from tensile strength measurements for additive-free and additive-containing specimens at an additive/CF ratio.

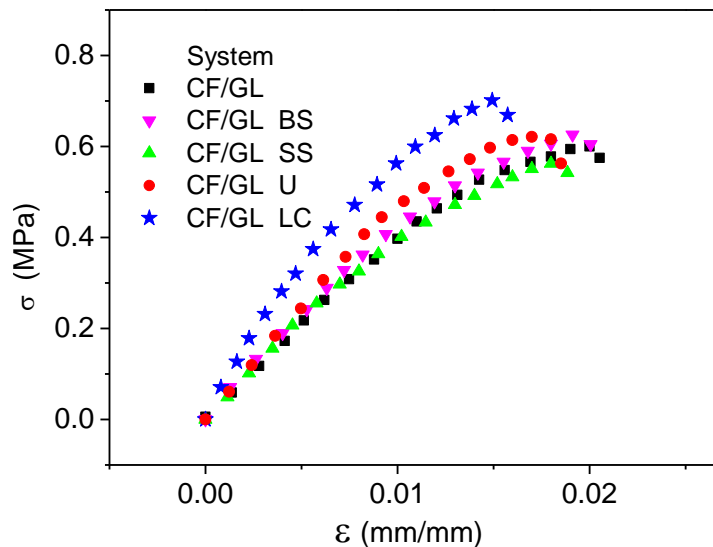


Figure 5.4-9: Stress versus strain curves from tensile strength measurements for different CF/GL and additive-containing probes.

All the curves exhibit a similar behaviour which consist of an initial linear elastic behaviour of high constant stress-strain slope yielding high values for the Young's modulus ( $E$ ), followed by a deformation stage with a continuous decrease in the stress-strain slope. A second constant slope is reached at the end of the plastic deformation stage. All the curves eventually reach a maximum value for the stress ( $\sigma_{\max}$ ) and the elongation at break ( $\epsilon_{\max}$ ). Only

LC leads to an apparent enhancement of the tensile strength profile, also leading to a slightly shorter strain value.

The values of stress-strain parameters ( $E$ ,  $\sigma_{max}$  and  $\epsilon_{max}$ ) and their corresponding standard deviations are plotted in Figure 5.4-10 for the additive-free and additive-containing specimens at 3 mg/g additive/CF ratio.

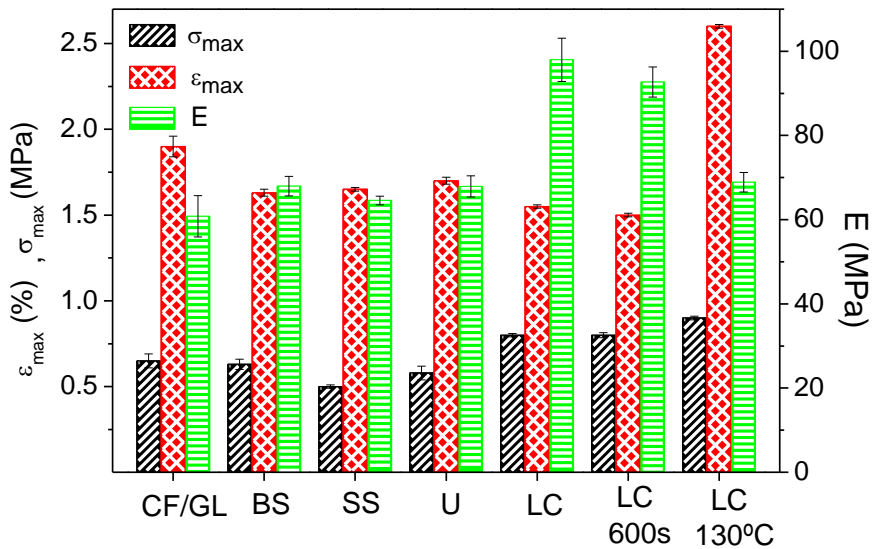


Figure 5.4-10: Parameters from tensile strength measurements: Maximum stress ( $\sigma_{max}$ ), elongation at break ( $\epsilon_{max}$ ) and Young's modulus ( $E$ ) for different CF/GL and additive-containing probes.

This figure puts forward once again that additive LC is the only one that improves parameters  $E$  and  $\sigma_{max}$  over the additive-free system, under the same processing conditions. On the other hand LC-added specimens exhibit lower values for  $\epsilon_{max}$ . The rest of additives lead to similar or even lower values of the three parameters. Figure 5.4-10 also shows the values for LC-added specimens moulded at longer time or higher temperature. As may be

observed, an increase in the packing time from 200 s up to 600 s does not yield any noticeable change in tensile parameters. This result indicates that after 200 s packing time, the probe is already closed by the solidified blend. On the other hand, an increase in the mould temperature leads to remarkable changes in tensile parameters. Thus, the maximum stress and above all the elongation at break undergo an apparent increase in value (ca. 12 and 70%, respectively), whereas the Young's modulus clearly decreases (ca. 30%) by increasing the mould temperature from 100 to 130 °C. Interestingly, it is the elongation at break the property that undergoes the most remarkable enhancement by favouring heat-induced crosslinking. In this way, the material exhibits higher toughness, in spite of being less strong. In fact, as stated by Lagrain et al. (2010), increasing the elongation at break of glassy, amorphous polymers typically goes at the expense of the elastic modulus. This compensation may also affect to the bending elastic properties of the bioplastic, thus explaining the small dependence of DMA profiles on moulding temperature.

Moreover, this behaviour is similar to that one found for other elastomeric materials such as rubber-based blends (Zarate-Ramirez, Martinez et al. 2011) and is consistent with the results from DMA measurements that show an extension of the rubbery plateau obtained at high temperature.

### 5.4.2. Crayfish-bioplasic with a synthetic polymer. Composite materials

A synthetic biodegradable polymer (PCL) were used to improve mechanical properties of CF-based bioplasic. This study can be considered as an alternative to the use of additives (previous section).

#### 5.4.2.1. Blends characterisation

##### 5.4.2.1.1. Preparation of blends by thermoplastic mixing

Figure 5.4-11 exhibits torque and temperature profiles as a function of mixing time for different CF/GL/PCL blends maintaining the same CF/GL ratio at ca. 2.3, using different PCL content, where the blend without PCL is used as the reference system.

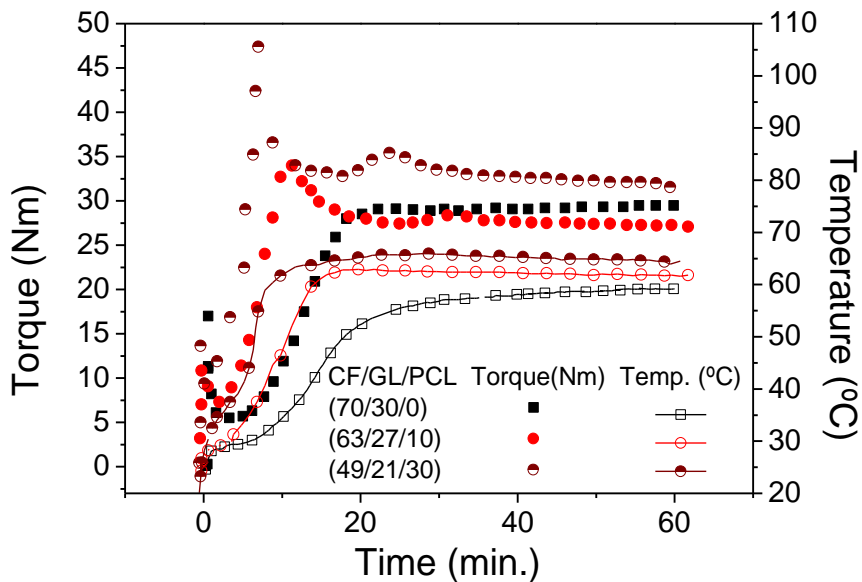


Figure 5.4-11: Evolution of torque and temperature over the mixing process for crayfish flour/glycerol/polycaprolactone (CF/GL/PCL) systems: at constant CF/GL ratio: (70/30/0), (63/27/10) and (49/21/30)

These results put forward the relevant dependence of torque and temperature on the CF/GL/PCL ratio. Thus, a rapid increase in torque up to a maximum value takes place, followed by an asymptotic decrease towards a plateau value. Temperature profiles generally follow an increase towards a plateau value. The time required to reach the plateau values for both variables (torque and temperature), which is roughly the same, is clearly dependent on the CF/GL/PCL ratio. This coincidence may be seen as a consequence of the development of exothermic crosslinking reactions during the mixing processes that involve both an increase in temperature and consistency (reflected in torque). Both profiles show also an initial induction period, being more evident for those blends displaying the slowest evolution. It is worth mentioning that a torque peak appears when unmelted PCL is present in the blend. Thus, the PCL melt point, which is reached at about 55 °C, is coincident with the maximum torque value. In other words, the torque does not start to decrease until the PCL melting point is exceeded.

As may be also observed in this figure, an increase in PCL content leads to a faster torque and temperature kinetics and, as a consequence, to an anticipation of both profiles. The effect also gives rise to a general increase in torque and temperature values at any time.

Figure 5.4-12 exhibits torque and temperature profiles as a function of mixing time for different CF/GL/PCL blends. This figure shows both profiles for blends containing 10% PCL at different CF/GL ratios.

As may be observe in this figure, the behaviour is quite similar to the previously found for systems at constant CF/GL ratio. Again, the temperature reached is above the PCL melting point, which ensures a homogenous mixing. However, the behaviour found for the system (60/30/10), seems to have an excess of glycerol, which lead to delay the plateau value.



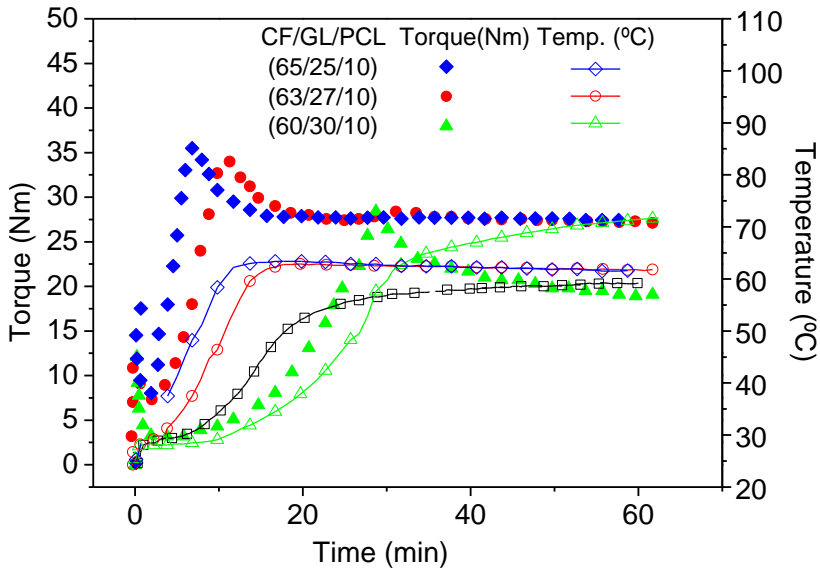


Figure 5.4-12: Evolution of torque and temperature over the mixing process for crayfish flour/glycerol/polycaprolactone (CF/GL/PCL) systems: at constant PCL concentration: (63/27/10), (60/30/10) and (65/25/10).

#### 5.4.2.1.2. Thermal characterization of blends

Heat flow patterns obtained from Differential Scanning Calorimetry (DSC) measurements are shown in Figure 5.4-13 and Figure 5.4-14. Figure 5.4-13 shows the thermogram for CF flour and for the reference system (CF/GL/PCL, 70/30/0), as well as the profiles corresponding to CF/GL/PCL blends at constant CF/GL ratio, as a function of PCL content. On the other and, Figure 5.4-14 displays the DSC results for CF/GL/PCL blends containing 10% PCL as a function of the CF/GL ratio.

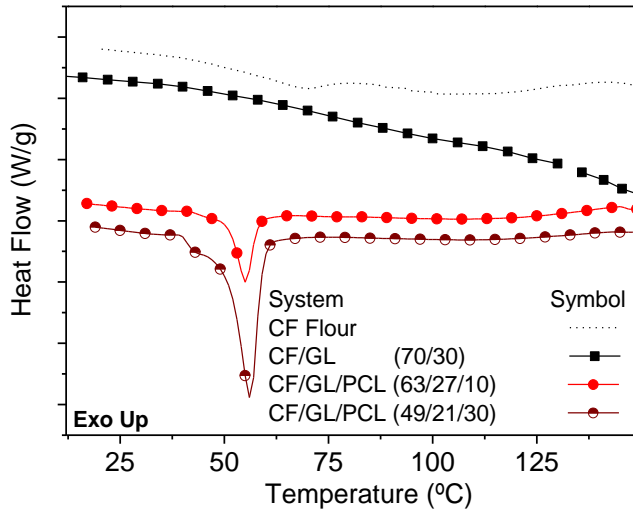


Figure 5.4-13: DSC profiles for crayfish flour and systems at constant CF/GL ratio: (70/30/0), (63/27/10) and (49/21/30) (A)

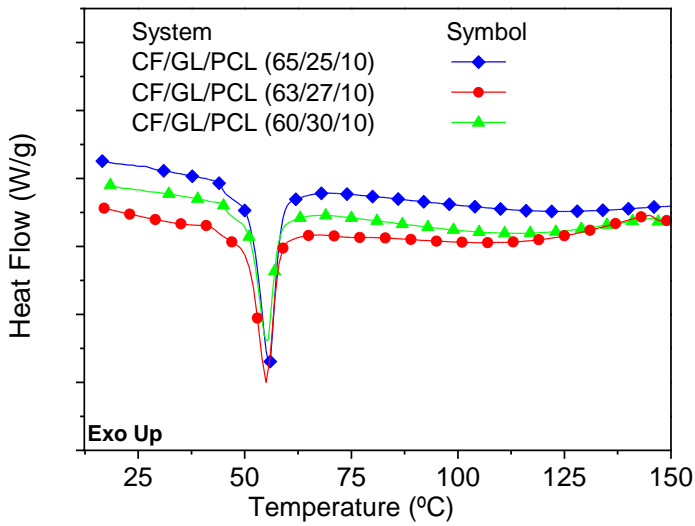


Figure 5.4-14: DSC profiles for systems at constant PCL concentration: (63/27/10), (60/30/10) and (65/25/10).

CF flour displays a typical endotherm of a fairly denatured protein system. This profile exhibits an endothermic first peak at 68 °C, a glass transition ( $T_g$ ) at ca. 92 °C, as well as a broad endothermic event between the  $T_g$  and 130 °C. The first thermal event can be attributed to the physical ageing effect, which was previously reported for this CF flour (Farahnaky, Guerrero et al. 2008). Physical ageing is a general phenomenon that occurs over time in glassy or partial glassy polymers below their  $T_g$  and is a manifestation of the non-equilibrium nature of the glassy state (Strink 1978, Anon 1997). The glass transition at around 90 °C is consistent with previous results reported by Farahnaky et al. (2008) for crayfish flour and Hashimoto et al. (2004) for fish muscle proteins. On the other hand, the broad endothermic event may be related to the huge variety of protein fractions of different molecular weight that constitute the CF flour as reported in a previous paper (Romero, Cordobes et al. 2011).

With regard to the endotherms obtained for the reference system the two endothermic events vanish. The total disappearance of the first endothermic peak, most probably as a consequence of mixing, confirms its physical ageing-driven nature. However, the glass transition remains roughly at the same temperature for all the blends studied.

In addition, it is worth mentioning that all the systems containing PCL display an apparent endothermic peak at ca. 55 °C, which is attributed to the PCL melting point. This peak becomes more pronounced with increasing PCL content.

The results obtained from DSC measurements also confirm the suitability of the temperature selected for the cylinder and mould, since the former (60 °C) is higher than the endothermic peak corresponding to the PCL melting whereas the later temperature (100 °C) is higher than the glass transition in

order to favour mobility and temperature-induced protein crosslinking (in combination with pressure).

### 5.4.2.2. Injection moulding process

Table 5.4-2 shows the conditions selected for the injection moulding process for each of the blends studied.

	T (°C)	Pressure (MPa)	Time (s)
<b>Pre-injection cylinder</b>	60	0.1	100
<b>Injection</b>	60	0.1-50	<1
<b>Packing stage</b>	100	50	20
	100	20	200

Table 5.4-2: Injection moulding parameters.

The processing parameters (temperature, pressure and time) values for the injection moulding process used in this study, which are similar to those used in the previous section. The values for the processing parameters at the pre-injection cylinder are selected to ensure a blend viscosity low enough to facilitate its injection into the mould. The residence time selected for the packing stage (right after injection) has been 220 s since no further enhancement has been noticed by increasing this period. In addition, exposition to high temperatures for a long time typically leads to protein degradation (i.e. via Maillard-type reactions) (Fayle, Gerrard et al. 2002).

### 5.4.3. Biocomposite characterisation

#### 5.4.3.1.1. Dynamic Mechanical Temperature Analysis

Figure 3.1-1 shows the values of the elastic modulus,  $E'$  from DMA temperature ramp test measurements. The reference system is compared

with those specimens with the same protein/plasticiser ratio (CF/GL/PCL: 63/27/10 and 49/21/30).

As may be observed, all the specimens studied show a similar profile for  $E'$  at low and medium temperature. In this way, an increase in temperature leads to a decrease in elastic modulus ( $E'$ ) that tends to reach a plateau value. However, it is remarkable that PCL containing samples exhibit higher elastic modulus provided that temperature remains below the PCL melting point. At the melting point the three samples show rather coincident values that undergo a decrease with increasing temperature. In fact, there is a region where the PCL-free specimen shows slightly higher  $E'$  values. Eventually a temperature is reached above which the decrease in  $E'$  found for the reference specimen becomes faster whereas the PCL-containing composites tend to reach a plateau region.

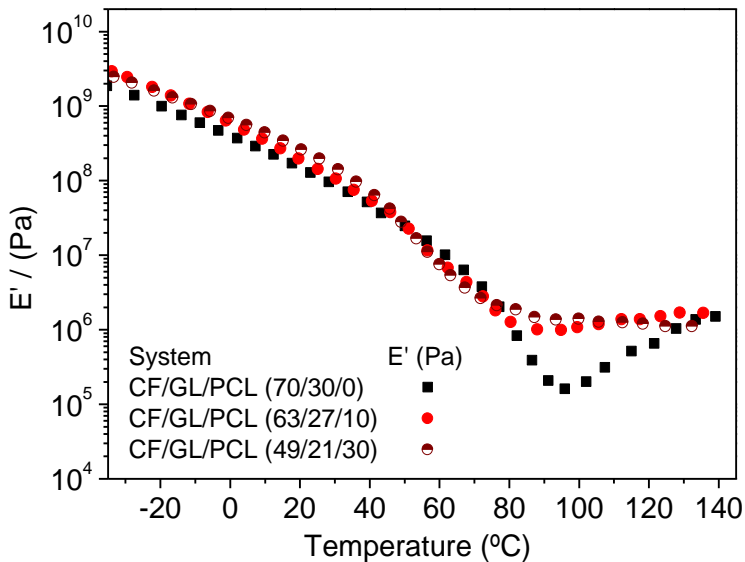


Figure 5.4-15: Storage modulus from DMA temperature ramp measurements performed at constant frequency (6.28 rad/s) and heating rate (3 °C/min) for CF/GL/PCL probes at constant CF/GL ratio: 70/30/0, 63/27/10, 49/21/30.

In addition, it is interesting to remark that the reference system shows a minimum in  $E'$  close to 100 °C, followed by an apparent enhancement of elastic properties increase, which is characteristic of a thermosetting potential (Jerez, Partal et al. 2007, Romero, Beaumal et al. 2011, Zarate-Ramirez, Martinez et al. 2011). In other words, an increase in the temperature of the packing stage would lead to a reinforcement of the biopolymer matrix. In contrast, the addition of PCL leads to a reduction in this potential than tends to disappear at the highest PCL content, where elastic properties remain rather independent on temperature. These results suggest that the melting of PCL results in a certain reduction in the free volume leading to an increase in physical interactions. In any case, the response in the high temperature region seems to be dominated by the presence of melted PCL.

Figure 5.4-16 shows the values of the elastic modulus,  $E'$  from DMA temperature ramp test measurements. The reference system is compared with those specimens with the same protein/plasticiser ratio (CF/GL/PCL: 63/27/10 and 49/21/30).

Furthermore, all probes studied display similar loss tangent profiles showing one single peak, which is related to a glass-like transition of the plasticized protein-based material. These unimodal profiles indicate a good compatibility between compounds, obtained for all systems after the injection moulding process. However, the increase in PCL content gives rise to a plasticising effect leading to a decrease in the peak temperature (from ca. 100 to 50 °C).

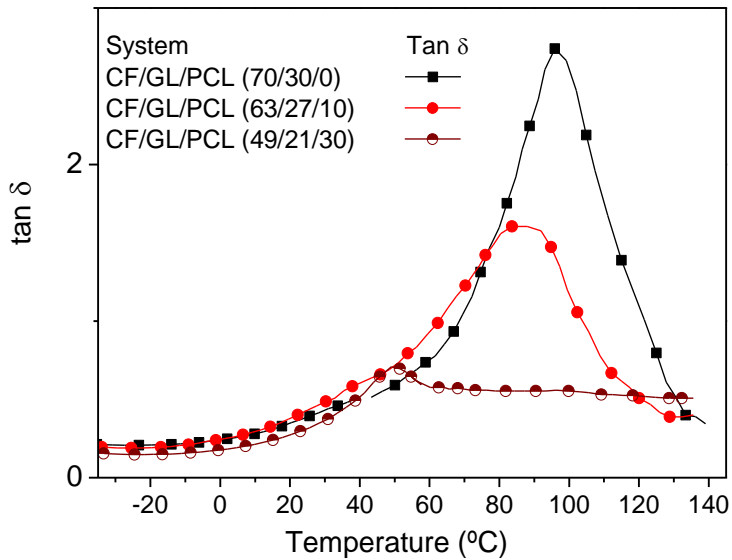


Figure 5.4-16:  $\tan \delta$  from DMA temperature ramp measurements performed at constant frequency (6.28 rad/s) and heating rate ( $3\text{ }^{\circ}\text{C}\cdot\text{min}^{-1}$ ) for CF/GL/PCL probes at constant CF/GL ratio: 70/30/0, 63/27/10, 49/21/30.

Figure 5.4-17 shows the values of the value of the storage modulus at 6.28 rad/s and  $20\text{ }^{\circ}\text{C}$  ( $E'_{1.20}$ ) in order to compare the behaviour of different biocomposite materials.

These results confirm the effect of PCL-induced increase in elasticity that takes place also at a higher CF/GL ratio. Moreover, at constant PCL content, an increase in CF/GL ratio also produces an increase in  $E'$  values. This effect is particularly noticeable at the highest PCL concentration, which suggests occurrence of a synergistic effect between CF and PCL. Similar results were reported by Aithani and Mohanty (2006), which found an increase in storage modulus for bioplastics containing PCL and corn gluten meal as the proportion of PCL increases.

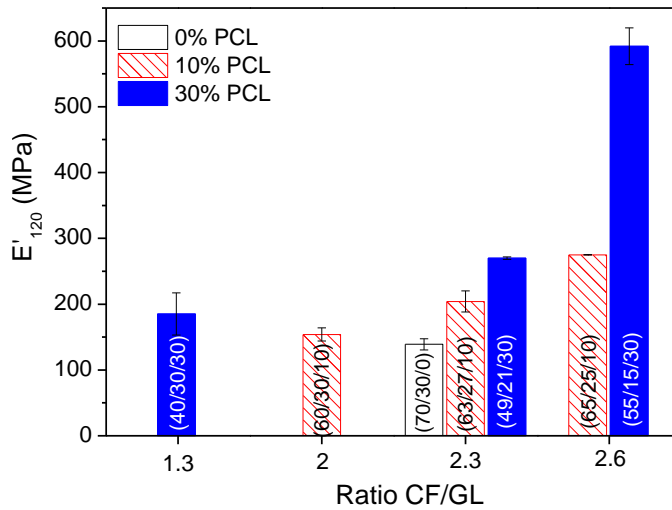


Figure 5.4-17: Storage modulus ( $E'_{120}$ ) obtained from DMA measurements for all CF/GL/PCL systems: (70/30/0), (65/25/10), (63/27/10), (60/30/10), (55/15/30), (49/21/30) and (40/30/30).

Figure 5.4-18 shows the value of the loss tangent at the peak temperature ( $\tan \delta_{\max}$ ), whose values ( $T_{\text{peak}}$ ) are also included in the plot values of some parameters selected

This figure shows how an increase in PCL content leads to a remarkable decrease in  $\tan \delta_{\max}$  and  $T_{\text{peak}}$  at the two CF/GL ratios studied, thus confirming the above mentioned plasticising effect of PCL. The increase in the CF/GL ratio gives rise to a different effect depending on the PCL concentration. At wt. 10% PCL a reduction for  $\tan \delta_{\max}$  and  $T_{\text{peak}}$  may also be observed, being much more noticeable for the former. On the other hand, for 30 wt. % PCL only slight changes in values take place. Thus,  $\tan \delta_{\max}$  undergoes a slight reduction followed by a moderate increase in value with increasing CF/GL ratio, while  $T_{\text{peak}}$  shows only a significant, but moderate, increase at the highest CF/GL ratio. This increase is probably what causes the final increase in  $\tan \delta_{\max}$ .



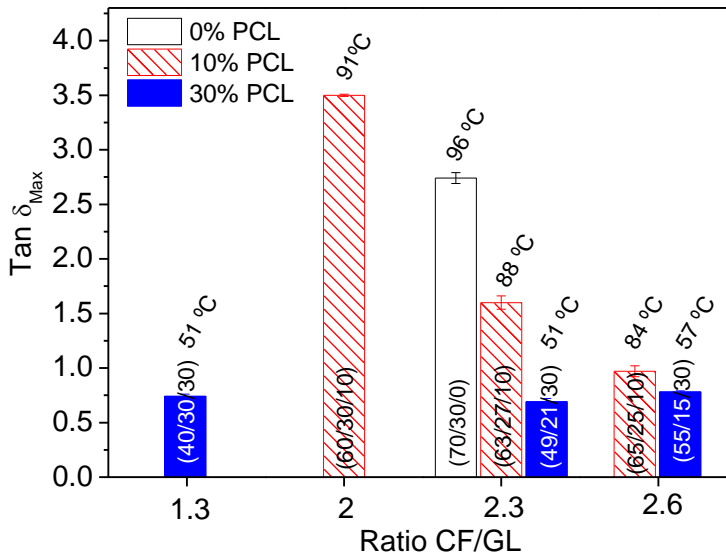


Figure 5.4-18: Loss tangent maximum ( $\tan \delta_{Max}$ ) obtained from DMA measurements for all CF systems, as well as the temperature reached

#### 5.4.3.1.2. Uniaxial tensile strength measurements

Stress-strain curves for the reference specimen CF/GL (70/30), and for composite samples containing the same ratio protein plasticiser (CF/GL/PCL: 63/27/10 and 49/21/30) are shown in Figure 5.4-19.

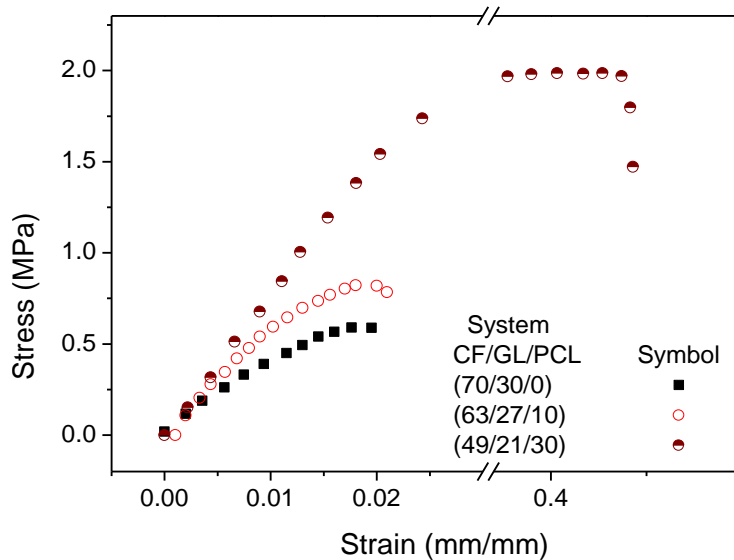


Figure 5.4-19: Tensile strength curve for systems at constant CF/GL ratio

All curves exhibit an initial linear elastic behaviour of high constant stress-strain slope yielding high values for the Young’s modulus (E), followed by a plastic deformation stage with a continuous decrease in the stress-strain slope after the elastic limit. Eventually, all curves reach a maximum value for the stress ( $\sigma_{max}$ ) and the elongation at break ( $\epsilon_{max}$ ). Toughness (T), which expresses the ability to absorb mechanical energy up to the point of failure, has been calculated from the area under the stress-strain curve by the following equation (5.4-3):

$$T = \int_0^{\epsilon_{max}} \sigma(\epsilon) \cdot d\epsilon \tag{5.4-3}$$

Where T represents the toughness,  $\sigma$  the stress and  $\epsilon$  the strain.

Regarding the tensile properties obtained from tensile tests applied to CF/GL and CF/GL/PCL biocomposites, Figure 5.4-20, Figure 5.4-21 and Figure

## Results

5.4-22 show the values of the Young's modulus, elongation at break and toughness, respectively:

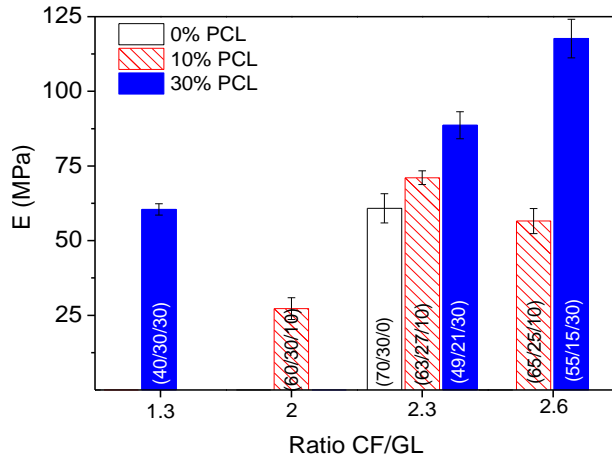


Figure 5.4-20: Young's modulus ( $E$ ) obtained from stress-strain curve for all CF/GL/PCL systems: (70/30/0), (65/25/10), (63/27/10), (60/30/10), (55/15/30), (49/21/30) and (40/30/30).

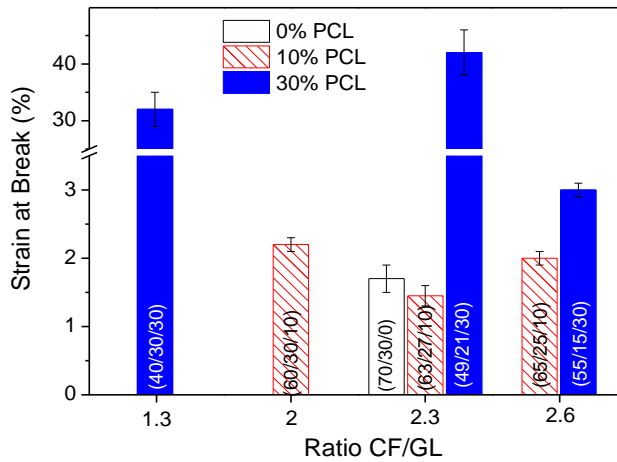


Figure 5.4-21: Elongation at break obtained from stress-strain curve for all CF/GL/PCL systems: (70/30/0), (65/25/10), (63/27/10), (60/30/10), (55/15/30), (49/21/30) and (40/30/30).

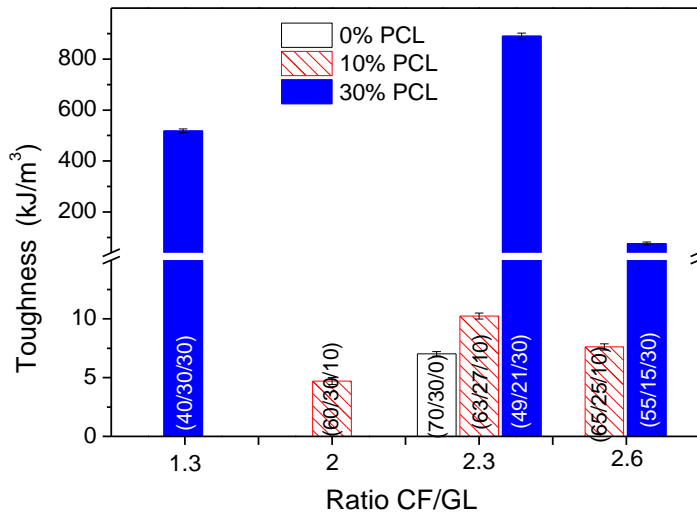


Figure 5.4-22: Toughness from stress-strain curve for all CF/GL/PCL systems: (70/30/0), (65/25/10), (63/27/10), (60/30/10), (55/15/30), (49/21/30) and (40/30/30).

As may be observed, higher values in  $E'$  and especially in  $\epsilon_{\max}$  and toughness are obtained by increasing PCL from 0 to 30%.

Moreover, an increase in the CF/GL ratio yields a different behaviour depending on PCL content. Those specimens containing 10 wt. % PCL display a maximum value in  $E$  as well as a minimum value in  $\epsilon_{\max}$ . As a result, a moderate increase in toughness takes place. It should be also taken into account that an increase in the CF/GL ratio also involves a decrease in the PCL/CF ratio. These results suggest that both ratios exert opposite effects, where the dominant effect seems to be the former at low CF content and the latter at high CF content. This balance can explain the occurrence of the maximum in  $E$  and minimum in  $\epsilon_{\max}$ .

On the other hand, an increase in PCL content up to 30 wt. % may lead to high values in  $E$  that exhibit a continuous increase with CF/GL ratio, but lead to particularly high values in  $\epsilon_{\max}$  that become less important for the highest

CF/GL ratio studied. The latter effect is so important in this case that toughness follows the same evolution. The final decrease in  $\epsilon_{\max}$  observed in Figure 5.4-21 and Figure 5.4-22 is probably because the specimen becomes brittle as a consequence of the high amount of polymer (CF+PCL).

It is also worth mentioning that a comparison of the elastic bending modulus ( $E'$ ) and the Young's modulus ( $E$ ) in Figure 5.4-17 and Figure 5.4-20, respectively, put forward the similar behaviour of both parameters. In fact, both parameters reflect the contribution of CF protein and PCL to the elastic response at small strain under bending or uniaxial tension deformations. All these results reveal that both polymers play a significant role on the elastic properties. In order to assess the contribution of each polymer (CF and PCL) a comparison between two systems containing the same polymer/GL ratio (40/30/30 and 60/30/10) may be carried out. It is apparent that the PCL yields higher contribution to the elastic response, particularly under uniaxial tensile tests. This dominant contribution of PCL can be extrapolated to the plastic deformation region since the 40/30/30 specimen shows much higher value in  $\epsilon_{\max}$ . The toughness also put forward this effect.

### 5.4.3.2. X-Ray Diffraction (XRD)

Figure 5.4-23 shows the X-ray diffraction spectra of the reference system and systems containing 10 wt. % PCL.

This figure reveals the characteristic pattern of PCL in its crystalline structure with the well-developed peaks at  $2\theta = 21.5^\circ$  and  $23.7^\circ$  in accordance with Vertuccio et al. (2009) that also reported a shoulder peak at about  $22.0^\circ$ . A further peak may be also observed at  $29.7^\circ$ , showing much lower intensity.

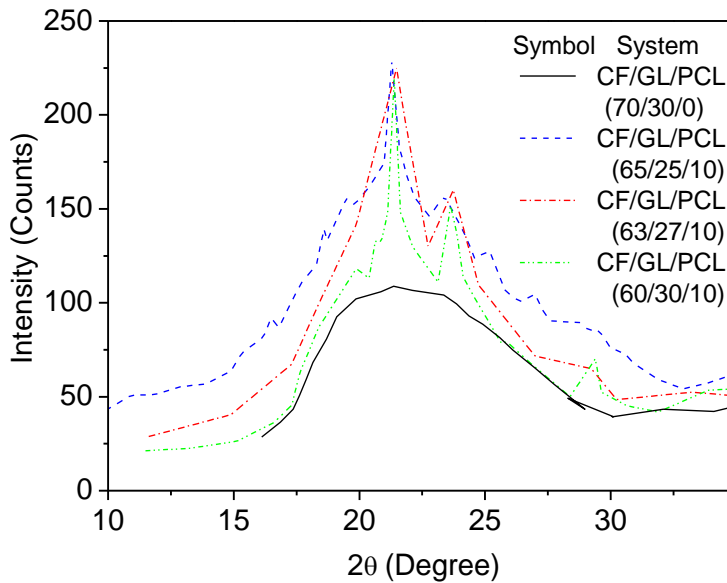


Figure 5.4-23: XRD for the reference system (70/30/0) and for CF/GL/PCL probes at constant PCL concentration: 10 wt. % of PCL: (65/25/10), (63/27/10) and (60/30/10)

As for the reference PCL-free specimen, the diffraction spectrum displays a broad peak that unfortunately is located at the same position of the two main peaks of PCL. This figure also shows how the incorporation of PCL up to 10 wt. % does not lead to any modification in the location ( $2\theta$  value) of the PCL peaks, but a progressive broadening effect takes place for both peaks as the protein content increases. According to Ungar (2004), X-ray diffraction peaks broaden when the crystal lattice becomes imperfect. Peaks broaden either when crystallites become smaller than about a micrometre or if lattice defects are present in large enough amount and there are two important causes: size and strain broadening. Therefore, in accordance with this statement, the results obtained for composites containing 10 wt. % PCL suggest that CF protein either inhibits the development of the PCL crystalline phase or favours the presence of lattice defects.

Figure 5.4-24 shows the X-ray diffraction spectra for systems containing 30 wt. % PCL: (55/15/30), (49/21/30) and (40/30/30).

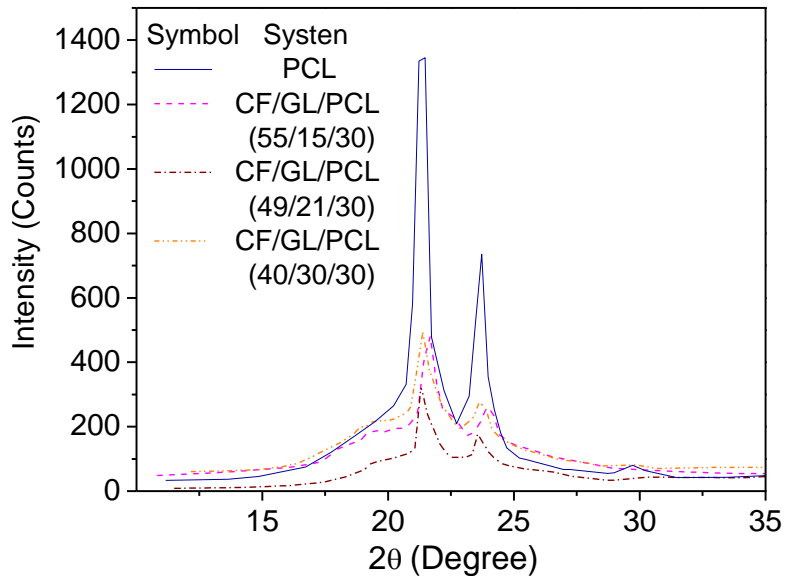


Figure 5.4-24: XRD for probes at constant PCL concentration: 30 wt. % (55/15/30), (49/21/30) and (40/30/30)

This figure shows how the diffraction spectra of the composites containing 30 wt. % PCL neither yield any particular modification in the location ( $2\theta$  value) of the PCL peaks. This fact means that the interplanar distance ( $d_{hkl}$ ) also remains unaltered, and as a consequence, the lattice structure does not suffer any change, regardless of the protein content of the composite specimen. These results suggest that amorphous sections are responsible for the protein-polymer system compatibility. Conversely, it can be observed that an increase in the total amount of synthetic polymer leads to remain unaltered crystalline sections. It is also worth pointing out that the crystalline phase of the PCL is well developed for composites containing 30 wt. % PCL, which suggests that the selected processing conditions do not affect to

the PCL crystalline morphology. In addition, these layers do not exhibit any broadening effect (neither size nor strain), thus indicating that the development of PCL crystalline phase is preserved after processing, which may well be related to the improvement of mechanical properties of these composites containing high percentage of PCL.

### **5.4.4. CF and CF2L protein-based bioplastic comparison**

In order to compare both protein systems (CF and CF2L) the ratio of protein-content to plasticiser was kept constant.

Then, if the protein content of the CF concentrate is  $64.2 \pm 0.9$  wt. %, the total amount of proteins in the bioplastic probes is about 45 wt. %. Thus, if the protein content of the CF2L system is  $78.6 \pm 0.9$  wt. %, the ratio protein/plasticiser should be 60/40.

For this reason, the systems compared were: CF/GL (70/30) and CF2L/GL (60/40), being all injection conditions for the new system that one selected from the previous study for CF protein concentrate.

Dynamic mechanical analysis and tensile test were performed to characterise the mechanical response of the new bioplastic.

#### **5.4.4.1. Dynamic Mechanical analysis**

Figure 5.4-25 shows a comparison between systems containing different crayfish powder (CF and CF2L) at the same protein/plasticiser ratio:



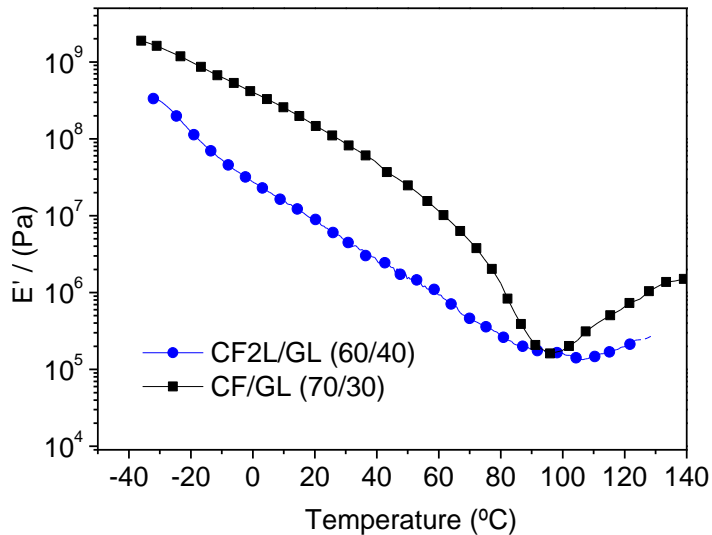


Figure 5.4-25: DMTA for the reference system CF/GL (70/30) and the system with CF2L protein concentrate CF2L/GL (60/40).

As may be observed, CF-based system has higher elastic modulus in the overall temperature interval studied. However, both bio-based plastic systems (CF and CF2L), exhibit similar behaviour. The increase of temperature leads to decrease the elastic modulus, until c.a. 100 °C where certain thermosetting potential seems to appear. The dramatic decrease of elastic modulus observed for CF/GL (70/30) probes was not found for CF2L/GL (60/40) probes, however elastic modulus for CF/GL (70/30) is never below CF2L/GL (60/40) modulus.

#### 5.4.4.2. Uniaxial tensile strength

Figure 5.4-26 shows the tensile strength measurements for systems CF and CF2L at the same protein/plasticiser ratio (70/30 and 60/40, respectively):

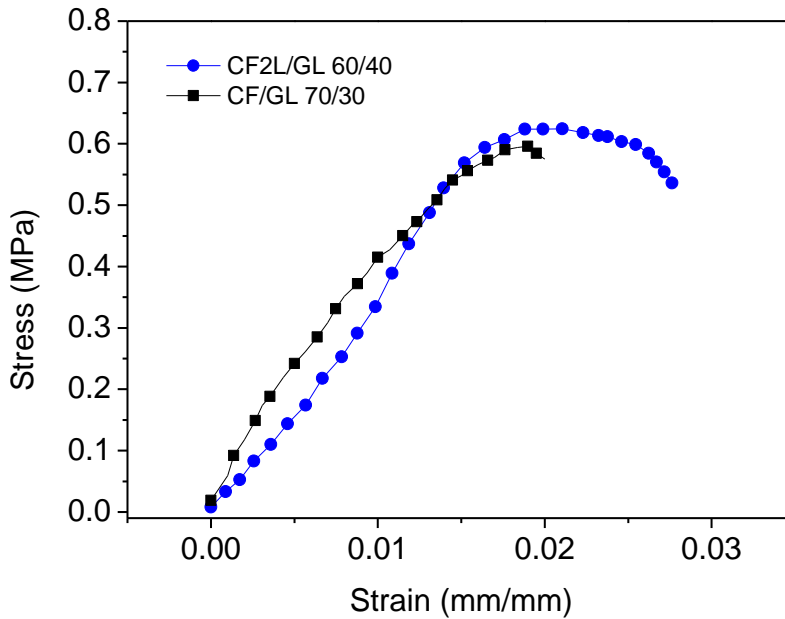


Figure 5.4-26: Tensile test for systems CF/GL and CF2L/GL at the same protein/plasticiser ratio (70/30 and 60/40, respectively)

Parameters obtained from these measurements are shown in Table 5.4-3:

System	Elongation at break (%)	Max. stress (MPa)	E (MPa)
CF/GL (70/30)	1.9 ± 0.2	0.60 ± 0.12	62.2 ± 4.5
CF2L/GL (60/40)	2.9 ± 0.3	0.62 ± 0.15	38.4 ± 5.1

Table 5.4-3: Parameters from tensile strength measurements for CF/GL (70/30) and CF2L/GL (60/40) systems.

Results from tensile tests show that both systems have comparable maximum stress value, however CF probes are more rigid, and as consequence these probes exhibit lower elongation at break and higher Young’s modulus. Both probes have comparable parameters.

*A la vida*

*Por todos esos momentos que me has dado,  
Por este ciclo que no estaba programado, pero que elegí sin saber a dónde  
llegaría ¿Qué hubiera sido de mí sin tus enseñanzas?*





## 6. Conclusions





### 6.1. Conclusions from protein characterisation

1. Crayfish protein concentrate, CF2L, contains a significant amount of the essential amino acids that would provide excellent nutritional quality to CF2L-containing products. Its nutritional value together with its high solubility makes this product fairly attractive as a food ingredient in different applications such as emulsions and gels. The CF2L protein system as well as their hydrolysates show a low protein denaturation, and a desirable sulfhydryl content for different applications (emulsions, gels and bioplastics). Surface hydrophobicity increase in the same way as degree of hydrolysis.





### 6.2. Conclusions from Crayfish-based Emulsions

2. Results from CF2L protein adsorption at liquid-liquid interfaces evidence a fast increase in surface pressure that tends to reach a pseudo-equilibrium value regardless of the pH. However, after fitting the curve to the Ward and Tordai model, the diffusion constant parameter indicates that protein diffusion takes place faster at pH 5.0 than at pH 3.0 or 8.0. This behaviour may be related to the absence of net charge close to the IEP. In contrast, fitting surface pressure data to a first order equation for the penetration stage reveals that this stage is favoured at pH 3.0.

3. Interfacial dilatational rheology measurements suggest that CF2L adsorbed interfaces are quite more packed or have larger Gibbs elasticity at pH 3.0, exhibiting higher values for the elastic modulus that correspond to a gel-like behaviour. However, dilatational measurements cannot determine the nature of the interactions or predict the stability of the interface.

4. CF2L-based high-oleic/water emulsions exhibit lower droplet sizes at pH 5.0, as a result of the higher surface pressure. However, the highest stability corresponds to emulsions prepared at pH 3.0, which show unflocculated unimodal distributions remaining unaltered in size over 2 months. On the other hand, droplet sizes show a strong influence on ageing time for emulsions prepared at pH 5.0 and 8.0, caused by coalescence. The increase in XG attenuates this effect to a great extent, although does not prevent an eventual emulsion destabilization.

5. Linear viscoelastic properties and steady flow properties of CF2L-based emulsions seem to be governed by protein-polysaccharide interactions that in turn depend on pH. Those interactions also seem to control the destabilization of the emulsions studied. These results support the key role of the polysaccharide in the formation of the gel-like network, either through

## *Conclusions*

formation of extensive flocculation (at pH 5.0 and 8.0) or through complexation with protein, favoured at pH 3.0.

6. Light scattering measurements and CLSM images confirm the emulsion stability behaviour found with DSD measurements as a function of pH. The former type of measurements put forward occurrence of coalescence and oiling-off at pH 5.0 and 8.0 after 14 days. CLSM illustrate a rather noticeable interface at pH 3.0.

### 6.3. Conclusions from Antioxidant Crayfish Gels

7. SAOS measurements reveal a strong dependence of gelation ability and gel strength on pH. Thus, near the IEP, the absence of net charges facilitates a proper development of gel network structures leading to fairly strong gel-like viscoelastic behaviour, with higher amount of disulphide bonds and enhanced WHC. On the other hand, at pH 8.0 and 2, the presence of repulsive interactions among charged protein surfaces tend to inhibit S-S bonds such that gel development is dominated by hydrophobic interactions, leading to weak gels with lower viscoelastic properties and WHC, particularly at pH 2 at which a large increase in the relative amount of the peptide fraction was found as a consequence of acidic hydrolysis.

8. The influence of protein hydrolysis is highly dependent on pH:

- At low pH, hydrolysis yields a reduction in interactions that involves a decrease in viscoelastic properties.
- At neutral pH, a moderate degree of hydrolysis brings about two opposite effects, inhibition of S-S bonds and enhancement of hydrophobic interactions and hydrogen bonds, resulting in a fairly invariable gel-like behaviour. However, WHC always decrease in consonance with the reduction of S-S bonds.
- On the other hand, at alkaline pH, an apparent enhancement of the gel network takes place at intermediate degree of hydrolysis, as a consequence of an increase in S-S bonds.

A high degree of hydrolysis generally leads to an apparent decrease of interactions that result in a dramatic decrease in viscoelastic properties and WHC.

## Conclusions

9. The highest antioxidant activity was obtained against ABTS and the lowest when FC was used, since this reagent is specific for phenol compounds. No particular influence of pH was found for DPPH or FC activity. However, pH exerts a dramatic increase on the activity against ABTS (around one decade). In general hydrolysates systems exhibit a higher antioxidant activity except against DPh=. This behaviour is remarkable for ABTS at pH 8.0 where antioxidant activity reaches twice the value for CF2L. Once again, a high degree of hydrolysis is not desirable, because antioxidant activity decreases.

### 6.4. Conclusions from Crayfish bioplastic

10. From the experimental results, it may be concluded that monitoring the torque over mixing of protein-based flour, additives and plasticizer it is useful to select the more suitable conditions (e.g. mixing time and formulation) in terms of energy efficiency. The addition of reducing agent (BS or SS), denaturing agent (U) or crosslinking promoter (LC), always yields an increase in energy efficiency at the mixing stage, leading to a remarkable reduction in the linear viscoelastic properties of blends, which is also important to select suitable operation conditions for injection moulding processing.

11. As for bioplastics, the additive developing a greater effect on mechanical properties is LC, which provides specimens showing a higher value for the Young's modulus, as well as a remnant thermosetting potential for further processing at high temperature. However, it is the maximum elongation the property that is remarkably enhanced by increasing the thermosetting temperature, which takes place at the expense of the Young's modulus. The maximum stress increase only when the temperature of the mould increase.

12. The combination of techniques such as mixing rheology of CF/GL/PCL, controlling torque and temperature profiles, and DSC is very useful for selecting suitable injection moulding parameters for processing blends.

13. CF/GL/PCL biocomposites show a remarkable enhancement in mechanical properties as compared to CF/GL bioplastics, even when crystalline structure remains unaltered. Furthermore, the protein/plasticiser ratio also plays a relevant role. Thus, both polymers play a significant role on the elastic properties. However, the PCL yields a dominant contribution to the

## *Conclusions*

elastic response, particularly under uniaxial tensile tests, and confer a higher ability to absorb energy before rupture.

14. Finally, the feasibility of designing renewable and biodegradable composites have been demonstrated, which may be regarded as an alternative to conventional plastic materials, containing an important amount of CF, thereby finding value-added applications of these low valued by-products of the crayfish industry.



## 7. References

---





## References

A.O.A.C. (2000). Official Methods of Analysis. E.E.U.U., Association of Official Analytical Chemist.

Acton, J. C. and R. L. Dick (1988). "Functional roles of heat induces protein gelation in processed meat." Journal of the American Oil Chemists Society **65**(4): 497-497.

Aguilar, J. M., A. P. Batista, M. C. Nunes, F. Cordobes, A. Raymundo and A. Guerrero (2011). "From egg yolk/kappa-Carrageenan dispersions to gel systems: Linear viscoelasticity and texture analysis." Food Hydrocolloids **25**(4): 654-658.

Aithani, D. and A. K. Mohanty (2006). "Value-added new materials from byproduct of corn based ethanol industries: Blends of plasticized corn gluten meal and poly(epsilon-caprolactone)." Industrial & Engineering Chemistry Research **45**(18): 6147-6152.

Akay, M. (2012). Introduction to Polymer Science and Technology, Bookboon.

Aluru, S. (2005). Handbook of Computational Molecular Biology, CRC Press.

Amine, C., J. Dreher, T. Helgason and T. Tadros (2014). "Investigation of emulsifying properties and emulsion stability of plant and milk proteins using interfacial tension and interfacial elasticity." Food Hydrocolloids **39**: 180-186.

Anon (1997). "Thermal Characterization of Polymeric Materials edited by Edith A. Turi." Polym. Test. **16**(5): 523.

Apak, R., K. Gueclue, B. Demirata, M. Oezyuerrek, S. E. Celik, B. Bektasoglu, K. I. Berker and D. Oezyurt (2007). "Comparative evaluation of various total antioxidant capacity assays applied to phenolic compounds with the CUPRAC assay." Molecules **12**(7): 1496-1547.

Arranz, S., R. Cert, J. Perez-Jimenez, A. Cert and F. Saura-Calixto (2008). "Comparison between free radical scavenging capacity and oxidative stability of nut oils." Food Chemistry **110**(4): 985-990.

## References

Balaguer, M. P., J. Gomez-Estaca, R. Gavara and P. Hernandez-Muñoz (2011). "Biochemical Properties of Bioplastics Made from Wheat Gliadins Cross-Linked with Cinnamaldehyde." Journal of Agricultural and Food Chemistry **59**(24): 13212-13220.

Banerjee, S. and S. Bhattacharya (2012). "Food Gels: Gelling Process and New Applications." Critical Reviews in Food Science and Nutrition **52**(4): 334-346.

Barnes, H. A. (2000). A Handbook of Elementary Rheology, University of Wales, Institute of Non-Newtonian Fluid Mechanics.

Batchelor, G. K. (1977). "The effect of Brownian motion on the bulk stress in a suspension of spherical particles." Journal of Fluid Mechanics **83**(01): 97-117.

Bengoechea, C., F. Cordobes and A. Guerrero (2006). "Rheology and microstructure of gluten and soya-based o/w emulsions." Rheologica Acta **46**(1): 13-21.

Berker, K. I., F. A. O. Olgun, D. Ozyurt, B. Demirata and R. Apak (2013). "Modified Folin-Ciocalteu Antioxidant Capacity Assay for Measuring Lipophilic Antioxidants." Journal of Agricultural and Food Chemistry **61**(20): 4783-4791.

Beveridge, T., S. J. Toma and S. Nakai (1974). "Determination of SH-groups and SS-groups in some food proteins using Ellman's Reagent." Journal of Food Science **39**(1): 49-51.

Boulanouar, B., G. Abdelaziz, S. Aazza, C. Gago and M. Graca Miguel (2013). "Antioxidant activities of eight Algerian plant extracts and two essential oils." Industrial Crops and Products **46**: 85-96.

Brand-Williams, W., M. E. Cuvelier and C. Berset (1995). "Use of a free-radical method to evaluate antioxidant activity." Food Science and Technology-Lebensmittel-Wissenschaft & Technologie **28**(1): 25-30.

Buonocore, G. G., M. A. Del Nobile, A. Panizza, M. R. Corbo and L. Nicolais (2003). "A general approach to describe the antimicrobial agent release from

## References

highly swellable films intended for food packaging applications." Journal of Controlled Release **90**(1): 97-107.

Cabra, V., E. Vazquez-Contreras, A. Moreno and R. Arreguin-Espinosa (2008). "The effect of sulfhydryl groups and disulphide linkage in the thermal aggregation of Z19 alpha-zein." Biochimica Et Biophysica Acta-Proteins and Proteomics **1784**(7-8): 1028-1036.

Calero, N., J. Munoz, P. W. Cox, A. Heuer and A. Guerrero (2013). "Influence of chitosan concentration on the stability, microstructure and rheological properties of O/W emulsions formulated with high-oleic sunflower oil and potato protein." Food Hydrocolloids **30**(1): 152-162.

Cano, M. P., A. Hernandez and B. DeAncos (1997). "High pressure and temperature effects on enzyme inactivation in strawberry and orange products." Journal of Food Science **62**(1): 85-88.

Cao, Y., E. Dickinson and D. J. Wedlock (1990). "Creaming and flocculation in emulsions containing polysaccharide." Food Hydrocolloids **4**(3): 185-195.

Careche, M., C. Alvarez and M. Tejada (1995). "Suwari and Kamaboko sardine gels - effect of heat-treatment on solubility of networks." Journal of Agricultural and Food Chemistry **43**(4): 1002-1010.

Castellani, O., S. Al-Assaf, M. Axelos, G. O. Phillips and M. Anton (2010). "Hydrocolloids with emulsifying capacity. Part 2-Adsorption properties at the n-hexadecane-Water interface." Food Hydrocolloids **24**(2-3): 121-130.

Clark, A. H., G. M. Kavanagh and S. B. Ross-Murphy (2001). "Globular protein gelation - theory and experiment." Food Hydrocolloids **15**(4-6): 383-400.

Cofrades, S., J. Carballo, M. Careche and F. J. Colmenero (1996). "Emulsifying properties of actomyosin from several species." Food Science and Technology-Lebensmittel-Wissenschaft & Technologie **29**(4): 379-383.

Cordobes, F., P. Partal and A. Guerrero (2004). "Rheology and microstructure of heat-induced egg yolk gels." Rheologica Acta **43**(2): 184-195.

## References

- Corradini, E., L. H. C. Mattoso, C. G. F. Guedes and D. S. Rosa (2004). "Mechanical, thermal and morphological properties of poly(epsilon-caprolactone)/zein blends." Polymers for Advanced Technologies **15**(6): 340-345.
- Cremades, O., J. Parrado, M. C. Alvarez-Ossorio, M. Jover, L. C. de Teran, J. F. Gutierrez and J. Bautista (2003). "Isolation and characterization of carotenoproteins from crayfish (*Procambarus clarkii*)." Food Chemistry **82**(4): 559-566.
- Creusot, N. and H. Gruppen (2007). "Enzyme-induced aggregation and gelation of proteins." Biotechnology Advances **25**(6): 597-601.
- Chalamaiah, M., B. D. Kumar, R. Hemalatha and T. Jyothirmayi (2012). "Fish protein hydrolysates: Proximate composition, amino acid composition, antioxidant activities and applications: A review." Food Chemistry **135**(4): 3020-3038.
- Chen, H. and Q. Zhong (2014). "Processes improving the dispersibility of spray-dried zein nanoparticles using sodium caseinate." Food Hydrocolloids **35**: 358-366.
- Damodaran, S. (1997). Food Proteins and Their Applications, Taylor & Francis.
- Damodaran, S., K. L. Parkin and O. R. Fennema (2007). Fennema's Food Chemistry, Fourth Edition, Taylor & Francis.
- De Graaf, L. A. (2000). "Denaturation of proteins from a non-food perspective." Journal of Biotechnology **79**(3): 299-306.
- di Gioia, L. and S. Guilbert (1999). "Corn protein-based thermoplastic resins: Effect of some polar and amphiphilic plasticizers." Journal of Agricultural and Food Chemistry **47**(3): 1254-1261.
- Dickinson, E. and D. J. McClements (1995). Advances In Food Colloids, Springer.

## References

Dowd, J. E. and D. S. Riggs (1965). "A COMPARISON OF ESTIMATES OF MICHAELIS-MENTEN KINETIC CONSTANTS FROM VARIOUS LINEAR TRANSFORMATIONS." Journal of Biological Chemistry **240**(2): 863-&.

Elias, R. J., S. S. Kellerby and E. A. Decker (2008). "Antioxidant activity of proteins and peptides." Critical Reviews in Food Science and Nutrition **48**(5): 430-441.

Ellis, G. P. (1959). The Maillard Reaction. Advances in Carbohydrate Chemistry. L. W. Melville, Academic Press. **Volume 14**: 63-134.

Erni, P., E. J. Windhab and P. Fischer (2011). "Emulsion Drops with Complex Interfaces: Globular Versus Flexible Proteins." Macromolecular Materials and Engineering **296**(3-4): 249-262.

Espinoza, M., C. Olea-Azar, H. Speisky and J. Rodriguez (2009). "Determination of reactions between free radicals and selected Chilean wines and transition metals by ESR and UV-vis technique." Spectrochimica Acta Part a-Molecular and Biomolecular Spectroscopy **71**(5): 1638-1643.

Etheridge, R. D., G. M. Pesti and E. H. Foster (1998). "A comparison of nitrogen values obtained utilizing the Kjeldahl nitrogen and Dumas combustion methodologies (Leco CNS 2000) on samples typical of an animal nutrition analytical laboratory." Animal Feed Science and Technology **73**(1-2): 21-28.

Ezhilarasi, P. N., D. Indrani, B. S. Jena and C. Anandharamakrishnan (2013). "Freeze drying technique for microencapsulation of Garcinia fruit extract and its effect on bread quality." Journal of Food Engineering **117**(4): 513-520.

FAO (1985). "Energy and protein requirements. Report of a joint FAO/WHO/UNU Expert Consultation." World Health Organization technical report series **724**: 1-206.

Farahnaky, A., A. Guerrero, S. E. Hill and J. R. Mitchell (2008). "Physical ageing of crayfish flour at low moisture contents." Journal of Thermal Analysis and Calorimetry **93**(2): 595-598.

## References

- Fayle, S. E., J. A. Gerrard and R. S. o. Chemistry (2002). The Maillard Reaction, Royal Society of Chemistry.
- Felix, M., J. E. Martin-Alfonso, A. Romero and A. Guerrero (2014). "Development of albumen/soy biobased plastic materials processed by injection molding." Journal of Food Engineering **125**: 7-16.
- Fetters, L. J., D. J. Lohse, D. Richter, T. A. Witten and A. Zirkel (1994). "Connection between polymer molecular-weight, density, chain dimensions, and melt viscoelastic properties " Macromolecules **27**(17): 4639-4647.
- Filipczak, K., M. Wozniak, P. Ulanski, L. Olah, G. Przybytniak, R. M. Olkowski, M. Lewandowska-Szumiel and J. M. Rosiak (2006). "Poly (epsilon-caprolactone) biomaterial sterilized by E-beam irradiation." Macromolecular Bioscience **6**(4): 261-273.
- Floch, C., E. Alarcon-Gutierrez and S. Criquet (2007). "ABTS assay of phenol oxidase activity in soil." Journal of Microbiological Methods **71**(3): 319-324.
- Folin, O. and V. Ciocalteu (1927). "On tyrosine and tryptophane determinations in proteins." Journal of Biological Chemistry **73**(2): 627-650.
- Fountoulakis, M. and H. W. Lahm (1998). "Hydrolysis and amino acid composition analysis of proteins." Journal of Chromatography A **826**(2): 109-134.
- Freer, E. M., K. S. Yim, G. G. Fuller and C. J. Radke (2004). "Interfacial rheology of globular and flexible proteins at the hexadecane/water interface: Comparison of shear and dilatation deformation." Journal of Physical Chemistry B **108**(12): 3835-3844.
- Frumkin, A. (1925). "The capillary curve of higher fatty acids and the constitutive equation of the surface layer." Zeitschrift Fur Physikalische Chemie--Stochiometrie Und Verwandtschaftslehre **116**(5/6): 466-484.
- Fuller, G. G. and J. Vermant (2012). "Complex Fluid-Fluid Interfaces: Rheology and Structure." Annual Review of Chemical and Biomolecular Engineering, Vol 3 **3**: 519-543.

## References

Galazka, V. B. and D. A. Ledward (1995). Developments in high pressure food processing. London, Sterling Publications International.

Geiger, W., P. Alcorlo, A. Baltanas and C. Montes (2005). "Impact of an introduced Crustacean on the trophic webs of Mediterranean wetlands." Biological Invasions **7**(1): 49-73.

Gomez-Guillen, M. C., A. J. Borderias and P. Montero (1997). "Chemical interactions of nonmuscle proteins in the network of sardine (*Sardina pilchardus*) muscle gels." Food Science and Technology-Lebensmittel-Wissenschaft & Technologie **30**(6): 602-608.

Gomez-Guillen, M. C., P. Montero, M. T. Solas and A. J. Borderias (1998). "Thermally induced aggregation of giant squid (*Dosidicus gigas*) mantle proteins. Physicochemical contribution of added ingredients." Journal of Agricultural and Food Chemistry **46**(9): 3440-3446.

Gomez-Martinez, D., P. Partal, I. Martinez and C. Gallegos (2009). "Rheological behaviour and physical properties of controlled-release gluten-based bioplastics." Bioresource Technology **100**(5): 1828-1832.

Greene, D. H. and J. K. Babbitt (1990). "Control of muscle softening and protease-parasite interactions in arrowtooth flounder *Atheresthes-stomias*." Journal of Food Science **55**(2): 579-580.

Hashimoto, K., S. Watabe, M. Kono and K. Shiro (1979). "Muscle protein-composition of sardine and mackerel." Bulletin of the Japanese Society of Scientific Fisheries **45**(11): 1435-1441.

Hashimoto, T., T. Suzuki, T. Hagiwara and R. Takai (2004). "Study on the glass transition for several processed fish muscles and its protein fractions using differential scanning calorimetry." Fisheries Science **70**(6): 1144-1152.

Hegg, P. O. (1982). "Conditions for the formation of heat-induced gels of some globular food proteins." Journal of Food Science **47**(4): 1241-1244.

Hereman, K., J. Van Camp and A. Huyghebaert (1997). High pressure effects on proteins. In:

## References

. Food Proteins and their Application in Foods. S. D. a. A. Paraf. New York, Marcel Dekker, Inc: 473-502.

Hermansson, A. M. (1986). "Soy protein gelation." JAOCS, J. Am. Oil Chem. Soc. **63**(5): 658-666.

Hernandez-Izquierdo, V. M. and J. M. Krochta (2008). "Thermoplastic processing of proteins for film formation - A review." Journal of Food Science **73**(2): R30-R39.

Hoover, D. G., C. Metrick, A. M. Papineau, D. F. Farkas and D. Knorr (1989). "Application of high hydrostatic pressure on foods to inactivate pathogenic and spoilage organism for extension of shelf life." Food Technology **49**: 99.

Hopkins, A. D., B. H. Hite and T. F. Watson (1899). The effect of pressure in the preservation of milk, West Virginia Agricultural Experiment Station.

Huang, X., Y. Kakuda and W. Cui (2001). "Hydrocolloids in emulsions: particle size distribution and interfacial activity." Food Hydrocolloids **15**(4-6): 533-542.

Hui, Y. H. (2006). Handbook of Food Science, Technology, and Engineering, Taylor & Francis.

Iannace, S., N. Deluca, L. Nicolais, C. Carfagna and S. J. Huang (1990). "Physical characterization of incompatible blends of Polymethylmethacrylate and Polycaprolactone." Journal of Applied Polymer Science **41**(11-12): 2691-2704.

Irissin-Mangata, J., G. Bauduin, B. Boutevin and N. Gontard (2001). "New plasticizers for wheat gluten films." European Polymer Journal **37**(8): 1533-1541.

ISO, U.-E. (2012). Plastics - Determination of tensile properties - Part 2: Test conditions for moulding and extrusion plastics Switzerland, International Organization for Standardization. **527-2**.



## References

- Janssen, J. M. H. and H. E. H. Meijer (1995). "Dynamics of liquid-liquid mixing - A 2-zone model." Polymer Engineering and Science **35**(22): 1766-1780.
- Jayasundera, M., B. Adhikari, P. Aldred and A. Ghandi (2009). "Surface modification of spray dried food and emulsion powders with surface-active proteins: A review." Journal of Food Engineering **93**(3): 266-277.
- Jerez, A., P. Partal, I. Martinez, C. Gallegos and A. Guerrero (2007). "Protein-based bioplastics: effect of thermo-mechanical processing." Rheologica Acta **46**(5): 711-720.
- Jin, W.-G., H.-T. Wu, X.-S. Li, B.-W. Zhu, X.-P. Dong, Y. Li and Y.-H. Fu (2014). "Microstructure and inter-molecular forces involved in gelation-like protein hydrolysate from neutrase-treated male gonad of scallop (*Patinopecten yessoensis*)." Food Hydrocolloids **40**: 245-253.
- Kato, A. and S. Nakai (1980). "Hydrophobicity determined by a fluorescence probe method and its correlation with surface-properties of proteins." Biochimica Et Biophysica Acta **624**(1): 13-20.
- Kikuzaki, H., M. Hisamoto, K. Hirose, K. Akiyama and H. Taniguchi (2002). "Antioxidant properties of ferulic acid and its related compounds." Journal of Agricultural and Food Chemistry **50**(7): 2161-2168.
- Kim, Y. S., J. Yongsawatdigul, J. W. Park and S. Thawornchinsombut (2005). "Characteristics of sarcoplasmic proteins and their interaction with myofibrillar proteins." Journal of Food Biochemistry **29**(5): 517-532.
- Kirjavainen, J. and K. Westman (1999). "Natural history and development of the introduced signal crayfish, *Pacifastacus leniusculus*, in a small, isolated Finnish lake, from 1968 to 1993." Aquatic Living Resources **12**(6): 387-401.
- Kong, B. and Y. L. Xiong (2006). "Antioxidant activity of zein hydrolysates in a liposome system and the possible mode of action." Journal of Agricultural and Food Chemistry **54**(16): 6059-6068.

## References

Kontogiorgos, V., C. G. Biliaderis, V. Kiosseoglou and G. Doxastakis (2004). "Stability and rheology of egg-yolk-stabilized concentrated emulsions containing cereal beta-glucans of varying molecular size." Food Hydrocolloids **18**(6): 987-998.

Kristinova, V., R. Mozuraityte, I. Storro and T. Rustad (2009). "Antioxidant Activity of Phenolic Acids in Lipid Oxidation Catalyzed by Different Prooxidants." Journal of Agricultural and Food Chemistry **57**(21): 10377-10385.

Krochta, J. M. (2002). "Proteins as raw materials for films and coatings: Definitions, current status, and opportunities." Protein-Based Films and Coatings: 1-41.

Lagrain, B., B. Goderis, K. Brijs and J. A. Delcour (2010). "Molecular Basis of Processing Wheat Gluten toward Biobased Materials." Biomacromolecules **11**(3): 533-541.

Lanier, T. C., P. Carvajal and J. Yongsawatdigul (2004). Surimi Gelation Chemistry, Surimi and Surimi

Seafood, Boca Raton.

Lanier, T. C., P. Carvajal and J. Yongsawatdigul (2005). "Surimi gelation chemistry." Food Sci. Technol. (Boca Raton, FL, U. S.) **142**(Surimi and Surimi Seafood (2nd Edition)): 435-489.

Lehninger, A. L., D. L. Nelson and M. M. Cox (2005). Lehninger Principles of Biochemistry, W. H. Freeman.

Lemanska, K., H. Szymusiak, B. Tyrakowska, R. Zielinski, A. Soffers and I. Rietjens (2001). "The influence of pH on antioxidant properties and the mechanism of antioxidant action of hydroxyflavones." Free Radical Biology and Medicine **31**(7): 869-881.

Lindroth, P. and K. Mopper (1979). "High-performance liquid-chromatographic determination of subpicomole amounts of amino-acids by

## References

precolumn fluorescence derivatization with Ortho-Phthaldialdehyde." Analytical Chemistry **51**(11): 1667-1674.

Liu, Q., H. Bao, C. Xi and H. Miao (2014). "Rheological characterization of tuna myofibrillar protein in linear and nonlinear viscoelastic regions." Journal of Food Engineering **121**: 58-63.

Liu, R., S.-M. Zhao, B.-J. Xie and S.-B. Xiong (2011). "Contribution of protein conformation and intermolecular bonds to fish and pork gelation properties." Food Hydrocolloids **25**(5): 898-906.

Lucassenreynnders, E. H., J. Lucassen, P. R. Garrett, D. Giles and F. Hollway (1975). "Dynamic surface measurements as a tool to obtain equation-of-state data for soluble monolayers." Advances in Chemistry Series(144): 272-285.

Lyklema, J. (2000). Fundamentals of Interface and Colloid Science: Liquid-Fluid Interfaces, Elsevier Science.

Mao, R., J. Tang and B. G. Swanson (2001). "Water holding capacity and microstructure of gellan gels." Carbohydrate Polymers **46**(4): 365-371.

Markwell, M. A. K., S. M. Haas, L. L. Bieber and N. E. Tolbert (1978). "Modification of Lowry procedure to simplify protein determination in membrane and lipoprotein samples." Analytical Biochemistry **87**(1): 206-210.

Martin-Alfonso, J. E., M. Felix, A. Romero and A. Guerrero (2014). "Development of new albumen based biocomposites formulations by injection moulding using chitosan as physicochemical modifier additive." Composites Part B-Engineering **61**: 275-281.

McClements, D. J. (2004). Food Emulsions: Principles, Practice and Techniques. Florida, Boca Raton.

Mezger, T. G. (2006). The Rheology Handbook, Vincentz Network.

Mezger, T. G. (2014). The Rheology Handbook: For Users of Rotational and Oscillatory Rheometers, Vincentz Network.

Miki, W. (1991). "Biological functions and activities of animal carotenoids." Pure and Applied Chemistry **63**(1): 141-146.

## References

Miliauskas, G., P. R. Venskutonis and T. A. van Beek (2004). "Screening of radical scavenging activity of some medicinal and aromatic plant extracts." Food Chemistry **85**(2): 231-237.

Miller, R. and J. Spinelli (1982). "The effect of protease inhibitors on proteolysis in parasitized pacific whiting, *merluccius-productus*, muscle." Fishery Bulletin **80**(2): 281-286.

Mine, Y., E. Li-Chan, B. Jiang and Editors (2010). Bioactive Proteins And Peptides As Functional Foods And Nutraceuticals, Wiley-Blackwell.

Nandan, B., L. D. Kandpal and G. N. Mathur (2004). "Poly(ether ether ketone)/poly(aryl ether sulfone) blends: Melt rheological behavior." Journal of Polymer Science Part B-Polymer Physics **42**(8): 1548-1563.

Nenadis, N., O. Lazaridou and M. Z. Tsimidou (2007). "Use of reference compounds in antioxidant activity assessment." Journal of Agricultural and Food Chemistry **55**(14): 5452-5460.

Nenadis, N., L. F. Wang, M. Tsimidou and H. Y. Zhang (2004). "Estimation of scavenging activity of phenolic compounds using the ABTS(center dot+) assay." Journal of Agricultural and Food Chemistry **52**(15): 4669-4674.

Nieto-Nieto, T. V., Y. X. Wang, L. Ozimek and L. Chen (2014). "Effects of partial hydrolysis on structure and gelling properties of oat globular proteins." Food Research International **55**: 418-425.

Noskov, B. and A. Mikhailovskaya (2013). "Adsorption kinetics of globular proteins and protein/surfactant complexes at the liquid-gas interface." Soft Matter **9**(39): 9392-9402.

Ortiz, S. E. M., M. C. Puppo and J. R. Wagner (2004). "Relationship between structural changes and functional properties of soy protein isolates-carrageenan systems." Food Hydrocolloids **18**(6): 1045-1053.

Pal, R. (2000). "Shear Viscosity Behavior of Emulsions of Two Immiscible Liquids." Journal of Colloid and Interface Science **225**(2): 359-366.

## References

Pal, R. (2001). "Novel viscosity equations for emulsions of two immiscible liquids." Journal of Rheology **45**(2): 509-520.

Pallos, F. M., G. H. Robertson, A. E. Pavlath and W. J. Orts (2006). "Thermoformed wheat gluten biopolymers." Journal of Agricultural and Food Chemistry **54**(2): 349-352.

Pearson, A. M. (1983). Developments in Food Proteins, Vol. 2, Applied Science Publishers.

Pérez, O. E., C. C. Sánchez, A. M. R. Pilosof and J. M. Rodríguez Patino (2009). "Kinetics of adsorption of whey proteins and hydroxypropyl-methyl-cellulose mixtures at the air–water interface." Journal of Colloid and Interface Science **336**(2): 485-496.

Petursson, S., E. A. Decker and D. J. McClements (2004). "Stabilization of oil-in-water emulsions by cod protein extracts." Journal of Agricultural and Food Chemistry **52**(12): 3996-4001.

Phan-Thien, N. and R. I. Tanner (1999). Viscoelastic finite volume method. Rheology Series. D. D. K. D.A. Siginer and R. P. Chhabra, Elsevier. **Volume 8**: 331-359.

Plastics-Europe. (2008). "The Compelling Facts about Plastics. An Analysis of Plastics Production, Demand and Recovery for 2006 in Europe.", 2008, from [http://epro-plasticsrecycling.com/\\_verwaltung/members/downloads/Brochure\\_Facts.pdf](http://epro-plasticsrecycling.com/_verwaltung/members/downloads/Brochure_Facts.pdf).

Puppo, M. C. and M. C. Añon (1998). "Structural properties of heat-induced soy protein gels as affected by ionic strength and pH." Journal of Agricultural and Food Chemistry **46**(9): 3583-3589.

Queguiner, C., E. Dumay, C. Cavalier and J. C. Cheftel (1989). "Reduction of streptococcus-thermophilus in a whey-protein isolate by low moisture extrusion cooking without loss of functional-properties." International Journal of Food Science and Technology **24**(6): 601-612.

## References

Quintana, J. M., A. N. Califano, N. E. Zaritzky, P. Partal and J. M. Franco (2002). "Linear and nonlinear viscoelastic behavior of oil-in-water emulsions stabilized with polysaccharides." Journal of Texture Studies **33**(3): 215-236.

Rahman, M. and C. S. Brazel (2004). "The plasticizer market: an assessment of traditional plasticizers and research trends to meet new challenges." Progress in Polymer Science **29**(12): 1223-1248.

Ramirez-Suarez, J. C., K. Addo and Y. L. Xiong (2005). "Gelation of mixed myofibrillar/wheat gluten proteins treated with microbial transglutaminase." Food Research International **38**(10): 1143-1149.

Ramos, O. L., R. N. Pereira, R. Rodrigues, J. A. Teixeira, A. A. Vicente and F. Xavier Malcata (2014). "Physical effects upon whey protein aggregation for nano-coating production." Food Research International **66**(0): 344-355.

Redl, A., M. H. Morel, J. Bonicel, S. Guilbert and B. Vergnes (1999). "Rheological properties of gluten plasticized with glycerol: dependence on temperature, glycerol content and mixing conditions." Rheologica Acta **38**(4): 311-320.

Rocheffort, W. E. and S. Middleman (1987). "Rheology of xanthan gum - salt, temperature, and strain effects in oscillatory and steady shear experiments." Journal of Rheology **31**(4): 337-369.

Rodriguez Patino, J. M., M. R. Rodriguez Nino and C. C. Sanchez (1999). "Adsorption of whey protein isolate at the oil-water interface as a function of processing conditions: a rheokinetic study." Journal of agricultural and food chemistry **47**(6): 2241-2248.

Rodríguez Patino, J. M., M. R. Rodríguez Niño and C. Carrera Sánchez (2007). "Physico-chemical properties of surfactant and protein films." Current Opinion in Colloid & Interface Science **12**(4-5): 187-195.

Romero, A., V. Beaumal, E. David-Briand, F. Cordobes, M. Anton and A. Guerrero (2011). "Interfacial and emulsifying behaviour of crayfish protein isolate." Lwt-Food Science and Technology **44**(7): 1603-1610.

## References

Romero, A., V. Beaumal, E. David-Briand, F. Cordobes, A. Guerrero and M. Anton (2011). "Interfacial and Oil/Water Emulsions Characterization of Potato Protein Isolates." Journal of Agricultural and Food Chemistry **59**(17): 9466-9474.

Romero, A., V. Beaumal, E. David-Briand, F. Cordobes, A. Guerrero and M. Anton (2012). "Interfacial and emulsifying behaviour of rice protein concentrate." Food Hydrocolloids **29**(1): 1-8.

Romero, A., C. Bengoechea, F. Cordobés and A. Guerrero (2009). "Application of thermal treatments to enhance gel strength and stability of highly concentrated crayfish-based emulsions." Food Hydrocolloids **23**(8): 2346-2353.

Romero, A., F. Cordobes, A. Guerrero and M. C. Puppo (2011). "Crayfish protein isolated gels. A study of pH influence." Food Hydrocolloids **25**(6): 1490-1498.

Romero, A., F. Cordobés, M. C. Puppo, A. Guerrero and C. Bengoechea (2008). "Rheology and droplet size distribution of emulsions stabilized by crayfish flour." Food Hydrocolloids **22**(6): 1033-1043.

Romero, A., F. Cordobes, M. C. Puppo, A. Guerrero and C. Bengoechea (2008). "Rheology and droplet size distribution of emulsions stabilized by crayfish flour." Food Hydrocolloids **22**(6): 1033-1043.

Romero, A., F. Cordobes, M. C. Puppo, A. Villanueva, J. Pedroche and A. Guerrero (2009). "Linear viscoelasticity and microstructure of heat-induced crayfish protein isolate gels." Food Hydrocolloids **23**(3): 964-972.

Rosentrater, K. A. and A. W. Otieno (2006). "Considerations for manufacturing bio-based plastic products." Journal of Polymers and the Environment **14**(4): 335-346.

Ryan, J. T., R. P. Ross, D. Bolton, G. F. Fitzgerald and C. Stanton (2011). "Bioactive Peptides from Muscle Sources: Meat and Fish." Nutrients **3**(9): 765-791.

## References

Sagis, L. M. C. and P. Fischer (2014). "Nonlinear rheology of complex fluid–fluid interfaces." Current Opinion in Colloid & Interface Science **19**(6): 520-529.

Sagis, L. M. C., K. N. P. Humblet-Hua and S. van Kempen (2014). "Nonlinear stress deformation behavior of interfaces stabilized by food-based ingredients." Journal of Physics-Condensed Matter **26**(46): 9.

Sakanaka, S., Y. Tachibana, N. Ishihara and L. R. Juneja (2005). "Antioxidant properties of casein calcium peptides and their effects on lipid oxidation in beef homogenates." Journal of Agricultural and Food Chemistry **53**(2): 464-468.

Sanchez, M., M. Berjano, A. Guerrero and C. Gallegos (2001). "Emulsification rheokinetics of nonionic surfactant-stabilized oil-in-water emulsions." Langmuir **17**(18): 5410-5416.

Sano, T., T. Ohno, H. Otsukafuchino, J. J. Matsumoto and T. Tsuchiya (1994). "Carp natural actomyosin - thermal-denaturation mechanism." Journal of Food Science **59**(5): 1002-1008.

Sarmadi, B. H. and A. Ismail (2010). "Antioxidative peptides from food proteins: A review." Peptides (N. Y., NY, U. S.) **31**(10): 1949-1956.

Sarmadi, B. H. and A. Ismail (2010). "Antioxidative peptides from food proteins: A review." Peptides **31**(10): 1949-1956.

Schramm, G. (2000). A Practical Approach to Rheology and Rheometry. Germany, Gebroeder HAAKE.

Sharma, S. and I. Luzinov (2012). "Water Aided Fabrication of Whey and Albumin Plastics." Journal of Polymers and the Environment **20**(3): 681-689.

Singleton, V. L., R. Orthofer and R. M. Lamuela-Raventos (1999). "Analysis of total phenols and other oxidation substrates and antioxidants by means of Folin-Ciocalteu reagent." Oxidants and Antioxidants, Pt A **299**: 152-178.

Slizyte, R., R. Mozuraityte, O. Martinez-Alvarez, E. Falch, M. Fouchereau-Peron and T. Rustad (2009). "Functional, bioactive and antioxidative



## References

properties of hydrolysates obtained from cod (*Gadus morhua*) backbones." Process Biochemistry **44**(6): 668-677.

Sorgentini, D. A., J. R. Wagner, E. L. Arrese and M. C. Anon (1991). "Water Imbibing Capacity of Soy Protein Isolates: Influence of Protein denaturation." Journal of Agricultural and Food Chemistry **39**(8): 1386-1391.

Soroudi, A. and I. Jakubowicz (2013). "Recycling of bioplastics, their blends and biocomposites: A review." European Polymer Journal **49**(10): 2839-2858.

Spatafora, C., E. Barbagallo, V. Amico and C. Tringali (2013). "Grape stems from Sicilian *Vitis vinifera* cultivars as a source of polyphenol-enriched fractions with enhanced antioxidant activity." Lwt-Food Science and Technology **54**(2): 542-548.

Standard, A. (2001). Standard test Method for Water Absorption of Plastics. West Conshohocken, PA. **D570**.

Stratil, P., B. Klejdus and V. Kuban (2006). "Determination of total content of phenolic compounds and their antioxidant activity in vegetables - Evaluation of spectrophotometric methods." Journal of Agricultural and Food Chemistry **54**(3): 607-616.

Strink, C. E. (1978). Physical Aging in Amorphous Polymers and Other Materials, Elsevier.

Tadros, T. F. (2013). Emulsion Formation and Stability, Wiley.

Tang, C.-H. (2008). "Thermal denaturation and gelation of vicilin-rich protein isolates from three *Phaseolus* legumes: A comparative study." Lwt-Food Science and Technology **41**(8): 1380-1388.

Tasneem, M., F. Siddique, A. Ahmad and U. Farooq (2014). "Stabilizers: Indispensable Substances in Dairy Products of High Rheology." Critical Reviews in Food Science and Nutrition **54**(7): 869-879.

Taylor, W. (1957). "Formol titration - An evaluation of its various modifications." Analyst **82**(976): 488-498.

## References

Tcholakova, S., N. D. Denkov, I. B. Ivanov and B. Campbell (2006). "Coalescence stability of emulsions containing globular milk proteins." Advances in Colloid and Interface Science **123**: 259-293.

Tewari, G., D. S. Jayas and R. A. Holley (1999). "High pressure processing of foods: an overview." Sciences des Aliments(19): 619-661.

Thannhauser, T. W., Y. Konishi and H. A. Scheraga (1984). "Sensitive quantitative-analysis of disulfide bonds in polypeptides and proteins." Analytical Biochemistry **138**(1): 181-188.

Torgersen, H. and R. T. Toledo (1977). "Physical-properties of protein preparations related to their functional characteristics in comminuted meat systems." Journal of Food Science **42**(6): 1386-1391.

Toth, J. (2002). Adsorption, Taylor & Francis.

Ungar, T. (2004). "Micro structural parameters from X-ray diffraction peak broadening." Scripta Materialia **51**(8): 777-781.

Verbeek, C. J. R. and d. B. L. E. van (2010). "Extrusion Processing and Properties of Protein-Based Thermoplastics." Macromol. Mater. Eng. **295**(Copyright (C) 2013 American Chemical Society (ACS). All Rights Reserved.): 10-21.

Vertuccio, L., G. Gorrasi, A. Sorrentino and V. Vittoria (2009). "Nano clay reinforced PCL/starch blends obtained by high energy ball milling." Carbohydrate Polymers **75**(1): 172-179.

Verwijlen, T., L. Imperiali and J. Vermant (2014). "Separating viscoelastic and compressibility contributions in pressure-area isotherm measurements." Advances in Colloid and Interface Science **206**: 428-436.

Vieira, M. G. A., M. A. da Silva, L. O. dos Santos and M. M. Beppu (2011). "Natural-based plasticizers and biopolymer films: A review." European Polymer Journal **47**(3): 254-263.

## References

- Vilasoa-Martinez, M., J. Lopez-Hernandez and M. A. Lage-Yusty (2007). "Protein and amino acid contents in the crab, *Chionoecetes opilio*." Food Chemistry **103**(4): 1330-1336.
- Wagner, J. R. and M. C. Anon (1990). "Influence of denaturation, hydrophobicity and sulfhydryl content on solubility and water absorbing capacity of soy protein isolates." Journal of Food Science **55**(3): 765-770.
- Walker, R. B. and J. D. Everette (2009). "Comparative Reaction Rates of Various Antioxidants with ABTS Radical Cation." Journal of Agricultural and Food Chemistry **57**(4): 1156-1161.
- Walstra, P. (1993). "Principles of emulsion formation." Chemical Engineering Science **48**(2): 333-349.
- Ward, A. F. H. and L. Tordai (1946). "Time-dependence of boundary tensions of solutions. 1. The role of diffusion in time-effects." Journal of Chemical Physics **14**(7): 453-461.
- Weiss, M., M. Manneberg, J.-F. Juranville, H.-W. Lahm and M. Fountoulakis (1998). "Effect of the hydrolysis method on the determination of the amino acid composition of proteins." Journal of Chromatography A **795**(2): 263-275.
- Wijmans, C. M. and E. Dickinson (1998). "Simulation of interfacial shear and dilatational rheology of an adsorbed protein monolayer modeled as a network of spherical particles." Langmuir **14**(25): 7278-7286.
- Williams, P. A. and G. O. Phillips (2003). GUMS | Food Uses. Encyclopedia of Food Sciences and Nutrition (Second Edition). B. Caballero. Oxford, Academic Press: 3001-3007.
- Winter, H. H. (1987). "Can the gel point of a cross-linking polymer be detected by the  $G'$  -  $G''$  crossover?" Polymer Engineering and Science **27**(22): 1698-1702.
- Wojdylo, A., J. Oszmianski and R. Czemerzys (2007). "Antioxidant activity and phenolic compounds in 32 selected herbs." Food Chemistry **105**(3): 940-949.

## References

Wootton-Beard, P. C., A. Moran and L. Ryan (2011). "Stability of the total antioxidant capacity and total polyphenol content of 23 commercially available vegetable juices before and after in vitro digestion measured by FRAP, DPPH, ABTS and Folin-Ciocalteu methods." Food Research International **44**(1): 217-224.

Wu, C. S. (2003). "Physical properties and biodegradability of maleated-polycaprolactone/starch composite." Polymer Degradation and Stability **80**(1): 127-134.

Xiong, Y. L. (2004). 5 - Muscle proteins. Proteins in Food Processing. R. Y. Yada, Woodhead Publishing: 100-122.

Yoon, W. B., S. Gunasekaran and J. W. Park (2004). "Characterization of thermorheological behaviour of Alaska pollock and Pacific whiting surimi." Journal of Food Science **69**(7): E338-E343.

Zarate-Ramirez, L. S., I. Martinez, A. Romero, P. Partal and A. Guerrero (2011). "Wheat gluten-based materials plasticised with glycerol and water by thermoplastic mixing and thermomoulding." Journal of the Science of Food and Agriculture **91**(4): 625-633.

Zheng, X.-q., J.-t. Wang, X.-l. Liu, Y. Sun, Y.-j. Zheng, X.-j. Wang and Y. Liu (2015). "Effect of hydrolysis time on the physicochemical and functional properties of corn glutelin by Protamex hydrolysis." Food Chemistry **172**: 407-415.

## 8. Appendix





# Development of crayfish protein-PCL biocomposite material processed by injection moulding



M. Félix, A. Romero<sup>\*</sup>, J.E. Martín-Alfonso, A. Guerrero

Departamento de Ingeniería Química, Universidad de Sevilla, Facultad de Química, 41012, Sevilla, Spain

## ARTICLE INFO

### Article history:

Received 26 January 2015

Received in revised form

4 March 2015

Accepted 16 March 2015

Available online 21 March 2015

### Keywords:

A. Polymer-matrix composites (PMCs)

B. Rheological properties

B. Thermomechanical

E. Injection moulding

## ABSTRACT

A combination of crayfish flour (CF, with 60% protein) and Polycaprolactone (PCL) was successfully used to prepare biocomposites by a process that consists of two stages: mixing with glycerol (GL) as plasticizer and injection moulding of CF/GL/PCL blends. Mixing rheometry and Differential Scanning Calorimetry (DSC) measurements were found to be useful to select suitable injection moulding conditions. A remarkable enhancement in mechanical properties was found for PCL containing systems, even when crystalline structure remains unaltered. PCL yields a dominant contribution to the elastic response and confer a higher ability to absorb energy before rupture, but also the protein/plasticiser ratio must be considered.

© 2015 Elsevier Ltd. All rights reserved.

## 1. Introduction

The exceptional properties of plastics, that have even lead to replace other traditional materials such as metal and wood in many applications, have fostered a continuous demand growth, following a trend which has been increasing since 1950s [1]. However, petroleum production costs have also been increasing, subsequently leading to a continuous rise in oil products. For these reasons, the development of eco-friendly polymeric materials that could contribute to reduce petroleum dependence and is becoming more urgently required. In fact, the development of biodegradable materials with suitable properties has been a great research challenge to the scientific community of polymer materials during recent years [2]. Nowadays, society has been interested in the use of renewable biomass to manufacture high-quality, cost-competitive and biodegradable consumer goods as a means to reduce the consumption and dependence on petroleum, as well as, to diminish environmental pollution [3,4].

For many years, proteins, lipids and polysaccharides have been selected as a source of biopolymer materials [5–8]. Regarding proteins, most studies have used plant proteins such as zein, wheat gluten or soybean in order to manufacture bioplastic materials [9–11]. Moreover, animal proteins (milk proteins, collagen,

gelatine, egg albumen ...) have also been used to obtain bioplastics [12–15].

A further protein source consists of using those by-products, surpluses and wastes that are produced in large quantities every year by the food industry. This alternative also involves important environmental benefits derived from waste reduction. An excellent example of this source is featured by the freshwater red-swamp crayfish (*Procambarus Clarkii*), which has undergone a fast growth due to the initial lack of predators, abundant food and favourable environmental conditions [16]. Previous results have demonstrated the ability of proteins from low value-added crayfish by-products in the stabilization of emulsions [17] and the formation of thermal-induced gel products [18].

Protein coming from crayfish (CF) may be used to develop bioplastic materials with significant advantages since they are derived from a sustainable bioresource, exhibit fast biodegradability and can be processed in much the same way as conventional synthetic polymers [19]. Traditionally, protein films are processed by casting method [20], however classical polymer processing techniques (compression moulding or extrusion) are being increasingly used in this field [21,22]. Among them, injection moulding is a fairly attractive operation that deserves particular attention. Typically in this process, proteins are mixed with a plasticiser in order to reduce intermolecular forces among polymer chains, increasing mobility and reducing the glass transition [7]. Thereafter, polymeric blends are subjected to suitable thermal conditions, being injected at high pressure into the mould cavity [12].

<sup>\*</sup> Corresponding author. Tel.: +34 955420984; fax: +34 954556447.  
E-mail address: [alromero@us.es](mailto:alromero@us.es) (A. Romero).

The optimization of processing conditions is essential in order to achieve the desirable properties of the final product. This fact is particularly relevant in protein-based materials that require a proper thermoplastic mixing with a suitable plasticiser, and may even come to show a predominant thermoset character upon injection moulding.

There is not much information on the use of blends containing polycaprolactone (PCL) and protein blends in order to produce biocomposite materials. PCL is classified as a polyester from fossil source, which has been widely used as the polymer matrix in the development of new materials. It is highly flexible, biodegradable, biocompatible and easy to process [23,24]. PCL can be blended with a variety of other polymers to improve their properties [25]. In fact, blending a natural polymer with polyester is an interesting way to reduce costs and to improve the biodegradability of the resulting polymer blends [26].

The overall objective of this work is to develop CF/PCL biocomposite plastic materials plasticised with glycerol (GL) by means of two-stage processing that consists of mixing and injection moulding, using different CF/GL/PCL ratios. Rheological and differential scanning calorimetry (DSC) measurements of CF/GL/PCL blends have been carried out in order to select suitable processing parameters (temperature and residence time in the pre-injection mixing chamber as well as the temperature of the mould). Properties of moulded specimens have been eventually assessed by dynamic mechanical analysis, X-Ray diffraction and tensile strength measurements.

## 2. Material and methods

### 2.1. Materials

Crayfish flour (CF) was obtained from ALFOCAN S.A. (Isla Mayor, Seville, Spain). The protein content was determined in quadruplicate as % N  $\times$  6.25 using a LECO CHNS-932 nitrogen micro analyser (Leco Corporation, St. Joseph, MI, USA) [27] being 65 wt.%. Glycerol (GL) was purchased from Panreac Química, S.A. (Spain) and PCL (Capa™ FB100) was supplied by Perstorp (Sweden).

### 2.2. Preparation of samples

Different CF/GL/PCL systems have been selected for this study using different CF/GL ratios (1.3, 2.0, 2.3 and 2.6) and different PCL content (0, 10 and 30%). The PCL-free system (denoted by 70/30/0) has been used as the reference.

CF/GL/PCL blends were manufactured by a thermomechanical procedure which includes two stages, previously mixing CF and PCL by hand: Initially, these blends were mixed in a two-blade counter-rotating batch mixer Haake PolyLab QC (ThermoHaake, Germany) at 25 °C and 50 rpm for 60 min, monitoring the torque and temperature during mixing. Secondly, the biocomposite blends obtained after the mixing process were subsequently processed by injection moulding using a Minijet Piston Injection Moulding System II (ThermoHaake, Germany) to obtain biocomposites specimens. Three stages are considered over this process: the pre-injection

stage, the injection itself and the after-injection packing stage. Table 1 shows the processing parameters (temperature, pressure and time) values for the injection moulding process used in this study, which is similar to those used in previous papers [28,29]. The values for the processing parameters at the pre-injection cylinder are selected to ensure a blend viscosity low enough to facilitate its injection into the mould. The residence time selected for the packing stage (right after injection) has been 220 s since no further enhancement has been noticed by increasing this period. In addition, exposition to high temperatures for a long time typically leads to protein degradation (i.e. via Maillard-type reactions) [30].

Two types of moulds were used to prepare CF/GL/PCL specimens: a 60  $\times$  10  $\times$  1 mm rectangular shape mould for DMTA experiments and a Dumpbell type specimen defined by ISO 527-2 [31] for Tensile Properties of Plastics.

### 2.3. Characterization of blends

#### 2.3.1. Differential scanning calorimetry (DSC)

DSC experiments were performed with a Q20 (TA Instruments, USA), using 5–10 mg samples, in hermetic aluminium pans. A heating rate of 10 °C/min was selected. The sample was purged with a nitrogen flow of 50 mL/min.

### 2.4. Characterization of biocomposites

#### 2.4.1. Dynamic mechanical temperature analysis (DMTA)

DMTA tests were carried out with a RSA3 (TA Instruments, New Castle, DE, USA), on rectangular specimens using dual cantilever bending. All the experiments were carried out at constant frequency (1 Hz) and strain (between 0.01 and 0.30%, within the linear viscoelastic region). The selected heating rate was 3 °C min<sup>-1</sup>. All the samples were coated with Dow Corning high vacuum grease to avoid water loss.

#### 2.4.2. X-ray diffraction (XRD)

XRD studies of the specimens were carried out using a D8 Discover (BRUKER, Massachusetts, USA) (45 kV, 100 mA) equipped with Cu K $\alpha$  radiation ( $\lambda$  = 0.1516 nm) in order to visualise different crystalline phases that may indicate systems whose microstructure could be different.

#### 2.4.3. Tensile strength measurements

Tensile tests were performed by using the Insight 10 kN Electromechanical Testing System (MTS, Eden Prairie, MN, USA), according to by ISO 527-2 [31] for Tensile Properties of Plastics. Tensile strength parameters were evaluated from at least three duplicates for each product using type IV probes and an extensional rate of 1 mm/min at room temperature.

### 2.5. Statistical analysis

Statistical analysis was performed using t-test and one-way analysis of variance (ANOVA,  $p < 0.05$ ) by means of the statistical package SPSS 18. Standard deviations from some selected parameters were calculated.

## 3. Results and discussion

### 3.1. Preparation of blends by thermoplastic mixing

Fig. 1 exhibits torque and temperature profiles as a function of mixing time for different CF/GL/PCL blends. Fig. 1A, shows two profiles for blends maintaining the same CF/GL ratio at ca. 2.3, using different PCL content, where the blend without PCL is used as the

**Table 1**

Standard values used as injection moulding parameters for the pre-injection cylinder, injection stage and packing stage.

	T (°C)	Pressure (MPa)	Time (s)
Pre-injection cylinder	60	0.1	100
Injection	60	0.1–50	<1
Packing stage	100	50	20
	100	20	200



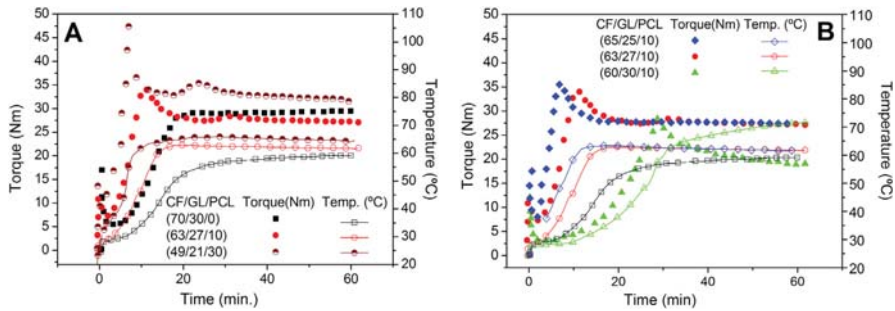


**Fig. 1.** Evolution of torque and temperature over the mixing process for crayfish flour/glycerol/polycaprolactone (CF/GL/PCL) systems: (A) at constant CF/GL ratio: 70/30/0, 63/27/10 and 49/21/30; (B) at constant PCL concentration: 65/25/10, 63/27/10 and 60/30/10.

reference system. On the other hand, those blends containing 10% PCL at different CF/GL ratios are plotted in Fig. 1B.

These results put forward the relevant dependence of torque and temperature on the CF/GL/PCL ratio. Thus, a rapid increase in torque up to a maximum value takes place, followed by an asymptotic decrease towards a plateau value. Temperature profiles generally follow an increase towards a plateau value. The time required to reach the plateau values for both variables (torque and temperature), which is roughly the same, is clearly dependent on the CF/GL/PCL ratio. This coincidence may be seen as a consequence of the development of exothermic crosslinking reactions during the mixing processes that involve both an increase in temperature and consistency (reflected in torque). Both profiles show also an initial induction period, being more evident for those blends displaying the slowest evolution. It is worth mentioning that a torque peak appears when unmelted PCL is present in the blend. Thus, the PCL melt point, which is reached at about 55 °C, is coincident with the maximum torque value. In other words, the torque does not start to decrease until the PCL melting point is exceeded.

As may be observed in Fig. 1A, an increase in PCL content leads to a faster torque and temperature kinetics and, as a consequence, to an anticipation of both profiles. The effect also gives rise to a general increase in torque and temperature values at any time. Similar behaviour can be observed by increasing the CF/GL ratio (Fig. 1B).

### 3.2. Thermal characterization of blends

Heat flow patterns obtained from Differential Scanning Calorimetry (DSC) measurements are shown in Fig. 2. Fig. 2A shows the thermogram for CF flour and for the reference system (CF/GL/PCL, 70/30/0), as well as the profiles corresponding to CF/GL/PCL blends at constant CF/GL ratio, as a function of PCL content. On the other hand, Fig. 2B displays the DSC results for CF/GL/PCL blends containing 10% PCL as a function of the CF/GL ratio.

CF flour displays a typical endotherm of a fairly denatured protein system. This profile exhibits an endothermic first peak at 68 °C, a glass transition ( $T_g$ ) at ca. 92 °C, as well as a broad endothermic event between the  $T_g$  and 130 °C. The first thermal event can be attributed to the physical ageing effect, which was previously reported for this CF flour [32]. Physical ageing is a general phenomenon that occurs over time in glassy or partial glassy polymers below their  $T_g$  and is a manifestation of the non-equilibrium nature of the glassy state [33,34]. The glass transition at around 90 °C is consistent with previous results reported by Farahnaky et al. [32] for crayfish flour and Hashimoto et al. [35] for fish muscle proteins. On the other hand, the broad endothermic event may be related to the huge variety of protein fractions of different molecular weight that constitute the CF flour as reported in a previous paper [18].

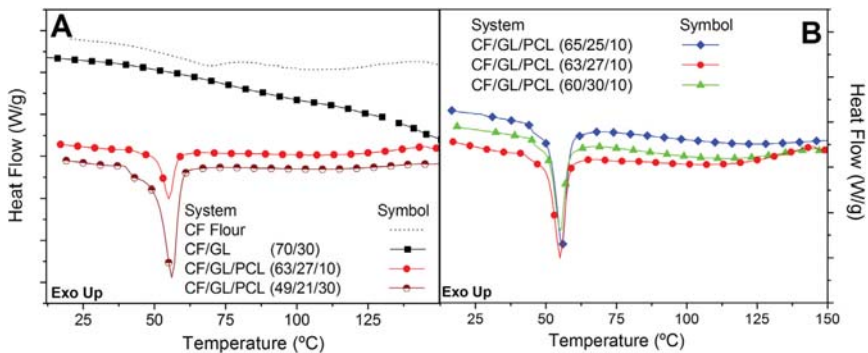


**Fig. 2.** DSC profiles for crayfish flour and CF/GL/PCL blends: (A) at constant CF/GL ratio: 70/30/0, 63/27/10 and 49/21/30; (B) at constant PCL concentration: 65/25/10, 63/27/10 and 60/30/10.

With regard to the endotherms obtained for the reference system the two endothermic events vanish. The total disappearance of the first endothermic peak, most probably as a consequence of mixing, confirms its physical ageing-driven nature. However, the glass transition remains roughly at the same temperature for all the blends studied.

In addition, it is worth mentioning that all the systems containing PCL display an apparent endothermic peak at ca. 55 °C, which is attributed to the PCL melting point. This peak becomes more pronounced with increasing PCL content, as may be observed in Fig. 2.

The results obtained from DSC measurements also confirm the suitability of the temperature selected for the cylinder and mould, since the former (60 °C) is higher than the endothermic peak corresponding to the PCL melting whereas the later temperature (100 °C) is higher than the glass transition in order to favour mobility and temperature-induced protein crosslinking (in combination with pressure).

### 3.3. Mechanical characterization of biocomposites

#### 3.3.1. Dynamic mechanical temperature analysis

Fig. 3 shows the values of the elastic modulus,  $E'$  (Fig. 3A), and the loss tangent,  $\tan \delta$  (Fig. 3B), as a function of temperature (from -30 °C to 140 °C) obtained from DMA measurements. The reference system is compared with those specimens with the same protein/plasticiser ratio (CF/GL/PCL: 63/27/10 and 49/21/30).

As may be observed in Fig. 3A, all the specimens studied show a similar profile for  $E'$  at low and medium temperature. In this way, an increase in temperature leads to a decrease in elastic modulus ( $E'$ ) that tends to reach a plateau value. It is remarkable, however, that PCL containing samples exhibit higher elastic modulus provided that temperature remains below the PCL melting point. At the melting point the three samples show rather coincident values that undergo a decrease with increasing temperature. In fact, there is a region where the PCL-free specimen shows slightly higher  $E'$  values. Eventually a temperature is reached above which the decrease in  $E'$  found for the reference specimen becomes faster whereas the PCL-containing composites tend to reach a plateau region.

In addition, it is interesting to remark that the reference system shows a minimum in  $E'$  close to 100 °C, followed by an apparent enhancement of elastic properties increase, which is characteristic of a thermosetting potential [36–38]. In other words, an increase in the temperature of the packing stage would lead to a reinforcement of the biopolymer matrix. In contrast, the addition of PCL leads to a

reduction in this potential than tends to disappear at the highest PCL content, where elastic properties remain rather independent on temperature. These results suggest that the melting of PCL results in a certain reduction in the free volume leading to an increase in physical interactions. In any case, the response in the high temperature region seems to be dominated by the presence of melted PCL.

Furthermore, all probes studied display similar loss tangent profiles (Fig. 3B) showing one single peak, which is related to a glass-like transition of the plasticized protein-based material. These unimodal profiles indicate a good compatibility between compounds, obtained for all systems after the injection moulding process. However, the increase in PCL content gives rise to a plasticising effect leading to a decrease in the peak temperature (from ca. 100 to 50 °C).

Fig. 4 shows the values of some parameters selected in order to compare the behaviour of different biocomposite materials. The first one (shown in Fig. 4A) corresponds to the value of the storage modulus at 1 Hz and 20 °C ( $E'_{1,20}$ ) and the second is the value of the loss tangent at the peak temperature ( $\tan \delta_{\max}$ ), whose values ( $T_{\text{peak}}$ ) are also included in the plot (Fig. 4B). These results confirm the effect of PCL-induced increase in elasticity that takes place also at a higher CF/GL ratio. Moreover, at constant PCL content, an increase in CF/GL ratio also produces an increase in  $E'$  values. This effect is particularly noticeable at the highest PCL concentration, which suggests occurrence of a synergistic effect between CF and PCL. Similar results were reported by Aithani and Mohanty [39], which found an increase in storage modulus for bioplastics containing PCL and corn gluten meal as the proportion of PCL increase.

Fig. 4B shows how an increase in PCL content leads to a remarkable decrease in  $\tan \delta_{\max}$  and  $T_{\text{peak}}$  at the two CF/GL ratios studied, thus confirming the above mentioned plasticising effect of PCL. The increase in the CF/GL ratio gives rise to a different effect depending on the PCL concentration. At wt. 10% PCL a reduction for  $\tan \delta_{\max}$  and  $T_{\text{peak}}$  may also be observed, being much more noticeable for the former. On the other hand, for 30 wt. % PCL only slight changes in values take place. Thus,  $\tan \delta_{\max}$  undergoes a slight reduction followed by a moderate increase in value with increasing CF/GL ratio, while  $T_{\text{peak}}$  shows only a significant, but moderate, increase at the highest CF/GL ratio. This increase is probably what causes the final increase in  $\tan \delta_{\max}$ .

#### 3.3.2. X-ray diffraction (XRD)

Fig. 5 shows the X-ray diffraction spectra of several samples. As may be observed, the diffractogram of the reference system and systems containing 10 wt. % PCL have been plotted in Fig. 5A, while

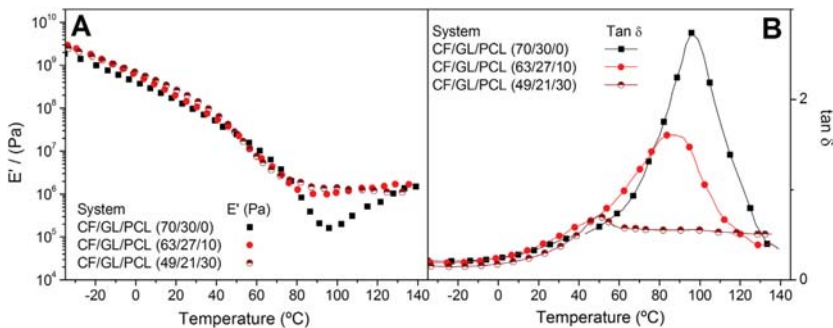


Fig. 3. DMA temperature ramp measurements performed at constant frequency (1 Hz) and heating rate (3 °C min<sup>-1</sup>) for CF/GL/PCL injection moulded specimens at constant CF/GL ratio: 70/30/0, 63/27/10, 49/21/30: (A) Storage modulus ( $E'$ ); and (B) loss tangent ( $\tan \delta$ ).

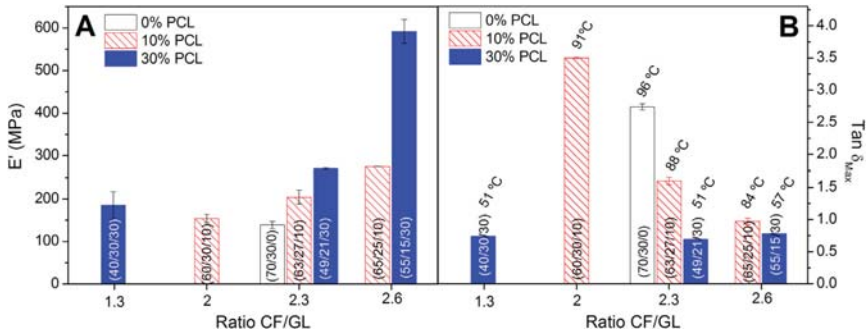


Fig. 4. Linear viscoelastic functions from DMA measurements for all CF/GL/PCL studied systems: 70/30/0, 65/25/10, 63/27/10, 60/30/10, 55/15/30, 49/21/30 and 40/30/30: (A) Storage modulus ( $E'$ ); (B) loss tangent ( $\tan \delta$ ).

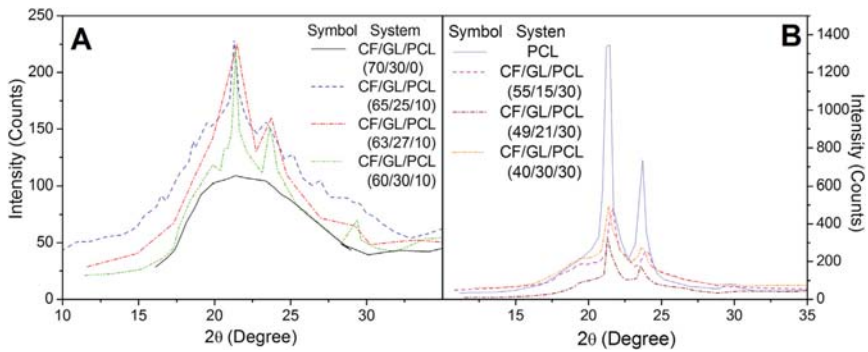


Fig. 5. X-Ray Diffraction measurements (XRD) for CF/GL/PCL specimens: (A) containing 10 wt.% PCL: 65/25/10, 63/27/10 and 60/30/10, as well as the reference specimen 70/30/0; (B) containing 30 wt.% PCL: 55/15/30, 49/21/30 and 40/30/30, as well as PCL powder.

PCL pure and systems containing 30 wt. % PCL have been represented in Fig. 5B. This figure reveals the characteristic pattern of PCL in its crystalline structure with the well-developed peaks at  $2\theta = 21.5^\circ$  and  $23.7^\circ$  in accordance with Vertuccio et al., 2009 that also reported a shoulder peak at about  $22.0^\circ$  [40]. A further peak may be also observed at  $29.7^\circ$ , showing much lower intensity.

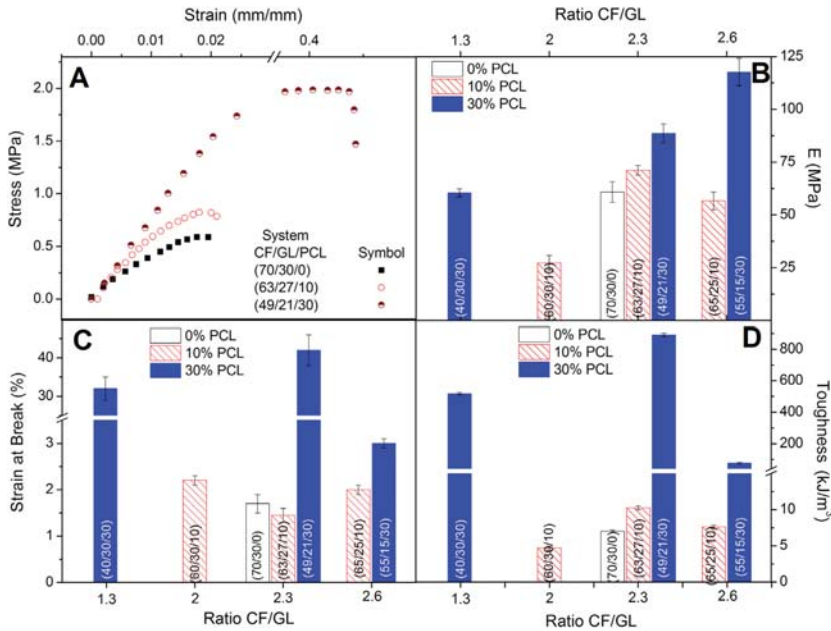
As for the reference PCL-free specimen shown in Fig. 5A, the diffraction spectrum displays a broad peak that unfortunately is located at the same position of the two main peaks of PCL. This figure also shows how the incorporation of PCL up to 10 wt. % does not lead to any modification in the location ( $2\theta$  value) of the PCL peaks, but a progressive broadening effect takes place for both peaks as the protein content increases. According to Ungar [41], X-ray diffraction peaks broaden when the crystal lattice becomes imperfect. Peaks broaden either when crystallites become smaller than about a micrometer or if lattice defects are present in large enough amount and there are two important causes: size and strain broadening. Therefore, in accordance with this statement, the results obtained for composites containing 10 wt. % PCL suggest that CF protein either inhibits the development of the PCL crystalline phase or favours the presence of lattice defects.

Fig. 5B shows how the diffraction spectra of the composites containing 30 wt. % PCL neither yield any particular modification in the location ( $2\theta$  value) of the PCL peaks. This fact means that the interplanar distance ( $d_{hkl}$ ) also remains unaltered, and as a consequence, the lattice structure does not suffer any change, regardless of the protein content of the composite specimen. These results

suggest that amorphous sections are responsible for the protein-polymer system compatibility. Conversely, it can be observed that an increase in the total amount of synthetic polymer leads to remain unaltered crystalline sections. It is also worth pointing out that the crystalline phase of the PCL is well developed for composites containing 30 wt. % PCL, which suggests that the selected processing conditions do not affect to the PCL crystalline morphology. In addition, these layers do not exhibit any broadening effect (neither size nor strain), thus indicating that the development of PCL crystalline phase is preserved after processing, which may well be related to the improvement of mechanical properties of these composites containing high percentage of PCL.

### 3.3.3. Uniaxial tensile strength measurements

The results obtained from uniaxial strength measurements are shown in Fig. 6. Stress-strain curves for the reference specimen CF/GL (70/30), and for composite samples containing the same ratio protein plasticiser (CF/GL/PCL: 63/27/10 and 49/21/30) are shown in Fig. 6A. All curves exhibit an initial linear elastic behaviour of high constant stress-strain slope yielding high values for the Young's Modulus ( $E$ ), followed by a plastic deformation stage with a continuous decrease in the stress-strain slope after the elastic limit. Eventually, all curves reach a maximum value for the stress ( $\sigma_{max}$ ) and the strain at break ( $\epsilon_{max}$ ). Toughness ( $T$ ), which expresses the ability to absorb mechanical energy up to the point of failure, has been calculated from the area under the stress-strain curve by the following equation:



**Fig. 6.** Results from uniaxial Tensile Strength measurements for the specimens studied 70/30/0, 65/25/10, 63/27/10, 60/30/10, 55/15/30, 49/21/30 and 40/30/30: (A) Tensile stress-strain curves (only for specimens at constant CF/GL ratio: 70/30/0, 63/27/10 and 49/21/30); (B) Young's modulus (E); (C) strain at break ( $\epsilon_{\text{max}}$ ); (D) Toughness (T).

$$T = \int_0^{\epsilon_{\text{max}}} \sigma(\epsilon) \cdot d\epsilon \quad (1)$$

Regarding the tensile properties obtained from tensile tests applied to CF/GL, and CF/GL/PCL bio-composites, Fig. 6B–D show the values of the Young's Modulus, strain at break and toughness, respectively. As may be observed, higher values in E and especially in  $\epsilon_{\text{max}}$  and toughness are obtained by increasing PCL from 0 to 30%.

Moreover, an increase in the CF/GL ratio yields a different behaviour depending on PCL content. Those specimens containing 10 wt.% PCL display a maximum value in E as well as a minimum value in  $\epsilon_{\text{max}}$ . As a result, a moderate increase in toughness takes place. It should be also taken into account that an increase in the CF/GL ratio also involves a decrease in the PCL/CF ratio. These results suggest that both ratios exert opposite effects, where the dominant effect seems to be the former at low CF content and the latter at high CF content. This balance can explain the occurrence of the maximum in E and minimum in  $\epsilon_{\text{max}}$ .

On the other hand, an increase in PCL content up to 30 wt.% may lead to high values in E that exhibit a continuous increase with CF/GL ratio, but lead to particularly high values in  $\epsilon_{\text{max}}$  that become less important for the highest CF/GL ratio studied. The latter effect is so important in this case that toughness follows the same evolution. The final decrease in  $\epsilon_{\text{max}}$  observed in Fig. 6C and D is probably because the specimen becomes brittle as a consequence of the high amount of polymer (CF + PCL).

It is also worth mentioning that a comparison of the elastic bending modulus ( $E'$ ) and the Young's modulus (E) in Figs. 4A and 6B, respectively, put forward the similar behaviour of both parameters. In fact, both parameters reflect the contribution of CF protein and PCL to the elastic response at small strain under bending or uniaxial tension deformations. All these results reveal

that both polymers play a significant role on the elastic properties. In order to assess the contribution of each polymer (CF and PCL) a comparison between two systems containing the same polymer/GL ratio (40/30/30 and 60/30/10) may be carried out. It is apparent that the PCL yields higher contribution to the elastic response, particularly under uniaxial tensile tests. This dominant contribution of PCL can be extrapolated to the plastic deformation region since the 40/30/30 specimen shows much higher value in  $\epsilon_{\text{max}}$ . The toughness also put forward this effect.

#### 4. Concluding remarks

From the experimental results, it may be concluded that mixing process of protein-based flour, plasticiser and synthetic polymer can be controlled by monitoring the torque and temperature profiles in order to select the most suitable mixing time. The combination of techniques such as mixing rheology and DSC are very useful for selecting suitable injection moulding parameters for processing blends. In this way, it could be claimed that a bioplastic exhibiting desirable properties can be made by means of injection moulding, using a suitable formulation (crayfish flour, glycerol and PCL) and selecting proper thermomechanical processing conditions (injection pressure, temperature and residence time in the pre-injection chamber and temperature in the mould).

From the mechanical characterisation of the CF/GL/PCL bio-composites, it can be pointed out the remarkable enhancement in mechanical properties obtained for PCL containing systems even when crystalline structure remains unaltered. Furthermore, as regards the bio-composite formulation, not only the contribution of PCL is important but also the protein/plasticiser ratio plays a role. Thus, both polymers play a significant role on the elastic properties, however, the PCL yields a dominant contribution to the elastic response, particularly under uniaxial tensile tests and confer a higher ability to absorb energy before rupture.

The present work demonstrates the feasibility of designing renewable and biodegradable composites, which may be regarded as an alternative to conventional plastic materials, containing an important amount of CF, thereby finding value-added applications of these by-products of the crayfish industry.

### Acknowledgements

This work is part of a research project sponsored by Andalusian Government, (Spain) (project TEP-6134) and by “Ministerio de Economía y Competitividad” from Spanish Government (Ref. MAT2011-29275-C02-02/01). The authors gratefully acknowledge their financial support. The authors also acknowledge to the Microanalysis Service, X-Ray and Functional Characterisation Service (CITIUS-Universidad de Sevilla) for providing full access and assistance to the LECO–CHNS–932, D8 Discover (Bruker) equipment and DSC Q20 Calorimetry (TA instruments), respectively.

### References

- [1] Plastics\_Europe. The Compelling facts about plastics. An analysis of plastics production, demand and Recovery for 2006 in Europe. EUPC (the European Plastics Converters), EPRO (European Association of Plastics Recycling and Recovery Organisations), & EuPr (the European Plastics Recycles); 2008.
- [2] Ray SS, Bousmina M. Biodegradable polymers and their layered silicate nano composites: In greening the 21st century materials world. *Prog Mater Sci* 2005;50(8):962–1079.
- [3] Rosentrater KA, Otieno AW. Considerations for manufacturing bio-based plastic products. *J Polym Environ* 2006;14(4):335–46.
- [4] Tummala P, Liu WJ, Drzal LT, Mohanty AK, Misra M. Influence of plasticizers on thermal and mechanical properties and morphology of soy-based bioplastics. *Industrial Eng Chem Res* 2006;45(22):7491–6.
- [5] Averous L. Biodegradable multiphase systems based on plasticized starch: a review. *J Macromol Science Polymer Rev* 2004;C44(3):231–74.
- [6] De Graaf LA. Denaturation of proteins from a non-food perspective. *J Biotechnol* 2000;79(3):299–306.
- [7] Irissin–Mangata J, Bauduin G, Boutevin B, Gontard N. New plasticizers for wheat gluten films. *Eur Polym J* 2001;37(8):1533–41.
- [8] Koch K, Gillgren T, Stading M, Andersson R. Mechanical and structural properties of solution-cast high-amylose maize starch films. *Int J Biol Macromol* 2010;46(1):13–9.
- [9] Cui B, Gontard N, Guilbert S. Proteins as agricultural polymers for packaging production. *Cereal Chem* 1998;75(1):1–9.
- [10] Jerez A, Partal P, Martínez I, Gallegos C, Guerrero A. Rheology and processing of gluten based bioplastics. *Biochem Eng J* 2005;26(2–3):131–8.
- [11] Zheng H, Tan ZA, Zhan YR, Huang J. Morphology and properties of soy protein plastics modified with chitin. *J Appl Polym Sci* 2003;90(13):3676–82.
- [12] Fernandez-Espada L, Bengoechea C, Cordobes F, Guerrero A. Linear viscoelasticity characterization of egg albumen/glycerol blends with applications in material moulding processes. *Food Bioprod Process* 2013;91(C4):319–26.
- [13] Arshad MU, Jamil N, Naheed N, Hasnain S. Analysis of bacterial strains from contaminated and non-contaminated sites for the production of biopolymers. *Afr J Biotechnol* 2007;6(9):1115–21.
- [14] Maiborodin IV, Beregovoi EA, Shevela AI, Kuznetsova IV, Barannik MI, Manaev AA, et al. Morphological tissue changes after the implantation of a biodegradable material on collagen basis. *Morfol St Petersburg Russ* 2013;144(6):63–8.
- [15] Gómez-Martínez D, Partal P, Martínez I, Gallegos C. Gluten-based bioplastics with modified controlled-release and hydrophilic properties. *Industrial Crops Prod* 2013;43(0):704–10.
- [16] Geiger W, Alcorlo P, Baltanas A, Montes C. Impact of an introduced Crustacean on the trophic webs of Mediterranean wetlands. *Biol Invasions* 2005;7(1):49–73.
- [17] Romero A, Cordobes F, Puppo MC, Guerrero A, Bengoechea C. Rheology and droplet size distribution of emulsions stabilized by crayfish flour. *Food Hydrocoll* 2008;22(6):1033–43.
- [18] Romero A, Cordobes F, Guerrero A, Puppo MC. Crayfish protein isolated gels. A study of pH influence. *Food Hydrocoll* 2011;25(6):1490–8.
- [19] Sharma S, Luzinov I. Water aided fabrication of whey and albumin plastics. *J Polym Environ* 2012;20(3):681–9.
- [20] Genadios A. Proteins based films and coating. New York: CRC Press; 2002.
- [21] Jerez A, Partal P, Martínez I, Gallegos C, Guerrero A. Egg white-based bioplastics developed by thermomechanical processing. *J Food Eng* 2007;82(4):608–17.
- [22] Gonzalez-Gutierrez J, Partal P, Garcia-Morales M, Gallegos C. Effect of processing on the viscoelastic, tensile and optical properties of albumen/starch-based bioplastics. *Carbohydr Polym* 2011;84(1):308–15.
- [23] Filipczak K, Wozniak M, Ulanski P, Olah L, Przybytniak G, Olkowski RM, et al. Poly (epsilon-caprolactone) biomaterial sterilized by E-beam irradiation. *Macromol Biosci* 2006;6(4):261–73.
- [24] Wu CS. Physical properties and biodegradability of maleated-polycaprolactone/starch composite. *Polym Degrad Stab* 2003;80(1):127–34.
- [25] Iannace S, Deluca N, Nicolais L, Carfagna C, Huang SJ. Physical characterization of incompatible blends of polymethylmethacrylate and Polycaprolactone. *J Appl Polym Sci* 1990;41(11–12):2691–704.
- [26] Corradini E, Mattoso LHC, Guedes CGF, Rosa DS. Mechanical, thermal and morphological properties of poly(epsilon-caprolactone)/zein blends. *Polym Adv Technol* 2004;15(6):340–5.
- [27] Etheridge RD, Pesti GM, Foster EH. A comparison of nitrogen values obtained utilizing the Kjeldahl nitrogen and Dumas combustion methodologies (Leco CNS 2000) on samples typical of an animal nutrition analytical laboratory. *Animal Feed Sci Technol* 1998;73(1–2):21–8.
- [28] Felix M, Martin-Alfonso JE, Romero A, Guerrero A. Development of albumen/soy biobased plastic materials processed by injection molding. *J Food Eng* 2014;125:7–16.
- [29] Martin-Alfonso JE, Felix M, Romero A, Guerrero A. Development of new albumen based biocomposites formulations by injection moulding using chitosan as physicochemical modifier additive. *Compos Part B-Engineering* 2014;61:275–81.
- [30] Fayle SE, Gerrard JA. Chemistry RSo. The maillard reaction. Royal Society of Chemistry; 2002.
- [31] ISO U-E. Plastics - determination of tensile properties - part 2: test conditions for moulding and extrusion plastics Switzerland. International Organization for Standardization; 2012.
- [32] Farahnaky A, Guerrero A, Hill SE, Mitchell JR. Physical ageing of crayfish flour at low moisture contents. *J Therm Analysis Calorim* 2008;93(2):595–8.
- [33] Strink CE. Physical aging in amorphous polymers and other materials. Elsevier; 1978.
- [34] Anon. Thermal characterization of polymeric materials edited by Edith a. Turi *Polym Test* 1997;16(5):523.
- [35] Hashimoto T, Suzuki T, Hagiwara T, Takai R. Study on the glass transition for several processed fish muscles and its protein fractions using differential scanning calorimetry. *Fish Sci* 2004;70(6):1144–52.
- [36] Zarate-Ramirez LS, Martínez I, Romero A, Partal P, Guerrero A. Wheat gluten-based materials plasticized with glycerol and water by thermoplastic mixing and thermomoulding. *J Sci Food Agric* 2011;91(4):625–33.
- [37] Jerez A, Partal P, Martínez I, Gallegos C, Guerrero A. Protein-based bioplastics: effect of thermo-mechanical processing. *Rheol Acta* 2007;46(5):711–20.
- [38] Romero A, Beaumal V, David-Briand E, Cordobes F, Anton M, Guerrero A. Interfacial and emulsifying behaviour of crayfish protein isolate. *Lwt-Food Sci Technol* 2011;44(7):1603–10.
- [39] Aithani D, Mohanty AK. Value-added new materials from byproduct of corn based ethanol industries: blends of plasticized corn gluten meal and poly(epsilon-caprolactone). *Industrial Eng Chem Res* 2006;45(18):6147–52.
- [40] Vertuccio L, Gorraasi G, Sorrentino A, Vittoria V. Nano clay reinforced PCL/starch blends obtained by high energy ball milling. *Carbohydr Polym* 2009;75(1):172–9.
- [41] Ungar T. Micro structural parameters from X-ray diffraction peak broadening. *Scr Mater* 2004;51(8):777–81.



# Development of crayfish bio-based plastic materials processed by small-scale injection moulding

Manuel Felix,\* Alberto Romero, Felipe Cordobes and Antonio Guerrero

## Abstract

**BACKGROUND:** Protein has been investigated as a source for biodegradable polymeric materials. This work evaluates the development of plastic materials based on crayfish and glycerol blends, processed by injection moulding, as a fully biodegradable alternative to conventional polymer-based plastics. The effect of different additives, namely sodium sulfite or bisulfite as reducing agents, urea as denaturing agent and L-cysteine as cross-linking agent, is also analysed.

**RESULTS:** The incorporation of any additive always yields an increase in energy efficiency at the mixing stage, but its effect on the mechanical properties of the bioplastics is not so clear, and even dampened. The additive developing a greater effect is L-cysteine, showing higher Young's modulus values and exhibiting a remnant thermosetting potential. Thus, processing at higher temperature yields a remarkable increase in extensibility.

**CONCLUSION:** This work illustrates the feasibility of crayfish-based green biodegradable plastics, thereby contributing to the search for potential value-added applications for this by-product.

© 2014 Society of Chemical Industry

**Keywords:** bioplastic; crayfish protein; mixing blends; rheology; tensile strength test

## INTRODUCTION

The freshwater red-swamp crayfish (*Procambarus clarkii*) was introduced into Europe in the early 1960s. Since then, this species has undergone a fast widespread growth due to its resistance to fungal disease as well as to favourable weather conditions, abundant food and a lack of predators.<sup>1</sup> This fact has driven the development of a strong local crayfish industry at the marshes of the Guadalquivir River in Spain. This development has also led to the generation of a large amount of crayfish surpluses, as is frequently the case in the fish and shellfish industry.<sup>2</sup> According to recent estimations by the Food and Agriculture Organization the total world output of fish represented 156 million tonnes in 2011. Unfortunately, a high proportion of this amount is not eventually used for human food consumption. Thus, according to the USDA, up to 45% of fish and shellfish that enters the USA retail food market is not eaten and, as a consequence, ends as wastes. Therefore, a search for any value-added application to these surpluses is becoming a real priority.

With regard to crayfish surpluses, some applications based on the functional properties of crayfish protein fraction have previously been assessed. Thus, interfacial properties of crayfish protein isolate (CFPI) have been studied<sup>3–5</sup> in order to address the good performance of crayfish protein in emulsion stabilisation.<sup>6,7</sup> Thermal properties of crayfish flour<sup>8</sup> and CFPI in aqueous solution have also been studied in order to assess thermally induced enhancement of emulsion stability<sup>9</sup> as well as the potential of crayfish in the manufacture of surimi-like products based on its ability to form a gel.<sup>10,11</sup>

A currently attractive way to valorise these by-products is through their use as renewable resources in the manufacture of 'green materials', replacing difficult-to-degrade plastic materials made from oil-based synthetic polymers. Nowadays, some important applications for bioplastics are beginning to emerge in the areas of packaging, food production, pharmaceuticals, electronics, automotive industry and biomedicine. Thus, among other applications bioplastics can be used in food packaging, fruit coating, encapsulation, textiles, absorbent materials or tissue engineering.<sup>12–14</sup> This wide variety of potential applications allows us to envisage an increasing use of biobased-plastic materials. Thus, according to European Bioplastics, the production capacity for bioplastics is predicted to increase from approximately 700 000 tons in 2010 to 1.7 Mtons by 2015.<sup>12</sup> However, like other bio-based innovations, bioplastics have struggled to achieve market share such that, at present, bioplastics constitute less than 0.5% of world plastics consumption.<sup>15</sup> Therefore, it is still necessary to intensify the efforts in research and development, and in innovation in this field.

Some biopolymers can directly replace synthetically derived materials in traditional applications or they simply possess unique

\* Correspondence to: Manuel Felix, Departamento de Ingeniería Química, Universidad de Sevilla, Facultad de Química, 41012 Seville, Spain.  
E-mail: mfelix@us.es

Departamento de Ingeniería Química, Universidad de Sevilla, Facultad de Química, 41012 Seville, Spain

properties that could open up a range of new commercial opportunities. In any case, it is essential that bio-based materials exhibit suitable physico-chemical properties. In this sense, cellulose, starch, polysaccharides and protein have become increasingly competitive in recent years as substitutes for petrochemicals, in view of the increase in oil production costs. Both environmental and economic factors are expected to entail the development of new plastic materials such as those using by-products with high protein content.<sup>16</sup> In this respect, proteins are exceptionally versatile materials, both in the sources from which they can be obtained and in the wide variety of possible modifications, which can be helpful in tailoring their properties to the particular requirements of a specific application. Proteins present significant advantages in that they are derived from a sustainable resource and can be processed in much the same way as conventional synthetic polymers.<sup>13</sup> However, proteins are generally mixed with a plasticiser in order to reduce intermolecular forces among polymer chains, increasing mobility and reducing the glass transition.<sup>17</sup>

Traditionally, protein films<sup>18–20</sup> are processed by a casting method; however, classical polymer processing techniques (compression moulding or extrusion) are being increasingly used in this field.<sup>21–24</sup> Among them, injection moulding is a fairly attractive operation that has not received due attention yet. Thus, studies on protein-based biodegradable polymeric materials processed by injection moulding are scarce.<sup>25,26</sup>

Typically in this process, polymeric materials are subjected to suitable thermal conditions, being injected at high pressure into the mould cavity. Optimisation of processing conditions is essential to achieve the desired properties of the final product. This is particularly relevant in protein-based materials that require thermoplastic mixing with a proper plasticiser but benefit from a predominant thermoset character upon injection moulding.<sup>26</sup> Besides, additives such as reducing agents may be helpful in order to reduce the average molecular weight of protein aggregates, thus facilitating both mixing and moulding processes. Thus, some authors studied the influence of reducing agents on the properties of thermo-moulded wheat gluten bioplastics,<sup>27</sup> soy protein isolate,<sup>28–30</sup> starch<sup>31</sup> or flax fibres.<sup>32</sup> The effect of adding a denaturing agent, such as urea has also been analysed on bioplastics processed by extrusion<sup>33</sup> or compression moulding.<sup>34–36</sup> As for the use of L-cysteine as cross-linking agent, Sun *et al.*<sup>37</sup> have recently evaluated its performance on thermo-moulded gluten-based plastics. However, no information about crayfish-based bioplastics with or without reducing, denaturing or cross-linker agents has been found.

The overall objective is to evaluate the potential development of plasticised crayfish bio-based plastic materials by means of a conventional and highly versatile polymer processing technique, such as injection moulding, as an alternative to moulded materials based on polymers derived from fossil fuels. A further objective is to analyse the effect of using different additives on the properties of crayfish-based products, using glycerol as the plasticiser. The additives assessed in this study were sodium sulfite or bisulfite as reducing agents, urea as denaturing agent and L-cysteine as cross-linking agent. A small-scale plunger-type injection moulding machine was used in this study to obtain crayfish-based specimens from crayfish/glycerol/additive blends, previously mixed by means of a mixing rheometer that allows the torque and temperature to be recorded during mixing. Rheological and differential scanning calorimetry measurements of these blends were also carried out in order to obtain information that may be used in the selection of suitable processing parameters for injection moulding operations

(e.g. temperature and residence time in the pre-injection cylinder as well as the temperature of the mould).

## EXPERIMENTAL

### Materials

Crayfish flour was obtained from ALFOCAN S.A. (Isla Mayor, Seville, Spain). The protein content of the crayfish flour, determined in quadruplicate as % N  $\times$  6.25 using a LECO CHNS-932 nitrogen micro analyser (Leco Corporation, St Joseph, MI, USA), was  $642 \pm 9 \text{ g kg}^{-1}$ . Glycerol (used as plasticiser) and additives (sodium sulfite, sodium bisulfite, urea and L-cysteine) were purchased from Panreac Química, S.A. (Barcelona, Spain).

### Free sulfhydryl groups

Free sulfhydryl groups of protein samples were determined using the method developed by Beveridge *et al.*<sup>38</sup> Samples were suspended ( $10 \text{ g L}^{-1}$ ) in buffer containing  $0.086 \text{ mol L}^{-1}$  Tris-HCl,  $0.09 \text{ mol L}^{-1}$  glycine,  $4 \text{ mmol L}^{-1}$  EDTA and  $8 \text{ mol L}^{-1}$  urea, at pH 8. Dispersions were stirred at  $25^\circ\text{C}$  during 10 min at 500 rpm in a thermomixer and then centrifuged at  $15\,000 \times g$  (10 min,  $10^\circ\text{C}$ ). Supernatant was incubated with Ellman's reagent [5,5'-dithiobis-(2-nitrobenzoic acid) (DTNB); 4 g DTNB  $\text{L}^{-1}$  methanol]. Absorbance at 412 nm was measured in a Genesis-20 spectrophotometer (Thermo Scientific, Waltham, MA, USA). The molar extinction coefficient of 3-thio-6-nitrobenzoate (TNB;  $13\,600 \text{ M}^{-1} \text{ cm}^{-1}$ ) was used. Protein concentration of extracts was determined by the Bradford method.

### Sample preparation

Blends with different crayfish flour/glycerol (CF/GL) ratios were manufactured by a thermomechanical procedure which consisted of two stages. Firstly, selected blends containing  $700 \text{ g kg}^{-1}$  crayfish flour and  $300 \text{ g kg}^{-1}$  glycerol (denoted 70/30) were mixed in a two-blade counter-rotating batch mixer Haake PolyLab QC (ThermoHaake, Karlsruhe, Germany) at  $25^\circ\text{C}$  and 50 rpm for 60 or 20 min, monitoring the torque and temperature during mixing. Secondly, the dough-like materials obtained after mixing were subsequently processed by injection moulding using a MiniJet Piston Injection Molding System II (ThermoHaake) to obtain bioplastic specimens. Two moulds were used to prepare two types of specimens: (1) a  $60 \times 10 \times 1 \text{ mm}$  rectangular-shaped specimen, to be used for both dynamic mechanical temperature analysis (DMTA) experiments and transparency measurements, and (2) a dumb-bell-type specimen defined by ISO 527–2:1993 for determining the tensile properties of plastics.

### Characterisation of blends

The most suitable processing variables such as temperatures in the pre-injection cylinder or in the mould were selected after performing temperature ramp tests and differential scanning calorimetry measurements (results not shown).

### Rheological measurements

Dough-like materials were characterised by small amplitude oscillatory shear measurements, using a controlled-strain rheometer, in order to select the optimum conditions for injection moulding: (Mars II from Haake, Karlsruhe, Germany). The geometry used has been a plate and plate geometry (diameter, 25 mm) with a rough surface and a gap between plates of 1 mm. Low viscosity

Dow Corning 200 fluid was used as sealant to avoid sample drying. Strain sweep small amplitude oscillatory shear tests were also performed in order to establish the linear visco-elasticity range. Temperature ramp tests were carried out at  $5\text{ }^{\circ}\text{C min}^{-1}$  from 20 to  $100\text{ }^{\circ}\text{C}$  and time sweep tests were performed for 1800 s at a selected constant temperature. Linear visco-elastic properties ( $G'$ ,  $G''$ ) were monitored at a constant frequency of  $6.28\text{ rad s}^{-1}$ . All the systems studied had the same thermo-rheological history before performing any rheological test.

### Characterisation of bioplastics

#### Dynamic mechanical temperature analysis

DMTA tests were carried out with a RSA3 (TA Instruments, New Castle, DE, USA), on rectangular probes using dual cantilever bending. All the experiments were carried out at constant frequency ( $6.28\text{ rad s}^{-1}$ ) and strain (between 0.01 and 0.3%, within the linear visco-elastic region). The selected heating rate was  $3\text{ }^{\circ}\text{C min}^{-1}$ . All the samples were coated with Dow Corning high vacuum grease to avoid water loss.

#### Tensile strength measurements

Tensile tests were performed by using an Insight 10 kN Electromechanical Testing System (MTS, Eden Prairie, MN, USA), according to ISO 527-2:1993 for tensile properties of plastics. Tensile stress and elongation at break were evaluated from at least three duplicates for each product using type IV probes and an extensional rate of  $100\text{ mm min}^{-1}$  at room temperature.

#### Statistical analysis

At least three replicates of each measurement were carried out. Statistical analyses were performed using a *t*-test and one-way analysis of variance (ANOVA,  $P < 0.05$ ) by using the statistical package SPSS 18 (SPSS, Chicago, IL, USA). Standard deviations from some selected parameters were calculated.

## RESULTS AND DISCUSSION

### Thermoplastic mixing of blends

Figure 1 shows both torque and temperature profiles as a function of mixing time for blends obtained at different CF/GL ratios, as well as their visual appearance after mixing. These results show

the remarkable dependence of these parameters on the CF/GL ratio. Thus, a rapid increase in torque up to a maximum value takes place for the system having less amount of plasticiser, denoted as 80/20, which represents the CF/GL weight ratio. This evolution is readily followed by an asymptotic decrease towards a plateau value. In contrast, the system 70/30 shows a moderate growth in torque showing no maximum value but a slow tendency to a plateau value. The profile of the system 60/40 only shows an initial increase in torque, although very slight, being dominated by a constant torque value over mixing time. In general, the evolution of temperature over time is very similar to the torque profile where an increase takes place excepting for the lowest CF/GL ratio. Both increases in torque and temperature may be attributed to shear-induced exothermic reactions, by S—S bonds formation, developed during the mixing process.

As a consequence of the above-mentioned differences in torque profile, the specific mechanical energy (SME) input for mixing is also quite different. This characteristic parameter of mixing may be defined as follows:<sup>39</sup>

$$\text{SME} = \frac{\omega}{m} \int_0^{t_{\text{mix}}} M(t) dt \quad (1)$$

where  $\omega$  (in  $\text{rad s}^{-1}$ ) is the mixing speed,  $m$  (in g) is the sample mass,  $M(t)$  (in N m) is the torque and  $t_{\text{mix}}$  (in s) is the mixing time. The values of the SME parameter for these three systems are included in Fig. 1. A remarkable increase in this parameter can be observed with the CF/GL ratio. This effect takes also place at the higher concentrations in spite of the fact that the plateau torque values are relatively close to each other.

From the visual appearance observed in Fig. 1, system 80/20 does not seem to contain enough amount of plasticiser to obtain an easy-to-handle material, giving rise to a granulated powder instead of a homogeneous dough-like blend. In fact, this is the system displaying the highest torque values, which correspond to the highest rheological consistency. On the other hand, the highest amount of glycerol in the 60/40 system provides a neat dough-like appearance to the blend. This is also consistent with the lowest torque values obtained (associated with a lower consistency) after the mixing process. The 70/30 system shows intermediate behaviour between both limits, although it is closer to the most concentrated protein-based blend. In the present study, the 80/20 system has been discarded because of the high energy

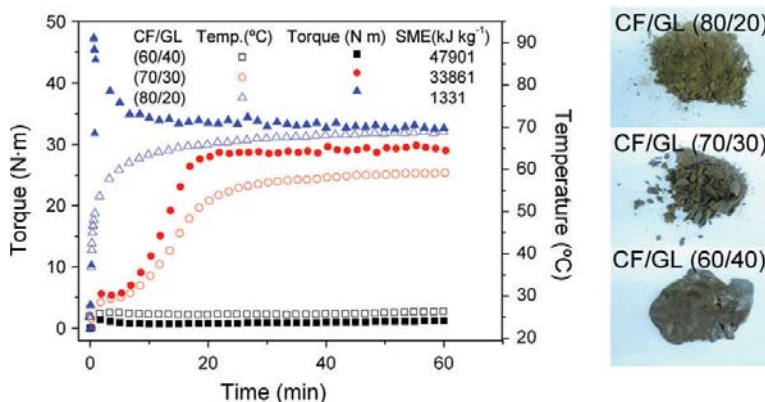


**Figure 1.** Mixing torque and temperature profiles and images for crayfish flour/glycerol (CF/GL) systems (80/20, 70/30 and 60/40).



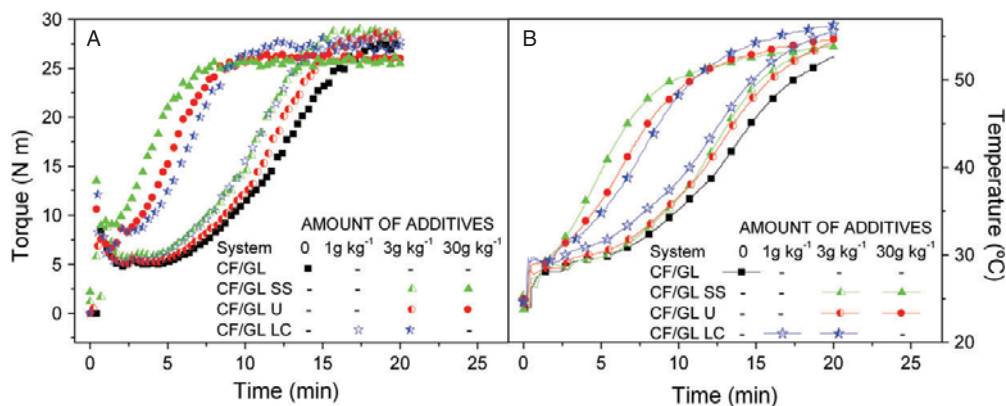


**Figure 2.** Evolution of mixing torque (A) and temperature (B) as a function of mixing time or additive-containing system (sodium sulfite, urea and L-cysteine). SS, sodium sulfite; U, urea; LC, L-cysteine.

input required for mixing. Moreover, this system has proven to be difficult to inject (results not shown). On the other hand, systems containing a low protein/glycerol ratio may be injected easily but the final bioplastic materials tend to exude the excess glycerol. Exudation is a well-known phenomenon described in the polymer–plasticiser literature and should be avoided in order to prevent contamination of the surrounding materials (e.g. in food packaging).<sup>40</sup> This seems to be the case for the 60/40 system. As a result, the 70/30 system was selected as the most suitable to obtain a homogeneous and easily injectable CF/GL blend.

Figure 2 shows the evolution of torque (Fig. 2A) and temperature (Fig. 2B) as a function of time for different 70/30 CF/GL blends prepared using sodium sulfite as reducing agent, urea as denaturing agent, or L-cysteine as cross-linking promoter at different concentrations (3 and 30 g kg<sup>-1</sup> protein for sodium sulfite and urea or 1 and 3 g kg<sup>-1</sup> for L-cysteine).

These results generally show that any of the additives used induces an anticipation of the torque profile, particularly at the highest additive concentrations. No differences in the torque profile are noticed at the two different concentrations of sodium bisulfite (data not shown). The highest amount of additive (corresponding to sodium sulfite or urea) also yields lower torque plateau values, which may be considered beneficial for the processability of blends, for example under injection moulding. Temperature–time profiles show the same type of evolution for all the additives and concentrations in spite of the fact that an air stream was used as a cooling fluid. No differences are found in the final values for the highest sodium sulfite or urea content in this case. The only difference found between temperature and torque profiles is that the former undergo a further delay in time, which may be related to the air-cooling effect.

It is interesting to notice that although all the additives in Fig. 2 led to an apparent anticipation in torque and temperature profiles, different mechanisms are involved depending on the additive used. Urea is a widely used denaturing agent that induces disruption of physical interactions among protein molecules. On the other hand sodium sulfite, acting as a reducing agent, induces disruption of S—S bonds. As a consequence, protein–plasticiser mixing is favoured in both cases resulting in a faster kinetics over the additive-free system. L-Cysteine is an amino acid that provides a free sulfhydryl group/molecule and therefore facilitates formation of S—S bonds with protein segments to form cystine

groups.<sup>41</sup> In this way, L-cysteine initiates the formation of exothermic S—S bonds, progressively increasing the temperature, which leads to anticipation of both torque and temperature profiles. In fact, this additive gives rise to the fastest anticipation for the same additive content. In addition, the highest temperatures reached by the L-cysteine-containing blend suggest the occurrence of a higher cross-linking degree as compared to the other systems.

It may be also noted that the system is not still properly mixed at times shorter than that that corresponding to the maximum torque. Therefore, as a general rule, the range of mixing times for subsequent blend processing is selected once the plateau torque value is reached such that a good degree of homogeneity is assured.

Another interesting parameter to compare different mixing processes is the relative energy input (REI), which is defined as follows:

$$REI (\%) = \frac{SME_{\min}(a, c)}{SME_{\min}(0)} \times 100 \quad (2)$$

where  $SME_{\min}(0)$  and  $SME_{\min}(a, c)$  are the SME values at which the torque reaches 95% of the maximum value for the profile of the additive free blend and additive *a* at concentration *c*, respectively. Therefore, REI is an index of the reduction in energy input relative to that that required for mixing the additive free blend.

The values of  $SME_{20}$  and REI parameters for all these additives are shown in Fig. 3A and B, respectively. The SME values for sodium bisulfite are also included in this figure.  $SME_{20}$  is the specific mechanical energy supplied, as defined in Eqn (1), after mixing for 20 min.

As may be observed in Fig. 3, an increase in additive concentration always leads to an apparent increase in the parameter  $SME_{20}$ , as a consequence of the above-mentioned anticipation of the torque profile. If the same additive concentration is used, this increase is particularly remarkable for L-cysteine and, in any case, is only moderate when sodium bisulfite is used.

The results obtained with parameter REI confirm the relevant effect of the addition of L-cysteine at constant additive concentration. Thus, estimation tendencies from the results obtained indicate that the additive/protein ratio required to achieve a 50% REI would be 33 g kg<sup>-1</sup> for urea and 27 g kg<sup>-1</sup> for sodium sulfite, whereas a ratio as low as 4.4 g kg<sup>-1</sup> would be required by using L-cysteine.

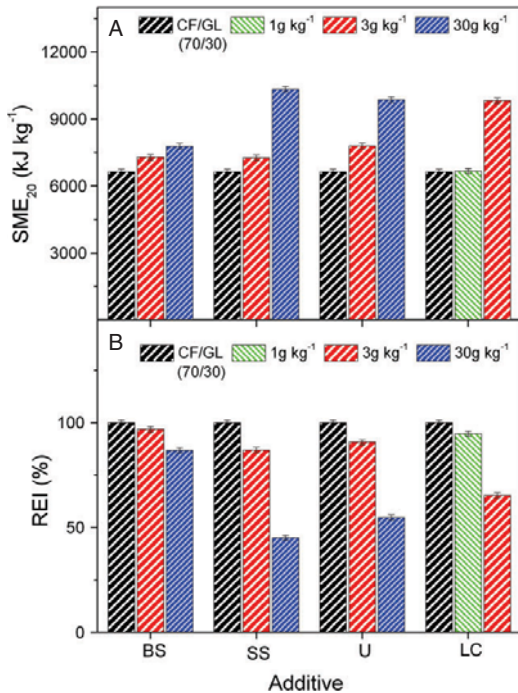


**Figure 3.** (A) Specific mechanical energy (SME) after mixing for 20 min and (B) reduction in energy input (REI) for different crayfish flour/glycerol (CF/GL) blends (additive-free, sodium bisulfite, sodium sulfite, urea or L-cysteine). BS, sodium bisulfite; SS, sodium sulfite; U, urea; LC, L-cysteine.

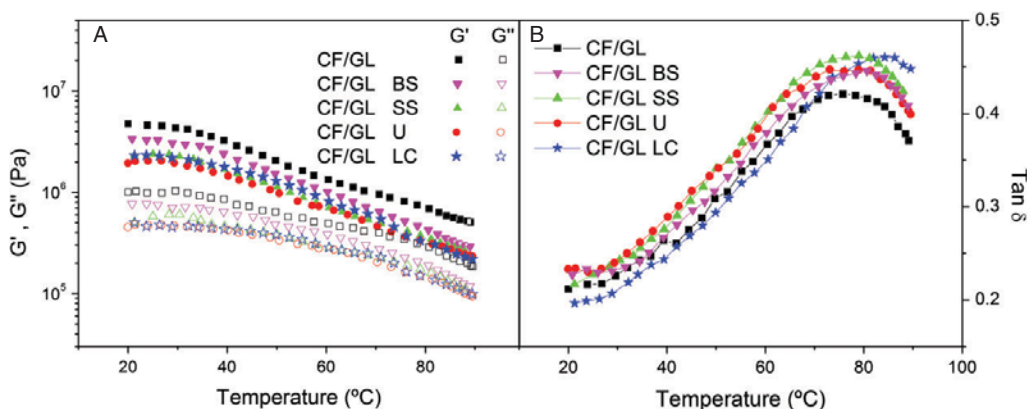
#### Temperature ramps

Figure 4 shows the dependence of linear visco-elastic functions on temperature for different blends containing 3 g additive kg<sup>-1</sup> crayfish protein. The additive free blend is also displayed in this figure. All the additives studied induce a reduction in  $G'$  and  $G''$  in the experimental temperature range. As for  $\tan \delta$  profiles, all of them show a similar elastic-dominant behaviour characterised

by the presence of a broad distribution showing a maximum value. This maximum has been also found at 70 °C by differential scanning calorimetry measurements for the CF/GL system (results not shown), being associated to a glass-like transition of the protein fraction. Most of additive-containing blends show this smooth thermal induced glass transition in the same temperature range than the additive free system (70–83 °C). However, a shift in this event towards higher values (80–87 °C) takes place when L-cysteine is used as additive.

It should be mentioned that the cooling–setting stage after mixing leads to noticeable differences between the visco-elastic properties of additive-free and additive-containing CF/GL blends. Once again, the additive showing the poorest effect is sodium bisulfite. However, the cooling–setting stage does not induce any apparent difference in  $G'$  or  $G''$  among the other three additives (Fig. 4A), in spite of the fact that the expected mechanism would be different. Thus, sodium sulfite is expected to reduce the visco-elastic properties of CF/GL blends by breaking some disulfide bonds, although the effect does not seem take place at a high extent. A similar mechanism should explain the behaviour found for sodium bisulfite-containing blends, which becomes more important above 60 °C. In contrast, urea may show a double effect. Firstly, as reported by Verbeek and Van den Berg,<sup>42</sup> urea may play the role of a plasticiser at a concentration as low as that used in this study, not showing any cross-linking effect. Secondly, urea, as a denaturing agent, tends to inhibit the recovery of physical interactions over the cooling–setting stage. In fact, the latter effect seems to be more relevant than the former, as no differences in the  $\tan \delta$  peak can be detected in Fig. 4B. According to this figure, the L-cysteine-containing blend is the only one showing the  $\tan \delta$  peak at higher temperature than the additive-free system. This effect may be related to a higher cross-linking extent, as previously mentioned (Fig. 2B). However, this higher degree of cross-linking does not involve any increase in  $G'$  and  $G''$ . On the contrary, the results are similar to those shown by urea- and sodium sulfite-containing blends. An explanation for this effect should be related to the inhibition of physical interactions development over the cooling–setting stage.

In any case, the addition of any of the additives used leads to a potential enhancement of the moulding processability of CF/GL blends, where rheological properties are regarded as the key



**Figure 4.** (A) Storage modulus ( $G'$ ) and loss modulus ( $G''$ ), and (B) loss tangent ( $\tan \delta$ ), at 1 Hz and 5 °C min<sup>-1</sup>, as a function of temperature for different crayfish flour/glycerol (CF/GL) blends (additive-free or 3 g kg<sup>-1</sup> sodium bisulfite, sodium sulfite, urea or L-cysteine). BS, sodium bisulfite; SS, sodium sulfite; U, urea; LC, L-cysteine.

**Table 1.** Standard values of injection moulding parameters for the pre-injection cylinder, injection and packing stage

Parameter	T (°C)	Pressure (MPa)	Time (s)
Pre-injection cylinder	60	0.1	100 <sup>a</sup>
Injection	60–100	0.1–50	<1
Packing stage	100 or 130	50	20
	100 or 130	20	200 <sup>a</sup>

<sup>a</sup> For a system containing L-cysteine, 130 °C and 600 s were also used.

factor. In other words, additives contribute to facilitate injection of CF-based blends. Similar results were found by Pallos *et al.*<sup>43</sup> for thermoformed wheat gluten modified by reducing agents and additives.

### Injection moulding process

Table 1 shows the conditions selected for the injection moulding process for each of the blends studied. Processing parameters for the pre-injection cylinder are selected taking into account that the elastic properties of CF/GL blends should be reduced to some extent (typically  $G'$  should be in the order of  $1 \times 10^6$  Pa or below). On the other hand, the temperature should not be increased excessively in order to prevent thermally induced protein cross-linking effects before the injection stage. For the same reason, the residence time in the cylinder should not be long. Under such premises the parameters selected for the first stage have been 60 °C and 100 s.

As for the mould processing conditions, the temperature has to be high enough to ensure the normal development of thermal and pressure-induced protein cross-linking reactions. On the other hand, exposure to high temperatures for a long time typically leads to protein degradation (i.e. via Maillard-type reactions). Therefore, 100 °C and 20 s have been selected as the moulding temperature and time, respectively. The injection pressure selected in this case has been 50 MPa. Once the blend has been injected into the mould, a further stage is performed at the same temperature for a residence time long enough (10 s) to allow for the development

of protein cross-linking to achieve the final network structure. The residence time selected has been 200 s since no further enhancement has been noted by increasing this period.

### Mechanical characterisation of bioplastics

#### Dynamic mechanical temperature analysis

Figure 5 shows the values of the elastic modulus,  $E'$ , as a function of temperature (from -30 °C to 140 °C) obtained from dynamic mechanical analysis (DMA) measurements for additive-free CF/GL specimens and CF/GL probes containing 3 g kg<sup>-1</sup> additive. Figure 5A compares the influence of different additives (sodium bisulfite, sodium sulfite, urea and L-cysteine) for specimens moulded at 100 °C for 200 s, whereas Fig. 5B shows the effect of different moulding conditions for L-cysteine-containing specimens.

As may be observed in Fig. 5A, all the specimens show similar profiles for  $E'$  and also for  $E''$  (data not shown), undergoing a remarkable decrease with increasing temperature. The decrease tends to reach a plateau value at high temperature. In some cases the  $E'$  profile eventually evolves to an increase in value, indicating a certain thermosetting potential. DMA profiles for the additive-free, urea and sodium bisulfite specimens do not display any significant difference, in spite of the effect observed on the visco-elastic properties of their corresponding blends (Fig. 4A). Sodium sulfite-containing specimens show lower  $E'$  values at low temperature but higher values in the high temperature region as compared to the reference (additive-free) system. This system also evolves in a more gradual way than the other bioplastic specimens, particularly at high temperature, showing no thermosetting potential region. This behaviour may be associated with the ability of sodium sulfite to impair disulfide bridges. Thus, the results obtained after application of the procedure devised by Beveridge *et al.*<sup>38</sup> indicate that the concentration of free sulfhydryl groups in crayfish flour is increased from  $19 \pm 3$  mmol kg<sup>-1</sup> to  $300 \pm 17$  mmol kg<sup>-1</sup> after addition of 3 g sodium sulfite kg<sup>-1</sup> protein.

As for L-cysteine specimens, they show a rather similar DMA profile at low and medium temperature but there is also an apparent increase in  $E'$  at high temperature, which reveals that this system still exhibits a marked remnant thermosetting potential for further processing.

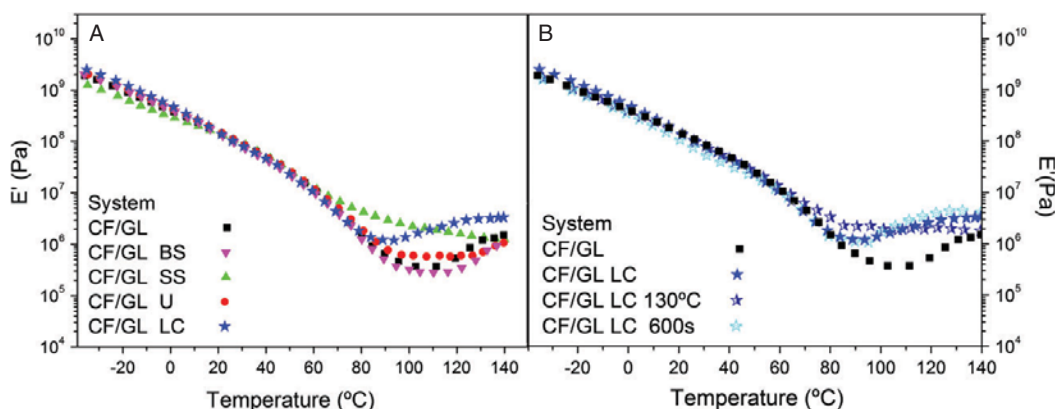


**Figure 5.** Storage modulus ( $E'$ ) values from dynamic mechanical analysis (DMA) temperature ramp measurements carried out at 1 Hz and 3 °C min<sup>-1</sup> for different crayfish flour/glycerol (CF/GL) systems: (A) additive-containing (sodium bisulfite, sodium sulfite, urea or L-cysteine) specimens; and (B) L-cysteine-containing specimens processed at different moulding temperature (100 or 130 °C) and packing time (200 or 600 s). The additive-free CF/GL is included as a reference. BS, sodium bisulfite; SS, sodium sulfite; U, urea; LC, L-cysteine.

This increase may be a consequence of different cross-linking reactions involving S—S bond formation, SH—SS interchange<sup>44</sup> and also non-disulfide bonds. Thus, Rombouts *et al.*<sup>45</sup> reported a heat-induced reduction in  $\epsilon$ -amino groups, being most likely the result of isopeptide bond formation in combination with Maillard and/or other heat-induced reactions. These authors also found that lysine- and glutamine-containing peptides from high molecular weight glutenin sub-units also induced the formation of isopeptide bonds, thereby demonstrating that cross-linking did not solely depend on the availability of cysteine or cystine residues. In this sense, it is interesting to note that crayfish protein is rich in the amino acids glutamine and lysine.<sup>46</sup>

In order to explore this potential L-cysteine-containing specimens were processed using different moulding conditions over the packing stage, increasing either the packing time in the mould at 100 °C and 20 MPa (up to 600 s) or the moulding temperature at 20 MPa over 200 s (up to 130 °C). DMA results for these new L-cysteine-containing specimens are shown in Fig. 5B. As may be observed, the increase in moulding time does not lead to any noticeable change in the DMA profile, which suggests that the time selected for the former specimens is long enough to complete the cross-linking stage. On the other hand, an increase in moulding temperature leads to a plateau value for  $E'$  in the high-temperature region. However, this change in moulding conditions does not drive any particular enhancement in the visco-elastic bending properties below 60 °C. This behaviour is somehow unexpected since the occurrence of the above-mentioned thermosetting potential typically involves an enhancement of mechanical properties.<sup>21,47,48</sup> A possible explanation for this lack of enhancement may be found in the fact that some degradation of specimens has been observed at 130 °C and above. Probably, this degradation is related to other components (e.g. lipids content) rather than protein but it may produce some alterations of mechanical properties. Thus, using a defatted crayfish protein concentrate instead of crayfish flour would be a better choice in order to process at higher temperatures.

#### Measurements of the uniaxial tensile strength

Figure 6A displays the results of stress–strain curves obtained from tensile strength measurements for additive-free and additive-containing specimens at an additive/CF ratio. All the

curves exhibit a similar behaviour which consist of an initial linear elastic behaviour of high constant stress–strain slope yielding high values for the Young's modulus ( $E$ ), followed by a deformation stage with a continuous decrease in the stress–strain slope. A second constant slope is reached at the end of the plastic deformation stage. All the curves eventually reach a maximum value for the stress ( $\sigma_{\max}$ ) and the strain at break ( $\epsilon_{\max}$ ). Only L-cysteine leads to an apparent enhancement of the tensile strength profile, also leading to a slightly shorter strain value. The values of these parameters ( $E$ ,  $\sigma_{\max}$  and  $\epsilon_{\max}$ ) and their corresponding standard deviations are plotted in Fig. 6B for the additive-free and additive-containing specimens at 3 g kg<sup>-1</sup> additive/CF ratio. This figure indicates once again that additive L-cysteine is the only one that improves parameters  $E$  and  $\sigma_{\max}$  over the additive-free system, under the same processing conditions. On the other hand L-cysteine-added specimens exhibit lower values for  $\epsilon_{\max}$ . The remainder of the additives lead to similar or even lower values of the three parameters. Figure 6B also shows the values for L-cysteine-added specimens moulded at longer time or higher temperature. As may be observed, an increase in the packing time from 200 s up to 600 s does not yield any noticeable change in tensile parameters. This result indicates that after 200 s packing time the sprue is already closed by the solidified blend. On the other hand, an increase in the mould temperature leads to remarkable changes in tensile parameters. Thus, the maximum stress and, above all, the strain at break undergo an apparent increase in value (approx. 12% and 70%, respectively), whereas the Young's modulus clearly decreases (approx. 30%) by increasing the mould temperature from 100 to 130 °C. Interestingly, the maximum elongation is the property that undergoes the most remarkable enhancement by favouring heat-induced cross-linking. In this way, the material exhibits greater toughness, in spite of being less strong. In fact, as stated by Lagrain *et al.*,<sup>49</sup> increasing the elongation at break of glassy, amorphous polymers typically goes at the expense of the elastic modulus. This compensation may also affect the bending elastic properties of the bioplastic, thus explaining the small dependence of DMA profiles on moulding temperature.

Moreover, this behaviour is similar to that found for other elastomeric materials such as rubber-based blends<sup>50</sup> and is consistent with the results from DMA measurements that show an extension of the rubbery plateau obtained at high temperature.

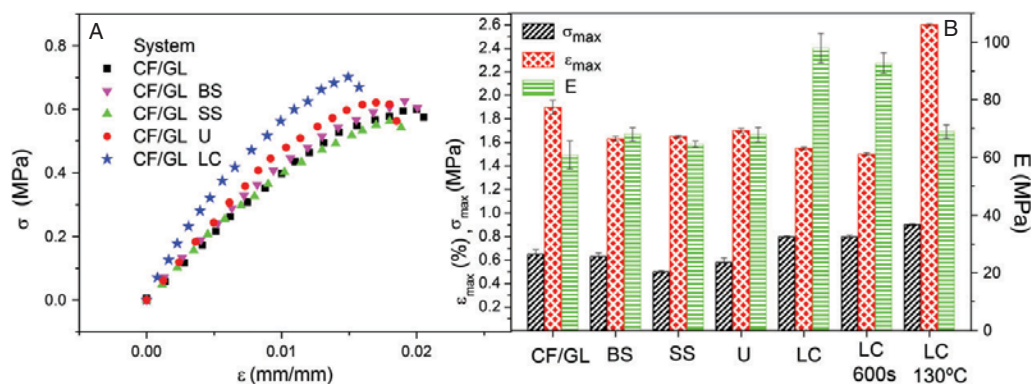


**Figure 6.** Results from tensile strength measurements for different crayfish flour/glycerol (CF/GL) systems: additive-free or 3 g kg<sup>-1</sup> additive-containing specimens (sodium bisulfite, sodium sulfite, urea or L-cysteine). (A) Stress–strain curves, and (B) parameters from tensile strength measurements: maximum stress ( $\sigma_{\max}$ ), strain at break ( $\epsilon_{\max}$ ) and Young's modulus ( $E$ ). BS, sodium bisulfite; SS, sodium sulfite; U, urea; LC, L-cysteine.



## CONCLUSIONS

From the experimental results, it may be concluded that monitoring the torque over mixing of protein-based flour, additives and plasticiser it is useful to select the more suitable conditions (e.g. mixing time and formulation) in terms of energy efficiency. Characterisation of the rheological properties of blends (particularly their dependence on temperature) is also important to select suitable operation conditions for injection moulding processing.

The addition of reducing agent (sodium bisulfite or sodium sulfite), denaturing agent (urea) or cross-linking promoter (L-cysteine), always yields an increase in energy efficiency (i.e. a decrease in REI value) at the mixing stage, leading to a remarkable reduction in the linear visco-elastic properties of blends.

In contrast, the effect of the additives on the mechanical properties of the final bioplastic material is not so clear, particularly for the results from DMA measurements. The additive developing a greater effect is L-cysteine, which provides specimens showing a higher value for the Young's modulus, as well as a remnant thermosetting potential for further processing at high temperature. This potential typically involves an enhancement of mechanical properties.<sup>21,47,48,51</sup> However, in this study the maximum elongation is the property that is remarkably enhanced by increasing the thermosetting temperature. This moulding temperature-driven enhancement is clearly at the expense of the Young's modulus, such that the effect on the bending elastic modulus is dampened.

The present work puts forward the feasibility of developing crayfish-based green biodegradable plastics, thereby finding potential value-added applications for this protein concentrate by-product. However, much research is still needed in order to further explore the potential of crayfish in this field. Thus, from the results obtained, it seems to be an advisable strategy to investigate the possible synergetic effects resulting from the combination of the different additives studied. This combination could be studied by incorporating each additive at the mixing stage, according to the following sequence: (1) urea, to facilitate disruption of physical interactions; (2) sodium sulfite, to induce breakage of disulfide bonds; and (3) L-cysteine to anticipate and improve mixing efficiency and to promote subsequent cross-linking at the moulding stage.

## ACKNOWLEDGEMENTS

This work is part of a research project sponsored by Andalusian Government (Spain) (project TEP-6134) and by the 'Ministerio de Economía y Competitividad' from Spanish Government (Ref. MAT2011-29275-C02-02). The authors gratefully acknowledge their financial support. The authors also acknowledge the Microanalysis Service (CITIUS-Universidad de Sevilla) for providing full access and assistance with the LECO-CHNS-932 equipment.

## REFERENCES

- Geiger W, Alcorlo P, Baltanas A and Montes C, Impact of an introduced Crustacean on the trophic webs of Mediterranean wetlands. *Biol Invasions* **7**:49–73 (2005).
- Kirjavainen J and Westman K, Natural history and development of the introduced finnish crayfish, *Pacifastacus leniusculus*, in a small, isolated Finnish lake, from 1968 to 1993. *Aquat Living Resour* **12**:387–401 (1999).
- Romero A, Beaumal V, David-Briand E, Cordobes F, Anton M and Guerrero A, Interfacial and emulsifying behaviour of crayfish protein isolate. *LWT—Food Sci Technol* **44**:1603–1610 (2011).
- Romero A, Verwijlen T, Guerrero A and Vermant J, Interfacial behaviour of crayfish protein isolate. *Food Hydrocolloids* **30**:470–476 (2013).
- Romero A, Verwijlen T, Guerrero A and Vermant J, Interfacial properties of crayfish protein isolate/chitosan mixed films. *Food Hydrocolloids* **32**:395–401 (2013).
- Romero A, Cordobes F, Puppo MC, Guerrero A and Bengoechea C, Rheology and droplet size distribution of emulsions stabilized by crayfish flour. *Food Hydrocolloids* **22**:1033–1043 (2008).
- Romero A, Cordobes F and Guerrero A, Influence of pH on linear viscoelasticity and droplet size distribution of highly concentrated O/W crayfish flour-based emulsions. *Food Hydrocolloids* **23**:244–252 (2009).
- Farahnaky A, Guerrero A, Hill SE and Mitchell JR, Physical ageing of crayfish flour at low moisture contents. *J Therm Anal Calorim* **93**:595–598 (2008).
- Romero A, Bengoechea C, Cordobes F and Guerrero A, Application of thermal treatments to enhance gel strength and stability of highly concentrated crayfish-based emulsions. *Food Hydrocolloids* **23**:2346–2353 (2009).
- Romero A, Cordobes F, Puppo MC, Villanueva A, Pedroche J and Guerrero A, Linear viscoelasticity and microstructure of heat-induced crayfish protein isolate gels. *Food Hydrocolloids* **23**:964–972 (2009).
- Romero A, Cordobes F, Guerrero A and Cecilia Puppo M, Crayfish protein isolated gels. A study of pH influence. *Food Hydrocolloids* **25**:1490–1498 (2011).
- Soroudi A and Jakubowicz I, Recycling of bioplastics, their blends and biocomposites: A review. *Eur Polym J* **49**:2839–2858 (2013).
- Sharma S and Luzinov I, Water aided fabrication of whey and albumin plastics. *J Polym Environ* **20**:681–689 (2012).
- Yoo SR and Krochta JM, Whey protein–polysaccharide blended edible film formation and barrier, tensile, thermal and transparency properties. *J Sci Food Agric* **91**:2628–2636 (2011).
- Shen L, Haufe J and Patel MK *Product Overview and Market Projection of Emerging Bio-Based Plastics PRO-BIP 2009*. Utrecht University, Utrecht (2009).
- DiGregorio BE, Biobased performance bioplastic: Mirel. *Chem Biol* **16**:1–2 (2009).
- Irissin-Mangata J, Bauduin G, Boutevin B and Gontard N, New plasticizers for wheat gluten films. *Eur Polym J* **37**:1533–1541 (2001).
- Prommakool A, Sajjaanantakul T, Janjarasskul T and Krochta JM, Whey protein–okra polysaccharide fraction blend edible films: tensile properties, water vapor permeability and oxygen permeability. *J Sci Food Agric* **91**:362–369 (2011).
- Rossi-Marquez G, Han JH, Garcia-Almendarez B, Castano-Tostado E and Regalado-Gonzalez C, Effect of temperature, pH and film thickness on nisin release from antimicrobial whey protein isolate edible films. *J Sci Food Agric* **89**:2492–2497 (2009).
- Rayner M, Cioffi V, Maves B, Stedman P and Mittal GS, Development and application of soy-protein films to reduce fat intake in deep-fried foods. *J Sci Food Agric* **80**:777–782 (2000).
- Jerez A, Partal P, Martinez I, Gallegos C and Guerrero A, Protein-based bioplastics: effect of thermo-mechanical processing. *Rheol Acta* **46**:711–720 (2007).
- Gonzalez-Gutierrez J, Partal P, Garcia-Morales M and Gallegos C, Effect of processing on the viscoelastic, tensile and optical properties of albumen/starch-based bioplastics. *Carbohydr Polym* **84**:308–315 (2011).
- Brauer S, Meister F, Gottlobler RP and Nechwatal A, Preparation and thermoplastic processing of modified plant proteins. *Macromol Mater Eng* **292**:176–183 (2007).
- Fernandez-Pan I, Mendoza M and Mate JI, Whey protein isolate edible films with essential oils incorporated to improve the microbial quality of poultry. *J Sci Food Agric* **93**:2986–2994 (2013).
- Nanda MR, Misra M and Mohanty AK, Mechanical performance of soy–hull-reinforced bioplastic composites: a comparison with polypropylene composites. *Macromol Mater Eng* **297**:184–194 (2012).
- Felix M, Martin-Alfonso JE, Romero A and Guerrero A, Development of albumen/soy biobased plastic materials processed by injection molding. *J Food Eng* **125**:7–16 (2014).
- Min Z, Song Y and Zheng Q, Influence of reducing agents on properties of thermo-molded wheat gluten bioplastics. *J Cereal Sci* **48**:794–799 (2008).
- Nanda PK, Rao KK, Kar RK and Nayak PL, Biodegradable polymers – Part VI – Biodegradable plastics of soy protein isolate modified with thiourea. *J Therm Anal Calorim* **89**:935–940 (2007).

- 29 Nayak P, Sasmal A, Nanda PK, Nayak PL, Kim J and Chang Y-W, Preparation and characterization of edible films based on soy protein isolate–fatty acid blends. *Polym–Plast Technol* **47**:466–472 (2008).
- 30 Swain SN, Biswal SM, Nanda PK and Nayak PL, Biodegradable soy-based plastics: Opportunities and challenges. *J Polym Environ* **12**:35–42 (2004).
- 31 Shin BY, Narayan R, Lee SI and Lee TJ, Morphology and rheological properties of blends of chemically modified thermoplastic starch and polycaprolactone. *Polym Eng Sci* **48**:2126–2133 (2008).
- 32 Wrobel-Kwiatkowska M, Czemplik M, Kulma A, Zuk M, Kaczmar J, Dyminska L, *et al.*, New biocomposites based on bioplastic flax fibers and biodegradable polymers. *Biotechnol Prog* **28**:1336–1346 (2012).
- 33 Pickering KL, Verbeek CJR and Viljoen C, The effect of aqueous urea on the processing, structure and properties of CGM. *J Polym Environ* **20**:335–343 (2012).
- 34 Yue HB, Cui YD, Shuttleworth PS and Clark JH, Preparation and characterisation of bioplastics made from cottonseed protein. *Green Chem* **14**:2009–2016 (2012).
- 35 Verbeek CJR and van den Berg LE, Development of proteinous bioplastics using bloodmeal. *J Polym Environ* **19**:1–10 (2011).
- 36 Liu DG and Zhang LN, Structure and properties of soy protein plastics plasticized with acetamide. *Macromol Mater Eng* **291**:820–828 (2006).
- 37 Sun S, Song Y and Zheng Q, Morphologies and properties of thermo-molded biodegradable plastics based on glycerol-plasticized wheat gluten. *Food Hydrocolloids* **21**:1005–1013 (2007).
- 38 Beveridge T, Toma SJ and Nakai S, Determination of SH-groups and SS-groups in some food proteins using Ellman's reagent. *J Food Sci* **39**:49–51 (1974).
- 39 Redl A, Morel MH, Bonicel J, Guilbert S and Vergnes B, Rheological properties of gluten plasticized with glycerol: dependence on temperature, glycerol content and mixing conditions. *Rheol Acta* **38**:311–320 (1999).
- 40 Rahman M and Brazel CS, The plasticizer market: An assessment of traditional plasticizers and research trends to meet new challenges. *Prog Polym Sci* **29**:1223–1248 (2004).
- 41 Rombouts I, Lagrain B, Delcour JA, Ture H, Hedenqvist MS, Johansson E, *et al.*, Crosslinks in wheat gluten films with hexagonal close-packed protein structures. *Ind Crop Prod* **51**:229–235 (2013).
- 42 Verbeek CJR and van den Berg LE, Extrusion processing and properties of protein-based thermoplastics. *Macromol Mater Eng* **295**:10–21 (2010).
- 43 Pallos FM, Robertson GH, Pavlath AE and Orts WJ, Thermoformed wheat gluten biopolymers. *J Agric Food Chem* **54**:349–352 (2006).
- 44 Gerrard JA, Protein–protein crosslinking in food: methods, consequences, applications. *Trends Food Sci Technol* **13**:391–399 (2002).
- 45 Rombouts I, Lagrain B, Brunnbauer M, Koehler P, Brijs K and Delcour JA, Identification of isopeptide bonds in heat-treated wheat gluten peptides. *J Agric Food Chem* **59**:1236–1243 (2011).
- 46 Cremades O, Parrado J, Alvarez-Ossorio MC, Jover M, de Teran LC, Gutierrez JF, *et al.*, Isolation and characterization of carotenoproteins from crayfish (*Procambarus clarkii*). *Food Chem* **82**:559–566 (2003).
- 47 Zarate-Ramirez LS, Martinez I, Romero A, Partal P and Guerrero A, Wheat gluten-based materials plasticised with glycerol and water by thermoplastic mixing and thermomoulding. *J Sci Food Agric* **91**:625–633 (2011).
- 48 Gómez-Martínez D, Partal P, Martínez I and Gallegos C, Rheological behaviour and physical properties of controlled-release gluten-based bioplastics. *Bioresour Technol* **100**:1828–1832 (2009).
- 49 Lagrain B, Goderis B, Brijs K and Delcour JA, Molecular basis of processing wheat gluten toward biobased materials. *Biomacromolecules* **11**:533–541 (2010).
- 50 Pire M, Norvez S, Iliopoulos I, Le Rossignol B and Leibler L, Imidazole-promoted acceleration of crosslinking in epoxidized natural rubber/dicarboxylic acid blends. *Polymer* **52**:5243–5249 (2011).
- 51 Jerez A, Partal P, Martinez I, Gallegos C and Guerrero A, Egg white-based bioplastics developed by thermomechanical processing. *J Food Eng* **82**:608–617 (2007).